

Syracuse University

SURFACE

Dissertations - ALL

SURFACE

December 2016

Development of multicomponent coupled-cluster theory and its application to nanoclusters and molecular systems

Benjamin Harrison Ellis
Syracuse University

Follow this and additional works at: <https://surface.syr.edu/etd>



Part of the [Physical Sciences and Mathematics Commons](#)

Recommended Citation

Ellis, Benjamin Harrison, "Development of multicomponent coupled-cluster theory and its application to nanoclusters and molecular systems" (2016). *Dissertations - ALL*. 572.

<https://surface.syr.edu/etd/572>

This Dissertation is brought to you for free and open access by the SURFACE at SURFACE. It has been accepted for inclusion in Dissertations - ALL by an authorized administrator of SURFACE. For more information, please contact surface@syr.edu.

Abstract

Many theoretical and computational methods are based upon the Born-Oppenheimer approximation. This approximation greatly simplifies the search for a wave function that describes all electrons and nuclei in a chemical system. This is accomplished by assuming that the motion of nuclei and electrons are vastly different; the motion of the two particle types is decoupled. While the BO approximation is ubiquitous in computational and theoretical studies, it is not always justifiable. There are two main cases where this approximation is not valid. The first is when nuclear and electronic motion cannot be decoupled. Decoupling the motion leads to incorrect observations and conclusions drawn. The second case is when a chemical system has more than one type of particle to be treated without the Born-Oppenheimer approximation. For these types of systems, a different and more general interpretation of the Born-Oppenheimer approximation must be made where multiple particle types can be investigated whose motion is not decoupled from one another. In order to investigate systems that are classified in this more inclusive interpretation, new computational theories and methods are needed. To accomplish this task, the multicomponent coupled-cluster method has been developed. In its present form, this new computational method is capable of treating two types of particles without decoupling their motion. The fundamental theories and methods for multicomponent coupled-cluster theory are discussed before the derivation and resulting multicomponent coupled-cluster equations are discussed. This method was then used to study excited electronic states in molecular systems and semiconductor quantum dots via the electron-hole representation. It was also used to calculate ground state energy of the positronium hydride system. These projects sparked further interest in the consequences of the Born-Oppenheimer approximation's application to chemical systems and how it compares to a non Born-Oppenheimer treatment.

DEVELOPMENT OF MULTICOMPONENT
COUPLED-CLUSTER THEORY AND ITS
APPLICATION TO NANOCCLUSERS AND
MOLECULAR SYSTEMS

BY

BENJAMIN H ELLIS

B.S., UNIVERSITY OF WISCONSIN-MADISON, 2011

M.PHIL., SYRACUSE UNIVERSITY, 2013

DISSERTATION SUBMITTED IN PARTIAL FULFILLMENT OF THE REQUIREMENTS
FOR THE DEGREE OF DOCTOR OF PHILOSOPHY IN CHEMISTRY

SYRACUSE UNIVERSITY

DECEMBER 2016

© Copyright by Benjamin H Ellis, 2016.

All rights reserved.

Acknowledgements

First and foremost, I would like to thank my advisor Professor Arindam Chakraborty. Throughout my time in graduate school, Ari has guided my academic growth and inspired me to follow my intellectual passions. I am grateful for his tutelage and support. I may not have fully convinced you on Python just yet, but your time will come!

I also want to thank my parents, Tom and Maureen. They always urged me to follow my passions and to do what I found most interesting in life. They have supported and encouraged me in my journey to graduate school, and continue to do so as I move on to the next phase of my life. Thank you both, so much, for all that you do for me. I am also thankful for the support of my brother, Lann, and sister-in-law, Jackie. They have been great friends, great visitors, and great hosts to me during my years in the program. I also want to thank my girlfriend, Julie, and her family for their support. Thank you to Daisy for being a great companion, hiking buddy, movie enthusiast, and couch potato with me.

I'd like to also thank my lab mates and friends at Syracuse. Specifically I'd like to thank Chris Blanton, Jen Elward, Mike Bayne, and Jeremey Scher. You were all great lab mates. You were all great at providing help on projects when I needed it. More importantly, you all made being in lab fun. I will fondly remember gathering around the coffee pot, excitedly smelling freshly opened beans, and doing our best to play coffee critic.

Let us think the unthinkable, let us
do the undoable, let us prepare to
grapple with the ineffable itself, and
see if we may not eff it after all.

Douglas Adams

Contents

Abstract	i
Acknowledgements	iv
List of Tables	x
List of Figures	xiii
1 Multicomponent systems in chemistry	1
1.1 Introduction	1
1.2 Single component description	2
1.3 Multicomponent description	4
1.3.1 Subatomic particles bound to molecular systems	5
1.3.2 Quasiparticle representation	5
1.3.3 Non Born-Oppenheimer affects	7
1.4 This work	7
2 Single component quantum chemistry	9
2.1 The Hartree-Fock method	10
2.2 Second quantization	16
2.2.1 Creation and annihilation operators	17
2.2.2 Anticommutation relationships	18
2.2.3 Fermi vacuum and normal ordering	20
2.2.4 Wick's theorem	21

2.2.5	Normal ordered Hamiltonian	24
2.2.6	Slater-Condon rules	25
2.3	Configuration interaction theory	26
2.3.1	Full configuration interaction	27
2.3.2	Configuration interaction singles and doubles	29
2.3.3	Consequences of truncating the CI wave function	30
2.3.4	Recent developments in configuration interaction	31
2.4	Coupled-cluster theory	32
2.4.1	Choosing an excitation operator	33
2.4.2	Similarity transformation and the Baker-Campbell-Hausdorff expansion	35
2.4.3	The CCSD equations	36
2.4.4	Size consistency and the CC wave function	38
2.4.5	Relating CC to CI	38
3	Multicomponent methods in quantum chemistry	41
3.1	Multicomponent Hartree-Fock	43
3.1.1	Choice of the multicomponent Fock operator	46
3.2	Multicomponent second quantization	49
3.3	Multicomponent configuration interaction	51
3.3.1	Multicomponent full configuration interaction wave function	52
3.3.2	Truncating the multicomponent configuration interaction wave function	53
4	Multicomponent coupled-cluster theory	55
4.1	Introduction	55
4.2	Theory	60
4.2.1	Construction of the vacuum states	60

4.2.2	Effective normal-ordered Hamiltonian	62
4.2.3	The mcCC Equations	65
4.3	Implementation details	78
4.4	Computational details	82
4.5	Results	82
4.5.1	Model-A single component Hooke's atom	82
4.5.2	Model-B multicomponent Hooke's atom	84
4.5.3	Positronium hydride system	85
4.5.4	Excitonic systems	86
4.5.5	Biexcitonic system	88
4.6	Conclusion	92
4.A	Calculation parameters	93
5	Investigating biexcitons in semiconductor quantum dots	95
5.1	Introduction	95
5.2	Theory	97
5.3	Results	105
5.4	Conclusion	111
5.A	Material and basis parameters	112
6	Applying multicomponent coupled-cluster method to molecular systems	115
6.1	Traditional methods for studying excited electronic states	116
6.1.1	Configuration interaction singles	117
6.1.2	Equation-of-motion coupled-cluster	119
6.1.3	Time dependent Hartree-Fock	120
6.2	Electron-hole representation	124
6.3	Linear response theory	125

6.3.1	Time dependent many body systems	125
6.3.2	General linear response theory	127
6.3.3	Density linear response	129
6.3.4	Perturbation theory approach	131
6.4	Preliminary results	133
7	Investigating mass and confinement effects in multicomponent systems	136
7.1	Introduction	136
7.2	Theory	138
7.2.1	The Born-Oppenheimer Approximation for single component systems	140
7.2.2	The Born-Oppenheimer Approximation for multicomponent systems	143
7.3	Method	147
7.4	Computational details	150
7.5	Results	151
7.6	Conclusion	153
7.A	System parameters	156
8	Conclusion	158
	Bibliography	161
	Curriculum Vitae	180

List of Tables

2.1	Slater-Condon Rules	14
2.2	Number of determinants in the CISD and FCI wave functions.	31
3.1	Type I-II coupling term Slater-Condon Rules	45
4.1	Important properties for systems studied.	83
4.2	Total energy of Model-A Hooke's atom in Hartrees.	84
4.3	Total energy of the Model-B Hooke's atom in Hartrees.	85
4.4	Total energy of positronium hydride (PsH) given in Hartrees.	85
4.5	Total exciton energy calculated from mcHF and correlation energy from mcCCSD, mcCCSD-SD, and mcFCI methods reported in Hartrees as function of k	87
4.6	Exciton binding energy calculated using mcHF, mcCCSD, mcCCSD-SD, and mcFCI methods reported in eV as function of k	88
4.7	Total biexciton energy calculated from mcHF and correlation energy from mcCCSD, mcCCSD-S, mcCCSD-SD, and mcFCI methods reported in Hartrees as function of k	90
4.8	Biexciton binding energy calculated using mcHF, mcCCSD, mcCCSD-S, mcCCSD-SD, and mcFCI methods reported in meV as function of k	91

4.9	Values of the exponents for the [4s4p4d] GTO basis functions (in atomic units) for the Hooke's atom calculations.	93
4.10	Values of the exponents for the [6s3p1d] GTO basis functions (in atomic units) for the positronium hydride (PsH) system.	94
4.11	Values of the exponents for the [spd] GTO basis functions (in atomic units) used for calculating exciton and biexciton binding energies.	94
5.1	Exciton (E_{EB}) and biexciton (E_{BB}) binding energies (meV) calculated using the eh-mcCC method for the set of quantum dots investigated in this work.	106
5.2	Scaling law for exciton binding energies (E_{EB}) for CdSe, CdS, CdTe, and PbS quantum dots	109
5.3	Scaling law for biexciton binding energies (E_{BB}) for CdSe, CdS, CdTe, and PbS quantum dots	110
5.4	Masses (atomic units) for electron and hole and dielectric constant (ϵ) by QD composition	113
5.5	Parameters for the external potential (atomic units) and Gaussian exponent parameter (α) values (atomic units) for the basis per dot diameter (nm)	114
6.1	Multicomponent coupled-cluster excitations energies versus CIS, TDHF, and EOM-CCSD in Hartrees.	135
7.1	Linear fits and RMSE of $\langle V_{e^-,e^-} \rangle$, $\langle V_{e^+,e^+} \rangle$, $\langle V_{e^-,e^+} \rangle$, and $\langle V_{\text{total}} \rangle$ (E_h) versus $\frac{1}{\sqrt{\langle r_{e^+,e^+}^2 \rangle}}$ (au^{-1}) as calculated by mcFCI for the $2e^-, 2e^+$ system.	156
7.2	Linear fits and RMSE of $\langle V_{e^-,e^-} \rangle$, $\langle V_{H,H} \rangle$, $\langle V_{e^-,H} \rangle$, and $\langle V_{\text{total}} \rangle$ (E_h) versus $\frac{1}{\sqrt{\langle r_{H,H}^2 \rangle}}$ (au^{-1}) as calculated by mcFCI for the H_2 system.	156
7.3	Linear fit and RMSE of $\sqrt{\langle r_{e^-,e^-}^2 \rangle}$ (au) versus $\sqrt{\langle r_{x^+,x^+}^2 \rangle}$ (au) as calculated with mcFCI.	157

7.4	Linear fit and RMSE of $\langle V_{e^-,e^-} \rangle (E_h)$ versus $\frac{1}{\sqrt{\langle r_{e^-,e^-}^2 \rangle}}$ (au ⁻¹) as calculated with mcFCI.	157
7.5	External potential (k in atomic units) and Gaussian exponent parameters (α , in atomic units) for each $2e^-$, $2e^+$ and H_2 calculation.	157

List of Figures

1.1	The all electron representation (left) versus the electron-hole representation (right) of an excited electronic state.	6
4.1	Wick's theorem	80
4.2	Many-to-one mapping of the molecular integrals. Set A contains the list of input integrals. Set B is a subset of A that contains the list of non-zero unique integrals. The terms $h_{p_2q_2r_2s_2}$ and $h_{p_3q_3r_3s_3}$ are assumed to have identical numerical values and are mapped to a single term in set B. The term $h_{p_4q_4r_4s_4}$ is assumed to be zero and is not included in set B.	81
4.3	Dependence of exciton binding energy calculated using mcCCSD, mcCCSD-SD, and mcFCI on the strength of the confinement potential.	89
4.4	Dependence of biexciton binding energy calculated using mcCCSD, mcCCSD-S, mcCCSD-SD, and mcFCI on the strength of the confinement potential.	92
5.1	Hugenholtz skeleton diagrams for one-body operators. The square and the dot symbols represent the Hamiltonian and the excitation operators, respectively.	103

5.2	Hugenholtz skeleton diagrams for two-body operators. The square and the dot symbols represent the Hamiltonian and the excitation operators, respectively.	104
5.3	Exciton binding energies (E_{EB}) for CdSe QDs, calculated using eh-mcCC, are compared with other studies by Inamdar <i>et al.</i> , Franceschetti <i>et al.</i> , Wang <i>et al.</i> , Querner <i>et al.</i> , Jasieniak <i>et al.</i> , Kucur <i>et al.</i> , Muelenberg <i>et al.</i> , and Elward <i>et al.</i>	105
5.4	Biexciton binding energies (E_{BB}) for CdSe QDs, calculated using eh-mcCC, are compared to other studies by Sewall <i>et al.</i> , Acherman <i>et al.</i> , Bonati <i>et al.</i> , and Dworak <i>et al.</i>	107
5.5	Exciton binding energy (E_{EB}) vs dot size.	108
5.6	Biexciton binding energy (E_{EB}) vs dot size.	109
5.7	Relative binding energies for CdSe, CdTe, CdS, and PbS quantum dots. The binding energies are normalized with respect to the exciton and biexciton binding energies of the smallest dot, respectively.	110
5.8	Parametric dependence of exciton binding energies (E_{EB}) on biexciton binding energies (E_{BB}) for the set of QDs investigated in this work.	111
7.1	Relationship of potential electron-electron, electron-positron, and positron-positron potential energies versus the average positron-positron distance.	153
7.2	Relationship of potential electron-electron, electron-hydrogen, and hydrogen-hydrogen potential energies versus the average hydrogen-hydrogen distance.	153
7.3	Inverse relationship of potential electron-electron, electron-positron, and positron-positron potential energies versus the average positron-positron.	154

7.4	Inverse relationship of potential electron-electron, electron-hydrogen, and hydrogen-hydrogen potential energies versus the average hydrogen-hydrogen distance.	154
7.5	Average positron-positron and hydrogen-hydrogen distance versus average electron-electron distance.	155
7.6	Average electron-electron potential energy versus the average electron-electron separation distance in the $2e^+$, $2e^-$ and H_2 systems.	155

Chapter 1

Multicomponent systems in chemistry

1.1 Introduction

The overarching goal of theoretical chemistry is to mathematically describe chemical and physical properties of chemical systems. Theoretical investigations into chemical systems have been used to explain thermodynamic and electronic properties, as well as study the spatial arrangement of atoms in a system. The field is continually growing by refining methodology, providing more and more accurate results, and by being applied to larger and more complex chemical systems.

Theoretical chemistry has many tools at its disposal to study chemical systems. The work discussed in this thesis will focus on methods that employ a wave function to describe chemical systems. A wave function is a mathematical object that describes the state of a chemical system, with dependence on the coordinates of every particle within that system. The wave function is then solved for using the Schrödinger equation. This equation has a Hamiltonian operator, which calculates the kinetic and potential energy terms of every particle in the system, operating on the wave

function and yielding energy times that wave function back,

$$H\Psi^{\text{exact}} = E\Psi^{\text{exact}}. \quad (1.1)$$

Solving this eigenvalue problem for a molecular system is a very difficult task. The nuclear and electronic particles are in constant motion. On top of that, the positions of electrons and nuclei are correlated; the electrons repel one another, while simultaneously being attracted to the nuclei. The same is true for the nuclei - these particles repel one another but are attracted to the negatively charged electrons.

Solving the Schrödinger equation in the current form proves to be an incredibly difficult task. For molecular systems, alleviating the complexity of the problem comes in the form of the Born-Oppenheimer approximation. This approximation is one of the most important approximations in the field and has been the foundation of many quantum chemical methodologies and investigations since its institution in 1927[1]. The next section, [section 1.2](#), will qualitatively describe the BO approximation and how it relates to quantum chemistry and the molecular Schrödinger equation. While this section will highlight the utility of the BO approximation, it is not universally applicable. There are systems where the BO approximation is invalid, and these will be introduced in [section 1.3](#).

1.2 Single component description

The exact wave function for a chemical system with two particle types (electrons and nuclei) is defined as,

$$\Psi^{\text{exact}}(\mathbf{r}, \mathbf{R}) = \sum_i \sum_j w_{i,j} \Psi_i^e(\mathbf{r}, \mathbf{R}) \Psi_j^N(\mathbf{R}). \quad (1.2)$$

In the above equation, \mathbf{r} are the electronic coordinates while \mathbf{R} are the nuclear coordinates. Substituting this form of the wave function into the Schrödinger equation produces a prohibitively complex problem to solve. The BO approximation simplifies the description of a chemical system by treating the motion of nuclei and electrons independently. Using this approach allows the exact wave function be approximated as

$$\Psi^{\text{exact}}(\mathbf{r}, \mathbf{R}) \approx \Psi^e(\mathbf{r}; \mathbf{R})\Psi^N(\mathbf{R}). \quad (1.3)$$

We can see that the electronic wave function is now only parametrically dependent on the nuclear coordinates, whereas in the exact wave function it was explicitly dependent. The electronic wave function is said to be single component now due to the fact that there is explicit dependence on a single particle type (the electrons). This approximation is justified later in [subsection 7.2.1](#).

The BO approximation has been used to great effect for studying both electronic and nuclear properties of chemical systems. Solution to the single component Schrödinger equation provides details about spectroscopic data [2, 3, 4, 5, 6, 7], molecular structure [8, 9, 10, 11, 12, 13], electron affinities and ionization potentials [14, 15, 16, 17, 18], excitation energies [19, 20, 21, 22], and so on.

Unfortunately, while the BO approximation has proven itself to be very useful, it is not without flaws. The most common interpretation identifies the particles as either electrons or nuclei (or in other language BO separated and non BO separated). While a vast majority of chemical systems fit this classification nicely, or can be abstracted to be described as such, it is not all-encompassing. Systems that cannot fit this description require that the wave function be augmented to encompass more particle types or for systems where the nuclear and electronic motion is not decoupled.

1.3 Multicomponent description

The exact wave function for a chemical system with three types of distinct particles is defined as,

$$\Psi^{\text{exact}}(\mathbf{r}^{\text{I}}, \mathbf{r}^{\text{II}}, \mathbf{R}^{\text{N}}) = \sum_i \sum_j w_{i,j} \Psi_i^{\text{I,II}}(\mathbf{r}^{\text{I}}, \mathbf{r}^{\text{II}}, \mathbf{R}^{\text{N}}) \Psi_j^{\text{N}}(\mathbf{R}^{\text{N}}). \quad (1.4)$$

This exact wave function is written to be more general in there are type I, type II and nuclei. An appropriate Hamiltonian will be defined that accounts for the extra potential and kinetic energies due to the addition of the type II particles. The form of this Hamiltonian is discussed in a later chapter. Solving for this wave function is an even more complicated process given the addition of extra particle types.

The BO approximation can be extended to this wave function by assuming that the motion of the nuclear particles is decoupled from that of type I and type II bodies. This interpretation of the BO approximation is defined below,

$$\Psi^{\text{exact}}(\mathbf{r}^{\text{I}}, \mathbf{r}^{\text{II}}, \mathbf{R}^{\text{BOS}}) \approx \Psi^{\text{I,II}}(\mathbf{r}^{\text{I}}, \mathbf{r}^{\text{II}}; \mathbf{R}^{\text{BOS}}) \Psi^{\text{BOS}}(\mathbf{R}^{\text{BOS}}). \quad (1.5)$$

Note that the particle types need not be nuclei or electrons but instead are generally defined as type I, type II, and BOS as this wave function can be applied to many types of multicomponent systems.

Using the multicomponent wave function is a very useful computational tool for investigating many interesting chemical systems. It can be used to investigate subatomic particles (such as positron or muon) bound to molecules, study excited electronic states, and include nuclear motions in the electronic wave function.

1.3.1 Subatomic particles bound to molecular systems

While it is not thought of as a typical chemical system, subatomic particles like positron and muon can bind to molecular systems. Positrons have the identical mass and spin of an electron (1 atomic unit and $\frac{1}{2}$) but have a +1 atomic unit charge. When electrons and positrons collide, they annihilate one another, emitting high energy electromagnetic radiation.

Understanding how these particles interact with molecular systems will help to explain the fundamental properties of matter and physical laws in the universe. Positrons and their interactions with electrons are used in spectroscopic applications. Positron emission tomography is a biological imaging technique that can be used to study and identify abnormalities and processes in living subjects [23, 24, 25, 26, 27]. Positron-based spectroscopic techniques are also used by material scientists to study defects of solids [28, 29, 30, 31].

In [chapter 4](#), a multicomponent study on positronium hydride (a positron bound to hydride) is presented.

1.3.2 Quasiparticle representation

Multicomponent wave functions can also be used to investigate electronically excited states. This fits into the multicomponent point of view by using the electron-hole representation of excitations. The electron-hole representation is an exact mathematical transformation that greatly simplifies an all-electron picture to the number of excited electrons and positively charged holes they leave behind. This quasiparticle transformation is well known and widely used in quantum chemistry and physics [32, 33].

In [Figure 1.1](#), the single component (all electron) and multicomponent representation are shown in a diagram. We see that on the left, all electrons in a system are considered when the excitation is investigated. In contrast, on the right, the

only electron considered is the one excited into the virtual states (states above the occupation level). We see that a hole quasiparticle is left behind, which must be considered in any theoretical treatment. This representation removes the complexity of considering all electrons, but inherits a different complexity in that multiple particle types, as well as the interactions between same type particles and different particle types, must now be accounted for. Higher order excitations can also be treated with the electron-hole representation.

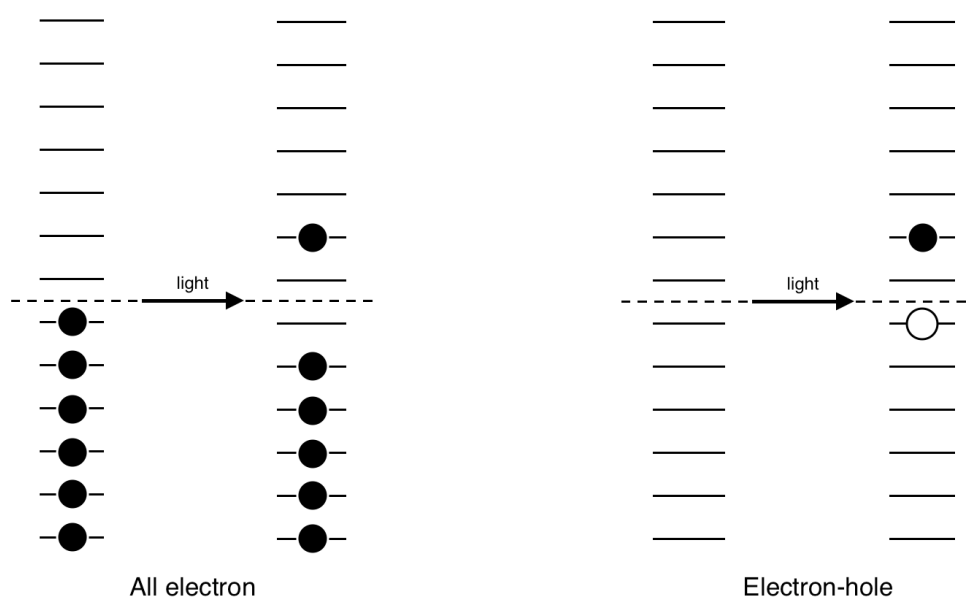


Figure 1.1: The all electron representation (left) versus the electron-hole representation (right) of an excited electronic state.

The electron-hole representation is often used to study excited states of systems with vast numbers of electrons such include bulk metals and semiconductor nanocrystals [34, 35, 36, 37, 38, 39, 40, 41, 42, 43, 44, 45, 46]. The research presented in this thesis was heavily influenced and inspired by the ability to study multiple excitations in semiconductor nanocrystals as they exhibit very interesting and highly tunable electronic and optical properties. In [chapter 4](#) and [chapter 5](#), investigations into these types of systems are presented.

1.3.3 Non Born-Oppenheimer affects

The multicomponent wave function can also be used to investigate non Born-Oppenheimer affects. In the single component representation, all nuclei are treated as fixed in space. There are several examples where nuclear motion is an important feature of chemical processes and properties of a system. Proton-coupled electron-transfer reactions are a great example where an electron and proton are transferred in a reaction nearly simultaneously [47, 48, 49, 50, 51, 52]. This process would be misrepresented with the BO approximation since the proton motion happens on a similar timescale to that of the electron. Proton tunneling is another example where the motion of a nuclear body cannot be ignored [53, 54, 55, 56, 57].

Motion of nuclear bodies can be treated in the multicomponent framework and presents a large amount of potential application projects for multicomponent methods. While the work in this thesis was mainly motivated by investigating electron-hole systems, some preliminary work on nuclear-electron studies was also done and is presented in [chapter 7](#).

1.4 This work

The work presented here involved using existing computational methods, and more specifically developing new ones, to study chemical systems where the BO approximation is inadequate. Before the studies are specifically discussed, the computational tools will be presented. Since approximate methods to solve the multicomponent Schrödinger equation is closely tied to the those that solve the single component Schrödinger equation, the single component methods will be briefly surveyed. These methods are the Hartree-Fock method, configuration interaction, and coupled-cluster. These single component theories are briefly surveyed in [chapter 2](#). Next, the multicomponent extensions of Hartree-Fock and configuration interaction will then be

discussed in [chapter 3](#). In the following chapter, the multicomponent coupled-cluster method will be derived and detailed in depth. This method was specifically developed over the past four years to study complex, multicomponent systems. As stated earlier, this method was then used to study positron-bound systems ([chapter 4](#)) and excited electronic states in both molecular systems and semiconductor quantum dots ([chapter 4](#) and [chapter 5](#)). This project also sparked curiosities about implications of the BO approximation and binding behavior of chemical systems treated without the BO approximation which is discussed in [chapter 7](#).

Chapter 2

Single component quantum chemistry

Single component, or electronic structure, theory is focused on finding solutions to the electronic wave function. We use the term single component here as a way of highlighting the fact that the electronic wave function only has explicit dependence on one particle type (the electrons). The wave function maintains parametric dependence on nuclei in the system. This is a result of invoking the Born-Oppenheimer approximation, which is detailed in [subsection 7.2.1](#). The Schrödinger equation for a single component system is defined as,

$$H^e \Psi^e(\mathbf{r}; \mathbf{R}) = E^e \Psi^e(\mathbf{r}; \mathbf{R}) \quad (2.1)$$

with the Hamiltonian being,

$$H^e = T^e(\mathbf{r}) + V^{e,N}(\mathbf{r}; \mathbf{R}) + V^{e,e}(\mathbf{r}). \quad (2.2)$$

The operators in the Hamiltonian calculate the kinetic, electron-nuclear, and electron-electron energies in the system.

Solutions for the electronic wave function give important information about chemical reactivity and properties. This chapter will introduce and discuss a select few explicit forms of the electronic wave function. These are the Hartree-Fock, configuration interaction, and coupled-cluster ansatz. The Hartree-Fock will be introduced first in [section 2.1](#) as it the basis of many other approximate wave functions, including configuration interaction and coupled-cluster. The forms of the configuration interaction ([section 2.3](#)) and coupled-cluster ([section 2.4](#)) wave functions will be detailed as well. They are significantly more complicated than that of the Hartree-Fock method. In general, these method are much more accurate, but are more computationally expensive and have other trade-offs which will be discussed.

2.1 The Hartree-Fock method

Electronic structure theory attempts to solve the electronic Schrödinger equation, [Equation 2.1](#). The research discussed in this dissertation expands the scope of electronic structure theory to encompass other particle types. Before that work is discussed, electronic structure theory will be presented so we have a foundation to build upon.

The terms of electronic Hamiltonian (which is now simply written as H instead of H^e) from [Equation 2.2](#) will be shortened to

$$H = H^{\text{core}} + V \tag{2.3}$$

where H^{core} is the one body operator,

$$H^{\text{core}} = -\frac{\hbar}{2m^e} \sum_i^N \nabla_i^2 - \sum_i^N \sum_A^M \frac{Z_A}{r_{iA}} \tag{2.4}$$

and V is the two body operator,

$$V = \sum_{i < j}^N \sum_j^N \frac{1}{r_{ij}}. \quad (2.5)$$

The electronic wave function depends explicitly on the coordinates of electrons. The coordinates of electrons are both their three-dimensional orientation and spin.

$$\mathbf{x} = \{\mathbf{r}, \omega\} \quad (2.6)$$

The electronic wave function, Φ^e , depends on the spatial-spin coordinates of all electrons in the system, $\Phi^e(\mathbf{x}_1, \mathbf{x}_2, \dots, \mathbf{x}_N)$. Including the spin in the coordinates is important because it will let us enforce the antisymmetry principle which states that interchange of any two electronic spatial-spin coordinates corresponds to a change in sign of the wave function.

$$\Phi^e(\dots, \mathbf{x}_i, \dots, \mathbf{x}_j, \dots) = -\Phi^e(\dots, \mathbf{x}_j, \dots, \mathbf{x}_i, \dots) \quad (2.7)$$

Requiring the wave function to be antisymmetric increases the complexity of the Schrödinger equation. We now must satisfy the eigenvalue problem with an eigenfunction that is antisymmetric.

Constructing an antisymmetric wave function will be approached from the bottom up. Ultimately, all of the wave functions discussed in this work will consist of at least one Slater determinant. Slater determinants are constructed from orbitals, which are single particle wave functions. A molecular orbital is a function of the spatial-spin

coordinates of a single electron and is shown in [Equation 2.8](#).

$$\chi(\mathbf{x}) = \begin{cases} \psi(\mathbf{r})\alpha(\omega) \\ \text{or} \\ \psi(\mathbf{r})\beta(\omega) \end{cases} \quad (2.8)$$

Molecular orbitals have dependence on spatial and spin functions which are ψ and α/β , respectively. The α and β functions are the two distinct S_z spin contributions an electron can have. The spatial and spin components of the molecular orbitals are orthonormal, thus molecular orbitals are orthonormal.

$$\int d\mathbf{r}\psi_i^*(\mathbf{r})\psi_j(\mathbf{r}) = \delta_{ij} \quad (2.9)$$

$$\int d\omega\alpha^*(\omega)\alpha(\omega) = \int d\omega\beta^*(\omega)\beta(\omega) = 1 \quad (2.10)$$

$$\int d\omega\alpha^*(\omega)\beta(\omega) = \int d\omega\beta^*(\omega)\alpha(\omega) = 0 \quad (2.11)$$

$$\int d\mathbf{x}\chi_i^*(\mathbf{x})\chi_j(\mathbf{x}) = \delta_{ij} \quad (2.12)$$

It is more convenient to use Dirac notation, so the orthonormal relationships can be expressed as

$$\langle\psi_i|\psi_j\rangle = \delta_{ij} \quad (2.13)$$

$$\langle\alpha|\alpha\rangle = \langle\beta|\beta\rangle = 1 \quad (2.14)$$

$$\langle\alpha|\beta\rangle = \langle\beta|\alpha\rangle = 0 \quad (2.15)$$

$$\langle\chi_i|\chi_j\rangle = \delta_{ij}. \quad (2.16)$$

Dirac notation used for the overlap integrals will also be used to when evaluating the one and two body molecular integrals from the Hamiltonian. They have the general

form,

$$\langle p | h^{\text{core}} | q \rangle = \int d\mathbf{x}_1 \chi_p^*(\mathbf{x}_1) h^{\text{core}} \chi_q(\mathbf{x}_1) \quad (2.17)$$

$$\langle pq | v | rs \rangle = \int d\mathbf{x}_1 d\mathbf{x}_2 \chi_p^*(\mathbf{x}_1) \chi_q^*(\mathbf{x}_2) r_{12}^{-1} \chi_r(\mathbf{x}_1) \chi_s(\mathbf{x}_2) \quad (2.18)$$

The form of these functions is general though and can be extended to other one or two body integrals. From this point on, Dirac notation will be the preferred notation.

Slater determinants are then constructed from these molecular orbitals. A Slater determinant will enforce the antisymmetry principle for electronic wave functions due to the properties of determinants. Interchanging any two columns would flip the sign of the determinant. It is shown below, with a normalization factor of $\frac{1}{\sqrt{N!}}$,

$$\Phi_{\text{SD}}(\mathbf{x}_1, \mathbf{x}_2, \dots, \mathbf{x}_N) = \frac{1}{\sqrt{N!}} \begin{vmatrix} \chi_1(\mathbf{x}_1) & \chi_2(\mathbf{x}_1) & \dots & \chi_N(\mathbf{x}_1) \\ \chi_1(\mathbf{x}_2) & \chi_2(\mathbf{x}_2) & \dots & \chi_N(\mathbf{x}_2) \\ \vdots & \vdots & \ddots & \vdots \\ \chi_1(\mathbf{x}_N) & \chi_2(\mathbf{x}_N) & \dots & \chi_N(\mathbf{x}_N) \end{vmatrix}. \quad (2.19)$$

Dirac notation also provides a shorthand notation for writing Slater determinants with the normalization factor included,

$$\Phi_{\text{SD}}(\mathbf{x}_1, \mathbf{x}_2, \dots, \mathbf{x}_N) = |\chi_i(\mathbf{x}_1) \chi_j(\mathbf{x}_2) \dots \chi_k(\mathbf{x}_N)\rangle \quad (2.20)$$

$$= |ij \dots k\rangle. \quad (2.21)$$

This simplified notation for Slater determinants will be used extensively.

Next, we must introduce how to compute elements of the Hamiltonian with respect to a given Slater determinant. These rules are outlined in [Table 2.1](#). These rules are for evaluating elements between determinants that have all the same orbitals occupied, have one noncoincidence, or two noncoincidences. All other terms are rigorously

zero. Note that the subscript A is for the antiymmetrized two body integral, which is required by the wave function [58]. It is defined as,

$$\langle pq|v|pq\rangle_A = \langle pq|v|pq\rangle - \langle pq|v|qp\rangle. \quad (2.22)$$

Table 2.1: **Slater-Condon Rules** [58]

Case 1: $ K\rangle = \dots ij\dots\rangle$	
$\langle K H^{\text{core}} K\rangle = \sum_i^N \langle i h^{\text{core}} i\rangle$	$\langle K V K\rangle = \sum_{i<j}^N \langle ij v ij\rangle_A$
Case 2: $ K\rangle = \dots ij\dots\rangle$ $ L\rangle = \dots aj\dots\rangle$	
$\langle K H^{\text{core}} L\rangle = \langle i h^{\text{core}} a\rangle$	$\langle K V L\rangle = \sum_j^N \langle ij v aj\rangle_A$
Case 3: $ K\rangle = \dots ij\dots\rangle$ $ L\rangle = \dots ab\dots\rangle$	
$\langle K H^{\text{core}} L\rangle = 0$	$\langle K V L\rangle = \langle ij v ab\rangle_A$

The Hartree-Fock (HF) method is one of the most widely used computational methods for solving the Schrödinger equation. In this section, the major points of the method will be surveyed. The HF method finds a solution for the wave function by minimizing energy with respect to a single Slater determinant,

$$E^{\text{HF}} = \langle \Phi|H|\Phi\rangle \quad (2.23)$$

$$= \sum_i^N \langle i|h^{\text{core}}|i\rangle + \sum_{i<j}^N \langle ij|v|ij\rangle_A \quad (2.24)$$

$$\frac{\partial E^{\text{HF}}}{\partial \chi_i} = 0. \quad (2.25)$$

In the expectation value calculation of energy, the h^{core} term is the one-body contributions from H and the V term is the antisymmetrized two-electron integral. Minimiz-

ing energy with respect to the molecular orbitals is done by minimizing the coefficients of individual basis functions in the (unique) spatial portions of each molecular orbital. Each spatial wave function can be expanded into a linear combination of K (theoretically this would be infinite, but a finite expansion is used) basis functions.

$$\psi_i(\mathbf{r}) = \sum_{\mu}^K C_{\mu i} \gamma(\mathbf{r}) \quad (2.26)$$

The coefficients are minimized via the HF equation,

$$f |\chi_i\rangle = \epsilon_i |\chi_i\rangle \quad (2.27)$$

where the Fock operator, f , has the following form,

$$f = h^{\text{core}} + v_{\text{HF}} \quad (2.28)$$

$$= h^{\text{core}} + \sum_j J_j - K_j. \quad (2.29)$$

The J and K terms are the Coulomb and exchange operators, respectively,

$$J_j \chi_i(\mathbf{x}_1) = \left[\int d\mathbf{x}_2 \chi_j^*(\mathbf{x}_2) \frac{1}{r_{12}} \chi_j(\mathbf{x}_2) \right] \chi_i(\mathbf{x}_1) \quad (2.30)$$

$$K_j \chi_i(\mathbf{x}_1) = \left[\int d\mathbf{x}_2 \chi_j^*(\mathbf{x}_2) \frac{1}{r_{12}} \chi_i(\mathbf{x}_2) \right] \chi_j(\mathbf{x}_1). \quad (2.31)$$

Now, by combining unique spatial contributions to each molecular orbital, we can rewrite the Hartree-Fock equation in terms of the basis via [Equation 2.26](#) for each unique spatial orbital ψ_i ,

$$f \sum_{\nu} C_{\nu i} \gamma_{\nu} = \epsilon_i \sum_{\nu} C_{\nu i} \gamma_{\nu}. \quad (2.32)$$

Left multiplying this equation by γ_μ^* and integrating over all space yields

$$\sum_{\nu} C_{\nu i} \underbrace{\int \gamma_{\nu}^* f \gamma_{\nu}}_{F_{\mu\nu}} = \epsilon_i \sum_{\nu} C_{\nu i} \underbrace{\int \gamma_{\mu}^* \gamma_{\nu}}_{S_{\mu\nu}} \quad (2.33)$$

$$\mathbf{FC} = \mathbf{SC}\epsilon. \quad (2.34)$$

With this final step, the Fock equation has been transformed into a matrix eigenvalue problem which can be solved using linear algebra techniques. The equation is then be solved self-consistently to optimize the Hartree-Fock wave function[58, 59].

The HF method is a tremendously useful computational tool. The problem is that the HF wave function can be inadequate to describe chemical systems. Remembering that the exact wave function is an infinite expansion of all possible states, it becomes apparent that using a single Slater determinant (even a highly optimized one), is a significant abstraction from the exact wave function because correlation effects are not accounted for. Other theories, such as configuration interaction and coupled-cluster, use many Slater determinants to describe the wave function. These theories will be discussed after second quantization is introduced.

2.2 Second quantization

Second quantization is a widely used mathematical formulation for many-body problems in quantum chemistry and quantum physics [60, 32, 59]. This representation is particularly useful when the number of particles in a system is unknown or ambiguous; however, the this work focuses on systems with fixed numbers of particles. In this work, second quantization will be heavily used because it enables operators in the Hamiltonian and the wave function to be manipulated efficiently and expressively. It is important to note that the formulations presented will apply to fermions.

That is, the wave function is taken to be antisymmetric. It is constructed from Slater determinants which consist of single particle basis functions as described earlier.

2.2.1 Creation and annihilation operators

To begin, we will discuss how second quantized creation and annihilation operators affect the Slater determinants from which the wave function is constructed. A creation operator, which will be denoted with a dagger, places a particle into the Slater determinant into a given spin orbital while an annihilation operator will remove a particle from a given spin orbital

$$i^\dagger |jk \dots z\rangle = |ijk \dots z\rangle, \quad (2.35)$$

$$i |ijk \dots z\rangle = |jk \dots z\rangle. \quad (2.36)$$

It's also important to note that a particle cannot be created in a spin orbital where one already exists and annihilation cannot occur on an orbital that is unoccupied (absent) from the determinant,

$$i^\dagger |ijk \dots z\rangle = i |jk \dots z\rangle = 0. \quad (2.37)$$

Second quantization also enforces the antisymmetry principle of the wave function. Creation and annihilation operations occur at the beginning of the Slater determinant. After the operation occurs, the determinant is lexically ordered and is accompanied with an appropriate sign based on the parity of the permutation (η_P),

$$p^\dagger |ijk \dots z\rangle = (-1)^{\eta_P} |ijk \dots p \dots z\rangle, \quad (2.38)$$

$$p |ijk \dots p \dots z\rangle = (-1)^{\eta_P} |ijk \dots z\rangle. \quad (2.39)$$

Slater determinants can also be written as a series of creation operations on the physical vacuum state (denoted by $|\rangle$),

$$i^\dagger j^\dagger k^\dagger \dots z^\dagger |\rangle = |ijk\dots z\rangle. \quad (2.40)$$

2.2.2 Anticommutation relationships

Second quantized operators obey a set of anticommutation relationships. These rules govern how groups of SQ operators behave. First we will look at how two creation operators behave. The operations give two possibilities,

$$p^\dagger q^\dagger |ijk\dots\rangle = |pqijk\dots\rangle \quad (2.41)$$

$$q^\dagger p^\dagger |ijk\dots\rangle = |qpijk\dots\rangle = -|pqijk\dots\rangle. \quad (2.42)$$

We see that the two Slater determinants differ in sign, thus

$$p^\dagger q^\dagger = -p^\dagger q^\dagger \quad (2.43)$$

$$[p^\dagger, q^\dagger]_+ = p^\dagger q^\dagger + q^\dagger p^\dagger = 0. \quad (2.44)$$

In the above expression, the $[A, B]_+$ notation is the anticommutator relationship

$$[A, B]_+ = AB + BA \quad (2.45)$$

$$[A, B]_+ = [B, A]_+. \quad (2.46)$$

It is important to note that the above relationship is also zero if either orbitals p or q are already occupied in the Slater determinant, or if $p = q$.

The next case to consider is two annihilation operators,

$$pq|qpijk\dots\rangle = p|pijk\dots\rangle = |ijk\dots\rangle \quad (2.47)$$

$$qp|qpijk\dots\rangle = -qp|pqijk\dots\rangle = -|qijk\dots\rangle = -|ijk\dots\rangle. \quad (2.48)$$

Once again, it is shown that the same determinant is generated, with a different sign, thus

$$pq = -qp \quad (2.49)$$

$$[p, q]_+ = 0. \quad (2.50)$$

Additionally, if the orbitals p or q do not exist in the determinant, or $p = q$, the relationship also resolves to zero.

The third case to consider is one creation and one annihilation operators. In these cases, one orbital is replaced by another according to the operators,

$$p^\dagger q |ijk\dots q\dots\rangle = |ijk\dots p\dots\rangle \quad (2.51)$$

$$qp^\dagger |qijk\dots\rangle = q|pqijk\dots\rangle = -q|qpijk\dots\rangle = -|pijk\dots\rangle \quad (p \neq q). \quad (2.52)$$

Once again, the same Slater determinant has been generated differing in sign, giving

$$[p^\dagger, q]_+ = 0 \quad (2.53)$$

for the case when $p \neq q$. When $p = q$, the relationship becomes (with p in the Slater determinant)

$$p^\dagger p |pijk\dots\rangle = |pijk\dots\rangle \quad (2.54)$$

$$pp^\dagger |pijk\dots\rangle = 0 \quad (2.55)$$

and (with p not in the Slater determinant)

$$p^\dagger p |ijk\dots\rangle = 0 \quad (2.56)$$

$$pp^\dagger |ijk\dots\rangle = |ijk\dots\rangle. \quad (2.57)$$

The anticommutator relationship for these cases is then

$$[p^\dagger, q]_+ = [q, p^\dagger]_+ = 1. \quad (2.58)$$

This relationship is broadly defined as

$$[p^\dagger, q]_+ = [q, p^\dagger]_+ = \delta_{pq} \quad (2.59)$$

to encompass both cases for $p = q$ and $p \neq q$.

2.2.3 Fermi vacuum and normal ordering

Manipulating strings of SQ operators will be introduced as it applies to the Fermi vacuum. The Fermi vacuum is a more convenient formalism to use for many particle systems as all other Slater determinants will be described relative to it. It may also be referred to as the reference state and is denoted by $|0\rangle$. This is usually taken to be the Hartree-Fock Slater determinant. Using the Fermi vacuum also introduces the particle-hole formalism. Hole states will be described by indices i, j, k, \dots while particle states will be described by a, b, c, \dots . Letters p, q, r, s, \dots can be used to describe either particle or hole states, depending on the context. Hole states are used to describe an orbital in the reference state from which an excitation occurs and particle states are the orbital where the electron is excited to. Examples of single and

double excitations are shown below (with $|0\rangle = |ijk\dots\rangle$),

$$|_i^a\rangle = a^\dagger i|0\rangle = |ajk\dots\rangle \quad (2.60)$$

$$|_{ij}^{ab}\rangle = a^\dagger b^\dagger ji|0\rangle = |abk\dots\rangle. \quad (2.61)$$

We see that any determinant can be described by some set of operators and the Fermi vacuum state.

SQ operators can be easily manipulated if they are normal ordered. When normal ordering operators with respect to the Fermi vacuum state, one must consider what state is being created and what state is being destroyed. In general, normal ordering moves creation and annihilation operators to the left or the right, depending on whether the operators are particle or hole operators. This is accomplished using the anticommutation relationships which were derived above. Normal ordering of hole states requires that all creation operators are moved to the left of all annihilation operators. For particle states, all annihilation operators must be to the left of creation operators. Normal ordering plays an important part when evaluating matrix elements in SQ notation. Operators that are in normal order will be in curly braces $\{AB\dots\}$. An important property of normal ordering is that the expectation values of normal ordered operators with respect to the Fermi vacuum state is zero,

$$\langle 0|\{ABC\dots\}|0\rangle = 0. \quad (2.62)$$

This property will be used extensively used in derivations presented here.

2.2.4 Wick's theorem

Computing elements of the Hamiltonian represented using SQ notation can be a very difficult task. Wick's theorem outlines how to handle this this task succinctly and

expediently. This is accomplished using what are called Wick's contractions. These contractions rely on the anticommutation relationships (which were previously derived and are summarized below) and normal ordering of SQ operators,

$$pq + qp = 0, \quad (2.63)$$

$$p^\dagger q^\dagger + q^\dagger p^\dagger = 0, \quad (2.64)$$

$$p^\dagger q + qp^\dagger = \delta_{pq}. \quad (2.65)$$

These rules will now be used to define normal products of SQ operators when computing expectation values of vacuum states. Creating normal products of SQ operators uses the anticommutation relationships to move all creation operators to the left of annihilation operators. The following example highlights how this is done,

$$pq^\dagger = [p, q^\dagger]_+ - q^\dagger p = \delta_{pq} - q^\dagger p. \quad (2.66)$$

This process used the anticommutation definition which resulted in the appearance of the delta function and the normal ordered product of pq^\dagger which is $-q^\dagger p$. Putting SQ operators in normal product form is useful as the expectation value with respect to the vacuum state will be zero.

With the vacuum state to which we relate to, we can now begin to discuss Wick's theorem by introducing a contraction. We define a contraction to be

$$\overline{AB} = AB - \{AB\} \quad (2.67)$$

where the operators in the curly braces are normal ordered. Given this relationship, the only contractions to be considered are Using the contractions defined above, it is possible normal order any set of SQ operators in a quick, succinct manner. When

contractions happen relative to the vacuum state, the only nonzero terms are

$$\overline{i^\dagger j} = i^\dagger j - \{i^\dagger j\} = i^\dagger j + j i^\dagger = \delta_{ij}, \quad (2.68)$$

$$\overline{ab^\dagger} = ab^\dagger - \{ab^\dagger\} = ab^\dagger + b^\dagger a = \delta_{ab} \quad (2.69)$$

For particle and hole operators. When the general indices (p, q, r, s, \dots) are considered the above relationship is obeyed,

$$\overline{i^\dagger q} = \delta_{iq} \quad (2.70)$$

$$\overline{p^\dagger j} = \delta_{pj} \quad (2.71)$$

$$\overline{ap^\dagger} = \delta_{ap} \quad (2.72)$$

$$\overline{qb^\dagger} = \delta_{qb}. \quad (2.73)$$

These relationships are important when using operators in SQ notation, which is discussed in the next section.

Wick's theorem then enables us to write the linear combinations of Kronecker delta functions and normal ordered SQ operators using contractions. This is generally expressed as follows,

$$\begin{aligned} ABC \dots XYZ \dots &= \{ABC \dots XYZ \dots\} \\ &+ \sum_{\text{singles}} \left\{ \overline{ABC \dots XYZ \dots} \right\} \\ &+ \sum_{\text{doubles}} \left\{ \overline{\overline{ABC \dots XYZ \dots}} \right\} + \dots \end{aligned} \quad (2.74)$$

where summation of contractions continues until all operators are contracted. This theorem also holds true for products of normal ordered operators since $\{ABC \dots\} \{XYZ \dots\} = \{ABC \dots XYZ \dots\}$. Wick's theorem is so powerful because it allows us to immediately identify which terms will equate to zero when

calculating expectation values with respect to the Fermi vacuum. An operator expectation value with respect to the Fermi vacuum will be zero unless all SQ operators are fully contracted,

$$\langle 0|A\dots B\dots C\dots D\dots|0\rangle = \sum \langle 0|\overbrace{A\dots B\dots C\dots D\dots}^{\text{fully contracted}}|0\rangle. \quad (2.75)$$

2.2.5 Normal ordered Hamiltonian

Now that properties of SQ operators and their relationship to the Fermi vacuum have been defined, we will define the Hamiltonian in SQ notation as

$$H = \sum_{pq} \langle p|h|q\rangle p^\dagger q + \frac{1}{4} \sum_{pqrs} \langle pq|v|rs\rangle_A p^\dagger q^\dagger sr. \quad (2.76)$$

Using Wick's theorem, the Hamiltonian can be normal ordered to give

$$\begin{aligned} H &= \sum_{pq} \langle p|h|q\rangle \{p^\dagger q\} + \sum_{pri} \langle pi|v|ri\rangle_A \{p^\dagger r\} + \frac{1}{4} \sum_{pqrs} \langle pq|v|rs\rangle_A \{p^\dagger q^\dagger sr\} \\ &+ \sum_i \langle i|h|i\rangle + \frac{1}{2} \sum_{ij} \langle ij|v|ij\rangle_A \end{aligned} \quad (2.77)$$

$$= \sum_{pq} \langle p|f|q\rangle \{p^\dagger q\} + \frac{1}{4} \sum_{pqrs} \langle pq|v|rs\rangle_A \{p^\dagger q^\dagger sr\} + \langle 0|H|0\rangle. \quad (2.78)$$

We can see that normal ordering reproduces the Hartree-Fock energy expression from the previous expression, $\langle \Phi|H|\Phi\rangle$, with the addition of other terms that did not contribute to that expression, but will in others. Also note that the Fock operator has been defined in SQ notation during the process of normal ordering of the Hamiltonian and that the asymmetric two body integrals evolved naturally. The normal ordered

Hamiltonian is often written as

$$H = F_N + V_N + \langle 0 | H | 0 \rangle \quad (2.79)$$

$$H = H_N + \langle 0 | H | 0 \rangle, \quad (2.80)$$

for convenience.

Normal ordering the Hamiltonian is a very useful mathematical tool because the expectation value of a normal ordered operator, with respect to the vacuum state, will always resolve to zero [60, 61],

$$\langle 0 | H_N | 0 \rangle = 0. \quad (2.81)$$

This relationship will come up again when deriving the coupled-cluster equations later this chapter in [section 2.4](#) and again in [chapter 4](#).

2.2.6 Slater-Condon rules

Using SQ notation, it is also possible to derive expressions for the matrix elements between Slater determinants. The derivation of these expressions is somewhat laborious as strings of SQ operators are written out, all possible full contractions are made, and resulting expressions are summed to give a final expression. Many times, the number of contractions is quite large (especially with two body operators), so these contractions are often done by computer. The resulting expressions were summarized in [Table 2.1](#).

An illustrative derivation of a one-body matrix element is shown,

$$\langle 0 | h |_i^a \rangle = \sum_{pq} \langle p | h | q \rangle \langle 0 | \{p^\dagger q\} \{a^\dagger i\} | 0 \rangle \quad (2.82)$$

$$= \sum_{pq} \langle p | h | q \rangle \langle 0 | \overbrace{\{p^\dagger q\} \{a^\dagger i\}} | 0 \rangle \quad (2.83)$$

$$= \sum_{pq} \langle p | h | q \rangle \langle 0 | \delta_{pi} \delta_{qa} | 0 \rangle \quad (2.84)$$

$$= \langle i | h | a \rangle. \quad (2.85)$$

Notice that the contraction

$$\overbrace{\{p^\dagger q\} \{a^\dagger i\}} \quad (2.86)$$

is zero. The generalized Wick's theorem lets us skip these internal contractions since they resolve to zero due to the fact that the operators are already normally ordered. Only contractions across normally ordered strings need to be resolved. A one-body term has been chosen simply because the number of possible contractions as the size of the SQ strings grow becomes unmanageable. As more SQ operators are included, the complexity arises from all possible permutations of contractions. Resolving all of these possibilities is time consuming and somewhat tedious, which is why such a simple example has been chosen. We see though, that this is the expression from Case 2 in [Table 2.1](#).

2.3 Configuration interaction theory

Configuration interaction is a theory that builds upon the Hartree-Fock model. The wave function is defined as a linear combination of Slater determinants. These Slater determinants include the reference (HF) state, and a collection of excited determi-

nants. Configuration interaction, or CI, is a rich field with many ways to approach the CI Schrödinger equation [58, 59].

2.3.1 Full configuration interaction

One such approach is to use the full configuration interaction (FCI) wave function. This wave function includes all excitations up to $N -$ tually excited determinants (where N is the number of electrons and M is the number of virtual orbitals). It has the following form,

$$\begin{aligned}
 |\Psi^{\text{FCI}}\rangle &= c_0 |0\rangle + \sum_i^N \sum_a^M c_{(i,a)} a^\dagger_i |0\rangle \\
 &+ \sum_{i<j}^N \sum_{a<b}^M c_{(ij,ab)} a^\dagger_i b^\dagger_j |0\rangle \\
 &+ \sum_{i<j<k}^N \sum_{a<b<c}^M c_{(ijk,abc)} a^\dagger_i b^\dagger_j c^\dagger_k |0\rangle + \dots
 \end{aligned} \tag{2.87}$$

$$= \sum_{\alpha} c_{\alpha} |\Phi_{\alpha}\rangle \tag{2.88}$$

The summation would continue until all possible electrons from the reference HF state ($|0\rangle$) were excited to virtual spin orbitals, which are spin orbitals above the Fermi level. Each excitation in the wave function also has an associated weight, c , that it contributes to the overall wave function. The shorthand from Equation 2.88 is adopted to easily discuss give determinants and their weights without concern for the actual form of the determinants.

The CI methodology is concerned with solving for these weights to understand what determinants are important in the overall wave function. This is done by substituting the CI wave function into the Schrödinger equation which gives,

$$H |\Psi^{\text{FCI}}\rangle = E^{\text{tot}} |\Psi^{\text{FCI}}\rangle. \tag{2.89}$$

The Schrödinger equation is then left multiplied by the FCI wave function to give

$$\langle \Psi^{\text{FCI}} | H | \Psi^{\text{FCI}} \rangle = E^{\text{tot}} \langle \Psi^{\text{FCI}} | \Psi^{\text{FCI}} \rangle. \quad (2.90)$$

The energy is then minimized with respect to the c coefficients,

$$E^{\text{tot}} = \min_c \frac{\langle \Psi^{\text{FCI}} | H | \Psi^{\text{FCI}} \rangle}{\langle \Psi^{\text{FCI}} | \Psi^{\text{FCI}} \rangle} \quad (2.91)$$

Elements of the Hamiltonian matrix and overlap matrix are as follows,

$$H_{\alpha,\beta} = \langle \Phi_\alpha | H | \Phi_\beta \rangle \quad (2.92)$$

$$S_{\alpha,\beta} = \langle \Phi_\alpha | \Phi_\beta \rangle. \quad (2.93)$$

The c coefficients represent the weights on each determinant in the wave function and are used to minimize total energy of the system.

The total energy can be written as reference (HF) energy plus correlation energy,

$$E^{\text{tot}} = E^{\text{ref}} + E^{\text{corr}}. \quad (2.94)$$

Correlation energy is the energy contribution from all Slater determinants aside from the HF determinant. Usually it is orders of magnitude smaller than the reference energy, but is immensely important in accurately describing physical properties.

In CI theory, FCI is particularly important because it represents an exact solution for a system with a finite basis. This property makes FCI one of the most useful methods, especially when highly accurate calculations are needed. Unfortunately, this also limits its applicability. If all possible excitations are included in the expansion of the CI wave function (as is the case with FCI), we quickly run into a scaling problem.

The FCI method scales factorially as

$$\binom{2K}{N} = \frac{2K!}{(2K - N)!N!} \quad (2.95)$$

where $2K$ is the number of spin orbitals (K being number of spatial orbitals) and N is the occupation number. With this scaling, FCI is limited to calculations on smaller systems that have small numbers of electrons and/or small basis sets.

2.3.2 Configuration interaction singles and doubles

While FCI is prohibitively expensive in many cases, there are truncations to the FCI wave function that are more computationally feasible. One of the most widely used truncations is configuration interaction singles and doubles, or CISD for short. The ansatz includes the reference HF state and all single and double excitations; it has the following form,

$$\begin{aligned} |\Psi^{\text{CISD}}\rangle = & c_0 |0\rangle + \sum_i^N \sum_a^M c_{(i,a)} a^\dagger_i |0\rangle \\ & + \sum_{i<j}^N \sum_{a<b}^M c_{(ij,ab)} a^\dagger_i b^\dagger_j |0\rangle. \end{aligned} \quad (2.96)$$

As was the case with FCI, this wave function can be substituted into the Schrödinger equation and then the eigenvalue problem can be solved with standard linear algebra methods.

Using a truncation to the FCI wave function like CISD can be very useful. FCI scales very poorly as seen from [Equation 2.95](#) where the expression for the total number of determinants was given. CISD will only include the single and double

excitations, so the number of excited determinants is given by,

$$\binom{N}{1} \binom{2K-N}{1} + \binom{N}{2} \binom{2K-N}{2}. \quad (2.97)$$

The number of determinants of a given excitation level is given by

$$\binom{N}{n} \binom{2K-N}{n} \quad (2.98)$$

where N is the number of electrons, K is the number of spin orbitals, and n is the excitation level. The size of the FCI versus the CISD space is illustrated below in [Table 2.2](#). It becomes immediately apparent how useful the CISD truncation truly is. In the larger systems, it eliminates orders of magnitudes of determinants. By eliminating vast numbers of determinants, it's possible to extend the method to larger systems, in terms of both electrons and basis functions, without incurring insurmountable computational cost. It is also worth noting that the table only shows the number of determinants in the expansion of the wave function, but the Hamiltonian matrix would be $N_{\text{det}} \times N_{\text{det}}$, which further illustrates the savings that the truncated wave function has.

2.3.3 Consequences of truncating the CI wave function

Unfortunately, truncating the CI wave function is not a perfect solution. The truncated CI wave functions do save on computational storage costs and CPU times, but lose some properties of the FCI wave function that were desirable.

Firstly, by truncating the FCI wave function, we no longer have an exact solution for a given basis due to the loss of higher order excitations. By extension then, CISD calculations will capture less correlation energy than their FCI counterparts. Sometimes this can mean inaccurate or incorrect insight into the physical properties of a chemical system. Secondly, truncating the CI wave function breaks a property

Table 2.2: Number of determinants in the CISD and FCI wave functions.

N	K	$N_{\text{det}}^{\text{CISD}}$	$N_{\text{det}}^{\text{FCI}}$
2	10	190	190
2	15	435	435
2	20	780	780
2	25	1225	1225
4	10	785	4845
4	15	2055	27405
4	20	3925	91390
4	25	6395	230300
10	10	2126	184756
10	15	8751	30045015
10	20	19876	847660528
10	25	35501	10272278170

called size consistency. Size consistency is a preferred, but not required, feature of any quantum chemical method. It states that the energy of some system XY , where X and Y are infinitely separated chemical systems, should be equal to the summed individual energies of X and Y . Mathematically, this is defined as [60],

$$\lim_{R_{XY} \rightarrow \infty} E(X + Y) = E(X) + E(Y). \quad (2.99)$$

At an infinite distance, two chemical systems should behave as independent particles, so intuitively size consistency should always be obeyed. If a method is size consistent, it will (more likely) predict dissociation curves and produce a more trustworthy potential energy surface.

2.3.4 Recent developments in configuration interaction

In the past few years, CI theory has seen great strides towards applying the methodology to larger chemical systems. This new method, full configuration interaction quantum Monte Carlo (FCIQMC)[62, 63, 64], and its relative, semistochastic quantum Monte Carlo (SQMC) [65], in principle, solves for the FCI wave function using

Monte Carlo techniques by generating excited determinants on-the-fly and computing the weighted contribution to the overall wave function. Based upon the coefficient c that is calculated, the determinant is either accepted or rejected. Determinants are continually generated until satisfactory convergence is achieved. In addition to reducing storage and computational costs, this new methodology will also retain size consistency.

FCIQMC represents a significant advancement for CI theory, which is worth noting. The theory won't be detailed further, though it remains an area of great interest for future work.

2.4 Coupled-cluster theory

Similar to CI, coupled-cluster (CC) theory uses a collection of determinants to define the wave function [60, 60, 61]. CC theory, uses an exponential ansatz for the wave function,

$$|\Psi^{\text{CC}}\rangle = e^T |0\rangle \quad (2.100)$$

with T being some excitation operator. In practice, the exponential operator is expanded into a Taylor series to give,

$$e^T = 1 + T + \frac{1}{2}T^2 + \frac{1}{3!}T^3 + \frac{1}{4!}T^4 + \dots \quad (2.101)$$

This expression can then be substituted back into the Schrödinger equation which will be the functional form for deriving the CC equations. Before that, though, we will discuss the choice of the T operator.

2.4.1 Choosing an excitation operator

The choice of the T operator is critical, as it defines how complex the wave function will be. The general form of a T excitation operator is

$$T_x = \frac{1}{x!^2} \sum_{ij\dots}^N \sum_{ab\dots}^M t_{ij\dots}^{ab\dots} \{a^\dagger i b^\dagger j \dots\} \quad (2.102)$$

where i, j are summed over occupied states and a, b are summed over virtual states and the t is an amplitude for the excitation. The two most common choices for the T operator are

$$T = T_2 \quad (\text{CCD}) \quad (2.103)$$

$$T = T_1 + T_2 \quad (\text{CCSD}). \quad (2.104)$$

The CCD operator was the original choice in CC theory, and includes only double excitations with respect to some reference state. The CCSD operator soon followed and has seen extensive use in quantum chemical investigations. It is more thorough than the CCD operator as it also includes all single excitations on the reference wave function and now resembles the CISD ansatz. In principle, the CC operator can be defined to include further excitations, though computational cost, once again, becomes a reason to exclude such contributions. The form of the T_1 and T_2 operators are as follows,

$$T_1 = \sum_i^N \sum_a^M t_i^a \{a^\dagger i\} \quad (2.105)$$

$$T_2 = \sum_{i<j}^N \sum_{a<b}^M t_{ij}^{ab} \{a^\dagger b^\dagger j i\}. \quad (2.106)$$

The CCSD T operator will be used when deriving the CC equations. It is accompanied by much more complexity than the CCD operator, but it is ultimately a more interesting wave function and will be built upon in later chapters.

The T amplitudes obey the antisymmetric nature of the wave function as well. That is, permuting indices in the excitation operator (which is accompanied by a permutation of the t amplitude indices), results in a change of sign which is illustrated using the T_2 amplitude,

$$t_{ij}^{ab} = -t_{ji}^{ab} = t_{ji}^{ba} = -t_{ij}^{ba}. \quad (2.107)$$

Symmetry must also be taken into account when products of t amplitudes are present.

Once the T operator is defined, the wave function can be substituted back into the Schrödinger equation yielding

$$H |\Psi_{\text{CCSD}}\rangle = E^{\text{tot}} |\Psi_{\text{CCSD}}\rangle \quad (2.108)$$

$$He^T |0\rangle = E^{\text{tot}} e^T |0\rangle \quad (2.109)$$

$$H_N e^T |0\rangle = E^{\text{corr}} e^T |0\rangle. \quad (2.110)$$

Moving from [Equation 2.109](#) to [Equation 2.110](#) was done by subtracting E^{ref} from both sides. The cluster operator is then expanded into a Taylor series which gives the following expression

$$e^T |0\rangle = \left[(1) + (T_1 + T_2) + \frac{1}{2}(T_1 + T_2)^2 + \frac{1}{3!}(T_1 + T_2)^3 + \dots \right] |0\rangle \quad (2.111)$$

$$\begin{aligned} &= |0\rangle + T_1 |0\rangle + T_2 |0\rangle + \frac{1}{2}T_1^2 |0\rangle + T_1 T_2 |0\rangle + \frac{1}{2}T_2^2 |0\rangle \\ &+ \frac{1}{3!}T_1^3 |0\rangle + \frac{1}{2}T_1 T_2^2 |0\rangle + \frac{1}{2}T_1^2 T_2 |0\rangle + \dots \end{aligned} \quad (2.112)$$

Though the summation is infinite, many terms in the expansion can be ignored. This will be addressed shortly.

2.4.2 Similarity transformation and the Baker-Campbell-Hausdorff expansion

The Hamiltonian will then be similarity transformed by multiplying the Schrödinger equation on the left by e^{-T} , which gives,

$$e^{-T}H_Ne^T|0\rangle = E^{\text{corr}}e^{-T}e^T|0\rangle. \quad (2.113)$$

Using the similarity transformed Hamiltonian enables a much more compact form the CC equations to be written by using the Baker-Campbell-Hausdorff expansion [60, 61]. This expansion lets $e^{-T}H_Ne^T$ to be rewritten using the anticommutator relationship of second-quantized operators as follows,

$$e^{-T}H_Ne^T = \left(1 - T + \frac{1}{2}T^2 - \frac{1}{3!}T^3 + \dots\right) H_N \left(1 + T + \frac{1}{2}T^2 + \frac{1}{3!}T^3 + \dots\right) \quad (2.114)$$

$$= H_N + [H_N, T] + \frac{1}{2} [[H_N, T], T] + \frac{1}{3!} [[[H_N, T], T], T] + \frac{1}{4!} [[[[H_N, T], T], T], T]. \quad (2.115)$$

Using Wick's theorem and the anticommutator relationship, the expression can be simplified via,

$$[H_N, T] = H_NT - TH_N = \{H_NT\} + \left\{ \overline{H_NT} \right\} - \{TH_N\} - \left\{ \overline{TH_N} \right\} \quad (2.116)$$

$$[H_N, T] = \left\{ \overline{H_NT} \right\} - \left\{ \overline{TH_N} \right\} \quad (2.117)$$

where the curly braces indicate a normal product and the contraction brace represents the sum of all normal products. Notice that all the terms that do not fully contract cancel as they contribute zero to the overall expression. Terms that do not full contract are called disconnected terms, while ones that fully contract are called connected. The CC expressions become very complex, so we only consider connected terms. If a subscript c is ever present in an equation, it assumes that only connected terms are including.

2.4.3 The CCSD equations

Using the similarity transformed Hamiltonian we then derive the CC equations using a series of projections. To arrive at the energy expression, the Schrödinger equation is left multiplied by the reference state, while the singles and doubles amplitudes equations are derived by left multiplying by singly and doubly excited Slater determinants which gives

$$\langle 0 | e^{-T} H_N e^T | 0 \rangle_c = E^{\text{corr}} \quad (2.118)$$

$$\langle S | e^{-T} H_N e^T | 0 \rangle_c = 0 \quad (2.119)$$

$$\langle D | e^{-T} H_N e^T | 0 \rangle_c = 0. \quad (2.120)$$

The singles and doubles projections are a set of all possible excitations on the reference state. Expanding the cluster operator gives the following equations,

$$\langle 0 | H_N \left[T_1 + \frac{1}{2!} T_1^2 + T_2 \right] | 0 \rangle_c = E^{\text{corr}} \quad (2.121)$$

$$\begin{aligned}
& \langle S | H_N \left[T_1 + T_1 T_2 + \frac{1}{2!} T_1^2 + \frac{1}{3!} T_1^3 + T_2 \right] \\
& + [-T_1^I] H_N \left[T_1 + \frac{1}{2!} T_1^2 + T_2 \right] |0\rangle_c = 0
\end{aligned} \tag{2.122}$$

$$\begin{aligned}
& \langle D | H_N \left[T_1 + T_1 T_2 + \frac{1}{2!} T_1^2 + \frac{1}{2!} T_1^2 T_2 + \frac{1}{3!} T_1^3 + \frac{1}{4!} T_1^4 + T_2 + \frac{1}{2!} T_2^2 \right] \\
& + [-T_1^I] H_N \left[T_1 + T_1 T_2 + \frac{1}{2!} T_1^2 + \frac{1}{3!} T_1^3 + T_2 \right] \\
& + [-T_2^I] H_N \left[T_1 + \frac{1}{2!} T_1^2 + T_2 \right] \\
& + \left[\frac{1}{2!} T_1^2 \right] H_N \left[T_1 + \frac{1}{2!} T_1^2 + T_2 \right] |0\rangle_c = 0.
\end{aligned} \tag{2.123}$$

The expanded CC equations are very complex quantities, especially considering that each T operator is actually a summation over occupied and virtual indices. In the expansion, we also see that the singles and doubles equations are coupled as t_1 and t_2 amplitudes show up in both amplitude equations. Additionally, the non-linearity of the CC equations is now obvious as the quadratic, cubic, and quartic terms are present shown.

In each CC equation, the excitation level (after operation by excitation operators) is, at most, two above the bra state. This is understood by contracting SQ operators using Wicks' theorem. This explains why the expansion of the e^T operator only went up the fourth order terms in [Equation 2.115](#). It also becomes apparent as to why further excitations are excluded from the T operator. Including triples or quadruples (CCSDT, CCSDTQ) would lead to enormous expressions. While solving the CC equations would become computationally prohibitive, equations that include the triples and quadruples amplitudes have been derived [\[60, 66, 67\]](#), though the amplitudes are calculated using different methodology, which we won't discuss.

2.4.4 Size consistency and the CC wave function

One concept that must be further addressed is the truncation of the T operator. In [subsection 2.3.3](#), the consequences of truncating the FCI wave function was explored. We established that a truncated CI wave function will not capture as much correlation energy as the FCI wave function. In fact, the FCI method will exactly solve a given basis. Furthermore, a truncated CI wave function breaks size consistency (defined in [Equation 2.99](#)). It is important to then discuss how the CC wave function behaves when the T operator is truncated.

In principle, one could define a full CC wave function that includes all possible excitations by using [Equation 2.102](#). As with the FCI wave function, this would yield an exact solution to a given basis. Once again, the exorbitant computational cost prohibits using an FCC wave function. We also saw that CC equations become complex much more quickly when compared to the CI equation which further stresses the need to truncate the wave function. As for size consistency, a truncated CC wave function (such as CCD or CCSD), will retain size consistency. This makes the CC method attractive as it can be used for calculating reaction coordinate diagrams and dissociation curves more reliably.

2.4.5 Relating CC to CI

A few final comparison must be made between the CC and CI methods. This discussion will use CCSD and CISD as examples, but it can be applied to any truncation of either wave function. The wave functions of of note are [Equation 2.96](#) for the CISD wave function and [Equation 2.111](#) for the CCSD wave function.

First, we will compare the CCSD amplitudes to the CISD coefficients. In the CISD method, each determinant gets a unique coefficient. In CCSD, that is not necessarily the case. CCSD assigns amplitudes, or products of amplitudes, to given excitations. Expanding the e^T operator causes cross terms to be present. Consequently, the

amplitudes and coefficients cannot necessarily be compared one-to-one. One has to use the non-linear terms in CC to equate the two,

$$c_S \approx t_S \quad (2.124)$$

$$c_D \approx t_D + \frac{1}{2}t_S t_S \quad (2.125)$$

where the S and D subscripts are for single or double excitations. This relationship grows in complexity quickly, as the triple and quadruple (T and Q) excitation terms would be

$$c_T \approx t_T + t_D t_S + \frac{1}{3!}t_S t_S t_S \quad (2.126)$$

$$c_Q \approx t_Q + \frac{1}{2}t_D t_D + \frac{1}{2}t_D t_S t_S + \frac{1}{4!}t_S t_S t_S t_S. \quad (2.127)$$

These terms are not present in the CCSD or CISD equations shown earlier, but illustrate the difficulty of directly comparing the two wave functions. This complexity is further exacerbated by the fact that t amplitude symmetry has to be taken into account when products of lower order terms are present. Using the double excitation as an example we would have

$$c_{(ij,ab)} \approx t_{ij}^{ab} + \frac{1}{2} \underbrace{(t_i^a t_j^b - t_j^a t_i^b + t_j^b t_i^a - t_i^b t_j^a)}_{t_S t_S} \quad (2.128)$$

with the further excitations having even more permutation complexity.

Secondly, in the CI section we discussed the number of determinants encompassed by CISD and FCI calculation (summarized in [Table 2.2](#)). The number of determinants in FCI was computationally prohibitive, but CISD proved to be a useful method to reduce this constraint. With CCSD, determinants have not yet been discussed. CC theory can avoid the complexity of Slater determinants by using SQ operator relationships and Wick's theorem. Wick's theorem still eliminates a vast number of

states in the CC equations just as the Slater-Condon rules did in CI theory. This is why the energy equation (Equation 2.121) couples only up to double excitations, why the singles amplitude equation (Equation 2.122) only couples up to triple excitations, the doubles amplitude equation (Equation 2.123) couples to quadruple excitations at most.

An important similarity that CCSD and CISD share is the number of optimizable parameters. The CISD method searches for coefficients for the ground state, singly excited states, and double excited states in the wave function. Similarly, the CCSD method searches for all single and double t amplitudes. The difference is in how these coefficients and amplitudes relate to the wave function. Since the CISD wave function is a linear combination, each state has a single coefficient value. In CCSD, the (expanded) cluster operator allows for combinations of t amplitudes to describe a given state. Additionally, exponential cluster operator in CCSD theory can use the higher order, non-linear terms to explain higher order excitations (such as triple and quadruple excitations) in a wave function, which is not possible in CISD without redefining the wave function.

Chapter 3

Multicomponent methods in quantum chemistry

The previous chapter briefly surveyed the basics of single component (electronic structure) theories. It focused on solutions to the electronic Schrödinger equation using the Hartree-Fock, configuration interaction, and coupled-cluster forms of the wave function.

This chapter will introduce multicomponent quantum chemical theories. These theories are used to investigate quantum chemical systems where the BO approximation is inadequate. Some of these types of systems were discussed earlier in [chapter 1](#). To begin, this chapter will assume that we are solving for the multicomponent wave function using the multicomponent Schrödinger equation,

$$H^{I,II}(\mathbf{r}^I, \mathbf{r}^{II}; \mathbf{R}^{\text{BOS}})\Psi^{I,II}(\mathbf{r}^I, \mathbf{r}^{II}; \mathbf{R}^{\text{BOS}}) = E^{I,II}(\mathbf{R}^{\text{BOS}})\Psi^{I,II}(\mathbf{r}^I, \mathbf{r}^{II}; \mathbf{R}^{\text{BOS}}). \quad (3.1)$$

The obvious difference from the single component case being that our wave function is now directly dependent on the coordinates of two particle types. BO separated bodies still have parametric dependence in this wave function. The Hamiltonian for

a multicomponent system is defined as

$$\begin{aligned}
 H^{I,II} &= T^I(\mathbf{r}^I) + V_{\text{ext}}^I(\mathbf{r}^I, \mathbf{R}^{\text{BOS}}) + V^{I,I}(\mathbf{r}^I) && \left. \vphantom{H^{I,II}} \right\} H^I \\
 &+ T^{II}(\mathbf{r}^{II}) + V_{\text{ext}}^{II}(\mathbf{r}^{II}, \mathbf{R}^{\text{BOS}}) + V^{II,II}(\mathbf{r}^{II}) && \left. \vphantom{H^{I,II}} \right\} H^{II} \\
 &+ V^{I,II}(\mathbf{r}^I, \mathbf{r}^{II}) && \left. \vphantom{H^{I,II}} \right\} V^{I,II}
 \end{aligned} \tag{3.2}$$

The Hamiltonian for a multicomponent system includes all terms in the single component Hamiltonian for each particle type. These are the kinetic energy, repulsive potential between particles of the same type, and external potential from BO separated bodies (see [Equation 2.4](#) and [Equation 2.5](#)). Adapting the single component operators to the multicomponent form also requires the addition of q^I and q^{II} to the external potential and two body operators to give

$$H^{\text{core}\alpha} = -\frac{\hbar}{2m^\alpha} \sum_i^N \nabla_i^2 - \sum_i^N \sum_A^M \frac{Z_A q^\alpha}{r_{iA}} \tag{3.3}$$

$$V = q^\alpha q^\alpha \sum_{i<j}^N \sum_j^N \frac{1}{r_{ij}}. \tag{3.4}$$

where α is either I or II. There is also the addition of a type I-II coupling term. The explicit forms of these terms can be taken from earlier definitions, with the exception of the $V^{I,II}$ coupling term which has the following form,

$$V^{I,II}(\mathbf{r}^I, \mathbf{r}^{II}) = q^I q^{II} \sum_i^{N^I} \sum_{i'}^{N^{II}} r_{ii'}^{-1}. \tag{3.5}$$

The goal of the remainder of this chapter is to draw parallels between single and multicomponent schools of thought. Extension and expansion of Hartree-Fock theory ([section 3.1](#)) and the configuration interaction method ([section 3.3](#)) will be presented in a way that builds upon the familiar single component theories. The key additions

and differences between the single component and multicomponent theories will be highlighted, while the underlying principles remains consistent.

3.1 Multicomponent Hartree-Fock

The multicomponent Schrödinger equation is a complex problem to solve. Like the single component counterpart, it is not exactly solvable, so we must approximate solutions. This approximation is the extension of Hartree-Fock theory to multicomponent chemical systems [68, 69, 70]. Similar to the single component formulation, multicomponent HF theory will use a single Slater determinant as an ansatz. The multicomponent theories presented in this and the following sections and chapter are for fermionic particles only. The omission of a formulation for bosonic particles is not because it is impossible to extend the theory; this choice was made due to the systems of interest.

We begin by defining the multicomponent wave function as a product of type I and type II functions,

$$\Psi^{I,II}(\mathbf{r}^I, \mathbf{r}^{II}; \mathbf{R}^{\text{BOS}}) = \Phi^I(\mathbf{x}^I; \mathbf{R}^{\text{BOS}})\Phi^{II}(\mathbf{x}^{II}; \mathbf{R}^{\text{BOS}}). \quad (3.6)$$

In this equation, the spatial spin coordinate has been reintroduced from [Equation 2.6](#). Both the type I and type II wave functions must obey the antisymmetry principle defined in [Equation 2.7](#). This antisymmetric property is enforced by defining each wave function to be a Slater determinant ([Equation 2.19](#)).

Each Slater determinant has its own, unique set of molecular orbitals. Particles from type I cannot occupy orbitals in the type II space and vice versa,

$$|\Phi^I(\mathbf{x}_1^I, \mathbf{x}_2^I, \dots, \mathbf{x}_N^I)\rangle = |\chi_i^I(\mathbf{x}_1^I) \chi_j^I(\mathbf{x}_2^I) \dots \chi_k^I(\mathbf{x}_N^I)\rangle \quad (3.7)$$

$$= |ij \dots k\rangle \quad (3.8)$$

$$|\Phi^{II}(\mathbf{x}_1^{II}, \mathbf{x}_2^{II}, \dots, \mathbf{x}_N^{II})\rangle = |\chi_i^{II}(\mathbf{x}_1^{II}) \chi_j^{II}(\mathbf{x}_2^{II}) \dots \chi_k^{II}(\mathbf{x}_N^{II})\rangle \quad (3.9)$$

$$= |i'j' \dots k'\rangle. \quad (3.10)$$

As with the Hamiltonian, type II indicies are accompanied by primes to easily distinguish them.

Elements of the multicomponent Hamiltonian are evaluated as such,

$$\begin{aligned} \langle \Phi^{I,II} | H^{I,II} | \Phi^{I,II} \rangle &= \langle \Phi_i^I \Phi_{i'}^{II} | (H^I + H^{II} + V^{I,II}) | \Phi_j^I \Phi_{j'}^{II} \rangle \\ &= \langle \Phi_i^I | H^I | \Phi_j^I \rangle \langle \Phi_{i'}^{II} | \Phi_{j'}^{II} \rangle + \langle \Phi_{i'}^{II} | H^{II} | \Phi_{j'}^{II} \rangle \langle \Phi_i^I | \Phi_j^I \rangle \\ &+ \langle \Phi_i^I \Phi_{i'}^{II} | V^{I,II} | \Phi_j^I \Phi_{j'}^{II} \rangle. \end{aligned} \quad (3.11)$$

The Hamiltonian is partitioned in such a way that the single component Slater-Condon rules can be applied from [Table 2.1](#) to the H^I and H^{II} terms. The result is the multiplied by the delta of the off type determinant. Note that these two terms do not include any type I-II interaction, as that is done in the $V^{I,II}$ term. The coupling term between type I and type II is resolved using its own set of rules since it has dependence on the coordinates of both type I and type II particles. The Slater-Condon rules for evaluation is shown in [Table 3.1](#). The integral form the the $V^{I,II}$ expression between spin orbitals is defined as,

$$\langle pp' | v^{I,II} | qq' \rangle = \int d\mathbf{x}_1^I d\mathbf{x}_1^{II} \chi_p^*(\mathbf{x}_1^I) \chi_{p'}^*(\mathbf{x}_1^{II}) r_{I,II}^{-1} \chi_q(\mathbf{x}_1^I) \chi_{q'}(\mathbf{x}_1^{II}) \quad (3.12)$$

Table 3.1: **Type I-II coupling term Slater-Condon Rules**

Case 1: $ K^I\rangle = \dots ij \dots\rangle$ $ K^{II}\rangle = \dots i'j' \dots\rangle$ $\langle K^I K^{II} V^{I,II} K^I K^{II} \rangle = \sum_i^{N^I} \sum_{i'}^{N^{II}} \langle ii' v^{I,II} ii' \rangle$	
Case 2A: $ K^I\rangle = \dots ij \dots\rangle$ $ L^I\rangle = \dots aj \dots\rangle$ $ K^{II}\rangle = \dots i'j' \dots\rangle$	Case 2B: $ K^I\rangle = \dots ij \dots\rangle$ $ K^{II}\rangle = \dots i'j' \dots\rangle$ $ L^{II}\rangle = \dots a'j' \dots\rangle$
$\langle K^I K^{II} V^{I,II} L^I K^{II} \rangle = \sum_{i'}^{N^{II}} \langle ai' v^{I,II} ai' \rangle \quad \langle K^I K^{II} V^{I,II} K^I L^{II} \rangle = \sum_i^{N^I} \langle ia' v^{I,II} ia' \rangle$	
Case 3: $ K^I\rangle = \dots ij \dots\rangle$ $ L^I\rangle = \dots aj \dots\rangle$ $ K^{II}\rangle = \dots i'j' \dots\rangle$ $ L^{II}\rangle = \dots a'j' \dots\rangle$	
$\langle K^I K^{II} V^{I,II} L^I L^{II} \rangle = \langle ii' v^{I,II} aa' \rangle$	

We now write the energy expression for a multicomponent system, below. The energy is a sum of single component energies for type I and type II particles as well as the the coupling term.

$$\begin{aligned}
 E^{\text{mcHF}} &= \langle \Phi^I \Phi^{II} | H | \Phi^I \Phi^{II} \rangle & (3.13) \\
 &= \sum_i^{N^I} \langle i | h^I | i \rangle + \sum_{i < j}^{N^I} \sum_j^{N^I} \langle ij | v^{I,I} | ij \rangle_A \\
 &\quad + \sum_{i'}^{N^{II}} \langle i' | h^{II} | i' \rangle + \sum_{i' < j'}^{N^{II}} \sum_{j'}^{N^{II}} \langle i'j' | v^{II,II} | i'j' \rangle_A \\
 &\quad + \sum_i^{N^I} \sum_{i'}^{N^{II}} \langle ii' | v^{I,II} | ii' \rangle. & (3.14)
 \end{aligned}$$

The energy is minimized with respect to the the molecular orbitals,

$$\frac{\partial E^{\text{mcHF}}}{\partial \chi_i^I} = \frac{\partial E^{\text{mcHF}}}{\partial \chi_{i'}^{II}} = 0 \quad \text{for } i = 1, \dots, N^I, i' = 1, \dots, N^{II} \quad (3.15)$$

Each set of molecular orbitals, for type I and type II particles, has a set of spatial orbitals. These spatial orbitals can be expanded into a set of the basis functions from [Equation 2.26](#). These coefficients can be optimized via the Fock equation. There are now two Fock equations, one for each type, with the following form,

$$f^{\text{I}} |\chi_i^{\text{I}}\rangle = \epsilon_i^{\text{I}} |\chi_i^{\text{I}}\rangle \quad (3.16)$$

$$f^{\text{II}} |\chi_{i'}^{\text{II}}\rangle = \epsilon_{i'}^{\text{II}} |\chi_{i'}^{\text{II}}\rangle. \quad (3.17)$$

An important step in mcHF theory is choosing the form of the Fock operator.

3.1.1 Choice of the multicomponent Fock operator

There are two obvious choices for the Fock operator that will be discussed. Both choices are valid, though one will be preferred over the other as it should provide a better approximation to the wave function and provide a lower energy.

The first form of the operators be the familiar single component Fock operator from [Equation 2.28](#). This choice neglects any coupling term that was present in the Hamiltonian and has the form,

$$\tilde{f}^{\text{I}} = h^{\text{I}} + v_{\text{HF}}^{\text{I}} \quad (3.18)$$

$$\tilde{f}^{\text{II}} = h^{\text{II}} + v_{\text{HF}}^{\text{II}}. \quad (3.19)$$

The Fock equation can then be solved self consistently and energy will be minimized independently for type I and type II particles. The scheme is shown below,

$$\langle \tilde{0}^{\text{I}} | H^{\text{I}} | \tilde{0}^{\text{I}} \rangle = \min_{\tilde{\Phi}^{\text{I}}} \langle \tilde{\Phi}^{\text{I}} | H^{\text{I}} | \tilde{\Phi}^{\text{I}} \rangle \quad (3.20)$$

$$\langle \tilde{0}^{\text{II}} | H^{\text{II}} | \tilde{0}^{\text{II}} \rangle = \min_{\tilde{\Phi}^{\text{II}}} \langle \tilde{\Phi}^{\text{II}} | H^{\text{II}} | \tilde{\Phi}^{\text{II}} \rangle. \quad (3.21)$$

The $|\tilde{0}^I\rangle$ and $|\tilde{0}^{II}\rangle$ are the optimized Slater determinants that are the Hartree-Fock wave function. Using the same scheme discussed in single component Hartree-Fock, we will arrive at the following matrix eigenvalue equation (originally described in [Equation 2.33](#)),

$$\mathbf{F}^I \mathbf{C}^I = \mathbf{S}^I \mathbf{C}^I \epsilon^I \quad (3.22)$$

$$\mathbf{F}^{II} \mathbf{C}^{II} = \mathbf{S}^{II} \mathbf{C}^{II} \epsilon^{II}. \quad (3.23)$$

Once these decoupled equations are solved, the overall mcHF wave function is a product of the two Slater determinants,

$$|\Phi_{\text{mcHF}}^{I,II}\rangle = |\tilde{0}^I\rangle |\tilde{0}^{II}\rangle = |\tilde{0}^I \tilde{0}^{II}\rangle. \quad (3.24)$$

In summary, this choice of the Fock operator solves the Fock equations in a decoupled manner and takes the product of results to be the mcHF wave function.

The second way to construct the Fock operator is to include a coupling term from the Hamiltonian. For the two particle types, the Fock operator is defined as

$$f^I = h^I + v_{\text{HF}}^I + \sum_{i'}^{N^{II}} \langle i' | v^{I,II} | i' \rangle \quad (3.25)$$

$$f^{II} = h^{II} + v_{\text{HF}}^{II} + \sum_i^{N^I} \langle i | v^{I,II} | i \rangle. \quad (3.26)$$

We can see that the $v^{I,II}$ coupling term has been added to the \tilde{f} operators just discussed. With this procedure, the minimization of energy will occur over the type I and type II Slater determinants simultaneously,

$$\langle 0^I 0^{II} | H | 0^I 0^{II} \rangle = \min_{\Phi^I, \Phi^{II}} \langle \Phi^I \Phi^{II} | H | \Phi^I \Phi^{II} \rangle. \quad (3.27)$$

This choice of the Fock operator will give rise to the following matrix equations,

$$\mathbf{F}^{\text{I}} [\mathbf{C}^{\text{II}}] \mathbf{C}^{\text{I}} = \mathbf{S}^{\text{I}} \mathbf{C}^{\text{I}} \epsilon^{\text{I}} \quad (3.28)$$

$$\mathbf{F}^{\text{II}} [\mathbf{C}^{\text{I}}] \mathbf{C}^{\text{II}} = \mathbf{S}^{\text{II}} \mathbf{C}^{\text{II}} \epsilon^{\text{II}}. \quad (3.29)$$

We see the manifestation of the coupling term in the matrix equations as well. The type I Fock matrix is dependent on the type II coefficients, and vice-versa. This coupled behavior is absent in the previous formulation of the Fock equations. Upon convergence, the multicomponent Hartree-Fock wave function will be determined and the energy will have been minimized over type I and II determinants simultaneously.

The mcHF wave function generated from the coupled type I-II Fock operators is preferred. Qualitatively, the particles of different types should experience a Coulombic potential from the other particles present in the system. Quantitatively, this method of constructing the wave function is preferred because it will provide a lower energy than that of the uncoupled construction of the wave function. This is a manifestation of the variational principle,

$$E^{\text{exact}} < \langle 0^{\text{I}} 0^{\text{II}} | H | 0^{\text{I}} 0^{\text{II}} \rangle \leq \langle \tilde{0}^{\text{I}} \tilde{0}^{\text{II}} | H | \tilde{0}^{\text{I}} \tilde{0}^{\text{II}} \rangle. \quad (3.30)$$

As the coupled Fock equations provide a lower energy approximation (that is still above the exact energy), the wave function constructed with this method is a better approximation to the exact wave function.

With the choice of Fock operator decided, the eigenvalue equation can be self-consistently satisfied until convergence is met, and the mcHF wave function will be found. As was the case in single component theory, sometimes a single Slater determinant will not yield enough information about a chemical system or energy will not be accurate enough. For these cases, we will look extend configuration interaction and coupled-cluster theory to multicomponent chemical systems. Before these theories are

discussed, we must first address second quantization as it relates to multicomponent systems.

3.2 Multicomponent second quantization

Multicomponent wave functions and the Hamiltonian are quite a bit more complicated than their single component counterparts. This section is meant to clarify and explain how second quantized operators and their rules should be applied to multicomponent systems. The rules and restrictions discussed here are all in addition to what is discussed in [section 2.2](#).

Creation and annihilation operators work the same as they did in single component theories. The only caveat being that there are now type I and type II operators. The type II operators will carry a prime. These type I and type II operators only operate in their space. A type I creation operator cannot put a particle of type I into a molecular orbital of type I within type II space, and vice versa. Creation and annihilation operations are contained to type space. A couple illustrative examples are as follows,

$$i^\dagger i'^\dagger |\Phi^{I,II}\rangle = i^\dagger |jk\dots z\rangle i'^\dagger |j'k'\dots z'\rangle \quad (3.31)$$

$$= |ijk\dots z\rangle |i'j'k'\dots z'\rangle \quad (3.32)$$

$$ii' |\Phi^{I,II}\rangle = i |ijk\dots z\rangle i' |i'j'k'\dots z'\rangle \quad (3.33)$$

$$= |jk\dots z\rangle |j'k'\dots z'\rangle. \quad (3.34)$$

These creation and annihilation operators for type I and type II particles then inherit all properties and rules previously discussed. Most notably, is that type I and type II particles are subject to Wick's theorem. Consequently, connected (non-zero)

expressions involving SQ operators must fully contract in type I and type II space simultaneously.

The multicomponent Hamiltonian will have the following form in SQ notation,

$$\begin{aligned}
H^{I,II} = & \sum_{pq} \langle p|h^I|q\rangle p^\dagger q + \sum_{pqrs} \langle pq|v^{I,I}|rs\rangle p^\dagger q^\dagger sr & \left. \vphantom{\sum_{pq}} \right\} H^I \\
& + \sum_{p'q'} \langle p'|h^{II}|q'\rangle p'^\dagger q' + \sum_{p'q'r's'} \langle p'q'|v^{II,II}|r's'\rangle p'^\dagger q'^\dagger s'r' & \left. \vphantom{\sum_{p'q'}} \right\} H^{II} \\
& + \sum_{pp'q'q} \langle pp'|v^{I,II}|qq'\rangle p^\dagger p'^\dagger qq' & \left. \vphantom{\sum_{pp'q'q}} \right\} V^{I,II}.
\end{aligned} \tag{3.35}$$

We see that it has two single component terms (H^I and H^{II}) and the coupled $V^{I,II}$ term. Since the multicomponent creation and annihilation operators obey all of the single component SQ laws, the multicomponent Hamiltonian can also be normal ordered. This will be presented in the following chapter though, as it won't be used when discussing multicomponent configuration interaction. Since all operators occur in their own type space, Wick's theorem can be applied independently to strings, and products of strings, of SQ operators. Wick's contractions will only happen between operators of the same type. Each contraction for a given type must be complete, as was the case with single component theory, in order to be considered a connected (non-zero) expression. This is the SQ extension of what was first presented in [Equation 3.11](#).

The addition of the type two particles does not greatly complicate the SQ rules and operations. It simply adds a greater level of computational complexity as products of contractions of type I and type II must now be considered. Since the resolution of SQ operations involving H^I and H^{II} were covered in the previous chapter, we will

focus solely on an example of a Hamiltonian element with the $V_N^{I,II}$ coupling term.

$$\langle 0^I 0^{II} | V_N^{I,II} |_{i i'}^{a a'} \rangle = \sum_{pq} \sum_{p'q'} \langle pp' | v^{I,II} | qq' \rangle \langle 0^I | \{p^\dagger q\} \{a^\dagger i\} | 0^I \rangle \langle 0^{II} | \{p'^\dagger q'\} \{a'^\dagger i'\} | 0^{II} \rangle \quad (3.36)$$

$$= \sum_{pq} \sum_{p'q'} \langle pp' | v^{I,II} | qq' \rangle \langle 0^I | \overbrace{\{p^\dagger q\} \{a^\dagger i\}} | 0^I \rangle \langle 0^{II} | \overbrace{\{p'^\dagger q'\} \{a'^\dagger i'\}} | 0^{II} \rangle \quad (3.37)$$

$$= \sum_{pq} \sum_{p'q'} \langle pp' | v^{I,II} | qq' \rangle \langle 0^I | \delta_{pi} \delta_{qa} | 0^I \rangle \langle 0^{II} | \delta_{p'i'} \delta_{q'a'} | 0^{II} \rangle \quad (3.38)$$

$$= \langle i i' | v^{I,II} | a a' \rangle. \quad (3.39)$$

We can see that the expression is the $v^{I,II}$ element times the product of contractions for type I particles times contractions for type II particles. This result is seen in [Table 3.1](#) as Case 3.

3.3 Multicomponent configuration interaction

The multicomponent Hartree-Fock method finds a single Slater determinant wave function for each particle type that minimizes the total energy of a given multicomponent system. There are times when a single determinant simply is not enough to adequately describe a system, however. Multicomponent configuration interaction (mcCI) approximates the wave function to be a linear combination of determinants for type I and type II particles. This section will extend single component configuration interaction theory to multicomponent systems [68, 69, 70].

3.3.1 Multicomponent full configuration interaction wave function

As stated, the wave function is a linear combination of Slater determinants for type I and type II particles. This is a greatly more complex wave function than the single component form. If we recall from [section 2.3](#), the CI wave function is a combination of all possible excitations on the reference state, $|0\rangle$. For multicomponent theory, we must include all possible excitations on reference states, $|0^I 0^{II}\rangle$. The mcFCI wave function can be written as,

$$\begin{aligned}
|\Psi_{\text{mcFCI}}\rangle &= c_{(0,0),(0',0')}^{I,II} |0^I 0^{II}\rangle \\
&+ \sum_i^{N^I} \sum_a^{M^I} c_{(i,a),(0',0')}^{I,II} a^\dagger i |0^I 0^{II}\rangle \\
&+ \sum_{i<j}^{N^I} \sum_j^{N^I} \sum_{a<b}^{M^I} \sum_b^{M^I} c_{(ij,ab),(0',0')}^{I,II} a^\dagger b^\dagger j i |0^I 0^{II}\rangle + \dots \\
&+ \sum_{i'}^{N^{II}} \sum_{a'}^{M^{II}} c_{(0,0),(i',a')}^{I,II} a'^\dagger i' |0^I 0^{II}\rangle \\
&+ \sum_{i'<j'}^{N^{II}} \sum_{j'}^{N^{II}} \sum_{a'<b'}^{M^{II}} \sum_{b'}^{M^{II}} c_{(0,0),(i'j',a'b')}^{I,II} a'^\dagger b'^\dagger j' i' |0^I 0^{II}\rangle + \dots \\
&+ \sum_i^{N^I} \sum_a^{M^I} \sum_{i'}^{N^{II}} \sum_{a'}^{M^{II}} c_{(i,a),(i',a')}^{I,II} a^\dagger i a'^\dagger i' |0^I 0^{II}\rangle \\
&+ \sum_{i<j}^{N^I} \sum_j^{N^I} \sum_{a<b}^{M^I} \sum_b^{M^I} \sum_{i'<j'}^{N^{II}} \sum_{j'}^{N^{II}} \sum_{a'<b'}^{M^{II}} \sum_{b'}^{M^{II}} c_{(ij,ab),(i'j',a'b')}^{I,II} a^\dagger b^\dagger j i a'^\dagger b'^\dagger j' i' |0^I 0^{II}\rangle \\
&+ \dots
\end{aligned} \tag{3.40}$$

The mcFCI wave function is such a complex quantity because the determinant space is a direct product of the type I FCI space and the type II FCI space. The mcFCI coefficients are not products of the single component counterparts, however. The coefficients of the mcFCI wave function are unique to each product of type I and type

II determinants. For ease, the mcFCI wave function can be written as,

$$|\Psi_{\text{mcFCI}}^{\text{I,II}}\rangle = \sum_{\alpha}^{N_{\text{mcFCI}}^{\text{I,II}}} c_{\alpha}^{\text{I,II}} |\Phi_{\alpha}^{\text{I,II}}\rangle. \quad (3.41)$$

The mcFCI wave function can be then solved by substituting the mcFCI wave function into the Schrödinger equation and left multiplying by the mcFCI wave function, then solving the resulting matrix eigenvalue equation,

$$H^{\text{I,II}}|\Psi^{\text{I,II}}\rangle = E_{\text{mcFCI}}|\Psi^{\text{I,II}}\rangle \quad (3.42)$$

$$\langle\Psi^{\text{I,II}}|H^{\text{I,II}}|\Psi^{\text{I,II}}\rangle = E_{\text{mcFCI}}\langle\Psi^{\text{I,II}}|\Psi^{\text{I,II}}\rangle \quad (3.43)$$

$$\sum_{\alpha}^{N_{\text{mcFCI}}^{\text{I,II}}} \sum_{\beta}^{N_{\text{mcFCI}}^{\text{I,II}}} c_{\alpha}^{\text{I,II}} c_{\beta}^{\text{I,II}} \langle\Phi_{\alpha}^{\text{I,II}}|H^{\text{I,II}}|\Phi_{\beta}^{\text{I,II}}\rangle = E_{\text{mcFCI}} \sum_{\alpha}^{N_{\text{mcFCI}}^{\text{I,II}}} \sum_{\beta}^{N_{\text{mcFCI}}^{\text{I,II}}} c_{\alpha}^{\text{I,II}} c_{\beta}^{\text{I,II}} \langle\Phi_{\alpha}^{\text{I,II}}|\Phi_{\beta}^{\text{I,II}}\rangle \quad (3.44)$$

$$\mathbf{Hc} = \mathbf{eSc}. \quad (3.45)$$

The mcFCI matrix equations are then solvable using standard techniques. The energy acquired by the mFCI method is exact for a given basis and is size consistent. These features make mcFCI an extremely power computational tool for studying chemical systems. Unfortunately, like its single component relative, mcFCI does not scale well as system and basis size increase. The mcFCI space is a product of the type I and type II single component FCI spaces.

3.3.2 Truncating the multicomponent configuration interaction wave function

In order to alleviate some of the computational cost inherent in the mcFCI method, the wave function can be truncated. Reducing the number of excited determinants accomplishes this task. Commonly, this will mean only including single and double excitations, though other truncations are also possible.

Truncating the mcCI wave function is very similar to what was done in the single component case first discussed in [subsection 2.3.2](#). In mcCI, truncating the wave function is more flexible than in the single component space since the wave function is a product of both single component (type I and type II) CI spaces. This allows more freedom when it comes to considering computational cost and enables the correlation effects to be scaled via the wave function.

Due to the sheer size of the mcCI space, a highly truncated wave function is usually the only option for multiparticle systems. In [Table 2.2](#), the number of determinants in a truncated wave function was shown for a single particle type. The mcCI wave function, which is a product of these spaces, scales very poorly which restricts the choice of truncation.

Unfortunately, any truncation of the mcFCI wave function has two negative effects. First, size consistency is broken. This concept was covered in [subsection 2.3.3](#). Additionally, a truncated mcFCI wave function will not produce an exact solution for a given basis. Outside of modestly sized systems, one must accept these consequences if the mcCI method is to be used.

Chapter 4

Multicomponent coupled-cluster theory

The theory and implementation details of the multicomponent coupled-cluster method will be discussed at length in this chapter. The theory is built upon the principles of single component coupled-cluster theory that was discussed in [section 2.4](#). The implementation details focus on reducing the memory footprint and reducing the CPU time (specifically in reference to Wick's contractions). The mcCC method was then used to study a few benchmark systems. The results gathered from mcCC will be compared against results from other researchers as well as configuration interaction results to verify validity. For the sake of completeness, this chapter briefly summarizes concepts covered in previous chapters.

4.1 Introduction

Systems that are made up of more than one type of quantum mechanical particle are defined as multicomponent systems. Multicomponent systems are ubiquitous in chemistry. Atoms and molecules, which are the building blocks of complex chemical systems, contain both electrons and nuclei and are intrinsically multicomponent in

nature. Similarly, molecules bound to other sub-atomic particles, such as positrons bound to molecular substrates [71] and muon-substituted compounds [72] also form multicomponent systems. Multicomponent terminology can also be extended to systems containing quasiparticles, [73] such as multiexcitons which are useful for describing electronic excitations in many-electron systems.

A multicomponent system is intrinsically a collection of interacting single component systems. Consequently, it inherits all of the complexity associated with the treatment of correlation in single component systems. The central challenge in theoretical investigations of multicomponent systems is the accurate description of the particle-particle correlation that exists not only between identical particles but also between particles of different types. The multicomponent wave function is a mathematically complex quantity and it is desirable to introduce simplifications to the exact form of the wave function for practical applications. For molecules, the Born-Oppenheimer (BO) approximation is a well-known approximation that introduces parametric dependence of the nuclear coordinates in the electronic wave function. As a consequence of the BO approximation, the exact multicomponent Schrödinger equation can be expressed as a set of two coupled single component equations for electrons and nuclei, respectively. Although the BO is a very useful approximation, it is important to recognize that it is still an approximation and there is an ever-increasing collection of experimental and theoretical findings that demonstrate its limitations. [74, 75, 76, 77, 78, 79, 68, 80, 81, 82, 83, 84, 85, 86] There are also other multicomponent quantum mechanical systems where the BO approximation is not a useful approximation. For example, electron-positron [87, 88, 89, 90] and multiexcitonic (electron-hole) systems [91, 36, 92, 37, 35, 34, 44, 41, 42, 93, 94, 95, 39, 40, 69, 70, 38] are systems where introducing BO separation leads to an unacceptable deviation from qualitative results.

In this work, we focus on multicomponent treatment of only two different types of particles, which are denoted as type I and II for the remainder of this article. The approach assumes that the coordinates of the heavy nuclei are BO separated (BOS) from the coordinates of the type I and II particles. Consequently, the exact multicomponent wave function is approximately factored as

$$\Psi_{\text{exact}}(\mathbf{r}^{\text{I}}, \mathbf{r}^{\text{II}}, \mathbf{R}^{\text{BOS}}) \approx \Psi(\mathbf{r}^{\text{I}}, \mathbf{r}^{\text{II}}; \mathbf{R}^{\text{BOS}})\chi(\mathbf{R}^{\text{BOS}}). \quad (4.1)$$

In the above expression, BO separated coordinates are collectively represented as \mathbf{R}^{BOS} . The exact multicomponent Hamiltonian can be written as the sum of two operators

$$H_{\text{exact}}(\mathbf{r}^{\text{I}}, \mathbf{r}^{\text{II}}, \mathbf{R}^{\text{BOS}}) = H(\mathbf{r}^{\text{I}}, \mathbf{r}^{\text{II}}; \mathbf{R}^{\text{BOS}}) + T_{\mathbf{R}^{\text{BOS}}} \quad (4.2)$$

where, $T_{\mathbf{R}^{\text{BOS}}}$ is the kinetic energy operators associated with the BO separated coordinates. The general form of the Hamiltonian for the multicomponent system is defined as

$$H(\mathbf{r}^{\text{I}}, \mathbf{r}^{\text{II}}; \mathbf{R}^{\text{BOS}}) = H^{\text{I}}(\mathbf{r}^{\text{I}}; \mathbf{R}^{\text{BOS}}) + H^{\text{II}}(\mathbf{r}^{\text{II}}; \mathbf{R}^{\text{BOS}}) + V^{\text{I,II}}(\mathbf{r}^{\text{I}}, \mathbf{r}^{\text{II}}) \quad (4.3)$$

where H^{I} and H^{II} are single component Hamiltonians for particle type I and II, respectively. The interaction between the two types of particles is described by the potential energy term, $V^{\text{I,II}}$. The total multicomponent Hamiltonian also admits parametric dependence on coordinates of particles (denoted by \mathbf{R}^{BOS}) that have been assumed to be BO-separated (BOS) from type I and II particles in the multicomponent wave function. Consequently, the multicomponent Hamiltonian presented above does not contain any kinetic energy operators associated with the BOS coordinates. The BOS coordinates in H are the generators of the external potentials $v_{\text{ext}}^{\text{I}}(\mathbf{r}^{\text{I}}; \mathbf{R}^{\text{BOS}})$

and $v_{\text{ext}}^{\text{II}}(\mathbf{r}^{\text{II}}; \mathbf{R}^{\text{BOS}})$ experienced by the type I and II particles, respectively. For example, in the case of multicomponent molecular systems, type I and II particles can be represented by electrons and protons and the remaining nuclei in the molecules will be treated by the BOS coordinates. In the case of quasiparticle systems, the (quasi) electrons and holes are treated as type I and II particles while all the nuclei in the system are treated using BOS coordinates. In both cases, the BOS coordinates will be responsible for the generation of the external potential experienced by the type I and II particles. This form of the multicomponent Hamiltonian has been used to describe various multicomponent interactions such as electron-proton interaction, [96, 97, 98, 71, 99, 100, 101, 76, 102] electron-positron interaction, [87, 89, 90] and electron-hole quasiparticle interaction. [36, 92, 37, 35, 34, 70, 69, 38] It is important to note that this approach is different from other multicomponent approaches such as the exact factorization method [103, 104, 105, 106, 107, 108, 109, 110, 111] and multicomponent (N -particle) density functional theory [75] that involve non-BO treatment of all particle types in a chemical system.

The overarching goal of this work is to present an approximate solution of the following multicomponent Schrödinger equation

$$H\Psi(\mathbf{r}^{\text{I}}, \mathbf{r}^{\text{II}}; \mathbf{R}^{\text{BOS}}) = E(\mathbf{R}^{\text{BOS}})\Psi(\mathbf{r}^{\text{I}}, \mathbf{r}^{\text{II}}; \mathbf{R}^{\text{BOS}}) \quad (4.4)$$

using a multicomponent coupled-cluster (mcCC) ansatz for the many-particle wave function. Coupled-cluster (CC) theory has been used successfully for studying electron-electron correlation in many-electron systems. [112, 113, 114, 115, 116, 117, 118, 119, 120, 121, 7, 122, 123, 124, 125, 126] In the context of multicomponent systems, the CC ansatz provides a balanced framework for a size-consistent and size-extensive treatment of many-particle correlation. The general theory of multicomponent CC for molecular Hamiltonian has been described earlier by Monkhorst. [127]

Application of CC to excitons has also been demonstrated by Sundholm et al. [69] and Vänskä et al. [70] for a two-band effective mass approximation Hamiltonian model. In this work we present a systematic derivation of the mcCC equation that is based on a multicomponent Hartree-Fock vacuum state. Coupled-cluster theory is a well known method with a large body of literature that describes its theory and implementation in electronic structure theory. [58, 60, 128, 61, 129, 130, 131, 132] The focus of this article is not to repeat the well-known derivations, but to highlight the key differences between the single component (electronic structure) and multicomponent coupled-cluster equations. In this work, we used the mcCC method to calculate ground state energies of multicomponent Hooke's atom, positronium hydride, and to calculate exciton and biexciton binding energies in multiexcitonic systems. Multiexcitonic systems are of particular interest due to the tremendous potential they have in photovoltaic and light harvesting applications. Theoretical investigations have been performed using an array of methods including configuration interaction,[39, 91, 70, 93, 133] quantum Monte Carlo,[39, 40] path integral Monte Carlo,[41, 38] Green's functions,[134] pseudopotentials,[95, 135] and coupled-cluster theory. [136, 69, 70] For each case, the mcCC results were benchmarked against full configuration interaction (FCI) calculations. The derivation of the mcCC equations, computer implementation of the t-amplitude equations, and details of the multiexcitonic systems are presented in the following sections.

4.2 Theory

4.2.1 Construction of the vacuum states

The multicomponent Hamiltonian in second quantized notation is defined as

$$\begin{aligned}
 H = & \sum_{pq} \langle p | h^{\text{I}} | q \rangle p^\dagger q & (4.5) \\
 & + \sum_{pqrs} \langle pq | v^{\text{I,I}} | rs \rangle p^\dagger q^\dagger sr \\
 & + \sum_{p'q'} \langle p' | h^{\text{II}} | q' \rangle p'^\dagger q' \\
 & + \sum_{p'q'r's'} \langle p'q' | v^{\text{II,II}} | r's' \rangle p'^\dagger q'^\dagger s'r' \\
 & + \sum_{pp'q'q'} \langle pp' | v^{\text{I,II}} | qq' \rangle p^\dagger p'^\dagger qq'
 \end{aligned}$$

where, the unprimed and primed operators represent type I and II particles, respectively. The form of the 1-particle and 2-particle operators are given (in atomic units) as

$$h^\alpha(\mathbf{r}^\alpha, \mathbf{R}^{\text{BOS}}) = \frac{-\hbar}{2m_\alpha} \nabla_\alpha^2 + v_{\text{ext}}^\alpha(\mathbf{r}^\alpha, \mathbf{R}^{\text{BOS}}) \quad \alpha = \text{I, II}, \quad (4.6)$$

$$v^{\alpha,\alpha}(\mathbf{r}^\alpha) = q^\alpha q^\alpha \epsilon^{-1} r_{\alpha\alpha}^{-1}, \quad (4.7)$$

$$v^{\text{I,II}}(\mathbf{r}^{\text{I}}, \mathbf{r}^{\text{II}}) = q^{\text{I}} q^{\text{II}} \epsilon^{-1} r_{\text{I,II}}^{-1}. \quad (4.8)$$

For electron-nuclear and electron-positron systems, the dielectric function is a constant ($\epsilon = 1$). For multiexcitonic systems, the electron-hole interaction is screened, and the screening can be described either by a constant dielectric value[92, 36, 137] or by a position dependent dielectric function. [94, 95]

We define the mcCC wave function by the following exponential ansatz,

$$\Psi_{\text{mcCC}}^{\text{I,II}}(\mathbf{r}^{\text{I}}, \mathbf{r}^{\text{II}}; \mathbf{R}^{\text{BOS}}) = e^{T^{\text{I,II}}} \Phi_0^{\text{I,II}}(\mathbf{r}^{\text{I}}, \mathbf{r}^{\text{II}}; \mathbf{R}^{\text{BOS}}), \quad (4.9)$$

where the BOS coordinates are shown explicitly using the standard semicolon convention. Traditionally in single-reference electronic structure coupled-cluster theory, the vacuum state Φ_0 is obtained from a Hartree-Fock (HF) calculation. For multicomponent systems, there are two different ways to construct the single component vacuum state. The first method involves the Hartree-Fock solution of the single component Hamiltonian as shown below with the states labeled as $|\tilde{0}^{\text{I}}\rangle$ and $|\tilde{0}^{\text{II}}\rangle$ for type I and II particles

$$\langle \tilde{0}^{\text{I}} | H^{\text{I}} | \tilde{0}^{\text{I}} \rangle = \min_{\Phi_{\text{SD}}^{\text{I}}} \langle \Phi_{\text{SD}}^{\text{I}} | H^{\text{I}} | \Phi_{\text{SD}}^{\text{I}} \rangle, \quad (4.10)$$

$$\langle \tilde{0}^{\text{II}} | H^{\text{II}} | \tilde{0}^{\text{II}} \rangle = \min_{\Phi_{\text{SD}}^{\text{II}}} \langle \Phi_{\text{SD}}^{\text{II}} | H^{\text{II}} | \Phi_{\text{SD}}^{\text{II}} \rangle. \quad (4.11)$$

The minimization in the above equations is performed over a set of single Slater determinants (Φ_{SD}). The total vacuum energy the above determinants is given as

$$\langle \tilde{0}^{\text{I}} \tilde{0}^{\text{II}} | H | \tilde{0}^{\text{I}} \tilde{0}^{\text{II}} \rangle = \langle \tilde{0}^{\text{I}} | H^{\text{I}} | \tilde{0}^{\text{I}} \rangle + \langle \tilde{0}^{\text{II}} | H^{\text{II}} | \tilde{0}^{\text{II}} \rangle + \langle \tilde{0}^{\text{I}} \tilde{0}^{\text{II}} | V^{\text{I,II}} | \tilde{0}^{\text{I}} \tilde{0}^{\text{II}} \rangle. \quad (4.12)$$

The second method for construction of the single component vacuum states is by solution of the multicomponent HF equation. We label these determinants by as $|0^{\text{I}}\rangle$ and $|0^{\text{II}}\rangle$ for type I and II particles, respectively and they are determined using the following energy minimization procedure

$$\langle 0^{\text{I}} 0^{\text{II}} | H | 0^{\text{I}} 0^{\text{II}} \rangle = \min_{\Phi_{\text{SD}}^{\text{I}}, \Phi_{\text{SD}}^{\text{II}}} \langle \Phi_{\text{SD}}^{\text{I}} \Phi_{\text{SD}}^{\text{II}} | H | \Phi_{\text{SD}}^{\text{I}} \Phi_{\text{SD}}^{\text{II}} \rangle. \quad (4.13)$$

The vacuum state $|0^I 0^{\text{II}}\rangle$ constructed from the multicomponent HF should be lower in energy than the vacuum state $|\tilde{0}^I \tilde{0}^{\text{II}}\rangle$ obtained using the single component HF method due to the variational principle,

$$\langle 0^I 0^{\text{II}} | H | 0^I 0^{\text{II}} \rangle \leq \langle \tilde{0}^I \tilde{0}^{\text{II}} | H | \tilde{0}^I \tilde{0}^{\text{II}} \rangle. \quad (4.14)$$

Because of this property, we have used multicomponent HF for construction of the single component vacuum states in all the calculations presented in [section 4.5](#). Multicomponent HF method has been used in earlier work for treating electron-proton correlation and the details of the method are not presented here to avoid repetition. [\[68, 77, 76, 138\]](#)

4.2.2 Effective normal-ordered Hamiltonian

The use of multicomponent HF instead of single component HF as the vacuum state has important implications on the general form of the CC equations, the vacuum energy, and the normal-ordering of the operators. The minimization procedure for multicomponent HF (shown in Eq. [\(4.13\)](#)) results in Fock operators for type I and II particles and is given as,

$$f^{\text{I}} = h^{\text{I}} + v_{\text{HF}}^{\text{I}} + \sum_{j'=1}^{N^{\text{II}}} \langle j' | v^{\text{I,II}} | j' \rangle \quad (4.15)$$

$$f^{\text{II}} = h^{\text{II}} + v_{\text{HF}}^{\text{II}} + \sum_{j=1}^{N^{\text{I}}} \langle j | v^{\text{I,II}} | j \rangle. \quad (4.16)$$

However, the Fock operators for the two types of particles are not independent of each other and are coupled because of the presence of the I-II coupling term. The

mcHF calculation is performed by iterative solution of the coupled SCF equation

$$f^I \chi_i^I = \epsilon_i^I \chi_i^I \quad (4.17)$$

$$f^{II} \chi_{i'}^{II} = \epsilon_{i'}^{II} \chi_{i'}^{II}. \quad (4.18)$$

The eigenfunction of the multicomponent Fock operators from Eq. (4.15) and Eq. (4.16) are used as the single-particle states in representing the creation and annihilation operators. The total vacuum energy obtained from the SCF step is additive and is made up of three components

$$\langle 0^I 0^{II} | H | 0^I 0^{II} \rangle = \langle 0^I 0^{II} | H^I | 0^I 0^{II} \rangle + \langle 0^I 0^{II} | H^{II} | 0^I 0^{II} \rangle + \langle 0^I 0^{II} | V^{I,II} | 0^I 0^{II} \rangle. \quad (4.19)$$

This relationship will be used in the definition of the normal-ordered Hamiltonian. Using Eq. (5.1), the single component normal ordered Hamiltonian is defined as

$$H^I = H_N^I + \langle 0^I | H^I | 0^I \rangle \quad (4.20)$$

where

$$H_N^I = \sum_{pq} \langle p | h^I | q \rangle \{ p^\dagger q \} + \sum_{pqi} \langle pi | v^{I,I} | qi \rangle_A \{ p^\dagger q \} + \frac{1}{4} \sum_{pqrs} \langle pq | v^{I,I} | rs \rangle_A \{ p^\dagger q^\dagger sr \} \quad (4.21)$$

The subscript "A" implies that both symmetric and antisymmetric combination of the integral are included in the expression shown below

$$\langle pq | v^{I,I} | rs \rangle_A = \langle pq | v^{I,I} | rs \rangle - \langle pq | v^{I,I} | sr \rangle. \quad (4.22)$$

The type I-II coupling operator in Eq. (7.32) can be expressed as the sum of three normal-ordered operators as shown below

$$V^{I,II} = V_N^{I,II} + W_N^I + W_N^{II} + \langle 00' | V^{I,II} | 00' \rangle \quad (4.23)$$

where

$$V_N^{I,II} = \sum_{pq} \sum_{p'q'} \langle pp' | v^{I,II} | qq' \rangle \{p^\dagger q\} \{p'^\dagger q'\} \quad (4.24)$$

$$W_N^I = \sum_{pq} \sum_{i'} \langle pi' | v^{I,II} | qi' \rangle \{p^\dagger q\} \quad (4.25)$$

$$W_N^{II} = \sum_i \sum_{p'q'} \langle ip' | v^{I,II} | iq' \rangle \{p'^\dagger q'\} \quad (4.26)$$

The total multicomponent Hamiltonian can then be written as sum of following normal-ordered operators,

$$H = H_N^I + H_N^{II} + V_N^{I,II} + W_N^I + W_N^{II} + \langle 0^I 0^{II} | H | 0^I 0^{II} \rangle \quad (4.27)$$

It is useful to define the following effective single component Hamiltonians \tilde{H}_N^I and \tilde{H}_N^{II} by incorporating W_N terms in expressions

$$\tilde{H}_N^I = H_N^I + W_N^I \quad (4.28)$$

$$\tilde{H}_N^{II} = H_N^{II} + W_N^{II}. \quad (4.29)$$

Using the above relationship, the total normal-ordered Hamiltonian is defined as

$$\tilde{H}_N = H - \langle 0^I 0^{II} | H | 0^I 0^{II} \rangle \quad (4.30)$$

$$= \tilde{H}_N^I + \tilde{H}_N^{II} + V_N^{I,II}. \quad (4.31)$$

4.2.3 The mcCC Equations

Using the normal-ordered Hamiltonian, the CC equation can be written in terms of the total correlation energy ΔE_{mcCC}

$$\tilde{H}_N e^T |0^I 0^{II}\rangle = \Delta E_{\text{mcCC}} e^T |0^I 0^{II}\rangle \quad (4.32)$$

where $\Delta E_{\text{mcCC}} = E_{\text{mcCC}} - \langle 0^I 0^{II} | H | 0^I 0^{II} \rangle$ and T is the cluster operator. In this work, we restrict the form of the cluster operator to include only single and double excitations as shown below

$$T = \sum_{ij}^2 \left[T_{ij}^{I,II} + (T_i^I + T_i^{II}) \delta_{ij} \right] \quad (4.33)$$

$$= T_1^I + T_2^I + T_1^{II} + T_2^{II} + T_{11}^{I,II} + T_{12}^{I,II} + T_{21}^{I,II} + T_{22}^{I,II}. \quad (4.34)$$

The T_1^I and T_2^I operators are identical to the single component CCSD operators and operate only on the type I space. The same holds true for the corresponding type II operators. The indices i, j are summed over the occupied space denoted by N while a, b indices are summed over the virtual space, M . The type II operators have primed indices to distinguish them from their type I counterparts.

$$T_1^I = \sum_i^N \sum_a^M t_i^a \{a^\dagger i\} \quad (4.35)$$

$$T_2^I = \frac{1}{4} \sum_{ij}^N \sum_{ab}^M t_{ij}^{ab} \{a^\dagger b^\dagger ji\} \quad (4.36)$$

$$T_1^{II} = \sum_{i'}^{N'} \sum_{a'}^{M'} t_{i'}^{a'} \{a'^\dagger i'\} \quad (4.37)$$

$$T_2^{\text{II}} = \frac{1}{4} \sum_{i'j'}^{N'} \sum_{a'b'}^{M'} t_{i'j'}^{a'b'} \{a'^{\dagger} b'^{\dagger} j' i'\} \quad (4.38)$$

The type I,II operators produce connected excitations in both the type I and II spaces.

These operators are expanded below,

$$T_{11}^{\text{I,II}} = \sum_i^N \sum_a^M \sum_{i'}^{N'} \sum_{a'}^{M'} t_{ii'}^{aa'} \{a^{\dagger} i\} \{a'^{\dagger} i'\} \quad (4.39)$$

$$T_{12}^{\text{I,II}} = \frac{1}{4} \sum_i^N \sum_a^M \sum_{i'j'}^{N'} \sum_{a'b'}^{M'} t_{ii'j'}^{aa'b'} \{a^{\dagger} i\} \{a'^{\dagger} b'^{\dagger} j' i'\} \quad (4.40)$$

$$T_{21}^{\text{I,II}} = \frac{1}{4} \sum_{ij}^N \sum_{ab}^M \sum_{i'}^{N'} \sum_{a'}^{M'} t_{ij i'}^{aa'b'} \{a^{\dagger} b^{\dagger} j i\} \{a'^{\dagger} i'\} \quad (4.41)$$

$$T_{22}^{\text{I,II}} = \frac{1}{16} \sum_{ij}^N \sum_{ab}^M \sum_{i'j'}^{N'} \sum_{a'b'}^{M'} t_{ij i' j'}^{aba'b'} \{a^{\dagger} b^{\dagger} j i\} \{a'^{\dagger} b'^{\dagger} j' i'\} \quad (4.42)$$

The cluster operator, as presented above, defines a multicomponent CCSD space.

The energy and the t amplitude expressions can be obtained by performing similarity-transformation on the normal-ordered Hamiltonian from Eq. (4.30),

$$e^{-T} \tilde{H}_N e^T |0^{\text{I}} 0^{\text{II}}\rangle = \Delta E_{\text{mcCC}} |0^{\text{I}} 0^{\text{II}}\rangle \quad (4.43)$$

which can be evaluated using the standard Baker-Campbell-Hausdorff (BCH) expansion[61, 60] shown below,

$$e^{-T} \tilde{H}_N e^T = \tilde{H}_N + [\tilde{H}_N, T] + \frac{1}{2} [[\tilde{H}_N, T], T] + \frac{1}{3!} [[[\tilde{H}_N, T], T], T] + \frac{1}{4!} [[[[\tilde{H}_N, T], T], T], T] \quad (4.44)$$

However, because of the multicomponent nature of the system, the number of terms in the BCH expansion is much larger than the single component expression. Substituting the expression with the Hamiltonian in Eq. (4.30) and the t amplitudes from Eq. (4.34), we arrive at the following set of equations,

$$[\tilde{H}_N, T] = \left[\sum_{K_1}^3 \tilde{H}_N^{(K_1)}, \sum_{L_1}^8 T^{(L_1)} \right] = \sum_{K_1}^3 \sum_{L_1}^8 [\tilde{H}_N^{(K_1)}, T^{(L_1)}] \quad (4.45)$$

$$[[\tilde{H}_N, T], T] = \sum_{K_1}^3 \sum_{L_1, L_2}^8 [[\tilde{H}_N^{(K_1)}, T^{(L_1)}], T^{(L_2)}] \quad (4.46)$$

$$[[[\tilde{H}_N, T], T], T] = \sum_{K_1}^3 \sum_{L_1, L_2, L_3}^8 [[[\tilde{H}_N^{(K_1)}, T^{(L_1)}], T^{(L_2)}], T^{(L_3)}] \quad (4.47)$$

$$[[[[\tilde{H}_N, T], T], T], T] = \sum_{K_1}^2 \sum_{L_1, L_2, L_3, L_4}^8 [[[[\tilde{H}_N^{(K_1)}, T^{(L_1)}], T^{(L_2)}], T^{(L_3)}], T^{(L_4)}] \quad (4.48)$$

where $\tilde{H}_N^{(K)}$ and $T^{(L)}$ are compact notations for the Hamiltonian and cluster operator and are defined as

$$\tilde{H}_N = \sum_K^3 \tilde{H}_N^{(K)} = \tilde{H}_N^I + \tilde{H}_N^{II} + V_N^{I,II} \quad (4.49)$$

$$T = \sum_L^8 T^{(L)} = T_1^I + T_2^I + T_1^{II} + T_2^{II} + T_{11}^{I,II} + T_{12}^{I,II} + T_{21}^{I,II} + T_{22}^{I,II}. \quad (4.50)$$

For the present ansatz of the mCC wave function, the number of commutators in the above expression is 9940 terms. However, not all of these terms contribute in all the

equations mentioned above, and the list of contributing terms in Eqs. (5.10)-(4.60) are presented in the supporting information.

The solution of the BCH expansion for the total multicomponent correlation energy results in the following expression,

$$\begin{aligned} \Delta E_{\text{mcCC}} = & \langle 0^{\text{I}}0^{\text{II}} | \tilde{H}_{\text{N}}^{\text{I}} [T_1^{\text{I}} + \frac{1}{2!} T_1^{\text{I}2} + T_2^{\text{I}}] | 0^{\text{I}}0^{\text{II}} \rangle \\ & + \langle 0^{\text{I}}0^{\text{II}} | \tilde{H}_{\text{N}}^{\text{II}} [T_1^{\text{II}} + \frac{1}{2!} T_1^{\text{II}2} + T_2^{\text{II}}] | 0^{\text{I}}0^{\text{II}} \rangle \\ & + \langle 0^{\text{I}}0^{\text{II}} | V_{\text{N}}^{\text{I,II}} [T_{11}^{\text{I,II}} + T_1^{\text{I}} + T_1^{\text{I}}T_1^{\text{II}} + T_1^{\text{II}}] | 0^{\text{I}}0^{\text{II}} \rangle. \end{aligned} \quad (4.51)$$

As expected, the total correlation energy can be written as the sum of correlation energies from the two components and the interaction between the two components. Analogous to the electronic CCSD expression, the correlation energies for type I and type II particles depend only on t_1 and t_2 amplitudes. In contrast, the contribution from I-II interaction depends only on t_1 and t_{11} amplitudes. It is important to note that although the expression for the type I correlation energy is identical to electronic CCSD, the t amplitudes in the expressions are not independent of type II t amplitudes but depend on type II amplitudes via Eq. (5.11) and Eq. (5.12). The determination of the total correlation energy depends on the converged t amplitude equations which require the simultaneous solution of a set of non-linear, coupled equations. Obtaining the t amplitude equations require projecting the similarity-transformed Hamiltonian onto a series of excited states denoted by $\langle K^{\text{I}}K^{\text{II}} |$. The following set of equations is the result of choosing $\langle K^{\text{I}}K^{\text{II}} |$ to be all combinations of vacuum, singly, and doubly excited states (represented as 0, S , and D , respectively) in both type I and type II

space.

$$\langle 0^I 0^{II} | e^{-T} \tilde{H}_N e^T | 0^I 0^{II} \rangle_c = \Delta E_{\text{mcCC}} \quad \text{correlation energy equation} \quad (4.52)$$

$$\langle S^I 0^{II} | e^{-T} \tilde{H}_N e^T | 0^I 0^{II} \rangle_c = 0 \quad t_1^I \quad \text{amplitude equation} \quad (4.53)$$

$$\langle D^I 0^{II} | e^{-T} \tilde{H}_N e^T | 0^I 0^{II} \rangle_c = 0 \quad t_2^I \quad \text{amplitude equation} \quad (4.54)$$

$$\langle 0^I S^{II} | e^{-T} \tilde{H}_N e^T | 0^I 0^{II} \rangle_c = 0 \quad t_1^{II} \quad \text{amplitude equation} \quad (4.55)$$

$$\langle 0^I D^{II} | e^{-T} \tilde{H}_N e^T | 0^I 0^{II} \rangle_c = 0 \quad t_2^{II} \quad \text{amplitude equation} \quad (4.56)$$

$$\langle S^I S^{II} | e^{-T} \tilde{H}_N e^T | 0^I 0^{II} \rangle_c = 0 \quad t_{11}^{I,II} \quad \text{amplitude equation} \quad (4.57)$$

$$\langle S^I D^{II} | e^{-T} \tilde{H}_N e^T | 0^I 0^{II} \rangle_c = 0 \quad t_{12}^{I,II} \quad \text{amplitude equation} \quad (4.58)$$

$$\langle D^I S^{II} | e^{-T} \tilde{H}_N e^T | 0^I 0^{II} \rangle_c = 0 \quad t_{21}^{I,II} \quad \text{amplitude equation} \quad (4.59)$$

$$\langle D^I D^{II} | e^{-T} \tilde{H}_N e^T | 0^I 0^{II} \rangle_c = 0 \quad t_{22}^{I,II} \quad \text{amplitude equation} \quad (4.60)$$

The expanded forms of these equations are shown below.

Energy expression ($\langle 0^I 0^{II} | e^{-T} H_N e^T | 0^I 0^{II} \rangle = \Delta E_{\text{mcCC}}$)

$$\langle 0^I 0^{II} | V_N^{I,II} [1 + T_{11}^{I,II} + T_1^I + T_1^I T_1^{II} + T_1^{II}] + \tilde{H}_N^{II} [1 + T_1^{II} + \frac{1}{2!} T_1^{II^2} + T_2^{II}] + \tilde{H}_N^I [1 + T_1^I + \frac{1}{2!} T_1^{I^2} + T_2^I] | 0^I 0^{II} \rangle = \Delta E_{\text{mcCC}}$$

Type I single amplitude ($\langle S^I 0^{II} | e^{-T} H_N e^T | 0^I 0^{II} \rangle = 0$)

$$\begin{aligned} & \langle S^I 0^{II} | V_N^{I,II} [1 + T_{11}^{I,II} + T_1^I + T_1^I T_{11}^{I,II} + T_1^I T_1^{II} + \frac{1}{2!} T_1^{I^2} + \frac{1}{2!} T_1^{I^2} T_1^{II} + T_1^{II} + T_{21}^{I,II} + T_2^I + T_2^I T_1^{II}] \\ & + [(-T_1^I)] V_N^{I,II} [1 + T_{11}^{I,II} + T_1^I + T_1^I T_1^{II} + T_1^{II}] + \tilde{H}_N^{II} [T_{11}^{I,II} + T_{12}^{I,II} + T_1^I + T_1^I T_1^{II} + T_1^I \frac{1}{2!} T_1^{II^2} \\ & + T_1^I T_2^{II} + T_1^{II} T_{11}^{I,II}] + [(-T_1^I)] \tilde{H}_N^{II} [1 + T_1^{II} + \frac{1}{2!} T_1^{II^2} + T_2^{II}] + \tilde{H}_N^I [1 + T_1^I + T_1^I T_2^I + \frac{1}{2!} T_1^{I^2} + \\ & \frac{1}{3!} T_1^{I^3} + T_2^I] + [(-T_1^I)] \tilde{H}_N^I [1 + T_1^I + \frac{1}{2!} T_1^{I^2} + T_2^I] | 0^I 0^{II} \rangle = 0 \end{aligned}$$

Type I double amplitude ($\langle D^I 0^{II} | e^{-T} H_N e^T | 0^I 0^{II} \rangle = 0$)

$$\begin{aligned} & \langle D^I 0^{II} | V_N^{I,II} [T_{11}^{I,II} + T_1^I + T_1^I T_{11}^{I,II} + T_1^I T_1^{II} + T_1^I T_{21}^{I,II} + T_1^I T_2^I + T_1^I T_2^I T_1^{II} + \frac{1}{2!} T_1^{I^2} + \frac{1}{2!} T_1^{I^2} T_{11}^{I,II} \\ & + \frac{1}{2!} T_1^{I^2} T_1^{II} + \frac{1}{3!} T_1^{I^3} + \frac{1}{3!} T_1^{I^3} T_1^{II} + T_{21}^{I,II} + T_2^I + T_2^I T_{11}^{I,II} + T_2^I T_1^{II}] + [(-T_2^I)] V_N^{I,II} [1 + T_{11}^{I,II} + T_1^I \end{aligned}$$

$$\begin{aligned}
& + T_1^I T_1^{II} + T_1^{II} + [(-T_1^I)] V_N^{I,II} [1 + T_{11}^{I,II} + T_1^I + T_1^I T_{11}^{I,II} + T_1^I T_1^{II} + \frac{1}{2!} T_1^{I^2} + \frac{1}{2!} T_1^{I^2} T_1^{II} + T_1^{II} \\
& + T_{21}^{I,II} + T_2^I + T_2^I T_1^{II}] + [\frac{1}{2!} T_1^{I^2}] V_N^{I,II} [1 + T_{11}^{I,II} + T_1^I + T_1^I T_1^{II} + T_1^{II}] + \tilde{H}_N^{II} [T_1^I T_{11}^{I,II} + T_1^I T_{12}^{I,II} \\
& + T_1^I T_1^{II} T_{11}^{I,II} + \frac{1}{2!} T_1^{I^2} + \frac{1}{2!} T_1^{I^2} T_1^{II} + \frac{1}{2!} T_1^{I^2} \frac{1}{2!} T_1^{II^2} + \frac{1}{2!} T_1^{I^2} T_2^{II} + T_1^{II} T_{21}^{I,II} + T_{21}^{I,II} + T_{22}^{I,II} + T_2^I + \\
& T_2^I T_1^{II} + T_2^I \frac{1}{2!} T_1^{II^2} + T_2^I T_2^{II}] + [(-T_2^I)] \tilde{H}_N^{II} [1 + T_1^{II} + \frac{1}{2!} T_1^{II^2} + T_2^{II}] + [(-T_1^I)] \tilde{H}_N^{II} [T_{11}^{I,II} + T_{12}^{I,II} \\
& + T_1^I + T_1^I T_1^{II} + T_1^I \frac{1}{2!} T_1^{II^2} + T_1^I T_2^{II} + T_1^{II} T_{11}^{I,II}] + [\frac{1}{2!} T_1^{I^2}] \tilde{H}_N^{II} [1 + T_1^{II} + \frac{1}{2!} T_1^{II^2} + T_2^{II}] + \tilde{H}_N^I [1 \\
& + T_1^I + T_1^I T_2^I + \frac{1}{2!} T_1^{I^2} + \frac{1}{2!} T_1^{I^2} T_2^I + \frac{1}{3!} T_1^{I^3} + \frac{1}{4!} T_1^{I^4} + T_2^I + \frac{1}{2!} T_2^{I^2}] + [(-T_2^I)] \tilde{H}_N^I [1 + T_1^I + \frac{1}{2!} T_1^{I^2} \\
& + T_2^I] + [(-T_1^I)] \tilde{H}_N^I [1 + T_1^I + T_1^I T_2^I + \frac{1}{2!} T_1^{I^2} + \frac{1}{3!} T_1^{I^3} + T_2^I] + [\frac{1}{2!} T_1^{I^2}] \tilde{H}_N^I [1 + T_1^I + \frac{1}{2!} T_1^{I^2} + \\
& T_2^I] |0^I 0^{II}\rangle = 0
\end{aligned}$$

Type II single amplitude ($\langle 0^I S^{II} | e^{-T} H_N e^T | 0^I 0^{II} \rangle = 0$)

$$\begin{aligned}
& \langle 0^I S^{II} | V_N^{I,II} [1 + T_{11}^{I,II} + T_{12}^{I,II} + T_1^I + T_1^I T_1^{II} + T_1^I \frac{1}{2!} T_1^{II^2} + T_1^I T_2^{II} + T_1^{II} + T_1^{II} T_{11}^{I,II} + \frac{1}{2!} T_1^{II^2} + \\
& T_2^{II}] + [(-T_1^{II})] V_N^{I,II} [1 + T_{11}^{I,II} + T_1^I + T_1^I T_1^{II} + T_1^{II}] + \tilde{H}_N^{II} [1 + T_1^{II} + T_1^{II} T_2^{II} + \frac{1}{2!} T_1^{II^2} + \frac{1}{3!} T_1^{II^3} \\
& + T_2^{II}] + [(-T_1^{II})] \tilde{H}_N^{II} [1 + T_1^{II} + \frac{1}{2!} T_1^{II^2} + T_2^{II}] + \tilde{H}_N^I [T_{11}^{I,II} + T_1^I T_{11}^{I,II} + T_1^I T_1^{II} + \frac{1}{2!} T_1^{I^2} T_1^{II} + \\
& T_1^{II} + T_{21}^{I,II} + T_2^I T_1^{II}] + [(-T_1^{II})] \tilde{H}_N^I [1 + T_1^I + \frac{1}{2!} T_1^{I^2} + T_2^I] |0^I 0^{II}\rangle = 0
\end{aligned}$$

Type II double amplitude ($\langle 0^I D^{II} | e^{-T} H_N e^T | 0^I 0^{II} \rangle = 0$)

$$\begin{aligned}
& \langle 0^I D^{II} | V_N^{I,II} [T_{11}^{I,II} + T_{12}^{I,II} + T_1^I T_1^{II} + T_1^I T_1^{II} T_2^{II} + T_1^I \frac{1}{2!} T_1^{II^2} + T_1^I \frac{1}{3!} T_1^{II^3} + T_1^I T_2^{II} + T_1^{II} + T_1^{II} T_{11}^{I,II} \\
& + T_1^{II} T_{12}^{I,II} + T_1^{II} T_2^{II} + \frac{1}{2!} T_1^{II^2} + \frac{1}{2!} T_1^{II^2} T_{11}^{I,II} + \frac{1}{3!} T_1^{II^3} + T_2^{II} + T_2^{II} T_{11}^{I,II}] + [(-T_2^{II})] V_N^{I,II} [1 + T_{11}^{I,II} \\
& + T_1^I + T_1^I T_1^{II} + T_1^{II}] + [(-T_1^{II})] V_N^{I,II} [1 + T_{11}^{I,II} + T_{12}^{I,II} + T_1^I + T_1^I T_1^{II} + T_1^I \frac{1}{2!} T_1^{II^2} + T_1^I T_2^{II} + \\
& T_1^{II} + T_1^{II} T_{11}^{I,II} + \frac{1}{2!} T_1^{II^2} + T_2^{II}] + [\frac{1}{2!} T_1^{II^2}] V_N^{I,II} [1 + T_{11}^{I,II} + T_1^I + T_1^I T_1^{II} + T_1^{II}] + \tilde{H}_N^{II} [1 + T_1^{II} \\
& + T_1^{II} T_2^{II} + \frac{1}{2!} T_1^{II^2} + \frac{1}{2!} T_1^{II^2} T_2^{II} + \frac{1}{3!} T_1^{II^3} + \frac{1}{4!} T_1^{II^4} + T_2^{II} + \frac{1}{2!} T_2^{II^2}] + [(-T_2^{II})] \tilde{H}_N^{II} [1 + T_1^{II} + \\
& \frac{1}{2!} T_1^{II^2} + T_2^{II}] + [(-T_1^{II})] \tilde{H}_N^{II} [1 + T_1^{II} + T_1^{II} T_2^{II} + \frac{1}{2!} T_1^{II^2} + \frac{1}{3!} T_1^{II^3} + T_2^{II}] + [\frac{1}{2!} T_1^{II^2}] \tilde{H}_N^{II} [1 + \\
& T_1^{II} + \frac{1}{2!} T_1^{II^2} + T_2^{II}] + \tilde{H}_N^I [T_{12}^{I,II} + T_1^I T_{12}^{I,II} + T_1^I T_1^{II} T_{11}^{I,II} + T_1^I \frac{1}{2!} T_1^{II^2} + T_1^I T_2^{II} + \frac{1}{2!} T_1^{I^2} \frac{1}{2!} T_1^{II^2} + \\
& \frac{1}{2!} T_1^{I^2} T_2^{II} + T_1^{II} T_{11}^{I,II} + T_1^{II} T_{21}^{I,II} + \frac{1}{2!} T_1^{II^2} + T_{22}^{I,II} + T_2^I \frac{1}{2!} T_1^{II^2} + T_2^I T_2^{II} + T_2^{II}] + [(-T_2^{II})] \tilde{H}_N^I [1 + \\
& T_1^I + \frac{1}{2!} T_1^{I^2} + T_2^I] + [(-T_1^{II})] \tilde{H}_N^I [T_{11}^{I,II} + T_1^I T_{11}^{I,II} + T_1^I T_1^{II} + \frac{1}{2!} T_1^{I^2} T_1^{II} + T_1^{II} + T_{21}^{I,II} + T_2^I T_{11}^{I,II}] \\
& + [\frac{1}{2!} T_1^{I^2}] \tilde{H}_N^I [1 + T_1^I + \frac{1}{2!} T_1^{I^2} + T_2^I] |0^I 0^{II}\rangle = 0
\end{aligned}$$

Type I, II single, single amplitude ($\langle S^I S^{II} | e^{-T} H_N e^T | 0^I 0^{II} \rangle = 0$)

$$\begin{aligned}
& \langle S^I S^{II} | V_N^{I,II} [1 + T_{11}^{I,II} + T_{12}^{I,II} + T_1^I + T_1^I T_{11}^{I,II} + T_1^I T_{12}^{I,II} + T_1^I T_1^{II} + T_1^I T_1^{II} T_{11}^{I,II} + T_1^I \frac{1}{2!} T_1^{II^2} + \\
& T_1^I T_2^{II} + \frac{1}{2!} T_1^I{}^2 + \frac{1}{2!} T_1^I{}^2 T_1^{II} + \frac{1}{2!} T_1^I{}^2 \frac{1}{2!} T_1^{II^2} + \frac{1}{2!} T_1^I{}^2 T_2^{II} + T_1^I + T_1^{II} T_{11}^{I,II} + T_1^{II} T_{21}^{I,II} + \frac{1}{2!} T_1^{II^2} + \\
& T_{21}^{I,II} + T_{22}^{I,II} + T_2^I + T_2^I T_1^{II} + T_2^I \frac{1}{2!} T_1^{II^2} + T_2^I T_2^{II} + T_2^{II}] + [(-T_{11}^{I,II})] V_N^{I,II} [1 + T_{11}^{I,II} + T_1^I + T_1^I T_1^{II} \\
& + T_1^{II}] + [(-T_1^I)] V_N^{I,II} [1 + T_{11}^{I,II} + T_1^I + T_1^I T_{11}^{I,II} + T_1^I T_1^{II} + \frac{1}{2!} T_1^I{}^2 + \frac{1}{2!} T_1^I{}^2 T_1^{II} + T_1^I + T_{21}^{I,II} + T_2^I \\
& + T_2^I T_1^{II}] + [(-T_1^I)] V_N^{I,II} [1 + T_{11}^{I,II} + T_{12}^{I,II} + T_1^I + T_1^I T_1^{II} + T_1^I \frac{1}{2!} T_1^{II^2} + T_1^I T_2^{II} + T_1^I + T_1^{II} T_{11}^{I,II} \\
& + \frac{1}{2!} T_1^{II^2} + T_2^I] + [(-T_1^I)(-T_1^{II})] V_N^{I,II} [1 + T_{11}^{I,II} + T_1^I + T_1^I T_1^{II} + T_1^{II}] + \tilde{H}_N^{II} [T_{11}^{I,II} + T_{12}^{I,II} + \\
& T_1^I + T_1^I T_1^{II} + T_1^I T_1^{II} T_2^{II} + T_1^I \frac{1}{2!} T_1^{II^2} + T_1^I \frac{1}{3!} T_1^{II^3} + T_1^I T_2^{II} + T_1^{II} T_{11}^{I,II} + T_1^{II} T_{12}^{I,II} + \frac{1}{2!} T_1^{II^2} T_{11}^{I,II} + \\
& T_2^{II} T_{11}^{I,II}] + [(-T_{11}^{I,II})] \tilde{H}_N^{II} [1 + T_1^I + \frac{1}{2!} T_1^{II^2} + T_2^{II}] + [(-T_1^I)] \tilde{H}_N^{II} [T_{11}^{I,II} + T_{12}^{I,II} + T_1^I + T_1^I T_1^{II} \\
& + T_1^I \frac{1}{2!} T_1^{II^2} + T_1^I T_2^{II} + T_1^{II} T_{11}^{I,II}] + [(-T_1^I)] \tilde{H}_N^{II} [1 + T_1^{II} + T_1^{II} T_2^{II} + \frac{1}{2!} T_1^{II^2} + \frac{1}{3!} T_1^{II^3} + T_2^{II}] + \\
& [(-T_1^I)(-T_1^{II})] \tilde{H}_N^{II} [1 + T_1^{II} + \frac{1}{2!} T_1^{II^2} + T_2^{II}] + \tilde{H}_N^I [T_{11}^{I,II} + T_1^I T_{11}^{I,II} + T_1^I T_1^{II} + T_1^I T_{21}^{I,II} + T_1^I T_2^I T_1^{II} \\
& + \frac{1}{2!} T_1^I{}^2 T_{11}^{I,II} + \frac{1}{2!} T_1^I{}^2 T_1^{II} + \frac{1}{3!} T_1^I{}^3 T_1^{II} + T_1^I + T_{21}^{I,II} + T_2^I T_{11}^{I,II} + T_2^I T_1^{II}] + [(-T_{11}^{I,II})] \tilde{H}_N^I [1 + T_1^I \\
& + \frac{1}{2!} T_1^I{}^2 + T_2^I] + [(-T_1^{II})] \tilde{H}_N^I [1 + T_1^I + T_1^I T_2^I + \frac{1}{2!} T_1^I{}^2 + \frac{1}{3!} T_1^I{}^3 + T_2^I] + [(-T_1^I)] \tilde{H}_N^I [T_{11}^{I,II} + \\
& T_1^I T_{11}^{I,II} + T_1^I T_1^{II} + \frac{1}{2!} T_1^I{}^2 T_1^{II} + T_1^{II} + T_{21}^{I,II} + T_2^I T_1^{II}] + [(-T_1^I)(-T_1^{II})] \tilde{H}_N^I [1 + T_1^I + \frac{1}{2!} T_1^I{}^2 + \\
& T_2^I] | 0^I 0^{II} \rangle = 0
\end{aligned}$$

Type I, II single, double amplitude ($\langle S^I D^{II} | e^{-T} H_N e^T | 0^I 0^{II} \rangle = 0$)

$$\begin{aligned}
& \langle S^I D^{II} | V_N^{I,II} [T_{11}^{I,II} + T_{11}^{I,II} T_{12}^{I,II} + T_{12}^{I,II} + T_1^I T_{11}^{I,II} + T_1^I T_{12}^{I,II} + T_1^I T_1^{II} + T_1^I T_1^{II} T_{11}^{I,II} + T_1^I T_1^{II} T_{12}^{I,II} + \\
& T_1^I T_1^{II} T_2^{II} + T_1^I \frac{1}{2!} T_1^{II^2} + T_1^I \frac{1}{2!} T_1^{II^2} T_{11}^{I,II} + T_1^I \frac{1}{3!} T_1^{II^3} + T_1^I T_2^{II} + T_1^I T_2^{II} T_{11}^{I,II} + \frac{1}{2!} T_1^I{}^2 T_1^{II} + \frac{1}{2!} T_1^I{}^2 T_1^{II} T_2^{II} \\
& + \frac{1}{2!} T_1^I{}^2 \frac{1}{2!} T_1^{II^2} + \frac{1}{2!} T_1^I{}^2 \frac{1}{3!} T_1^{II^3} + \frac{1}{2!} T_1^I{}^2 T_2^{II} + T_1^I + T_1^{II} T_{11}^{I,II} + T_1^{II} T_{12}^{I,II} + T_1^{II} T_{21}^{I,II} + T_1^{II} T_{22}^{I,II} + \\
& T_1^{II} T_2^{II} + \frac{1}{2!} T_1^{II^2} + \frac{1}{2!} T_1^{II^2} T_{11}^{I,II} + \frac{1}{2!} T_1^{II^2} T_{21}^{I,II} + \frac{1}{3!} T_1^{II^3} + T_{21}^{I,II} + T_{22}^{I,II} + T_2^I T_1^{II} + T_2^I T_1^{II} T_2^{II} + \\
& T_2^I \frac{1}{2!} T_1^{II^2} + T_2^I \frac{1}{3!} T_1^{II^3} + T_2^I T_2^{II} + T_2^{II} + T_2^{II} T_{11}^{I,II} + T_2^{II} T_{21}^{I,II}] + [(-T_{12}^{I,II})] V_N^{I,II} [1 + T_{11}^{I,II} + T_1^I + \\
& T_1^I T_1^{II} + T_1^{II}] + [(-T_{11}^{I,II})] V_N^{I,II} [1 + T_{11}^{I,II} + T_{12}^{I,II} + T_1^I + T_1^I T_1^{II} + T_1^I \frac{1}{2!} T_1^{II^2} + T_1^I T_2^{II} + T_1^{II} + \\
& T_1^{II} T_{11}^{I,II} + \frac{1}{2!} T_1^{II^2} + T_2^{II}] + [(-T_2^{II})] V_N^{I,II} [1 + T_{11}^{I,II} + T_1^I + T_1^I T_{11}^{I,II} + T_1^I T_1^{II} + \frac{1}{2!} T_1^I{}^2 + \frac{1}{2!} T_1^I{}^2 T_1^{II} \\
& + T_1^{II} + T_{21}^{I,II} + T_2^I + T_2^I T_1^{II}] + [(-T_1^{II})] V_N^{I,II} [1 + T_{11}^{I,II} + T_{12}^{I,II} + T_1^I + T_1^I T_{11}^{I,II} + T_1^I T_{12}^{I,II} + \\
& T_1^I T_1^{II} + T_1^I T_1^{II} T_{11}^{I,II} + T_1^I \frac{1}{2!} T_1^{II^2} + T_1^I T_2^{II} + \frac{1}{2!} T_1^I{}^2 + \frac{1}{2!} T_1^I{}^2 T_1^{II} + \frac{1}{2!} T_1^I{}^2 \frac{1}{2!} T_1^{II^2} + \frac{1}{2!} T_1^I{}^2 T_2^{II} + T_1^{II} \\
& + T_1^{II} T_{11}^{I,II} + T_1^{II} T_{21}^{I,II} + \frac{1}{2!} T_1^{II^2} + T_{21}^{I,II} + T_{22}^{I,II} + T_2^I + T_2^I T_1^{II} + T_2^I \frac{1}{2!} T_1^{II^2} + T_2^I T_2^{II} + T_2^{II}] +
\end{aligned}$$

Type I, II double, single amplitude ($\langle D^I S^{II} | e^{-T} H_N e^T | 0^I 0^{II} \rangle = 0$)

$$\begin{aligned}
& \langle D^I S^{II} | V_N^{I,II} [T_{11}^{I,II} + T_{11}^{I,II} T_{21}^{I,II} + T_{12}^{I,II} + T_1^I + T_1^I T_{11}^{I,II} + T_1^I T_{12}^{I,II} + T_1^I T_1^I + T_1^I T_1^I T_{11}^{I,II} + T_1^I T_1^I T_{21}^{I,II} \\
& + T_1^I \frac{1}{2!} T_1^{II^2} + T_1^I T_{21}^{I,II} + T_1^I T_{22}^{I,II} + T_1^I T_2^I + T_1^I T_2^I T_1^I + T_1^I T_2^I \frac{1}{2!} T_1^{II^2} + T_1^I T_2^I T_2^I + T_1^I T_2^I + \frac{1}{2!} T_1^{I^2} \\
& + \frac{1}{2!} T_1^{I^2} T_{11}^{I,II} + \frac{1}{2!} T_1^{I^2} T_{12}^{I,II} + \frac{1}{2!} T_1^{I^2} T_1^{II} + \frac{1}{2!} T_1^{I^2} T_1^I T_{11}^{I,II} + \frac{1}{2!} T_1^{I^2} \frac{1}{2!} T_1^{II^2} + \frac{1}{2!} T_1^{I^2} T_2^I + \frac{1}{3!} T_1^{I^3} + \\
& \frac{1}{3!} T_1^{I^3} T_1^{II} + \frac{1}{3!} T_1^{I^3} \frac{1}{2!} T_1^{II^2} + \frac{1}{3!} T_1^{I^3} T_2^I + T_1^{II} T_{11}^{I,II} + T_1^{II} T_{21}^{I,II} + T_{21}^{II} + T_{22}^{II} + T_2^I + T_2^I T_{11}^{I,II} + \\
& T_2^I T_{12}^{I,II} + T_2^I T_1^I + T_2^I T_1^I T_{11}^{I,II} + T_2^I \frac{1}{2!} T_1^{II^2} + T_2^I T_2^I] + [(-T_{21}^{I,II})] V_N^{I,II} [1 + T_{11}^{I,II} + T_1^I + T_1^I T_1^I \\
& + T_1^{II}] + [(-T_{11}^{I,II})] V_N^{I,II} [1 + T_{11}^{I,II} + T_1^I + T_1^I T_{11}^{I,II} + T_1^I T_1^I + \frac{1}{2!} T_1^{I^2} + \frac{1}{2!} T_1^{I^2} T_1^I + T_1^{II} + T_{21}^{II} \\
& + T_2^I + T_2^I T_1^I] + [(-T_1^{II})] V_N^{I,II} [T_{11}^{I,II} + T_1^I + T_1^I T_{11}^{I,II} + T_1^I T_1^I + T_1^I T_{21}^{I,II} + T_1^I T_2^I + T_1^I T_2^I T_1^I + \\
& \frac{1}{2!} T_1^{I^2} + \frac{1}{2!} T_1^{I^2} T_{11}^{I,II} + \frac{1}{2!} T_1^{I^2} T_1^{II} + \frac{1}{3!} T_1^{I^3} + \frac{1}{3!} T_1^{I^3} T_1^{II} + T_{21}^{II} + T_2^I + T_2^I T_{11}^{I,II} + T_2^I T_1^I] + [(-T_2^I)] \\
& V_N^{I,II} [1 + T_{11}^{I,II} + T_{12}^{I,II} + T_1^I + T_1^I T_1^I + T_1^I \frac{1}{2!} T_1^{II^2} + T_1^I T_2^I + T_1^{II} + T_1^{II} T_{11}^{I,II} + \frac{1}{2!} T_1^{II^2} + T_2^I] + \\
& [(-T_1^{II})(-T_2^I)] V_N^{I,II} [1 + T_{11}^{I,II} + T_1^I + T_1^I T_1^I + T_1^{II}] + [(-T_1^I)] V_N^{I,II} [1 + T_{11}^{I,II} + T_{12}^{I,II} + T_1^I + \\
& T_1^I T_{11}^{I,II} + T_1^I T_{12}^{I,II} + T_1^I T_1^I + T_1^I T_1^I T_{11}^{I,II} + T_1^I \frac{1}{2!} T_1^{II^2} + T_1^I T_2^I + \frac{1}{2!} T_1^{I^2} + \frac{1}{2!} T_1^{I^2} T_1^I + \frac{1}{2!} T_1^{I^2} \frac{1}{2!} T_1^{II^2} \\
& + \frac{1}{2!} T_1^{I^2} T_2^I + T_1^{II} + T_1^{II} T_{11}^{I,II} + T_1^{II} T_{21}^{I,II} + \frac{1}{2!} T_1^{II^2} + T_{21}^{II} + T_{22}^{II} + T_2^I + T_2^I T_1^I + T_2^I \frac{1}{2!} T_1^{II^2} + \\
& T_2^I T_2^I + T_2^{II}] + [(-T_{11}^{I,II})(-T_1^I)] V_N^{I,II} [1 + T_{11}^{I,II} + T_1^I + T_1^I T_1^I + T_1^{II}] + [(-T_1^I)(-T_1^{II})] V_N^{I,II} [1 \\
& + T_{11}^{I,II} + T_1^I + T_1^I T_{11}^{I,II} + T_1^I T_1^I + \frac{1}{2!} T_1^{I^2} + \frac{1}{2!} T_1^{I^2} T_1^I + T_1^{II} + T_{21}^{II} + T_2^I + T_2^I T_1^I] + [\frac{1}{2!} T_1^{I^2}] \\
& V_N^{I,II} [1 + T_{11}^{I,II} + T_{12}^{I,II} + T_1^I + T_1^I T_1^I + T_1^I \frac{1}{2!} T_1^{II^2} + T_1^I T_2^I + T_1^{II} + T_1^{II} T_{11}^{I,II} + \frac{1}{2!} T_1^{II^2} + T_2^I] \\
& + [(-T_1^{II}) \frac{1}{2!} T_1^{I^2}] V_N^{I,II} [1 + T_{11}^{I,II} + T_1^I + T_1^I T_1^I + T_1^{II}] + \tilde{H}_N^{II} [T_{11}^{I,II} T_{12}^{I,II} + T_1^I T_{11}^{I,II} + T_1^I T_{12}^{I,II} + \\
& T_1^I T_1^I T_{11}^{I,II} + T_1^I T_1^I T_{12}^{I,II} + T_1^I \frac{1}{2!} T_1^{II^2} T_{11}^{I,II} + T_1^I T_2^I T_{11}^{I,II} + \frac{1}{2!} T_1^{I^2} + \frac{1}{2!} T_1^{I^2} T_1^I + \frac{1}{2!} T_1^{I^2} T_1^I T_2^I + \\
& \frac{1}{2!} T_1^{I^2} \frac{1}{2!} T_1^{II^2} + \frac{1}{2!} T_1^{I^2} \frac{1}{3!} T_1^{II^3} + \frac{1}{2!} T_1^{I^2} T_2^I + T_1^{II} T_{21}^{I,II} + T_1^{II} T_{22}^{I,II} + \frac{1}{2!} T_1^{II^2} T_{21}^{I,II} + T_{21}^{II} + T_{22}^{II} + T_2^I \\
& + T_2^I T_1^I + T_2^I T_1^I T_2^I + T_2^I \frac{1}{2!} T_1^{II^2} + T_2^I \frac{1}{3!} T_1^{II^3} + T_2^I T_2^I + T_2^I T_{21}^{I,II}] + [(-T_{21}^{I,II})] \tilde{H}_N^{II} [1 + T_1^{II} + \\
& \frac{1}{2!} T_1^{II^2} + T_2^I] + [(-T_{11}^{I,II})] \tilde{H}_N^{II} [T_{11}^{I,II} + T_{12}^{I,II} + T_1^I + T_1^I T_1^I + T_1^I \frac{1}{2!} T_1^{II^2} + T_1^I T_2^I + T_1^{II} T_{11}^{I,II}] + \\
& [(-T_1^{II})] \tilde{H}_N^{II} [T_1^I T_{11}^{I,II} + T_1^I T_{12}^{I,II} + T_1^I T_1^I T_{11}^{I,II} + \frac{1}{2!} T_1^{I^2} + \frac{1}{2!} T_1^{I^2} T_1^I + \frac{1}{2!} T_1^{I^2} \frac{1}{2!} T_1^{II^2} + \frac{1}{2!} T_1^{I^2} T_2^I + \\
& T_1^{II} T_{21}^{I,II} + T_{21}^{II} + T_{22}^{II} + T_2^I + T_2^I T_1^I + T_2^I \frac{1}{2!} T_1^{II^2} + T_2^I T_2^I] + [(-T_2^I)] \tilde{H}_N^{II} [1 + T_1^{II} + T_1^{II} T_2^I + \\
& \frac{1}{2!} T_1^{II^2} + \frac{1}{3!} T_1^{II^3} + T_2^I] + [(-T_1^I)(-T_2^I)] \tilde{H}_N^{II} [1 + T_1^{II} + \frac{1}{2!} T_1^{II^2} + T_2^I] + [(-T_1^I)] \tilde{H}_N^{II} [T_{11}^{I,II} + T_{12}^{I,II} \\
& + T_1^I + T_1^I T_1^I + T_1^I T_1^I T_2^I + T_1^I \frac{1}{2!} T_1^{II^2} + T_1^I \frac{1}{3!} T_1^{II^3} + T_1^I T_2^I + T_1^{II} T_{11}^{I,II} + T_1^{II} T_{12}^{I,II} + \frac{1}{2!} T_1^{II^2} T_{11}^{I,II} \\
& + T_2^I T_{11}^{I,II}] + [(-T_{11}^{I,II})(-T_1^I)] \tilde{H}_N^{II} [1 + T_1^{II} + \frac{1}{2!} T_1^{II^2} + T_2^I] + [(-T_1^I)(-T_1^{II})] \tilde{H}_N^{II} [T_{11}^{I,II} + T_{12}^{I,II} \\
& + T_1^I + T_1^I T_1^I + T_1^I T_1^I T_2^I + T_1^I \frac{1}{2!} T_1^{II^2} + T_1^I \frac{1}{3!} T_1^{II^3} + T_1^I T_2^I + T_1^{II} T_{11}^{I,II} + \frac{1}{2!} T_1^{II^2} + \frac{1}{3!} T_1^{II^3} \\
& + T_2^I T_{11}^{I,II}] + [\frac{1}{2!} T_1^{I^2}] \tilde{H}_N^{II} [1 + T_1^{II} + T_1^{II} T_2^I + \frac{1}{2!} T_1^{II^2} + \frac{1}{3!} T_1^{II^3}
\end{aligned}$$

$$\begin{aligned}
& [T_{11}^{I,II} + T_1^I + T_1^I T_{11}^{I,II} + T_1^I T_1^{II} + T_1^I T_{21}^{I,II} + T_1^I T_2^I + T_1^I T_2^I T_1^{II} + \frac{1}{2!} T_1^{I^2} + \frac{1}{2!} T_1^{I^2} T_{11}^{I,II} + \frac{1}{2!} T_1^{I^2} T_1^{II} + \\
& \frac{1}{3!} T_1^{I^3} + \frac{1}{3!} T_1^{I^3} T_1^{II} + T_{21}^{I,II} + T_2^I + T_2^I T_{11}^{I,II} + T_2^I T_1^{II}] + [(-T_1^{II})] V_N^{I,II} [T_{11}^{I,II} + T_{11}^{I,II} T_{21}^{I,II} + T_{12}^{I,II} + T_1^I \\
& + T_1^I T_{11}^{I,II} + T_1^I T_{12}^{I,II} + T_1^I T_1^{II} + T_1^I T_1^{II} T_{11}^{I,II} + T_1^I T_1^{II} T_{21}^{I,II} + T_1^I \frac{1}{2!} T_1^{II^2} + T_1^I T_{21}^{I,II} + T_1^I T_{22}^{I,II} + T_1^I T_2^I \\
& + T_1^I T_2^I T_1^{II} + T_1^I T_2^I \frac{1}{2!} T_1^{II^2} + T_1^I T_2^I T_2^{II} + T_1^I T_2^{II} + \frac{1}{2!} T_1^{I^2} + \frac{1}{2!} T_1^{I^2} T_{11}^{I,II} + \frac{1}{2!} T_1^{I^2} T_{12}^{I,II} + \frac{1}{2!} T_1^{I^2} T_1^{II} + \\
& \frac{1}{2!} T_1^{I^2} T_1^{II} T_{11}^{I,II} + \frac{1}{2!} T_1^{I^2} \frac{1}{2!} T_1^{II^2} + \frac{1}{2!} T_1^{I^2} T_2^{II} + \frac{1}{3!} T_1^{I^3} + \frac{1}{3!} T_1^{I^3} T_1^{II} + \frac{1}{3!} T_1^{I^3} \frac{1}{2!} T_1^{II^2} + \frac{1}{3!} T_1^{I^3} T_2^{II} + T_1^{II} T_{11}^{I,II} \\
& + T_1^{II} T_{21}^{I,II} + T_{21}^{I,II} + T_{22}^{I,II} + T_2^I + T_2^I T_{11}^{I,II} + T_2^I T_{12}^{I,II} + T_2^I T_1^{II} + T_2^I T_1^{II} T_{11}^{I,II} + T_2^I \frac{1}{2!} T_1^{II^2} + T_2^I T_2^{II}] \\
& + [(-T_1^{II})(-T_{21}^{I,II})] V_N^{I,II} [1 + T_{11}^{I,II} + T_1^I + T_1^I T_1^{II} + T_1^{II}] + [(-T_{11}^{I,II})(-T_1^{II})] V_N^{I,II} [1 + T_{11}^{I,II} + \\
& T_1^I + T_1^I T_{11}^{I,II} + T_1^I T_1^{II} + \frac{1}{2!} T_1^{I^2} + \frac{1}{2!} T_1^{I^2} T_1^{II} + T_1^{II} + T_{21}^{I,II} + T_2^I + T_2^I T_1^{II}] + [\frac{1}{2!} T_1^{II^2}] V_N^{I,II} [T_{11}^{I,II} + \\
& T_1^I + T_1^I T_{11}^{I,II} + T_1^I T_1^{II} + T_1^I T_{21}^{I,II} + T_1^I T_2^I + T_1^I T_2^I T_1^{II} + \frac{1}{2!} T_1^{I^2} + \frac{1}{2!} T_1^{I^2} T_{11}^{I,II} + \frac{1}{2!} T_1^{I^2} T_1^{II} + \frac{1}{3!} T_1^{I^3} \\
& + \frac{1}{3!} T_1^{I^3} T_1^{II} + T_{21}^{I,II} + T_2^I + T_2^I T_{11}^{I,II} + T_2^I T_1^{II}] + [(-T_2^I)] V_N^{I,II} [T_{11}^{I,II} + T_{12}^{I,II} + T_1^I T_1^{II} + T_1^I T_1^{II} T_2^{II} \\
& + T_1^I \frac{1}{2!} T_1^{II^2} + T_1^I \frac{1}{3!} T_1^{II^3} + T_1^I T_2^{II} + T_1^{II} + T_1^{II} T_{11}^{I,II} + T_1^{II} T_{12}^{I,II} + T_1^{II} T_2^{II} + \frac{1}{2!} T_1^{II^2} + \frac{1}{2!} T_1^{II^2} T_{11}^{I,II} + \\
& \frac{1}{3!} T_1^{II^3} + T_2^{II} + T_2^{II} T_{11}^{I,II}] + [(-T_2^I)(-T_2^{II})] V_N^{I,II} [1 + T_{11}^{I,II} + T_1^I + T_1^I T_1^{II} + T_1^{II}] + [(-T_1^{II})(-T_2^I)] \\
& V_N^{I,II} [1 + T_{11}^{I,II} + T_{12}^{I,II} + T_1^I + T_1^I T_1^{II} + T_1^I \frac{1}{2!} T_1^{II^2} + T_1^I T_2^{II} + T_1^{II} + T_1^{II} T_{11}^{I,II} + \frac{1}{2!} T_1^{II^2} + T_2^{II}] + \\
& [(-T_2^I) \frac{1}{2!} T_1^{II^2}] V_N^{I,II} [1 + T_{11}^{I,II} + T_1^I + T_1^I T_1^{II} + T_1^{II}] + [(-T_1^I)] V_N^{I,II} [T_{11}^{I,II} + T_{11}^{I,II} T_{12}^{I,II} + T_{12}^{I,II} + \\
& T_1^I T_{11}^{I,II} + T_1^I T_{12}^{I,II} + T_1^I T_1^{II} + T_1^I T_1^{II} T_{11}^{I,II} + T_1^I T_1^{II} T_{12}^{I,II} + T_1^I T_1^{II} T_2^{II} + T_1^I \frac{1}{2!} T_1^{II^2} + T_1^I \frac{1}{2!} T_1^{II^2} T_{11}^{I,II} \\
& + T_1^I \frac{1}{3!} T_1^{II^3} + T_1^I T_2^{II} + T_1^I T_2^{II} T_{11}^{I,II} + \frac{1}{2!} T_1^{I^2} T_1^{II} + \frac{1}{2!} T_1^{I^2} T_1^{II} T_2^{II} + \frac{1}{2!} T_1^{I^2} \frac{1}{2!} T_1^{II^2} + \frac{1}{2!} T_1^{I^2} \frac{1}{3!} T_1^{II^3} + \\
& \frac{1}{2!} T_1^{I^2} T_2^{II} + T_1^{II} + T_1^{II} T_{11}^{I,II} + T_1^{II} T_{12}^{I,II} + T_1^{II} T_{21}^{I,II} + T_1^{II} T_{22}^{I,II} + T_1^{II} T_2^{II} + \frac{1}{2!} T_1^{II^2} + \frac{1}{2!} T_1^{II^2} T_{11}^{I,II} + \\
& \frac{1}{2!} T_1^{II^2} T_{21}^{I,II} + \frac{1}{3!} T_1^{II^3} + T_{21}^{I,II} + T_{22}^{I,II} + T_2^I T_1^{II} + T_2^I T_1^{II} T_2^{II} + T_2^I \frac{1}{2!} T_1^{II^2} + T_2^I \frac{1}{3!} T_1^{II^3} + T_2^I T_2^{II} + T_2^{II} + \\
& T_2^{II} T_{11}^{I,II} + T_2^{II} T_{21}^{I,II}] + [(-T_{12}^{I,II})(-T_1^I)] V_N^{I,II} [1 + T_{11}^{I,II} + T_1^I + T_1^I T_1^{II} + T_1^{II}] + [(-T_{11}^{I,II})(-T_1^I)] \\
& V_N^{I,II} [1 + T_{11}^{I,II} + T_{12}^{I,II} + T_1^I + T_1^I T_1^{II} + T_1^I \frac{1}{2!} T_1^{II^2} + T_1^I T_2^{II} + T_1^{II} + T_1^{II} T_{11}^{I,II} + \frac{1}{2!} T_1^{II^2} + T_2^{II}] + \\
& [(-T_1^I)(-T_2^{II})] V_N^{I,II} [1 + T_{11}^{I,II} + T_1^I + T_1^I T_1^{II} + T_1^I T_1^{II} + \frac{1}{2!} T_1^{I^2} + \frac{1}{2!} T_1^{I^2} T_1^{II} + T_1^{II} + T_{21}^{I,II} + T_2^I + \\
& T_2^I T_1^{II}] + [(-T_1^I)(-T_1^{II})] V_N^{I,II} [1 + T_{11}^{I,II} + T_{12}^{I,II} + T_1^I + T_1^I T_{11}^{I,II} + T_1^I T_{12}^{I,II} + T_1^I T_1^{II} + T_1^I T_1^{II} T_{11}^{I,II} \\
& + T_1^I \frac{1}{2!} T_1^{II^2} + T_1^I T_2^{II} + \frac{1}{2!} T_1^{I^2} + \frac{1}{2!} T_1^{I^2} T_1^{II} + \frac{1}{2!} T_1^{I^2} \frac{1}{2!} T_1^{II^2} + \frac{1}{2!} T_1^{I^2} T_2^{II} + T_1^{II} + T_1^{II} T_{11}^{I,II} + T_1^{II} T_{21}^{I,II} \\
& + \frac{1}{2!} T_1^{II^2} + T_{21}^{I,II} + T_{22}^{I,II} + T_2^I + T_2^I T_1^{II} + T_2^I \frac{1}{2!} T_1^{II^2} + T_2^I T_2^{II} + T_2^{II}] + [(-T_{11}^{I,II})(-T_1^I)(-T_1^{II})] \\
& V_N^{I,II} [1 + T_{11}^{I,II} + T_1^I + T_1^I T_1^{II} + T_1^{II}] + [(-T_1^I) \frac{1}{2!} T_1^{II^2}] V_N^{I,II} [1 + T_{11}^{I,II} + T_1^I + T_1^I T_{11}^{I,II} + T_1^I T_1^{II} + \\
& \frac{1}{2!} T_1^{I^2} + \frac{1}{2!} T_1^{I^2} T_1^{II} + T_1^{II} + T_{21}^{I,II} + T_2^I + T_2^I T_1^{II}] + [\frac{1}{2!} T_1^{I^2}] V_N^{I,II} [T_{11}^{I,II} + T_{12}^{I,II} + T_1^I T_1^{II} + T_1^I T_1^{II} T_2^{II} \\
& + T_1^I \frac{1}{2!} T_1^{II^2} + T_1^I \frac{1}{3!} T_1^{II^3} + T_1^I T_2^{II} + T_1^{II} + T_1^{II} T_{11}^{I,II} + T_1^{II} T_{12}^{I,II} + T_1^{II} T_2^{II} + \frac{1}{2!} T_1^{II^2} + \frac{1}{2!} T_1^{II^2} T_{11}^{I,II} +
\end{aligned}$$

$$\begin{aligned}
& + T_1^I + T_1^I T_1^{II} + T_1^I T_1^{II} T_2^{II} + T_1^I \frac{1}{2!} T_1^{II^2} + T_1^I \frac{1}{3!} T_1^{II^3} + T_1^I T_2^{II} + T_1^{II} T_{11}^{I,II} + T_1^{II} T_{12}^{I,II} + \frac{1}{2!} T_1^{II^2} T_{11}^{I,II} \\
& + T_2^{II} T_{11}^{I,II}] + [(-T_{11}^{I,II})(-T_1^I)(-T_1^{II})] \tilde{H}_N^{II}[1 + T_1^{II} + \frac{1}{2!} T_1^{II^2} + T_2^{II}] + [(-T_1^I) \frac{1}{2!} T_1^{II^2}] \tilde{H}_N^{II}[T_{11}^{I,II} \\
& + T_{12}^{I,II} + T_1^I + T_1^I T_1^{II} + T_1^I \frac{1}{2!} T_1^{II^2} + T_1^I T_2^{II} + T_1^{II} T_{11}^{I,II}] + [\frac{1}{2!} T_1^{II^2}] \tilde{H}_N^{II}[1 + T_1^{II} + T_1^{II} T_2^{II} + \frac{1}{2!} T_1^{II^2} \\
& + \frac{1}{2!} T_1^{II^2} T_2^{II} + \frac{1}{3!} T_1^{II^3} + \frac{1}{4!} T_1^{II^4} + T_2^{II} + \frac{1}{2!} T_2^{II^2}] + [(-T_2^{II}) \frac{1}{2!} T_1^{II^2}] \tilde{H}_N^{II}[1 + T_1^{II} + \frac{1}{2!} T_1^{II^2} + T_2^{II}] \\
& + [(-T_1^{II}) \frac{1}{2!} T_1^{II^2}] \tilde{H}_N^{II}[1 + T_1^{II} + T_1^{II} T_2^{II} + \frac{1}{2!} T_1^{II^2} + \frac{1}{3!} T_1^{II^3} + T_2^{II}] + [\frac{1}{2!} T_1^{II^2} \frac{1}{2!} T_1^{II^2}] \tilde{H}_N^{II}[1 + T_1^{II} \\
& + \frac{1}{2!} T_1^{II^2} + T_2^{II}] + \tilde{H}_N^I[T_{11}^{I,II} T_{21}^{I,II} + T_{12}^{I,II} + T_1^I T_{11}^{I,II} T_{21}^{I,II} + T_1^I T_{12}^{I,II} + T_1^I T_1^{II} T_{11}^{I,II} + T_1^I T_1^{II} T_{21}^{I,II} + \\
& T_1^I \frac{1}{2!} T_1^{II^2} + T_1^I T_{22}^{I,II} + T_1^I T_2^I T_{12}^{I,II} + T_1^I T_2^I T_1^{II} T_{11}^{I,II} + T_1^I T_2^I \frac{1}{2!} T_1^{II^2} + T_1^I T_2^I T_2^{II} + T_1^I T_2^{II} + \frac{1}{2!} T_1^{II^2} T_{12}^{I,II} \\
& + \frac{1}{2!} T_1^{II^2} T_1^{II} T_{11}^{I,II} + \frac{1}{2!} T_1^{II^2} T_1^{II} T_{21}^{I,II} + \frac{1}{2!} T_1^{II^2} \frac{1}{2!} T_1^{II^2} + \frac{1}{2!} T_1^{II^2} T_{22}^{I,II} + \frac{1}{2!} T_1^{II^2} T_2^I \frac{1}{2!} T_1^{II^2} + \frac{1}{2!} T_1^{II^2} T_2^I T_2^{II} + \\
& \frac{1}{2!} T_1^{II^2} T_2^{II} + \frac{1}{3!} T_1^{II^3} T_{12}^{I,II} + \frac{1}{3!} T_1^{II^3} T_1^{II} T_{11}^{I,II} + \frac{1}{3!} T_1^{II^3} \frac{1}{2!} T_1^{II^2} + \frac{1}{3!} T_1^{II^3} T_2^{II} + \frac{1}{4!} T_1^{II^4} \frac{1}{2!} T_1^{II^2} + \frac{1}{4!} T_1^{II^4} T_2^{II} + \\
& T_1^{II} T_{11}^{I,II} + T_1^{II} T_{21}^{I,II} + \frac{1}{2!} T_1^{II^2} + \frac{1}{2!} T_{21}^{I,II^2} + T_{22}^{I,II} + T_2^I T_{12}^{I,II} + T_2^I T_1^{II} T_{11}^{I,II} + T_2^I T_1^{II} T_{21}^{I,II} + T_2^I \frac{1}{2!} T_1^{II^2} \\
& + T_2^I T_{22}^{I,II} + T_2^I T_2^{II} + \frac{1}{2!} T_2^{II^2} \frac{1}{2!} T_1^{II^2} + \frac{1}{2!} T_2^{II^2} T_2^{II} + T_2^{II}] + [(-T_{22}^{I,II})] \tilde{H}_N^I[1 + T_1^I + \frac{1}{2!} T_1^{II^2} + T_2^I] \\
& + [(-T_{21}^{I,II})] \tilde{H}_N^I[T_{11}^{I,II} + T_1^I T_{11}^{I,II} + T_1^I T_1^{II} + \frac{1}{2!} T_1^{II^2} T_1^{II} + T_1^{II} + T_{21}^{I,II} + T_2^I T_1^{II}] + [(-T_{12}^{I,II})] \tilde{H}_N^I \\
& [1 + T_1^I + T_1^I T_2^I + \frac{1}{2!} T_1^{II^2} + \frac{1}{3!} T_1^{II^3} + T_2^I] + [\frac{1}{2!} T_{11}^{I,II^2}] \tilde{H}_N^I[1 + T_1^I + \frac{1}{2!} T_1^{II^2} + T_2^I] + [(-T_{11}^{I,II})] \tilde{H}_N^I \\
& [T_{11}^{I,II} + T_1^I T_{11}^{I,II} + T_1^I T_1^{II} + T_1^I T_{21}^{I,II} + T_1^I T_2^I T_1^{II} + \frac{1}{2!} T_1^{II^2} T_{11}^{I,II} + \frac{1}{2!} T_1^{II^2} T_1^{II} + \frac{1}{3!} T_1^{II^3} T_1^{II} + T_1^{II} + \\
& T_{21}^{I,II} + T_2^I T_{11}^{I,II} + T_2^I T_1^{II}] + [(-T_2^{II})] \tilde{H}_N^I[1 + T_1^I + T_1^I T_2^I + \frac{1}{2!} T_1^{II^2} + \frac{1}{2!} T_1^{II^2} T_2^I + \frac{1}{3!} T_1^{II^3} + \frac{1}{4!} T_1^{II^4} \\
& + T_2^I + \frac{1}{2!} T_2^{II^2}] + [(-T_1^{II})] \tilde{H}_N^I[T_{11}^{I,II} + T_1^I T_{11}^{I,II} + T_1^I T_1^{II} + T_1^I T_{21}^{I,II} + T_1^I T_2^I T_{11}^{I,II} + T_1^I T_2^I T_1^{II} + \\
& \frac{1}{2!} T_1^{II^2} T_{11}^{I,II} + \frac{1}{2!} T_1^{II^2} T_1^{II} + \frac{1}{2!} T_1^{II^2} T_{21}^{I,II} + \frac{1}{2!} T_1^{II^2} T_2^I T_1^{II} + \frac{1}{3!} T_1^{II^3} T_{11}^{I,II} + \frac{1}{3!} T_1^{II^3} T_1^{II} + \frac{1}{4!} T_1^{II^4} T_1^{II} + T_1^{II} + \\
& T_{21}^{I,II} + T_2^I T_{11}^{I,II} + T_2^I T_1^{II}] + [(-T_1^{II})(-T_{21}^{I,II})] \tilde{H}_N^I[1 + T_1^I + \frac{1}{2!} T_1^{II^2} + T_2^I] + [(-T_1^{II})(-T_2^{II})] \tilde{H}_N^I[1 + T_1^I + T_1^I T_2^I + \\
& \frac{1}{2!} T_1^{II^2} + \frac{1}{2!} T_1^{II^2} T_2^I + \frac{1}{3!} T_1^{II^3} + \frac{1}{4!} T_1^{II^4} + T_2^I + \frac{1}{2!} T_2^{II^2}] + [(-T_2^I)] \tilde{H}_N^I[T_{12}^{I,II} + T_1^I T_{12}^{I,II} + T_1^I T_1^{II} T_{11}^{I,II} + \\
& T_1^I \frac{1}{2!} T_1^{II^2} + T_1^I T_2^I + \frac{1}{2!} T_1^{II^2} \frac{1}{2!} T_1^{II^2} + \frac{1}{2!} T_1^{II^2} T_2^I + T_1^{II} T_{11}^{I,II} + T_1^{II} T_{21}^{I,II} + \frac{1}{2!} T_1^{II^2} + T_{22}^{I,II} + T_2^I \frac{1}{2!} T_1^{II^2} + \\
& T_2^I T_2^{II} + T_2^{II}] + [(-T_1^I)(-T_2^{II})] \tilde{H}_N^I[1 + T_1^I + \frac{1}{2!} T_1^{II^2} + T_2^I] + [(-T_1^{II})(-T_2^I)] \tilde{H}_N^I[T_{11}^{I,II} + T_1^I T_{11}^{I,II} \\
& + T_1^I T_1^{II} + \frac{1}{2!} T_1^{II^2} T_1^{II} + T_1^{II} + T_{21}^{I,II} + T_2^I T_1^{II}] + [(-T_2^I) \frac{1}{2!} T_1^{II^2}] \tilde{H}_N^I[1 + T_1^I + \frac{1}{2!} T_1^{II^2} + T_2^I] + [(-T_1^I)] \\
& \tilde{H}_N^I[T_{11}^{I,II} T_{21}^{I,II} + T_{12}^{I,II} + T_1^I T_{12}^{I,II} + T_1^I T_1^{II} T_{11}^{I,II} + T_1^I T_1^{II} T_{21}^{I,II} + T_1^I \frac{1}{2!} T_1^{II^2} + T_1^I T_{22}^{I,II} + T_1^I T_2^I \frac{1}{2!} T_1^{II^2} \\
& + T_1^I T_2^I T_2^{II} + T_1^I T_2^{II} + \frac{1}{2!} T_1^{II^2} T_{12}^{I,II} + \frac{1}{2!} T_1^{II^2} T_1^{II} T_{11}^{I,II} + \frac{1}{2!} T_1^{II^2} \frac{1}{2!} T_1^{II^2} + \frac{1}{2!} T_1^{II^2} T_2^I + \frac{1}{3!} T_1^{II^3} \frac{1}{2!} T_1^{II^2} + \\
& \frac{1}{3!} T_1^{II^3} T_2^{II} + T_1^{II} T_{11}^{I,II} + T_1^{II} T_{21}^{I,II} + \frac{1}{2!} T_1^{II^2} + T_{22}^{I,II} + T_2^I T_{12}^{I,II} + T_2^I T_1^{II} T_{11}^{I,II} + T_2^I \frac{1}{2!} T_1^{II^2} + T_2^I T_2^{II} + \\
& T_2^{II}] + [(-T_{12}^{I,II})(-T_1^I)] \tilde{H}_N^I[1 + T_1^I + \frac{1}{2!} T_1^{II^2} + T_2^I] + [(-T_{11}^{I,II})(-T_1^I)] \tilde{H}_N^I[T_{11}^{I,II} + T_1^I T_{11}^{I,II} + T_1^I T_1^{II}
\end{aligned}$$

$$\begin{aligned}
& + \frac{1}{2!}T_1^I T_1^{\text{II}} + T_1^{\text{II}} + T_{21}^{\text{I,II}} + T_2^I T_1^{\text{II}} + [(-T_1^I)(-T_2^{\text{II}})]\tilde{H}_N^{\text{I}}[1 + T_1^I + T_1^I T_2^I + \frac{1}{2!}T_1^{\text{I}^2} + \frac{1}{3!}T_1^{\text{I}^3} + T_2^I] \\
& + [(-T_1^I)(-T_1^{\text{II}})]\tilde{H}_N^{\text{I}}[T_{11}^{\text{I,II}} + T_1^I T_{11}^{\text{I,II}} + T_1^I T_1^{\text{II}} + T_1^I T_{21}^{\text{I,II}} + T_1^I T_2^I T_1^{\text{II}} + \frac{1}{2!}T_1^{\text{I}^2} T_{11}^{\text{I,II}} + \frac{1}{2!}T_1^{\text{I}^2} T_1^{\text{II}} \\
& + \frac{1}{3!}T_1^{\text{I}^3} T_1^{\text{II}} + T_1^{\text{II}} + T_{21}^{\text{I,II}} + T_2^I T_{11}^{\text{I,II}} + T_2^I T_1^{\text{II}}] + [(-T_{11}^{\text{I,II}})(-T_1^I)(-T_1^{\text{II}})]\tilde{H}_N^{\text{I}}[1 + T_1^I + \frac{1}{2!}T_1^{\text{I}^2} + \\
& T_2^I] + [(-T_1^I)\frac{1}{2!}T_1^{\text{I}^2}]\tilde{H}_N^{\text{I}}[1 + T_1^I + T_1^I T_2^I + \frac{1}{2!}T_1^{\text{I}^2} + \frac{1}{3!}T_1^{\text{I}^3} + T_2^I] + [\frac{1}{2!}T_1^{\text{I}^2}]\tilde{H}_N^{\text{I}}[T_{12}^{\text{I,II}} + T_1^I T_{12}^{\text{I,II}} \\
& + T_1^I T_1^{\text{II}} T_{11}^{\text{I,II}} + T_1^I \frac{1}{2!}T_1^{\text{I}^2} + T_1^I T_2^{\text{II}} + \frac{1}{2!}T_1^{\text{I}^2} \frac{1}{2!}T_1^{\text{II}^2} + \frac{1}{2!}T_1^{\text{I}^2} T_2^{\text{II}} + T_1^{\text{II}} T_{11}^{\text{I,II}} + T_1^{\text{II}} T_{21}^{\text{I,II}} + \frac{1}{2!}T_1^{\text{II}^2} + \\
& T_{22}^{\text{I,II}} + T_2^I \frac{1}{2!}T_1^{\text{II}^2} + T_2^I T_2^{\text{II}} + T_2^{\text{II}}] + [(-T_2^{\text{II}})\frac{1}{2!}T_1^{\text{I}^2}]\tilde{H}_N^{\text{I}}[1 + T_1^I + \frac{1}{2!}T_1^{\text{I}^2} + T_2^I] + [(-T_1^{\text{II}})\frac{1}{2!}T_1^{\text{I}^2}] \\
& \tilde{H}_N^{\text{I}}[T_{11}^{\text{I,II}} + T_1^I T_{11}^{\text{I,II}} + T_1^I T_1^{\text{II}} + \frac{1}{2!}T_1^{\text{I}^2} T_1^{\text{II}} + T_1^{\text{II}} + T_{21}^{\text{I,II}} + T_2^I T_1^{\text{II}}] + [\frac{1}{2!}T_1^{\text{I}^2} \frac{1}{2!}T_1^{\text{II}^2}]\tilde{H}_N^{\text{I}}[1 + T_1^I + \\
& \frac{1}{2!}T_1^{\text{I}^2} + T_2^I]|0^{\text{I}}0^{\text{II}}\rangle = 0
\end{aligned}$$

4.3 Implementation details

The implementation of the t amplitude equations was performed sequentially by first performing the contraction over one particle type followed by contraction over the other particle type. For a general t amplitude equation, this procedure is shown by the following equation

$$\begin{aligned}
\langle K^{\text{I}}K^{\text{II}}|e^{-T}H_N e^T|0^{\text{I}}0^{\text{II}}\rangle_c &= \langle K^{\text{II}}|\langle K^{\text{I}}|e^{-T}\tilde{H}_N^{\text{I}}e^T|0^{\text{I}}\rangle_c|0^{\text{II}}\rangle_c \quad (4.61) \\
&+ \langle K^{\text{I}}|\langle K^{\text{II}}|e^{-T}\tilde{H}_N^{\text{II}}e^T|0^{\text{II}}\rangle_c|0^{\text{I}}\rangle_c \\
&+ \langle K^{\text{I}}|\langle K^{\text{II}}|e^{-T}V_N e^T|0^{\text{II}}\rangle_c|0^{\text{I}}\rangle_c.
\end{aligned}$$

Contraction over indices of one particle type resulted in a set of single component operators. These operators (labeled as A^{I} , A^{II} , and B) are analogous to the effective operators in electronic structure CC theory (pg. 328 of Ref. [60]) and are defined in

Eqs. [Equation 4.62](#)-[Equation 4.64](#)

$$\begin{aligned}
 \langle K^{\text{II}} | e^{-T} \tilde{H}_{\text{N}}^{\text{II}} e^T | 0^{\text{II}} \rangle_c &= A_0^{\text{I}} \\
 &+ \sum_{ia} A_{ia}^{\text{I}} \{a^\dagger i\} \\
 &+ \sum_{ijab} A_{ijab}^{\text{I}} \{a^\dagger b^\dagger j i\} \\
 &+ \dots \text{(n-body terms)}.
 \end{aligned} \tag{4.62}$$

In general, the number of operators in the above expression is infinite because of the presence of the exponential operators. However, because the operator expression was projected onto a space that contains only at most doubly excited spaces $\langle D |$, all three-body and higher operators had zero contribution to the t amplitude equations. Analogous to the type I particles, the operators for the type II particles are defined as

$$\begin{aligned}
 \langle K^{\text{I}} | e^{-T} \tilde{H}_{\text{N}}^{\text{I}} e^T | 0^{\text{I}} \rangle_c &= A_0^{\text{II}} \\
 &+ \sum_{i'a'} A_{i'a'}^{\text{II}} \{a'^\dagger i'\} \\
 &+ \sum_{i'j'a'b'} A_{i'j'a'b'}^{\text{II}} \{a'^\dagger b'^\dagger j' i'\} \\
 &+ \dots \text{(n-body terms)}
 \end{aligned} \tag{4.63}$$

The contraction over the $V_{\text{N}}^{\text{I,II}}$ operators is defined as

$$\begin{aligned}
 \langle K^{\text{II}} | e^{-T} V_{\text{N}}^{\text{I,II}} e^T | 0^{\text{II}} \rangle_c &= \sum_{pq} B_{pq}^{\text{I}} \{p^\dagger q\} \\
 &+ \sum_{pqia} B_{pqia}^{\text{I}} \{p^\dagger a^\dagger i q\} \\
 &+ \dots \text{(n-body terms)}
 \end{aligned}$$

The main advantage of defining the single component effective operators A^I , A^{II} , and B is that the form of the operators are similar (but not identical) to the electronic structure CCSD equations. As a consequence, the evaluation and implementation of these operators benefited from the development of computer-assisted source code generation of electronic structure CC methods.[139, 140, 141, 142] In this work we developed a program to perform algebraic manipulation of the strings of second-quantized (SQ) operators. This program was largely inspired by the tensor contraction engine (TCE) [140, 143, 144, 145, 146, 147, 148, 149, 150] which has been used extensively for implementation of electronic structure CC methods. A subset of techniques used in the TCE method [151] was used for source-code generation and implementation of the t amplitude equations. The program uses the well-known results of the Wick’s expansion theorem, in which only fully contracted terms have non-zero contribution for a vacuum expectation value of the a string of SQ operators (Figure 4.1).[60] In the first

$$\langle \mathbf{0} | \{X_1 X_2 \dots\} \{\dots Y_{N-1} Y_N\} | \mathbf{0} \rangle = \langle \mathbf{0} | \overbrace{X_1 X_2 \dots Y_{N-1} Y_N} | \mathbf{0} \rangle \quad (\text{fully contracted})$$

Figure 4.1: Wick’s theorem

step, for a given string of SQ operators, the program generated a list of all valid fully-contracted terms. In the second step, reduction operations were performed to reduce the number of terms. The final step involved generation of the mcCC source code. The reduction operation is the key step for increasing the efficiency of the implementation. The SQ program performed index permutation operations and consolidated equivalent expressions to minimize the number of terms in the fully contracted list.

In addition to performing index manipulations, the SQ program performed additional reduction operations by using the numerical value of the molecular integrals (h_{pq} and h_{pqrs}). This was performed by eliminating all numerically zero terms from the set of molecular integrals and mapping the non-unique terms to a set of unique terms. This mapping of terms is illustrated in Figure 4.2, where set A is the set

of original integrals and set B is a subset of set A containing only unique, non-zero terms. In the reduction step, terms with $h_{pq} = 0$ and $h_{pqrs} = 0$ were eliminated at a

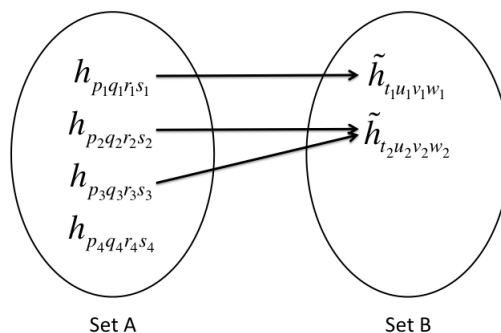


Figure 4.2: Many-to-one mapping of the molecular integrals. Set A contains the list of input integrals. Set B is a subset of A that contains the list of non-zero unique integrals. The terms $h_{p_2q_2r_2s_2}$ and $h_{p_3q_3r_3s_3}$ are assumed to have identical numerical values and are mapped to a single term in set B. The term $h_{p_4q_4r_4s_4}$ is assumed to be zero and is not included in set B.

very early stage of the calculation. The reduction process also performed additional consolidation for expressions with identical numerical values (for example $\tilde{h}_{t_2u_2v_2w_2}$ in [Figure 4.2](#)).

There are both advantages and disadvantages of using information from the molecular integrals for the reduction step. The main limitation is that the source code generation becomes system dependent and therefore the CC source code needs to be generated for each unique system. However, the advantage of a system dependent source code is that the generated code is highly optimized for the specific system under investigation and uses the intrinsic symmetries associated with the given system. The mapping of the integrals to the set of unique non-zero terms also helps in reducing the memory footprint.

The present version of the SQ program is still in the first iteration of its development cycle and is neither as general nor as efficient as the TCE. In future work

we envision interfacing the SQ program with the open-source version of the TCE for extending the implementation of mcCC theory.

4.4 Computational details

4.5 Results

The mcCC method was applied to a series of model systems to validate the theory and implementation. These systems are described in greater detail in the following subsections and their key properties are listed in [Table 4.1](#). Calculations were done on these systems using three different ansatz for the T operators as shown in the following equation

$$|\Psi_{\text{mcCCSD-SD}}\rangle = e^{T_1^{\text{I}}+T_2^{\text{I}}+T_1^{\text{II}}+T_2^{\text{II}}+T_{11}^{\text{I,II}}+T_{12}^{\text{I,II}}+T_{21}^{\text{I,II}}+T_{22}^{\text{I,II}}} |0^{\text{I}}0^{\text{II}}\rangle \quad (4.64)$$

$$|\Psi_{\text{mcCCSD-S}}\rangle = e^{T_1^{\text{I}}+T_2^{\text{I}}+T_1^{\text{II}}+T_2^{\text{II}}+T_{11}^{\text{I,II}}} |0^{\text{I}}0^{\text{II}}\rangle \quad (4.65)$$

$$|\Psi_{\text{mcCCSD}}\rangle = e^{T_1^{\text{I}}+T_2^{\text{I}}+T_1^{\text{II}}+T_2^{\text{II}}} |0^{\text{I}}0^{\text{II}}\rangle. \quad (4.66)$$

The suffix "-S" and "-SD" in the above expression are used to denote inclusion of connect I-II singles, and connect I-II singles and doubles operators, respectively. The three mcCC wave functions represent three different levels of approximations for treating correlation between type I and type II particles. We have compared the quality of these approximations with full configuration interaction calculations and results from these calculations are presented below.

4.5.1 Model-A single component Hooke's atom

The Hooke's atom is one of the few two-electron systems which can be solved exactly, making it an obvious choice for benchmarking the mcCC method. We label this

Table 4.1: **Important properties for systems studied.**

Property	Hooke's Model A	Hooke's Model B	PsH	Excitonic system	Biexcitonic system
Number of type I particles	2	1	2	1	2
Charge of type I particles	-1	-1	-1	-1	-1
Mass of type I particles	1	1	1	1	1
S_z for type I subsystem	0	$+\frac{1}{2}$	0	$+\frac{1}{2}$	0
Number of type II particles	0	1	1	1	2
Charge of type II particles	-	-1	+1	+1	+1
Mass of type II particles	-	1	1	1	1
S_z for type II subsystem	-	$-\frac{1}{2}$	$+\frac{1}{2}$	$-\frac{1}{2}$	0
Total spin(S)	0	0	$\frac{1}{2}$	0	0
Dielectric constant	1	1	1	1	1

system as "Model-A" and the Hamiltonian for this Hooke's atom is given by the following equation.

$$H_{\text{Hooke}}^{\text{Model-A}} = \sum_{i=1}^2 \left[\frac{-\hbar^2}{2m^{\text{I}}} \nabla_i^2 + \frac{1}{2} k^{\text{I}} (r_i^{\text{I}})^2 \right] + \frac{1}{r_{12}^{\text{I,I}}} \quad (4.67)$$

Notice that this Hamiltonian only includes type I particles - we do not include any type II particles and thus any type I-II coupling is absent. This calculation was done to ensure that the automated generation and solution of the single component CC ansatz ($|\Psi_{\text{CC}}\rangle = e^{T_1+T_2}|0\rangle$) would be correct. We have performed mcCC calculations on this Hamiltonian using [4s4p4d] GTO basis functions to allow for direct comparison to previous work.[152, 153, 154] The details of the GTO basis can be found in Table 4.9 located in section 4.A and the results from the calculations are presented in Table 4.2. The mcCC energy was found to be in very good agreement with the analytical ground state energy and was found to be higher than the analytical result by 0.76 mHartree. This result successfully demonstrates the single-component limit of the mcCC wave function.

Table 4.2: **Total energy of Model-A Hooke’s atom in Hartrees.**

Method	Total Energy	Ref.
Analytical	2.00000	[152, 153, 154]
mcHF	2.03844	This work
mcCC	2.00076	This work
mcFCI	2.00076	This work
FCI	2.00076	[152]

4.5.2 Model-B multicomponent Hooke’s atom

The Model-B Hooke’s atom is a hypothetical system that consist of treating two electrons in the Hooke’s atom as distinguishable particles. Specifically, the electron with alpha spin is labeled as type I particle, and electron with beta is labeled as type II particle. Using this labeling, the multicomponent Hamiltonian for this system is defined as

$$\begin{aligned}
 H_{\text{Hooke}}^{\text{Model-B}} = & \left[\frac{-\hbar^2}{2m^{\text{I}}} \nabla^2 + \frac{1}{2} k^{\text{I}} (r^{\text{I}})^2 \right] \\
 & + \left[\frac{-\hbar^2}{2m^{\text{II}}} \nabla^2 + \frac{1}{2} k^{\text{II}} (r^{\text{II}})^2 \right] \\
 & + \frac{1}{r_{12}^{\text{I,II}}}
 \end{aligned} \tag{4.68}$$

Because there is only one type I and one type II particle is present in the system, only the T_{11} term contributes to the correlation energy. Note that the mcCC calculation done for this system will only include T_1^{I} , T_1^{II} and $T_{11}^{\text{I,II}}$ operators in the ansatz due to only a single type I and single type II particle in the system. This Hamiltonian was used to perform mcCC calculations and the results are summarized in Table 4.3. The results from the mcCC calculations were found to be in very good agreement with previously published FCI results. The results from both Model-A and Model-B Hooke’s system demonstrates accurate implementation of the $(T_1^{\text{I}} + T_2^{\text{I}})$ and $T_{11}^{\text{I,II}}$ components of the mcCC ansatz.

Table 4.3: **Total energy of the Model-B Hooke’s atom in Hartrees.**

Method	Total Energy	Ref.
Analytical	2.00000	[152, 153, 154]
mcHF	2.03844	This work
mcCC	2.00076	This work
mcFCI	2.00076	This work
FCI	2.00076	[152]

Table 4.4: **Total energy of positronium hydride (PsH) given in Hartrees.**

Method	Ground state energy (Hartree)	Ref.
$E_{\text{NEO-HF}}$	-0.666872	[155, 156]
E_{mcHF}	-0.666872	This work
$E_{\text{mcCCSD-S}}$	-0.754000	This work
$E_{\text{mcCCSD-SD}}$	-0.758956	This work
$E_{\text{NEO-FCI}}$	-0.758965	[155, 156]

4.5.3 Positronium hydride system

The positronium hydride (PsH) molecule is a multicomponent system which can be viewed as a positron (e^+) bound to the H^- anion. The PsH system is a prototype for studying electron-positron correlation and has been studied using various theoretical methods including perturbation theory,[155] full configuration interaction (FCI),[155, 156] explicitly correlated methods.[157] In this work, we have performed mcCC calculation on the PsH system, where the two electrons were treated as type I particles, the single positron was treated as type II particle, and the proton was BO separated from the electron-positron subsystem. The mcCC calculations were performed using a set of [6s3p1d] GTO basis functions (shown in Table 4.10 in section 4.A) which was used earlier for FCI calculations[155, 156] and comparison of results between the two methods are presented in Table 4.4. The use of identical set of basis functions ensured a consistent comparison between the mcCC and FCI calculations. Comparison between mcCCSD-SD and FCI energies show very good agreement between the two methods demonstrating the effectiveness of mcCCSD-SD method

for treatment many-particle correlation. We note that the results are invariant to the definition of type I and type II particles and labeling the hole as type I and electrons as type II generate identical results. These results demonstrate accurate implementation of the $(T_{21}^{I,II} + T_{12}^{I,II})$ components of the mcCC ansatz.

4.5.4 Excitonic systems

The mcCC method was also used for computation of exciton binding energies. The external potential was approximated using the 3D parabolic potential defined below

$$v_{\text{ext}}^{\alpha} = \frac{1}{2}k^{\alpha}|\mathbf{r}^{\alpha}|^2 \quad \alpha = \text{I, II.} \quad (4.69)$$

A parabolic potential was chosen because they have been used extensively [158, 159, 160, 161, 162, 163, 164, 165, 166, 167, 37, 35, 36] to represent the confinement potential experienced by excitons in nanoparticles. The values of the force constant parameter, k , were selected such that the confining potential spanned from weakly confining region ($k = 1.0 \times 10^{-4}$ a.u.) to strongly confining region ($k = 5.0$ a.u.) The details of the excitonic systems are summarized in Table 4.1. The overall spin for the exciton was set at $S_{\text{exciton}} = 0$ and electron-hole pair in the exciton was assumed to have opposite spins. A set of [spd] GTO functions were used for electron and hole basis functions and the values for the exponents for each value of k is provided in section 4.A.

For all the excitonic and biexcitonic systems, the masses for the electron and holes were selected to be identical to each other. Although this choice of having identical electron and hole masses is not representative of realistic chemical systems, however this selection was made to impose stringent condition for testing the mcCC implementation. Specifically, one of the cornerstones of the BO approximation is the use of mass ratio (labeled $\kappa = (m_e/m_N)^{1/4}$) by Born and Oppenheimer to perform

perturbative expansion of the multicomponent wave function. [1, 168] By setting the electron and hole masses to be identical, we simulate the worst case scenario limit where the BO-approximation is not valid. In the same spirit, we also set the dielectric constant to one, which is a more stringent condition than found in chemical systems where the dielectric constant is greater than 1 because of dielectric screening.

In addition to mcCC calculations, we also performed multicomponent full configuration interaction (mcFCI) calculations on the eight excitonic systems in order to verify validity of the mcCC method. The mcFCI energy was obtained from the solution of the following equations

$$\Psi_{\text{mcFCI}} = \sum_i^{N_{\text{FCI}}^{\text{I}}} \sum_{i'}^{N_{\text{FCI}}^{\text{II}}} c_{ii'} \Phi_i^{\text{I}} \Phi_{i'}^{\text{II}} \quad (4.70)$$

$$E_{\text{mcFCI}} = \min_{\mathbf{c}} \langle \Psi_{\text{mcFCI}} | H | \Psi_{\text{mcFCI}} \rangle \quad (4.71)$$

and the mcFCI correlation energy ($\Delta E_{\text{mcFCI}} = E_{\text{mcFCI}} - E_{\text{mcHF}}$) was compared with the mcCC results. As shown in Table 4.5, the mcCC energies were found to be in excellent agreement with the mcFCI results. For the excitonic system, both mcCCSD

Table 4.5: **Total exciton energy calculated from mcHF and correlation energy from mcCCSD, mcCCSD-SD, and mcFCI methods reported in Hartrees as function of k .**

$k(\text{a.u.})$	E_{mcHF}	ΔE_{mcCCSD}	$\Delta E_{\text{mcCCSD-SD}}$	ΔE_{mcFCI}
0.0001	-0.06611	0.00000	-0.01008	-0.01008
0.0010	-0.06844	0.00000	-0.01526	-0.01526
0.0100	0.02282	0.00000	-0.02101	-0.02101
0.1000	0.47374	0.00000	-0.02554	-0.02554
0.2500	0.90931	0.00000	-0.02686	-0.02686
0.5000	1.42379	0.00000	-0.02763	-0.02763
1.0000	2.17547	0.00000	-0.02828	-0.02828
5.0000	5.48836	0.00000	-0.02942	-0.02942

and mcCCSD-S form of the CC wave functions are equivalent to the mcHF and

mcCCSD-SD wave functions, respectively and are not shown in [Table 4.5](#) to avoid repetition.

The results for the exciton binding energies are presented in [Table 4.6](#). Exciton binding energy (E_{EBE}) is defined as the difference in energies between the non-interacting and interaction electron-hole pair and is given by the following expression

$$E_{\text{EBE}} = \langle \Psi_0 | H | \Psi_0 \rangle - \langle \Psi_{\text{eh}} | H_{\text{eh}} | \Psi_{\text{eh}} \rangle \quad (4.72)$$

$$H_{\text{eh}} = H_0 + V_{\text{eh}} \quad (4.73)$$

where Ψ_{eh} and Ψ_0 are wave functions that minimizes the energy of the interacting (H_{eh}) and non-interacting (H_0) systems, respectively. The exciton binding energies calculated using the mcCC method were found to be in very good agreement with the mcFCI results. The exciton binding energy was found to increase with increasing

Table 4.6: Exciton binding energy calculated using mcHF, mcCCSD, mcCCSD-SD, and mcFCI methods reported in eV as function of k .

$k(\text{a.u.})$	mcHF	mcCCSD	mcCCSD-SD	mcFCI
0.0001	2.615	2.615	2.889	2.889
0.0010	4.444	4.444	4.859	4.859
0.0100	7.542	7.542	8.114	8.114
0.1000	12.924	12.924	13.619	13.619
0.2500	16.073	16.073	16.804	16.804
0.5000	18.981	18.981	19.733	19.733
1.0000	22.437	22.437	23.206	23.206
5.0000	33.194	33.194	33.994	33.994

strength of the confinement potential and its dependence on the force constant of the external potential is shown in [Figure 5.5](#).

4.5.5 Biexcitonic system

Biexcitons are bound two-electron, two-hole quasiparticles that are formed from two weakly interacting excitons. Using the mcCC method, we calculated total correlation

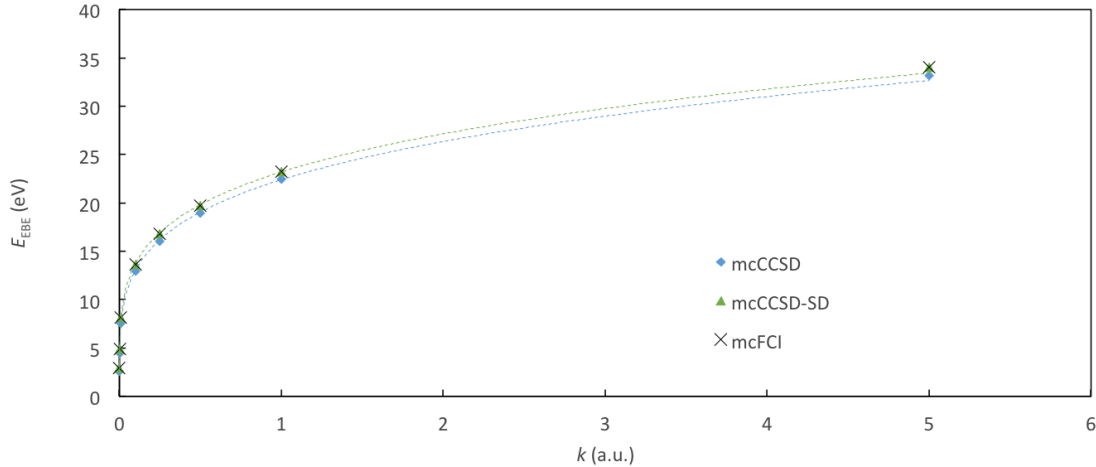


Figure 4.3: Dependence of exciton binding energy calculated using mcCCSD, mcCCSD-SD, and mcFCI on the strength of the confinement potential.

energy and biexciton binding energy for a set of eight model systems. Total correlation energy of the biexciton systems was calculated by subtracting the vacuum energy from total energy,

$$\Delta E_{\text{mcCC}} = E_{\text{mcCC}} - E_{\text{ref}} \quad (4.74)$$

and biexciton binding energy E_{BBE} was defined as the difference between the energies of the free excitons (E_X) and the total biexciton energy E_{X_2} . [39, 93]

$$E_{\text{BBE}} = E_{X_2} - 2E_X \quad (4.75)$$

The biexciton binding energy calculations were performed in three steps. In the first step, mcCC calculation on the fully interacting biexciton (2e,2h) was performed and the total biexcitonic energy was obtained. In the second step, mcCC calculation on the fully interacting exciton (1e,1h) was performed and the total exciton energy was obtained. In the final step, the biexciton binding energy was calculation using Eq.(4.75). The details of the biexcitonic systems are summarized in Table 4.1. Each of the eight biexcitonic systems consisted of electron-hole pairs with unit charges and

masses ($m^{\text{I}} = m^{\text{II}} = 1\text{a.u.}$). The dielectric function in Eq. (7.33) was assumed to be constant and was set to $\epsilon = 1$. The overall spin for the biexciton was set at $S_{\text{biexciton}} = 0$ and both electrons and holes separately were assumed to be spin-paired.

The correlation energies calculated using mcCCSD, mcCCSD-SD and mcFCI for the excitonic and biexcitonic systems are presented in Table 4.7. The comparison between mcCCSD-SD and mcFCI results shows very good agreement between the two methods for all values of k . The maximum difference between mcCCSD-SD and mcFCI correlation energy was found to be in the order of 10^{-5} Hartrees. In contrast, the mcCCSD calculations were found to underestimate the correlation energy and recovered only 19 – 34% of the mcFCI correlation energy for all values of the confinement potential. In contrast, the mcCCSD-S calculations were able to recover 85 – 99% of the mcFCI correlation energy. These results highlight the importance of including connected excitation operator in the mcCC wave function. The results also show that connected operators are important in both weak and strong confinement regions. The exciton and biexciton binding energies calculated using the methods

Table 4.7: Total biexciton energy calculated from mcHF and correlation energy from mcCCSD, mcCCSD-S, mcCCSD-SD, and mcFCI methods reported in Hartrees as function of k .

$k(\text{a.u.})$	E_{mcHF}	ΔE_{mcCCSD}	$\Delta E_{\text{mcCCSD-S}}$	$\Delta E_{\text{mcCCSD-SD}}$	ΔE_{mcFCI}
0.0001	-0.13221	-0.00501	-0.02291	-0.02666	-0.02666
0.0010	-0.13688	-0.01025	-0.03997	-0.04466	-0.04466
0.0100	0.04564	-0.01965	-0.06562	-0.07044	-0.07044
0.1000	0.94748	-0.03166	-0.09640	-0.10021	-0.10021
0.2500	1.81862	-0.03633	-0.10874	-0.11197	-0.11197
0.5000	2.84759	-0.03956	-0.11753	-0.12028	-0.12028
1.0000	4.35094	-0.04253	-0.12582	-0.12813	-0.12813
5.0000	10.97673	-0.04843	-0.14296	-0.14436	-0.14436

described above are presented in Table 4.8. The mcCCSD-SD binding energies were found to be in very good agreement with the mcFCI results. The mcCCSD results deviated from the mcFCI results and recovered 57 – 77% of the mcFCI binding en-

ergies. The mcCCSD-S calculations were found to recover 42 – 98% of the mcFCI binding energies. The results from [Table 4.7](#) and [Table 4.8](#) also show the role of cancellation of errors in biexciton binding energy calculations. For example, the correlation energy data from [Table 4.7](#) clearly show the advantage of the mcCCSD-S over the mcCCSD method. However, in biexciton binding energy calculations ([Table 4.8](#)) for some systems, the mcCCSD method outperformed the mcCCSD-S method due to coincidental favorable cancellation of errors. These results underscore the pitfall of using only biexciton binding energy data to assess quality of theoretical methods. The results in [Table 4.8](#) also highlight the importance of particle-particle correlation

Table 4.8: **Biexciton binding energy calculated using mcHF, mcCCSD, mcCCSD-S, mcCCSD-SD, and mcFCI methods reported in meV as function of k .**

$k(\text{a.u.})$	mcHF	mcCCSD	mcCCSD-S	mcCCSD-SD	mcFCI
0.0001	0	136	75	177	177
0.0010	0	279	257	385	385
0.0100	0	535	642	773	773
0.1000	0	861	1233	1337	1337
0.2500	0	989	1497	1585	1585
0.5000	0	1076	1694	1769	1769
1.0000	0	1157	1885	1948	1948
5.0000	0	1318	2289	2327	2327

in calculations of biexciton binding energy. Specifically, comparison of the mcHF and mcCCSD-SD results shows that the Hartree-Fock approximation is qualitatively inadequate capturing biexcitonic interactions. Comparing with mcCCSD results, we find that inclusion of e-e and h-h correlation can significantly improve the Hartree-Fock results. However, the quality of the improvement is a function of confinement potential. The dependence of the biexciton binding energy on the strength of the potential is shown in [Figure 5.6](#). As expected, we find that the biexciton is bound strongly in high confinement regions. This trend is consistent with the quantum confinement effect observed in optical properties of semiconductor nanoparticles. [Figure 5.6](#) also

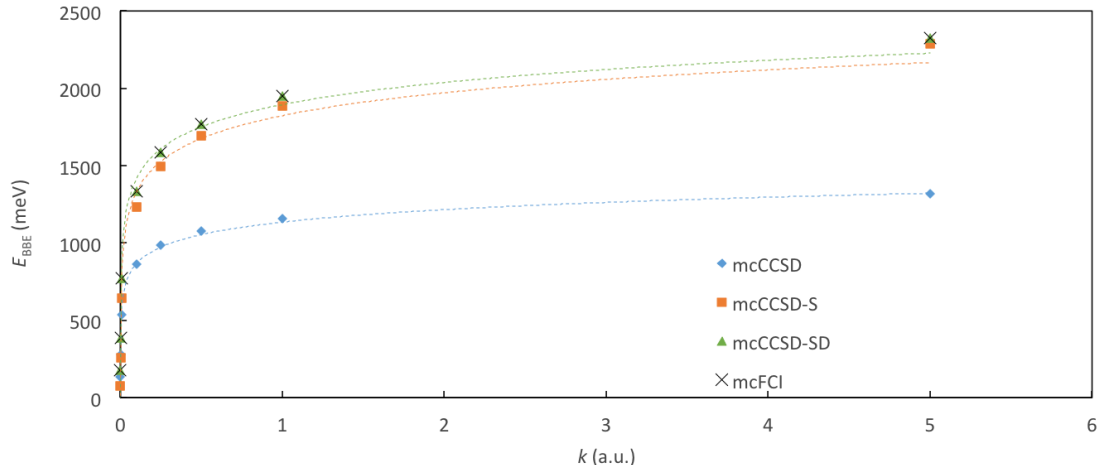


Figure 4.4: Dependence of biexciton binding energy calculated using mcCCSD, mcCCSD-S, mcCCSD-SD, and mcFCI on the strength of the confinement potential.

shows that the mcCCSD-S method outperforms the mcCCSD method in the high confinement region and is a computationally cost effective alternative to the much more expensive mcCCSD-SD method.

The mcCCSD-S calculations ran over ten times faster than the mcCCSD-SD calculations. Amplitude equations were set to converge to 1×10^{-8} which took roughly 48 hour fore the mcCCSD-SD calculations and about 4 hours for the mcCCSD-S calculations. Each calculation was done on TACC Stampede and used a single node (two Intel Xeon E5-2680 2.7GHz processors) running 16 threads.

4.6 Conclusion

In this work, we present the theoretical development and implementation details of the multicomponent coupled-cluster theory. This method was developed to investigate particle-particle correlation in many-particle multicomponent systems such as electron-proton, electron-positron, and electron-hole systems. Specifically, the construction of the multicomponent vacuum state, form of the cluster operator, and the expressions for the cluster amplitudes were discussed. The coupled-cluster equations

were implemented using a computer-assisted source code generation strategy employing an integral-driven approach. The developed method was used to investigate electron-hole quasiparticle interactions in biexcitonic systems by calculating total correlation energy and biexciton binding energies. These quantities were found to be in very good agreement with full configuration interaction results. Based on these calculations we conclude that (1) the mean-field approximation severely underestimates the biexciton binding energies and is not a suitable approximation for treating biexcitonic systems and (2) the inclusion of connected excitation operators in the multicomponent coupled-cluster wave function is crucial for accurate calculation of electron-hole correlation energy. The method presented here provides a foundation for extending multicomponent coupled-cluster theory and future work will explore perturbative approaches to connected excitation and linearized version of this method.

4.A Calculation parameters

Table 4.9: Values of the exponents for the [4s4p4d] GTO basis functions (in atomic units) for the Hooke’s atom calculations.^[152]

	α
1s	0.231598
2s	0.407633
3s	0.717471
4s	1.262815
1p	0.234844
2p	0.389490
3p	0.645973
4p	1.071350
1d	0.234204
2d	0.400061
3d	0.683376
4d	1.167326

Table 4.10: Values of the exponents for the [6s3p1d] GTO basis functions (in atomic units) for the positronium hydride (PsH) system.[156]

	α_{e^-}	α_{e^+}
1s	66.011	8.9346
2s	10.002	1.5904
3s	2.3585	0.51619
4s	0.73659	0.11092
5s	0.26847	0.052472
6s	0.049378	0.024562
1p	0.67771	0.47831
2p	0.19922	0.18726
3p	0.075304	0.069729
1d	0.17232	0.15439

Table 4.11: Values of the exponents for the [spd] GTO basis functions (in atomic units) used for calculating exciton and biexciton binding energies.

$k(\text{a.u.})$	α
0.0001	5.00×10^{-3}
0.0010	1.58×10^{-2}
0.0100	5.00×10^{-2}
0.1000	1.58×10^{-1}
0.2500	2.50×10^{-1}
0.5000	3.54×10^{-1}
1.0000	5.00×10^{-1}
5.0000	1.12

Chapter 5

Investigating biexcitons in semiconductor quantum dots

In this chapter, a study carried out with the multicomponent coupled-cluster method is presented. Previous calculations using the mcCC method were done on benchmark systems that all had known results. This work investigated how quantum dot material and size affects exciton, and more importantly biexciton binding energy. This scaling behavior has been heavily studied for excitons, though little work has been done for biexcitons.

5.1 Introduction

The electron-hole quasiparticle representation provides an intuitive description of electronic excitations in semiconductor nanoparticles. The generation of bound electron-hole pairs, also called excitons, is a central concept for investigating optical properties of quantum dots (QDs) and has been subject of intense research for a wide variety of applications in the fields of light-harvesting devices, [169, 170, 171, 172] light emitting devices, [173, 174, 175, 176] and biological imaging. [177, 178, 179, 180, 181, 182, 183, 184]

In addition to excitonic states, semiconductor materials have also been shown to exhibit multiexcitonic states, such as biexcitons, trions, and electron-hole liquid and droplets. The generation and dissociation of multiexcitons also have been the focus of intense research because of their application in light-harvesting systems. [171, 185, 186, 187, 188, 189, 190, 191] Multiexcitonic systems, such as biexcitons and electron-hole liquid and droplets, are characterized as bound states that consist of at least two quasiparticles. These systems are intrinsically different than a collection of non-interacting excitons because their photophysical properties depend strongly on the strength of the exciton-exciton interaction. In the case of a biexciton, the strength of this interaction is known as the biexciton binding energy, which is defined as the energy needed to dissociate a biexciton into a pair of non-interacting excitons ($E_{\text{BB}} = 2E_{\text{X}} - E_{\text{XX}}$). Typically, the exciton-exciton interaction is much weaker than an electron-hole interaction and consequently, biexciton binding energies are generally an order of magnitude lower than the exciton binding energies. Like excitons, the optical and electronic properties of biexcitons are also influenced by the quantum confinement effect. The biexcitonic interactions in QDs are influenced by the size and composition of the QD. In this work, we present a systematic investigation of the effect of QD size and composition on electron-hole interactions in biexcitonic systems. The binding energy can be separated into contributions from mean-field (Hartree-Fock) and electron-hole correlation. It is well-known from earlier studies[39, 192] that, unlike exciton binding energies, biexciton binding energies are dominated by the electron-hole correlation contribution. Because of this, it is imperative to have a highly accurate quantum chemical method for treating electron-hole correlation in biexcitonic systems. The dominance of the electron-hole correlation contribution also suggests that, when compared to excitonic systems, biexciton binding will be impacted differently by changes in the confinement potential of the QDs.

In this work, we present a systematic study of the effect of QD size on biexciton binding energy. Specifically, the work answers three critical questions in the field of biexcitonic systems: (1) what effect does QD dot size have on biexciton binding energies, (2) how does material of the QD affect the biexciton binding energies, and (3) how are the stabilities of biexcitons related to the stabilities of excitons. However, the theoretical investigation of biexciton binding is challenging for three reasons. First, the biexciton binding energy is typically in the range of 1-50 meV and requires high-precision quantum mechanical methods to calculate these quantities. Second, as previously mentioned, earlier studies have demonstrated that the biexciton binding energy is dominated by electron-hole correlation energy. Consequently, accurate descriptions of biexcitonic interaction demand accurate treatment of electron-hole correlation. Third, an accurate biexciton binding energy calculation requires a size-consistent treatment of electron-hole correlation. Using a size-consistent quantum mechanical method like the electron-hole multicomponent coupled-cluster (eh-mcCC) ansatz [192] will provide a balanced treatment of many-particle correlation (electron-electron, hole-hole, and electron-hole) for both the biexcitonic and excitonic systems.

5.2 Theory

The excitons and biexcitons are described using the electron-hole (eh) quasiparticle Hamiltonian, and the quasiparticle interactions are defined using screened-Coulomb interaction. This well-known Hamiltonian has been used in earlier studies[193, 194, 195, 196, 197] on excitonic and multiexcitonic systems. The electron-hole Hamiltonian

in second quantized notation is defined as

$$\begin{aligned}
H^{\text{eh}} = & \sum_{pq} \langle p|h^e|q\rangle p^\dagger q + \sum_{pqrs} \langle pq|v^{e,e}|rs\rangle p^\dagger q^\dagger sr \\
& + \sum_{p'q'} \langle p'|h^h|q'\rangle p'^\dagger q' + \sum_{p'q'r's'} \langle p'q'|v^{h,h}|r's'\rangle p'^\dagger q'^\dagger s'r' \\
& + \sum_{pp'qq'} \langle pp'|v^{e,h}|qq'\rangle p^\dagger p'^\dagger qq'
\end{aligned} \tag{5.1}$$

where, the unprimed and primed operators represent electron and hole quasiparticles, respectively. The material parameters for the Hamiltonian relevant for the systems investigated in this work are provided in Supporting Information. The multicomponent vacuum state, $|0^e0^h\rangle$, is obtained via multicomponent Hartree-Fock (mcHF) using the following scheme,

$$\langle 0^e0^h|H|0^e0^h\rangle = \min_{\Phi_{\text{SD}}^e \Phi_{\text{SD}}^h} \langle \Phi_{\text{SD}}^e \Phi_{\text{SD}}^h | H | \Phi_{\text{SD}}^e \Phi_{\text{SD}}^h \rangle \tag{5.2}$$

and the normal-ordered Hamiltonian is written as,

$$H_{\text{N}} = H - \langle 0^e0^h|H|0^e0^h\rangle. \tag{5.3}$$

The form of the mcCC wave function in this work is defined as

$$|\Psi_{\text{mcCC}}^{\text{e,h}}\rangle = e^{T_1^e + T_2^e + T_1^h + T_2^h + T_{11}^{\text{e,h}}} |0^e0^h\rangle \tag{5.4}$$

$$= e^T |0^e0^h\rangle. \tag{5.5}$$

where the cluster operators, the T_1^e , T_2^e , T_1^h , and T_2^h are equivalent to single-component coupled-cluster excitation operators (α being either e or h),

$$T_1^\alpha = \sum_i^N \sum_a^M t_i^\alpha \{a^\dagger i\} \tag{5.6}$$

$$T_2^\alpha = \frac{1}{4} \sum_{ij}^N \sum_{ab}^M t_{ij}^{ab} \{a^\dagger b^\dagger j i\} \quad (5.7)$$

The electronic T operators excite only in electronic space and hole T operators excite only in hole space. The $T_{11}^{\text{e,h}}$ operator, which is defined below, is a connected excitation operator that simultaneously performs single excitations in electronic and hole spaces.

$$T_{11}^{\text{e,h}} = \sum_i^N \sum_a^M \sum_{i'}^{N'} \sum_{a'}^{M'} t_{ii'}^{aa'} \{a^\dagger i\} \{a'^\dagger i'\} \quad (5.8)$$

The summation limits to N and M are to occupied and virtual states, respectively, and that hole indices are primed while electronic indices are not. The mcCC Schrödinger equation,

$$H_N e^T |0^e 0^h\rangle = \Delta E_{\text{mcCC}} e^T |0^e 0^h\rangle \quad (5.9)$$

will yield the six mcCC equations we need to solve after performing the similarity transformation and projecting into the appropriate states,

$$\langle 0^e 0^h | e^{-T} H_N e^T | 0^e 0^h \rangle_c = \Delta E_{\text{mcCC}} \quad (5.10)$$

$$\langle S^e 0^h | e^{-T} H_N e^T | 0^e 0^h \rangle_c = 0 \quad (5.11)$$

$$\langle D^e 0^h | e^{-T} H_N e^T | 0^e 0^h \rangle_c = 0 \quad (5.12)$$

$$\langle 0^e S^h | e^{-T} H_N e^T | 0^e 0^h \rangle_c = 0 \quad (5.13)$$

$$\langle 0^e D^h | e^{-T} H_N e^T | 0^e 0^h \rangle_c = 0 \quad (5.14)$$

$$\langle S^e S^h | e^{-T} H_N e^T | 0^e 0^h \rangle_c = 0. \quad (5.15)$$

Expanding the energy expression gives,

$$\begin{aligned} \Delta E_{\text{mcCC}} = \langle 0^e 0^h | V_N^{e,h} [1 + T_{11}^{e,h} + T_1^e + T_1^e T_1^h + T_1^h] + \\ H_N^h [1 + T_1^h + \frac{1}{2!} T_1^{h^2} + T_2^h] + \\ H_N^e [1 + T_1^e + \frac{1}{2!} T_1^{e^2} + T_2^e] | 0^e 0^h \rangle. \end{aligned} \quad (5.16)$$

The resulting singles equations are of the following form,

$$\begin{aligned} \langle S^e 0^h | V_N^{e,h} [1 + T_{11}^{e,h} + T_1^e + T_1^e T_{11}^{e,h} + T_1^e T_1^h + \frac{1}{2!} T_1^{e^2} + \frac{1}{2!} T_1^{e^2} T_1^h + T_1^h + T_2^e + T_2^e T_1^h] + \\ [(-T_1^e)] V_N^{e,h} [1 + T_{11}^{e,h} + T_1^e + T_1^e T_1^h + T_1^h] + \\ H_N^h [T_{11}^{e,h} + T_1^e + T_1^e T_1^h + T_1^e \frac{1}{2!} T_1^{h^2} + T_1^e T_2^h + T_1^h T_{11}^{e,h}] + \\ [(-T_1^e)] H_N^h [1 + T_1^h + \frac{1}{2!} T_1^{h^2} + T_2^h] + \\ H_N^e [1 + T_1^e + T_1^e T_2^e + \frac{1}{2!} T_1^{e^2} + \frac{1}{3!} T_1^{e^3} + T_2^e] + \\ [(-T_1^e)] H_N^e [1 + T_1^e + \frac{1}{2!} T_1^{e^2} + T_2^e] | 0^e 0^h \rangle = 0. \end{aligned} \quad (5.17)$$

The expanded doubles equation is,

$$\begin{aligned}
& \langle D^e 0^h | V_N^{e,h} [T_{11}^{e,h} + T_1^e + T_1^e T_{11}^{e,h} + T_1^e T_1^h + T_1^e T_2^e + T_1^e T_2^e T_1^h + \frac{1}{2!} T_1^{e^2} + \frac{1}{2!} T_1^{e^2} T_{11}^{e,h} + \frac{1}{2!} T_1^{e^2} T_1^h + \\
& \quad \frac{1}{3!} T_1^{e^3} + \frac{1}{3!} T_1^{e^3} T_1^h + T_2^e + T_2^e T_{11}^{e,h} + T_2^e T_1^h] + \\
& \quad [(-T_2^e)] V_N^{e,h} [1 + T_{11}^{e,h} + T_1^e + T_1^e T_1^h + T_1^h] + \\
& \quad [(-T_1^e)] V_N^{e,h} [1 + T_{11}^{e,h} + T_1^e + T_1^e T_{11}^{e,h} + T_1^e T_1^h + \frac{1}{2!} T_1^{e^2} + \frac{1}{2!} T_1^{e^2} T_1^h + T_1^h + T_2^e + T_2^e T_1^h] + \\
& \quad [\frac{1}{2!} T_1^{e^2}] V_N^{e,h} [1 + T_{11}^{e,h} + T_1^e + T_1^e T_1^h + T_1^h] + \\
& \quad H_N^h [T_1^e T_{11}^{e,h} + T_1^e T_1^h T_{11}^{e,h} + \frac{1}{2!} T_1^{e^2} + \frac{1}{2!} T_1^{e^2} T_1^h + \frac{1}{2!} T_1^{e^2} \frac{1}{2!} T_1^{h^2} + \frac{1}{2!} T_1^{e^2} T_2^h + \\
& \quad T_2^e + T_2^e T_1^h + T_2^e \frac{1}{2!} T_1^{h^2} + T_2^e T_2^h] + \\
& \quad [(-T_2^e)] H_N^h [1 + T_1^h + \frac{1}{2!} T_1^{h^2} + T_2^h] + \\
& \quad [(-T_1^e)] H_N^h [T_{11}^{e,h} + T_1^e + T_1^e T_1^h + T_1^e \frac{1}{2!} T_1^{h^2} + T_1^e T_2^h + T_1^h T_{11}^{e,h}] + \\
& \quad [\frac{1}{2!} T_1^{e^2}] H_N^h [1 + T_1^h + \frac{1}{2!} T_1^{h^2} + T_2^h] + \\
& \quad H_N^e [1 + T_1^e + T_1^e T_2^e + \frac{1}{2!} T_1^{e^2} + \frac{1}{2!} T_1^{e^2} T_2^e + \frac{1}{3!} T_1^{e^3} + \frac{1}{4!} T_1^{e^4} + T_2^e + \frac{1}{2!} T_2^{e^2}] + \\
& \quad [(-T_2^e)] H_N^e [1 + T_1^e + \frac{1}{2!} T_1^{e^2} + T_2^e] + [(-T_1^e)] H_N^e [1 + T_1^e + T_1^e T_2^e + \frac{1}{2!} T_1^{e^2} + \frac{1}{3!} T_1^{e^3} + T_2^e] + \\
& \quad [\frac{1}{2!} T_1^{e^2}] H_N^e [1 + T_1^e + \frac{1}{2!} T_1^{e^2} + T_2^e] | 0^e 0^h \rangle = 0. \tag{5.18}
\end{aligned}$$

The complementary singles and doubles equation for the hole particles are not repeated here for conciseness. The singles-singles amplitude equation is

$$\begin{aligned}
& \langle S^e S^h | V_N^{e,h} [1 + T_{11}^{e,h} + T_1^e + T_1^e T_{11}^{e,h} + T_1^e T_1^h + T_1^e T_1^h T_{11}^{e,h} + T_1^e \frac{1}{2!} T_1^{h^2} + \\
& T_1^e T_2^h + \frac{1}{2!} T_1^{e^2} + \frac{1}{2!} T_1^{e^2} T_1^h + \frac{1}{2!} T_1^{e^2} \frac{1}{2!} T_1^{h^2} + \frac{1}{2!} T_1^{e^2} T_2^h + T_1^h + T_1^h T_{11}^{e,h} + \frac{1}{2!} T_1^{h^2} + \\
& T_2^e + T_2^e T_1^h + T_2^e \frac{1}{2!} T_1^{h^2} + T_2^e T_2^h + T_2^h] + \\
& [(-T_{11}^{e,h})] V_N^{e,h} [1 + T_{11}^{e,h} + T_1^e + T_1^e T_1^h + T_1^h] + \\
& [(-T_1^h)] V_N^{e,h} [1 + T_{11}^{e,h} + T_1^e + T_1^e T_{11}^{e,h} + T_1^e T_1^h + \frac{1}{2!} T_1^{e^2} + \frac{1}{2!} T_1^{e^2} T_1^h + T_1^h + T_2^e + T_2^e T_1^h] + \\
& [(-T_1^e)] V_N^{e,h} [1 + T_{11}^{e,h} + T_1^e + T_1^e T_1^h + T_1^e \frac{1}{2!} T_1^{h^2} + T_1^e T_2^h + T_1^h + T_1^h T_{11}^{e,h} + \frac{1}{2!} T_1^{h^2} + T_2^h] + \\
& [(-T_1^e)(-T_1^h)] V_N^{e,h} [1 + T_{11}^{e,h} + T_1^e + T_1^e T_1^h + T_1^h] + \\
& H_N^h [T_{11}^{e,h} + T_1^e + T_1^e T_1^h + T_1^e T_1^h T_2^h + T_1^e \frac{1}{2!} T_1^{h^2} + T_1^e \frac{1}{3!} T_1^{h^3} + T_1^e T_2^h + \\
& T_1^h T_{11}^{e,h} + \frac{1}{2!} T_1^{h^2} T_{11}^{e,h} + T_2^h T_{11}^{e,h}] + \\
& [(-T_{11}^{e,h})] H_N^h [1 + T_1^h + \frac{1}{2!} T_1^{h^2} + T_2^h] + \\
& [(-T_1^h)] H_N^h [T_{11}^{e,h} + T_1^e + T_1^e T_1^h + T_1^e \frac{1}{2!} T_1^{h^2} + T_1^e T_2^h + T_1^h T_{11}^{e,h}] + \\
& [(-T_1^e)] H_N^h [1 + T_1^h + T_1^h T_2^h + \frac{1}{2!} T_1^{h^2} + \frac{1}{3!} T_1^{h^3} + T_2^h] + \\
& [(-T_1^e)(-T_1^h)] H_N^h [1 + T_1^h + \frac{1}{2!} T_1^{h^2} + T_2^h] + \\
& H_N^e [T_{11}^{e,h} + T_1^e T_{11}^{e,h} + T_1^e T_1^h + T_1^e T_2^e T_1^h + \frac{1}{2!} T_1^{e^2} T_{11}^{e,h} + \frac{1}{2!} T_1^{e^2} T_1^h + \frac{1}{3!} T_1^{e^3} T_1^h + \\
& T_1^h + T_2^e T_{11}^{e,h} + T_2^e T_1^h] + \\
& [(-T_{11}^{e,h})] H_N^e [1 + T_1^e + \frac{1}{2!} T_1^{e^2} + T_2^e] + \\
& [(-T_1^h)] H_N^e [1 + T_1^e + T_1^e T_2^e + \frac{1}{2!} T_1^{e^2} + \frac{1}{3!} T_1^{e^3} + T_2^e] + \\
& [(-T_1^e)] H_N^e [T_{11}^{e,h} + T_1^e T_{11}^{e,h} + T_1^e T_1^h + \frac{1}{2!} T_1^{e^2} T_1^h + T_1^h + T_2^e T_1^h] + \\
& [(-T_1^e)(-T_1^h)] H_N^e [1 + T_1^e + \frac{1}{2!} T_1^{e^2} + T_2^e] | 0^e 0^h \rangle = 0 \tag{5.19}
\end{aligned}$$

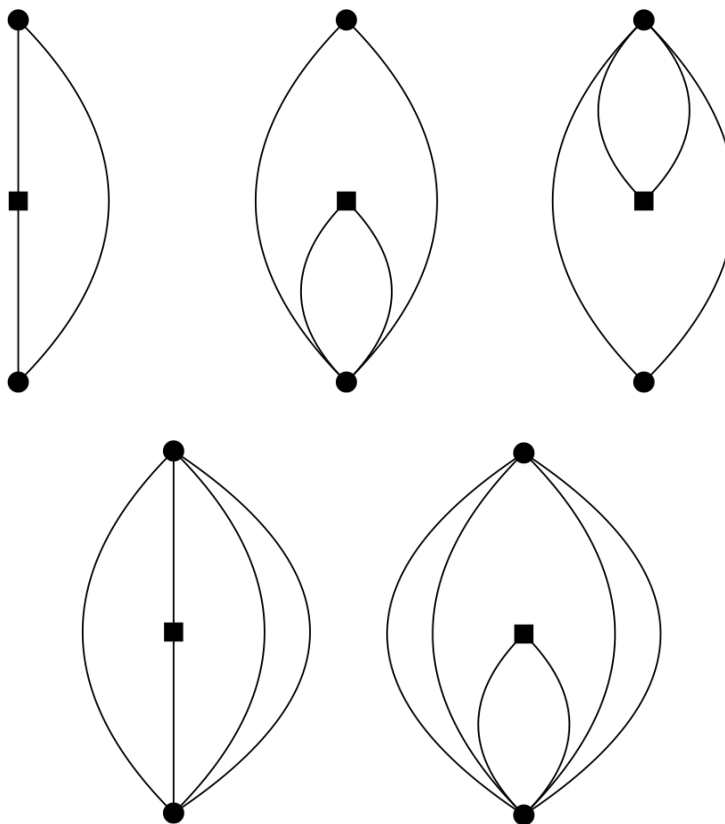


Figure 5.1: Hugenholtz skeleton diagrams for one-body operators. The square and the dot symbols represent the Hamiltonian and the excitation operators, respectively.

The equations for the t -amplitudes can be conveniently derived using the diagrammatic representation and in this work we have used the Hugenholtz diagrammatic representation. The Hugenholtz skeleton diagrams representing connected terms for the all one-body and two-body operators are presented in [Figure 5.1](#) and [Figure 5.2](#), respectively. Computer implementation of the t -amplitude equations were achieved using the computer-assisted source code generation procedure where the generalize Wick's contraction of strings of second-quantized operators was performed using symbolic algebraic manipulation.[\[148\]](#) After successful calculation of the correlation energy, the exciton binding energies were calculated by subtracting the total exciton energy (E_X) from the non-interacting energy of the electron and hole (E_e and E_h)

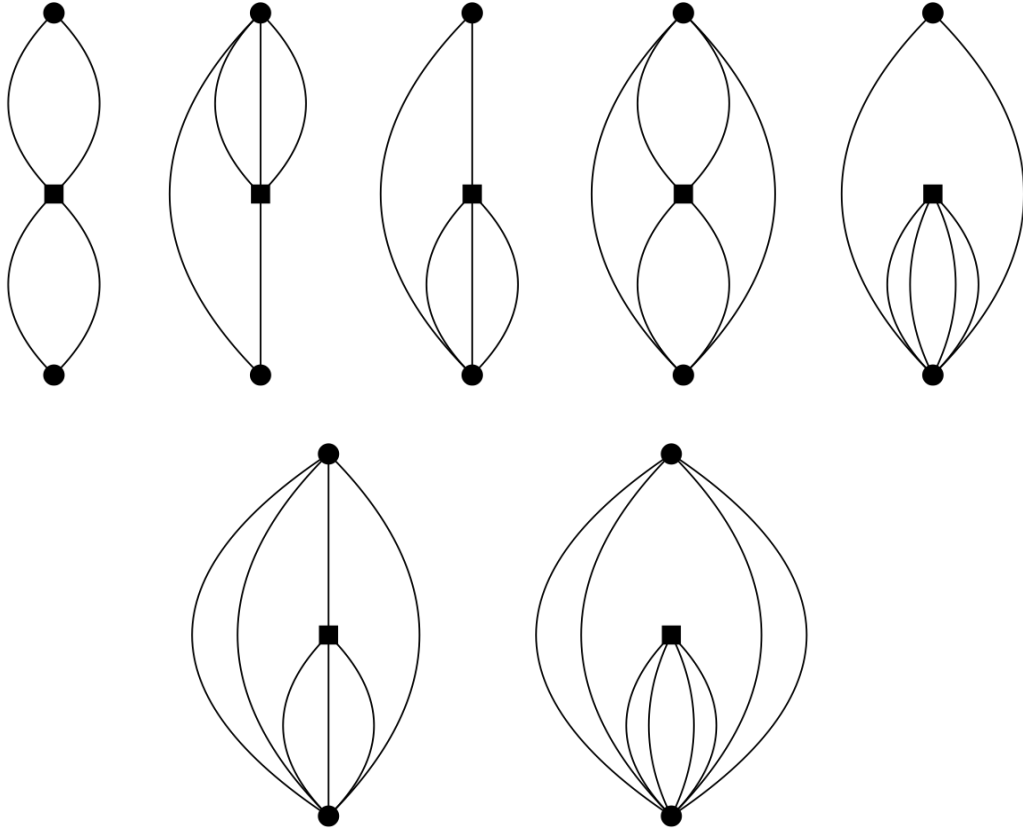


Figure 5.2: Hugenholtz skeleton diagrams for two-body operators. The square and the dot symbols represent the Hamiltonian and the excitation operators, respectively.

respectively,

$$E_{EB} = E_e + E_h - E_X. \quad (5.20)$$

Similarly, the biexciton binding energy was obtained by subtracting the total biexciton energy from a pair of non-interacting excitons.

$$E_{BB} = 2E_X - E_{XX} \quad (5.21)$$

5.3 Results

The effect of shape was investigated by performing calculations on QDs with diameters in the range of 1-20 nm. The effect of material type was investigated by selecting four semiconductor materials (CdSe, CdS, CdTe, and PbS). Exciton and biexciton binding energies as well as an estimated crystal formula for the entire set of dots are presented in Table 5.1. Of the material types investigated here, CdSe QDs have been studied most extensively and is, therefore, an excellent system for comparison. In Figure 5.3, we compare exciton binding energies obtained in this work using eh-mcCC to several other studies.

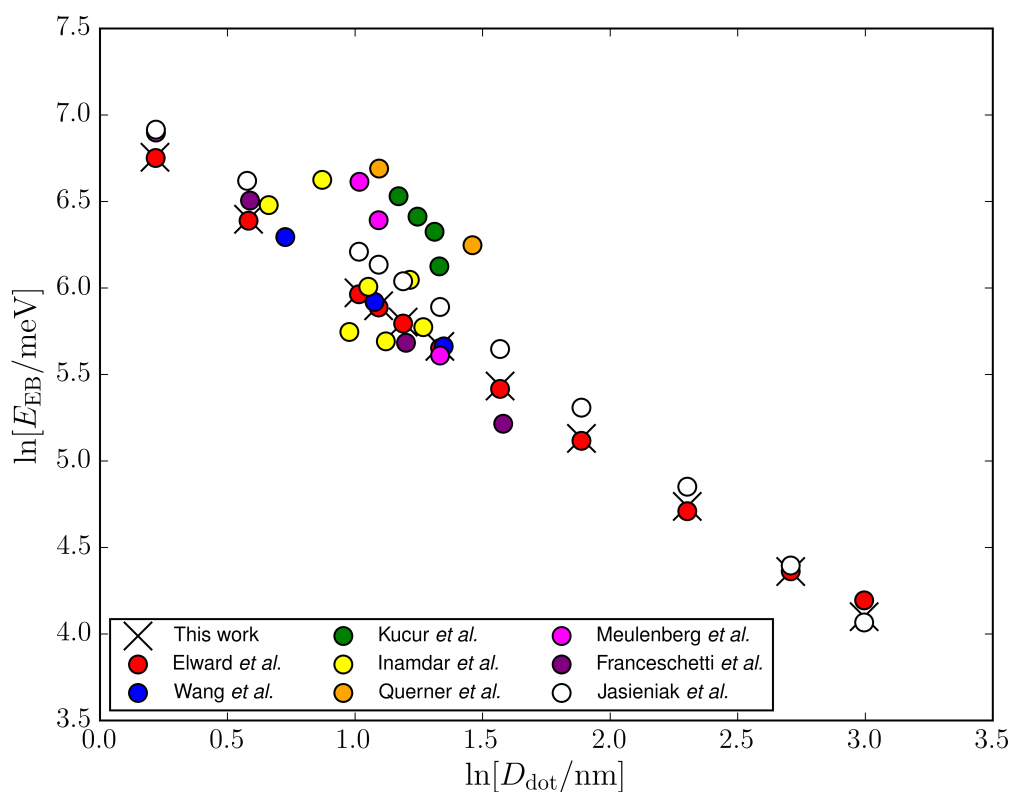


Figure 5.3: Exciton binding energies (E_{EB}) for CdSe QDs, calculated using eh-mcCC, are compared with other studies by Inamdar *et al.*, [198] Franceschetti *et al.*, [43] Wang *et al.*, [199] Querner *et al.*, [200] Jasieniak *et al.*, [201] Kucur *et al.*, [202] Muelenberg *et al.*, [203] and Elward *et al.* [36].

Table 5.1: Exciton (E_{EB}) and biexciton (E_{BB}) binding energies (meV) calculated using the eh-mcCC method for the set of quantum dots investigated in this work.

D_{dot} (nm)	CdSe			CdS			CdTe			PbS		
	Cd_xSe_y	E_{EB}	E_{BB}	Cd_xS_y	E_{EB}	E_{BB}	Cd_xTe_y	E_{EB}	E_{BB}	Pb_xS_y	E_{EB}	E_{BB}
1.24	$Cd_{18}Se_{18}$	859	17.8	$Cd_{20}S_{20}$	986	21.6	$Cd_{15}Te_{15}$	745	8.02	$Pb_{19}S_{19}$	306	0.874
1.79	$Cd_{54}Se_{54}$	600	17.0	$Cd_{61}S_{61}$	689	20.7	$Cd_{46}Te_{46}$	520	7.86	$Pb_{57}S_{57}$	213	0.868
2.76	$Cd_{196}Se_{196}$	392	15.8	$Cd_{224}S_{224}$	451	19.3	$Cd_{167}Te_{167}$	338	7.62	$Pb_{207}S_{207}$	138	0.863
2.98	$Cd_{247}Se_{247}$	364	15.5	$Cd_{281}S_{281}$	418	19.0	$Cd_{210}Te_{210}$	314	7.56	$Pb_{261}S_{261}$	128	0.861
3.28	$Cd_{329}Se_{329}$	331	15.2	$Cd_{375}S_{375}$	381	18.6	$Cd_{281}Te_{281}$	285	7.50	$Pb_{348}S_{348}$	117	0.861
3.79	$Cd_{508}Se_{508}$	288	14.5	$Cd_{579}S_{579}$	331	17.9	$Cd_{433}Te_{433}$	247	7.36	$Pb_{537}S_{537}$	101	0.856
4.80	$Cd_{1032}Se_{1032}$	229	13.5	$Cd_{1176}S_{1176}$	264	16.7	$Cd_{879}Te_{879}$	196	7.12	$Pb_{1091}S_{1091}$	79.8	0.850
6.60	$Cd_{2683}Se_{2683}$	169	11.8	$Cd_{3058}S_{3058}$	195	14.5	$Cd_{2286}Te_{2286}$	144	6.68	$Pb_{2836}S_{2836}$	58.2	0.835
10.0	$Cd_{9333}Se_{9333}$	114	9.33	$Cd_{10635}S_{10635}$	132	11.5	$Cd_{7952}Te_{7952}$	96.2	5.96	$Pb_{9863}S_{9863}$	38.5	0.812
15.0	$Cd_{31500}Se_{31500}$	78.4	6.82	$Cd_{35893}S_{35893}$	90.8	8.22	$Cd_{26839}Te_{26839}$	65.3	5.03	$Pb_{33288}S_{33288}$	25.8	0.778
20.0	$Cd_{74668}Se_{74668}$	60.3	5.15	$Cd_{85080}S_{85080}$	70.0	6.04	$Cd_{63617}Te_{63617}$	49.9	4.25	$Pb_{78904}S_{78904}$	19.4	0.742

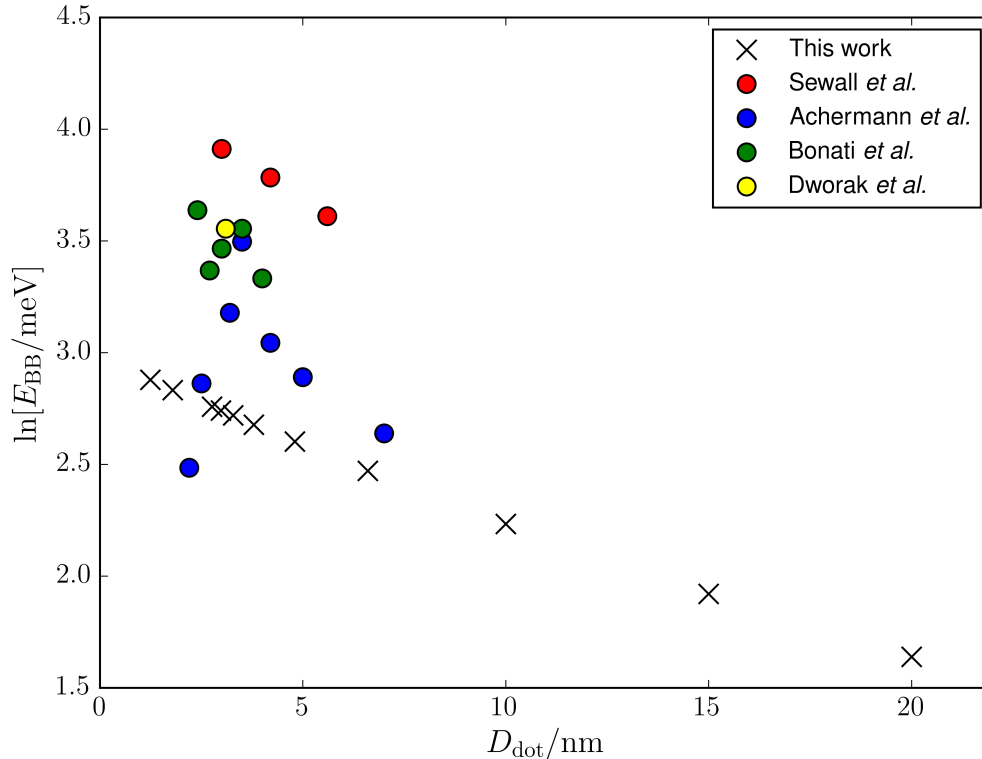


Figure 5.4: Biexciton binding energies (E_{BB}) for CdSe QDs, calculated using eh-mcCC, are compared to other studies by Sewall *et al.*, [204, 205] Achermann *et al.*, [206] Bonati *et al.*, [207] and Dworak *et al.* [208].

We find that eh-mcCC agrees very well with previous theoretical and experimental studies. [203, 201, 36, 43, 199] The log-log plot in Figure 5.3 also shows that the exciton binding energies in CdSe quantum dots scale as D^n . This well-known scaling behavior has been reported in both experimental and theoretical investigations. [203, 201, 36, 43, 199] The scaling of biexciton binding energies with respect to the diameter of CdSe QDs is presented in Figure 5.4. In general, we find that the biexciton binding energies are much smaller in magnitude than the corresponding exciton binding energies. The comparison with previously reported experimental results indicates that the biexciton binding energies are much more sensitive to factors influencing the confinement potential. This makes determination of biexciton binding

energies using both experimental and computational techniques challenging. Comparing theoretical and experimental results shows that calculated biexciton binding energies are underestimated for smaller dots, however, this difference decreases with increasing dot size.

The dependence of exciton and biexciton binding energies on dot size for other materials studied (CdS, CdTe, and PbS) is shown in [Figure 5.5](#) and [Figure 5.6](#), respectively. In all cases, we find that the trend observed in CdSe QDs is also seen

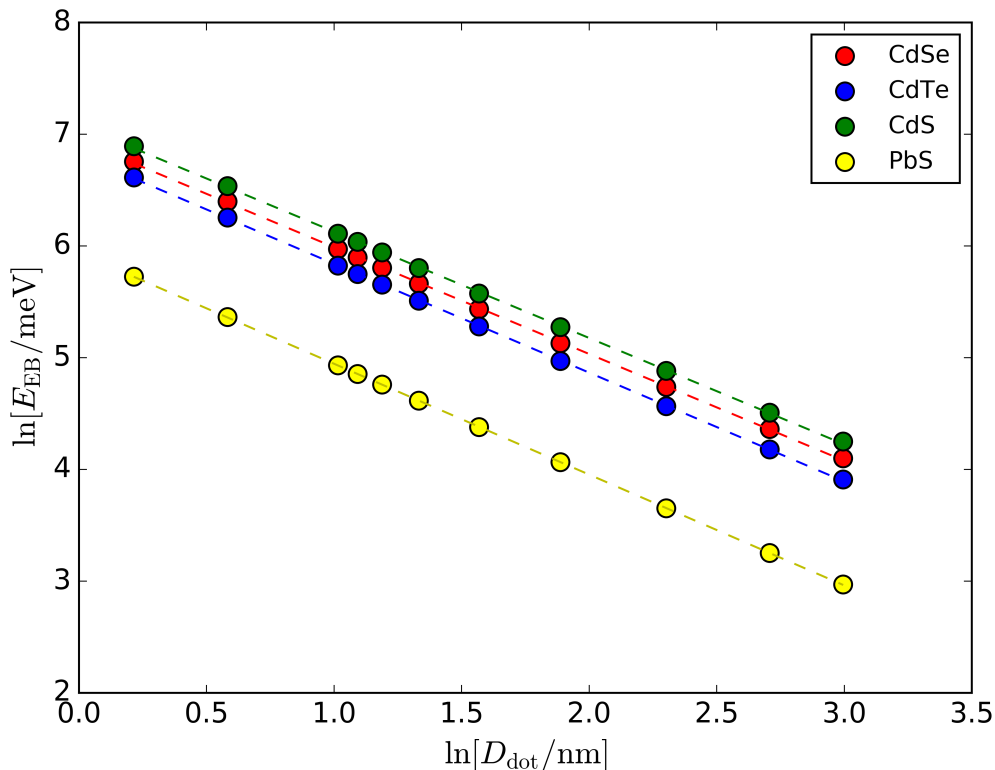


Figure 5.5: Exciton binding energy (E_{EB}) vs dot size.

in other material types. The analytical expression of the relationship between exciton binding energy to dot diameter can be obtained by performing linear regression analysis and the expressions for best-fit lines are presented in [Table 5.2](#). We find that the exponent of QD diameter (D_{dot}) is close to one and is relatively insensitive to material type. Comparing the scaling equations of exciton and biexciton binding

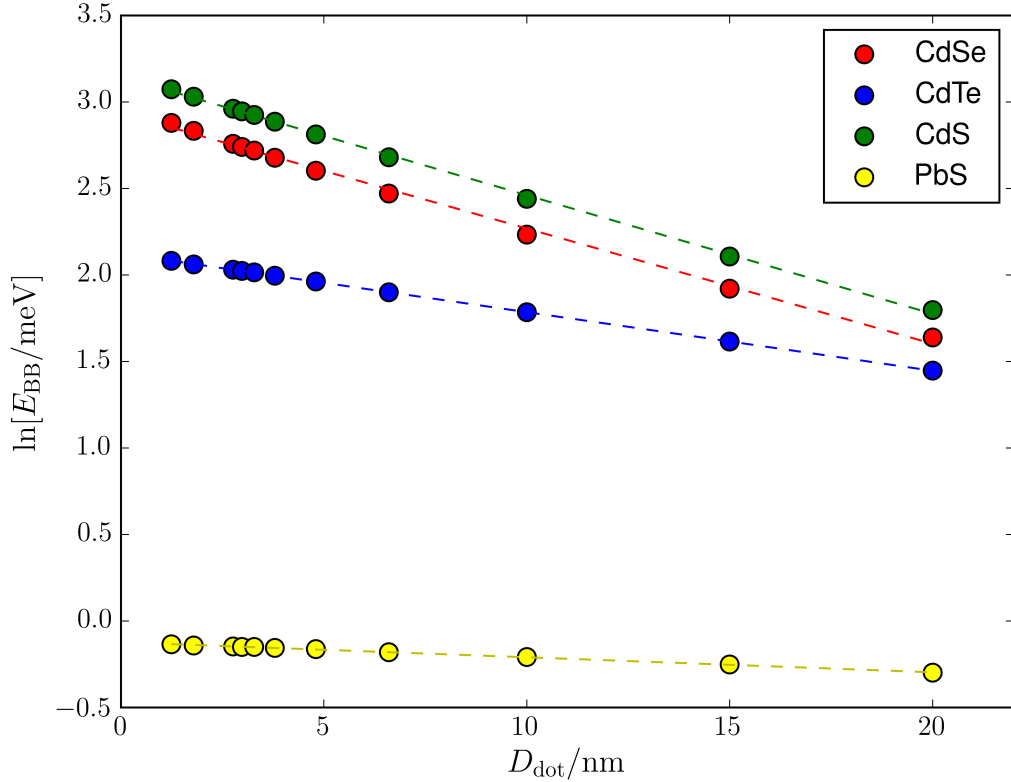


Figure 5.6: Biexciton binding energy (E_{EB}) vs dot size.

Table 5.2: Scaling law for exciton binding energies (E_{EB}) for CdSe, CdS, CdTe, and PbS quantum dots

Material	Scaling Law	Root Mean Square Error
CdSe	$\ln[E_{\text{BE}}/\text{meV}] = -0.956 \ln[D_{\text{dot}}/\text{nm}] + 6.944$	1.015×10^{-2}
CdS	$\ln[E_{\text{BE}}/\text{meV}] = -0.952 \ln[D_{\text{dot}}/\text{nm}] + 7.079$	1.122×10^{-2}
CdTe	$\ln[E_{\text{BE}}/\text{meV}] = -0.974 \ln[D_{\text{dot}}/\text{nm}] + 6.814$	6.533×10^{-3}
PbS	$\ln[E_{\text{BE}}/\text{meV}] = -0.992 \ln[D_{\text{dot}}/\text{nm}] + 5.938$	1.639×10^{-3}

energies (Table 5.2 and Table 5.3) shows that although both quantities decrease with increasing dot size, the scaling properties are completely different. Specifically, we find that the biexciton binding energies scale as $e^{-\alpha D}$ with respect to dot diameter. We also find that the scaling law for exciton binding energy is $D^{-\alpha}$, while that of biexciton binding energy is $e^{-\alpha D}$ (Figure 5.7). However, comparison of the slope of the two binding energies reveals that with increasing dot diameter the biexciton bind-

Table 5.3: Scaling law for biexciton binding energies (E_{BB}) for CdSe, CdS, CdTe, and PbS quantum dots

Material	Scaling Law	Root Mean Square Error
CdSe	$\ln[E_{BB}/\text{meV}] = -0.067[D_{\text{dot}}/\text{nm}] + 2.936$	2.062×10^{-2}
CdS	$\ln[E_{BB}/\text{meV}] = -0.070[D_{\text{dot}}/\text{nm}] + 3.150$	1.180×10^{-2}
CdTe	$\ln[E_{BB}/\text{meV}] = -0.034[D_{\text{dot}}/\text{nm}] + 2.124$	1.077×10^{-3}
PbS	$\ln[E_{BB}/\text{meV}] = -0.009[D_{\text{dot}}/\text{nm}] - 0.123$	1.555×10^{-3}

ing energies decrease at a slower rate than do exciton binding energies (Figure 5.7).

The results in Table 5.2 and Table 5.3 also show that biexciton binding energies

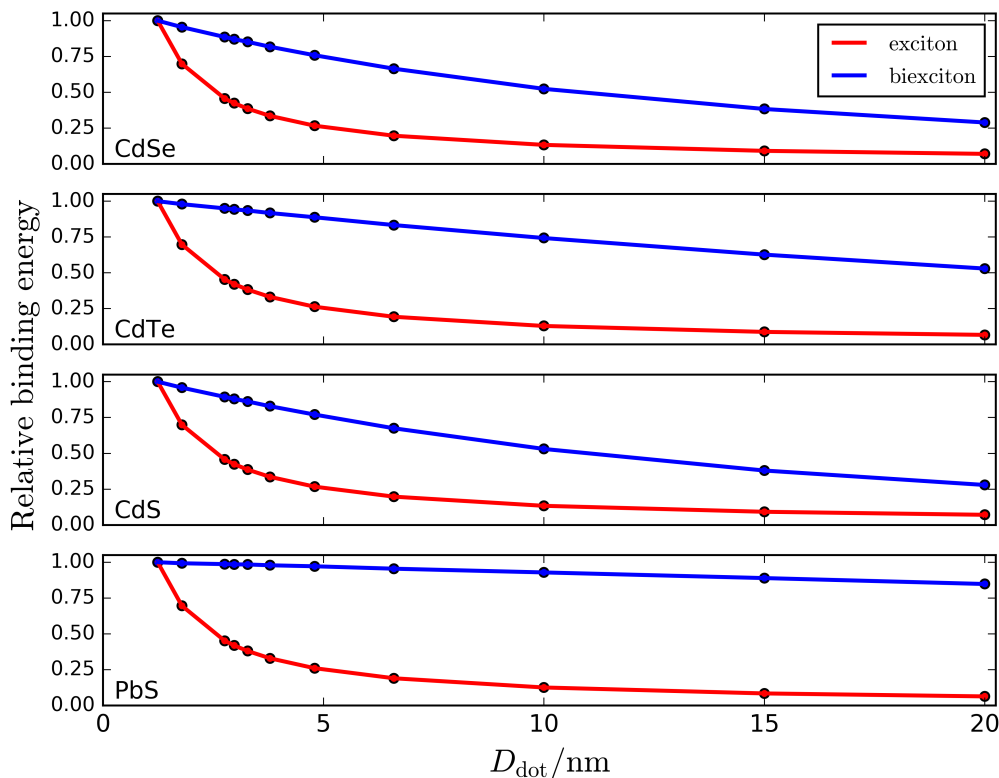


Figure 5.7: Relative binding energies for CdSe, CdTe, CdS, and PbS quantum dots. The binding energies are normalized with respect to the exciton and biexciton binding energies of the smallest dot, respectively.

are much more sensitive to changes in material type than are exciton binding energies. The parametric dependence of the two binding energies (Figure 5.8) reveals that

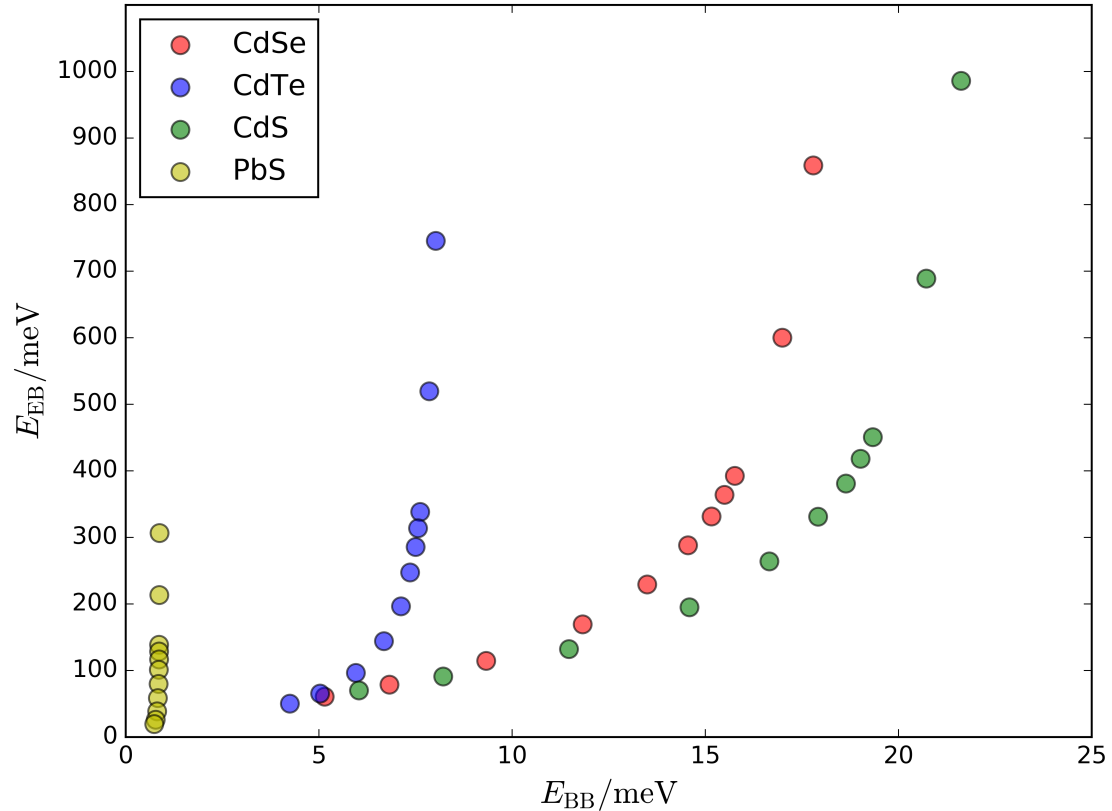


Figure 5.8: Parametric dependence of exciton binding energies (E_{EB}) on biexciton binding energies (E_{BB}) for the set of QDs investigated in this work.

both exciton and biexciton binding energies are positively correlated, however, this dependence is highly nonlinear.

5.4 Conclusion

In summary, this work presents a theoretical investigation of the effect of dot size on exciton and biexciton binding energies in semiconductor QDs. The electron-hole interactions in these systems were studied using the electron-hole multicomponent coupled-cluster method, and calculations were performed on four different material types. The results from these calculations revealed that biexciton binding energies follow different scaling laws than do excitonic binding energies. The results also

show that biexcitonic properties are, in general, more sensitive to material type. The dramatic difference in the scaling equations for biexciton binding energies compared to excitonic systems shows that the response of the biexcitonic system with respect to change in the confinement potential is fundamentally very different from the response shown by excitonic systems. We postulate that this effect is a consequence of many-body effects present in biexcitonic systems.

5.A Material and basis parameters

The electron-hole Hamiltonian used in this work is defined as follows,

$$H = H^e + V^{e,e} + H^h + V^{h,h} + V^{e,h} \quad (5.22)$$

where the exact forms of the operators (in atomic units) are given as,

$$H^\alpha = \sum_i^{N^\alpha} \frac{-\hbar}{2m_\alpha} \nabla_{i,\alpha}^2 + v_{\text{ext}}^\alpha(\mathbf{r}_i^\alpha, \mathbf{R}^{\text{BOS}}) \quad \alpha = e, h, \quad (5.23)$$

$$V^{\alpha,\alpha} = \sum_{i<j}^{N^\alpha} \frac{q^\alpha q^\alpha}{\epsilon r_{ij}^{\alpha\alpha}}, \quad (5.24)$$

$$V^{e,h}(\mathbf{r}^e, \mathbf{r}^h) = \sum_i^{N^e} \sum_j^{N^h} \frac{q^e q^h}{\epsilon r_{ij}^{e,h}}. \quad (5.25)$$

The ϵ is the dielectric function. We used a single-particle basis for the electrons and holes of [spd] Gaussian-type functions. The particles were confined in a parabolic potential [36, 37, 34, 192] that had the following form,

$$v_{\text{ext}}^\alpha = \frac{1}{2} k^\alpha |\mathbf{r}^\alpha|^2 \quad \alpha = e, h. \quad (5.26)$$

The scheme for determining parameters for the Gaussian functions and force constants per dot size is presented in previous work and will not be discussed here.[36]

Each composition also had corresponding effective masses for electrons and holes and dielectric constants.[209] For the systems in this work, the effective masses, dielectric constants, parameters for the Gaussian functions and force constants are given in Table 5.4 and Table 5.5, respectively.

Table 5.4: Masses (atomic units) for electron and hole and dielectric constant (ϵ) by QD composition[209]

	m^e	m^h	ϵ
CdSe	0.13	0.38	6.2
CdS	0.19	0.22	5.4
CdTe	0.12	0.13	7.1
PbS	0.08	0.075	17.2

Table 5.5: Parameters for the external potential (atomic units) and Gaussian exponent parameter (α) values (atomic units) for the basis per dot diameter (nm)

D_{dot}	α	CdSe			CdS			CdTe			PbS		
		k_e	k_h	k_e	k_e	k_h	k_e	k_e	k_h	k_e	k_h	k_e	k_h
1.24	2.94×10^{-2}	2.66×10^{-2}	9.10×10^{-3}	1.82×10^{-2}	1.57×10^{-2}	2.88×10^{-2}	2.66×10^{-2}	4.32×10^{-2}	2.66×10^{-2}	4.61×10^{-2}	4.32×10^{-2}	4.61×10^{-2}	
1.79	1.42×10^{-2}	6.22×10^{-3}	2.13×10^{-3}	4.26×10^{-3}	3.68×10^{-3}	6.74×10^{-3}	6.22×10^{-3}	1.01×10^{-2}	6.22×10^{-3}	1.08×10^{-2}	1.01×10^{-2}	1.08×10^{-2}	
2.76	5.98×10^{-3}	1.10×10^{-3}	3.76×10^{-4}	7.53×10^{-4}	6.50×10^{-4}	1.19×10^{-3}	1.10×10^{-3}	1.79×10^{-3}	1.10×10^{-3}	1.91×10^{-3}	1.79×10^{-3}	1.91×10^{-3}	
2.98	5.13×10^{-3}	8.10×10^{-4}	2.77×10^{-4}	5.54×10^{-4}	4.78×10^{-4}	8.77×10^{-4}	8.10×10^{-4}	1.32×10^{-3}	8.10×10^{-4}	1.40×10^{-3}	1.32×10^{-3}	1.40×10^{-3}	
3.28	4.24×10^{-3}	5.52×10^{-4}	1.89×10^{-4}	3.78×10^{-4}	3.26×10^{-4}	5.98×10^{-4}	5.52×10^{-4}	8.97×10^{-4}	5.52×10^{-4}	9.57×10^{-4}	8.97×10^{-4}	9.57×10^{-4}	
3.79	3.17×10^{-3}	3.09×10^{-4}	1.06×10^{-4}	2.11×10^{-4}	1.83×10^{-4}	3.35×10^{-4}	3.09×10^{-4}	5.02×10^{-4}	3.09×10^{-4}	5.36×10^{-4}	5.02×10^{-4}	5.36×10^{-4}	
4.80	1.98×10^{-3}	1.20×10^{-4}	4.12×10^{-5}	8.23×10^{-5}	7.11×10^{-5}	1.30×10^{-4}	1.20×10^{-4}	1.96×10^{-4}	1.20×10^{-4}	2.09×10^{-4}	1.96×10^{-4}	2.09×10^{-4}	
6.60	1.05×10^{-3}	3.39×10^{-5}	1.16×10^{-5}	2.32×10^{-5}	2.00×10^{-5}	3.68×10^{-5}	3.39×10^{-5}	5.51×10^{-5}	3.39×10^{-5}	5.88×10^{-5}	5.51×10^{-5}	5.88×10^{-5}	
10.00	4.57×10^{-4}	6.41×10^{-6}	2.19×10^{-6}	4.39×10^{-6}	3.79×10^{-6}	6.95×10^{-6}	6.41×10^{-6}	1.04×10^{-5}	6.41×10^{-6}	1.11×10^{-5}	1.04×10^{-5}	1.11×10^{-5}	
15.00	2.03×10^{-4}	1.26×10^{-6}	4.33×10^{-7}	8.65×10^{-7}	7.47×10^{-7}	1.37×10^{-6}	1.26×10^{-6}	2.06×10^{-6}	1.26×10^{-6}	2.19×10^{-6}	2.06×10^{-6}	2.19×10^{-6}	
20.00	1.14×10^{-4}	4.01×10^{-7}	1.37×10^{-7}	2.74×10^{-7}	2.37×10^{-7}	4.34×10^{-7}	4.01×10^{-7}	6.51×10^{-7}	4.01×10^{-7}	6.95×10^{-7}	6.51×10^{-7}	6.95×10^{-7}	

Chapter 6

Applying multicomponent coupled-cluster method to molecular systems

The electron-hole representation for investigating electronic excitations is often reserved for systems with large number of electrons. This chapter will discuss theory and preliminary results for smaller systems. To begin, traditional methods used to study excited electronic states will be introduced in [section 6.1](#). We will specifically focus on configuration interaction singles, equation-of-motion coupled-cluster theory, and time dependent Hartree-Fock theory as they are some of the most widely adopted methods. Next, ([section 6.3](#)) will introduce and explain the theoretical challenges of applying the electron-hole representation to molecular systems, and how they were resolved. The final section of this chapter, [section 6.4](#), will show representative results for using electron-hole methods to calculate electronic excitation energies.

6.1 Traditional methods for studying excited electronic states

Investigating electronically excited states is an important field in chemistry. Often times, the excited state of a molecular system possesses interesting properties that govern chemical processes. Information on excited electronic states is particularly important in fields like spectroscopy. Interpreting spectra relies on understanding the electronic and molecular structure of a given chemical species. Computationally studying the excited states is a very useful tool in predicting, justifying, and explaining features of spectroscopic data. There are also excited states which are optically inactive and unable to be studied spectroscopically.

Theoretical treatment of excited states is a rich field of study. There is a wide spectrum of methods designed to study excited state properties of chemical systems. In many cases, these methods can be derived from their ground state counterparts, as is the case with configuration interaction and coupled-cluster methodologies which were detailed earlier in [chapter 2](#). Calculation energy of excited electronic states permits the computation of the excitation energy. Excitation energy is the difference in energy between an excited state and the ground state. This is the energy required to transition from the ground state to the excited state.

This work will introduce a few of the most widely adopted excited state methods. These methods are the configuration interaction singles (CIS), equation-of-motion coupled-cluster (EOM-CC), and time-dependent Hartree-Fock (TDHF). CIS and EOM-CC methods will closely resemble the ground state discussions presented earlier. The TDHF method will introduce how time dependent methods can be used to investigate excited states. The key difference these methods have from earlier discussions will be in the form of the wave function and how it is used to calculate excitation energy. The problem with the more highly accurate excited state methods

is that they are computationally demanding. As was displayed earlier, transforming to the electron-hole representation can reduce computational cost. Using the electron-hole representation is accompanied with some issues, but overall should provide accurate results that are competitive with all electron methods, but at a lower cost.

One of the main issues with using the electron-hole representation is the presence of screening. In the all-electron representation, the electron-electron potential terms are obviously present. In electron-hole representation, all electrons, except those excited, have been abstracted away. All of the electron-electron interactions still must be accounted for in some way, and that is through screening. In electron-hole representation there is screening between electron-electron, hole-hole, and electron-hole interactions. The goal of this research is to develop a function that describes this screening.

Deriving an accurate screening function will be introduced using linear density response theory. Linear response theory is used in time-dependent density functional theory to calculate excitation energies. This work will use aspects of the theory to arrive at a screening function which can be used in electron-hole methodology.

6.1.1 Configuration interaction singles

Configuration interaction singles method, or CIS for short, expands configuration interaction theory (which was introduced in [section 2.3](#)) to calculate excitation energies [\[210\]](#). In ground state CI calculations, ground state energy was reached by projecting the Schrödinger equation onto the CI wave function,

$$\langle \Psi^{\text{CI}} | H | \Psi^{\text{CI}} \rangle = E^{\text{CI}} \langle \Psi^{\text{CI}} | \Psi^{\text{CI}} \rangle. \quad (6.1)$$

For excited electronic states, a similar approach can be used. The CIS wave function includes only single excitations on the reference state (which is obtained using the Hartree-Fock method),

$$|\Psi^{\text{CIS}}\rangle = \sum_i^N \sum_a^M c_{(i,a)} a^\dagger_i |\Phi_0\rangle. \quad (6.2)$$

The sum i is over the N occupied orbitals while a is over M virtual orbitals. The CIS energy is then obtained by substituting the CIS wave function into [Equation 6.1](#),

$$\sum_i^N \sum_a^M c_{(i,a)} H |i^a\rangle = E^{\text{CIS}} \sum_i^N \sum_a^M c_{(i,a)} |i^a\rangle \quad (6.3)$$

and then projected into elements of the CIS wave function giving

$$\sum_i^N \sum_a^M c_{(i,a)} \langle_j^b | H |i^a\rangle = E^{\text{CIS}} \sum_i^N \sum_a^M c_{(i,a)} \delta_{ij} \delta_{ab}. \quad (6.4)$$

The excitation energy with which we are interested is defined as

$$\omega_k = E_k^{\text{CIS}} - E^{\text{ref}} \quad (6.5)$$

where k is the desired excitation. To compute this quantity, the reference energy is subtracted from both sides of [Equation 6.4](#) to give

$$\sum_i^N \sum_a^M \{(\epsilon_a - \epsilon_i) \delta_{ij} \delta_{ab} + \langle ij | v | ab \rangle_A\} c_{(i,a)} = \omega_k \sum_i^N \sum_a^M c_{(i,a)} \delta_{ij} \delta_{ab}. \quad (6.6)$$

The ϵ values are orbital energies of the single particle orbitals i and a and the V term is the antisymmetrized two electron integral. This equation can then be solved using standard linear algebra techniques, which is apparent upon rewriting it in matrix

form,

$$\mathbf{A}\mathbf{C} = \omega\mathbf{C}. \quad (6.7)$$

The \mathbf{A} matrix is the Hamiltonian elements from the left side of [Equation 6.6](#).

The CIS method is very popular due to its relatively low computational cost. This low computational cost is associated with reduced accuracy, which other methods, such as EOM-CC and TDHF address.

6.1.2 Equation-of-motion coupled-cluster

Equation-of-motion coupled-cluster (EOM-CC) is another widely used method for calculating excited states of chemical systems [\[60\]](#). It is based upon the CC work first introduced in [section 2.4](#). In EOM-CC we consider the ground state and an excited state CC Schrödinger equation,

$$H_N |\Psi_0\rangle = \Delta E_0 |\Psi_0\rangle \quad H_N |\Psi_k\rangle = \Delta E_k |\Psi_k\rangle. \quad (6.8)$$

The goal, is then to calculate the difference in energy between the k^{th} state and the ground state,

$$\omega_k = \Delta E_k - \Delta E_0. \quad (6.9)$$

The ground state wave function is the familiar,

$$|\Psi_0\rangle = e^T |0\rangle \quad (6.10)$$

while the k^{th} wave function is given by

$$|\Psi_k\rangle = R_k |\Psi_0\rangle. \quad (6.11)$$

It is worth noting that one need not use the coupled-cluster ansatz from above. Other EOM methods exist, but CC theory is a focus of this work and is widely used in applications. The R_k operator excites the ground state wave function into the desired state. Generally, the similarity transformed Hamiltonian is used which gives the following equations

$$\mathcal{H} |\Psi_0\rangle = \Delta E_0 |\Psi_0\rangle \quad (6.12)$$

$$\mathcal{H} R_k |\Psi_0\rangle = \Delta E_k R_k |\Psi_0\rangle. \quad (6.13)$$

Left multiplying the top equation by R_k and subtracting it from the second gives

$$[\mathcal{H} R_k] |\Psi_0\rangle = (\Delta E_k - \Delta E_0) R_k |\Psi_0\rangle \quad (6.14)$$

$$[\mathcal{H} R_k] |\Psi_0\rangle = \omega_k R_k |\Psi_0\rangle. \quad (6.15)$$

Satisfaction of this eigenvalue equation yields the excitation energy of the k^{th} state. It's important to note that the EOM-CC equations directly eliminate shared terms in the ground and excited state expressions, making it more favorable than solving the ground state and excited state CC equations independently.

6.1.3 Time dependent Hartree-Fock

Another way excited states are theoretically investigated is by using time dependent methods. Here, we will discuss time dependent Hartree-Fock (TDHF) theory [210]. TDHF, and time dependent density functional theory (TDDFT) rely on using electronic density to compute excited electronic states. This is done by using the time dependent

Kohn-Sham equation shown below (with its adjoint),

$$i\frac{\partial}{\partial t}\mathbf{C} = \mathbf{F}\mathbf{C} \quad (6.16)$$

$$-i\frac{\partial}{\partial t}\mathbf{C}^\dagger = \mathbf{C}^\dagger\mathbf{F}. \quad (6.17)$$

These equations yield the KS equation in density matrix form,

$$\mathbf{F}\mathbf{P} - \mathbf{P}\mathbf{F} = i\frac{\partial}{\partial t}\mathbf{P} \quad (6.18)$$

where $\mathbf{P} = \mathbf{C}\mathbf{C}^\dagger$ is the electronic density and \mathbf{F} is the Fock matrix.

We assume that the system is in the ground state (and is unperturbed) which is denoted by the superscript (0),

$$\mathbf{F}^{(0)}\mathbf{P}^{(0)} - \mathbf{P}^{(0)}\mathbf{F}^{(0)} = 0 \quad (6.19)$$

Since we are interested in perturbing the system, the density and Fock matrices will be expanded,

$$\mathbf{P} = \mathbf{P}^{(0)} + \mathbf{P}^{(1)} + \dots \quad (6.20)$$

$$\mathbf{F} = \mathbf{F}^{(0)} + \mathbf{F}^{(1)} + \dots \quad (6.21)$$

These expressions can then be substituted into [Equation 6.18](#) to give

$$\mathbf{F}^{(0)}\mathbf{P}^{(1)} - \mathbf{P}^{(1)}\mathbf{F}^{(0)} + \mathbf{F}^{(1)}\mathbf{P}^{(0)} - \mathbf{P}^{(0)}\mathbf{F}^{(1)} = i\frac{\partial}{\partial t}\mathbf{P}^{(1)} \quad (6.22)$$

where the time dependent perturbation is give by a Fourier component,

$$g_{pq} = \frac{1}{2} (f_{pq}e^{-i\omega t} + f_{qp}^*e^{i\omega t}) \quad (6.23)$$

which is a one-electron operator. This perturbation results in a first order Fock matrix response, that is written in terms of the zeroth order Fock matrix,

$$F_{pq}^{(1)} = g_{pq} + \Delta F_{pq}^{(0)} \quad (6.24)$$

$$\Delta F_{pq}^{(0)} = \sum_{rs} \frac{\partial F_{pq}^{(0)}}{\partial P_{rs}} P_{rs}^{(1)}. \quad (6.25)$$

Likewise, the first order density matrix is defined as

$$P^{(1)} = \frac{1}{2} (d_{pq} e^{-i\omega t} + d_{qp}^* e^{i\omega t}) \quad (6.26)$$

where d_{pq} elements represent perturbation densities.

Substituting the expressions for $\mathbf{F}^{(1)}$ and $\mathbf{P}^{(1)}$ into [Equation 6.22](#), and gathering $e^{-i\omega t}$ terms gives,

$$\sum_q F_{pq}^{(0)} d_{qr} - d_{pq} F_{qr}^{(0)} + \left(f_{pq} + \sum_{st} \frac{\partial F_{pq}^{(0)}}{\partial P_{st}} d_{st} \right) P_{qr}^{(0)} - P_{pq}^{(0)} \left(f_{qr} + \sum_{st} \frac{\partial F_{qr}^{(0)}}{\partial P_{st}} d_{st} \right) = \omega d_{pr}. \quad (6.27)$$

The terms with $e^{i\omega t}$ yield the complex conjugate of this expression. Given that density matrices must be idempotent, we show that

$$\sum_q (P_{pq}^{(0)} P_{qr}^{(1)} + P_{pq}^{(1)} P_{qr}^{(0)}) = P_{pr}^{(1)}. \quad (6.28)$$

This restricts the form of the \mathbf{d} matrices such that only d_{ia} and d_{ai} elements will be non-zero (where i are occupied and a are virtual orbitals).

This results in the following equations,

$$F_{aa}^{(0)} x_{ai} - x_{ai} F_{ii}^{(0)} + \left(f_{ai} + \sum_{bj} \left\{ \frac{\partial F_{ai}}{\partial P_{bj}} x_{bj} + \frac{\partial F_{ai}}{\partial P_{jb}} y_{bj} \right\} \right) P_{ii}^{(0)} = \omega x_{ai} \quad (6.29)$$

$$F_{ii}^{(0)} y_{ai} - y_{ai} F_{aa}^{(0)} + P_{ii}^{(0)} \left(f_{ia} + \sum_{bj} \left\{ \frac{\partial F_{ia}}{\partial P_{bj}} x_{bj} + \frac{\partial F_{ia}}{\partial P_{jb}} y_{bj} \right\} \right) = \omega y_{ai} \quad (6.30)$$

where $x_{ai} = d_{ai}$ and $y_{ai} = d_{ia}$. This yields the following eigenvalue equation,

$$\begin{bmatrix} \mathbf{A} & \mathbf{B} \\ \mathbf{B}^* & \mathbf{A}^* \end{bmatrix} \begin{bmatrix} \mathbf{X} \\ \mathbf{Y} \end{bmatrix} = \omega \begin{bmatrix} \mathbf{1} & \mathbf{0} \\ \mathbf{0} & -\mathbf{1} \end{bmatrix} \begin{bmatrix} \mathbf{X} \\ \mathbf{Y} \end{bmatrix} \quad (6.31)$$

where \mathbf{A} was seen previously in the CIS equations. It has the following form,

$$A_{ia,jb} = \delta_{ij} \delta_{ab} (\epsilon_a - \epsilon_i) + \langle ij|v|ab \rangle_A. \quad (6.32)$$

The \mathbf{B} matrix elements are given to be

$$B_{ia,jb} = \langle ib|v|ja \rangle_A. \quad (6.33)$$

We see that a benefit the TDHF method has over the CIS method and EOM methods is that only the ground state wave function was needed to calculate the excitation energy. This can greatly reduce computational complexity while still delivering accurate results. It's worth mentioning that TDDFT extends the TDHF methodology, with the two body contributions in the \mathbf{A} and \mathbf{B} matrices includes an exchange-correlation functional f_{xc} .

6.2 Electron-hole representation

While methods like CIS and EOM-CC provide accurate calculations, they can be quite expensive. The wave function depends on $N \times D$ coordinates (N is the number of electrons and D is the number of dimensions). As system size increases, the wave function becomes a large quantity. This is especially true given that the CIS and EOM-CC wave functions must track large sets of excited determinants.

The electron-hole representation of excitations can simplify some of the computational complexity associated with these traditional methods. This concept was first introduced in [section 1.3](#) and has been used extensively in quantum chemical studies. These studies and related work were discussed in [chapter 4](#) and [chapter 5](#). Invoking the electron-hole representation is especially useful with large chemical systems, though it can be used for modestly sized systems as well.

One of the central challenges of using the electron-hole representation is accurately treating electron-hole screening. In electron-hole representation, an electron exists in a virtual orbital and a hole exists in an orbital from the Fermi vacuum. The issue is that, even though they are "hidden" in the electron-hole representation, other electrons in the system screen the electron-hole interaction (and electron-electron and hole-hole in the case where more than one electron and one hole are present). This screening was present in the work presented earlier via the dielectric constant in the electron-electron, hole-hole, and electron-hole operators.

This work looks to formulate a screening function that can accurately and quickly calculate screening to improve the accuracy of electron-hole excited state calculations. This will be accomplished by using linear response theory, which is heavily used in time-dependent density functional methodology. A major reason why linear response theory is attractive is because it only requires information about the ground state wave function to calculate excited state properties. Furthermore, (TD)DFT methodology does not require all information of the wave function, only the density,

to accomplish this which makes the screening function extendible to large, complex chemical systems.

6.3 Linear response theory

6.3.1 Time dependent many body systems

Thus far, only time independent formalism has been used to describe chemical systems. In this chapter, use time dependent techniques to investigate properties of interest.

The Hamiltonian for a system in a time dependent potential $v(\mathbf{r}, t)$ is defined as

$$H(t) = F + V(t) + W \quad (6.34)$$

where F and is the Fock operator and W is the electron-electron potential operator. The explicit form of $V(t)$ is

$$V(t) = \sum_i^N v(\mathbf{r}_i, t). \quad (6.35)$$

The corresponding Schrödinger equation for a time dependent system is

$$i \frac{\partial}{\partial t} \Psi(\mathbf{x}_1, \dots, \mathbf{x}_N, t) = H(t) \Psi(\mathbf{x}_1, \dots, \mathbf{x}_N, t) \quad (6.36)$$

which propagates over some time. Usually the system is initially in the ground state and the time dependent potential is enabled at t_0 . Taking this is always true the present discussion, the potential can be split into two terms,

$$v(\mathbf{r}, t) = v_0(\mathbf{r}) + v_1(\mathbf{r}, t)\theta(t - t_0). \quad (6.37)$$

For convenience, the Hamiltonian assume the following form,

$$H(t) = H_0 + H_1(t) \quad (6.38)$$

where F and W operators are in H_0 and $V(t)$ is $H_1(t)$.

The solution to the time dependent Schrödinger equation can be written in terms of a time evolution operator operating on the ground state wave function,

$$\Psi(t) = U(t, t_0)\Psi_0 \quad (6.39)$$

where $t_0 < t$. The form of the time evolution operator is given as

$$U(t, t_0) = e^{-iH_0(t-t_0)} \quad (6.40)$$

where H_0 is made up of the time independent contributions to the total Hamiltonian $H(t)$. These techniques are the foundation of linear response theory, which will be introduced shortly. The time evolution operator must also be expanded to give

$$U(t, t_0) = e^{-iH_0(t-t_0)}U_1(t, t_0). \quad (6.41)$$

Using the time dependent Schrödinger equation,

$$i\frac{\partial}{\partial t}U_1(t, t_0) = e^{-iH_0(t-t_0)}H_1(t)e^{-iH_0(t-t_0)}U_1(t, t_0). \quad (6.42)$$

The first order correction to the time evolution operator can then be approximated as

$$U_1(t, t_0) \approx 1 - i \int_{t_0}^t dt' e^{-iH_0(t'-t_0)}H_1(t')e^{-iH_0(t'-t_0)}. \quad (6.43)$$

If we assume that

$$H_1(t) = F(t)\beta \quad (6.44)$$

where β is some observable coupled to external force $F(t)$, the observable is written as

$$\beta(t) = e^{-iH_0(t-t_0)}\beta e^{-iH_0(t-t_0)}. \quad (6.45)$$

The first order approximation to the time evolution operator is then taken to be

$$U(t, t_0) \approx e^{-iH_0(t-t_0)} \left\{ 1 - i \int_{t_0}^t dt' F(t')\beta(t' - t_0) \right\}. \quad (6.46)$$

This expression will be useful in the discussion of linear response theory in the following section.

6.3.2 General linear response theory

The goal of linear response theory is to understand how, in this case time dependent, perturbations affect some observable of a quantum mechanical system as it relates to the unperturbed ground state [211, 212]. A observable α is found by taking the expectation value with respect to the wave function,

$$\alpha_i = \langle \Psi_i | \alpha | \Psi_i \rangle. \quad (6.47)$$

In this discussion we are principally concerned with perturbations to the ground state, so $i = 0$ unless otherwise noted. In the above equation, Ψ_i is a many-body wave function with some accompanying Hamiltonian H_0 . Note that the subscript 0 indicates that this is the static or $t_0 = 0$ state (introduced in [Equation 6.38](#)). The

perturbation affects the wave function and the expectation value of α is now time dependent,

$$\alpha(t) = \langle \Psi(t) | \alpha | \Psi(t) \rangle. \quad (6.48)$$

The difference between this time dependent observation and the static observation from Equation 6.47, $\alpha(t) - \alpha_0$ is defined as the response of α to the perturbation. Another notation that can be used with time dependence is the Heisenberg representation. In this notation, the time propagator is removed from that of the wave function and placed on the operator,

$$\alpha(t) = \langle \Psi(t) | \alpha | \Psi(t) \rangle \quad (6.49)$$

$$= \langle \Psi(t=0) | e^{iHt} \alpha e^{-iHt} | \Psi(t=0) \rangle \quad (6.50)$$

$$= \langle \Psi | \alpha(t) | \Psi \rangle. \quad (6.51)$$

This notation will be used when the density linear response function is discussed in the next section.

This response can be expanded into powers of the external force $F(t)$ to give

$$\alpha(t) - \alpha_0 = \alpha_1(t) + \alpha_3(t) + \alpha_2(t) + \dots \quad (6.52)$$

with the subscripts being the order of the response (linear, quadratic, cubic, and so on). The linear response, with which we are concerned, can then be defined as

$$\alpha_1(t) = -i \int_{t_0}^t dt' F(t') \langle \Psi_0 | [\alpha(t), \beta(t')] | \Psi_0 \rangle. \quad (6.53)$$

Given that the static Hamiltonian H_0 is time independent, the commutator above can be rewritten inside a response function as,

$$\chi_{\alpha,\beta}(t-t') = -i\theta(t-t') \langle \Psi_0 | [\alpha(t-t'), \beta] | \Psi_0 \rangle. \quad (6.54)$$

The θ function ensures causality, or that the perturbation happens at time $t' \leq t$.

The linear response function can then be written as,

$$\alpha_1(t) = \int_{-\infty}^{\infty} dt' \chi_{\alpha\beta}(t-t') F(t') \quad (6.55)$$

The response function is general for any quantum mechanical observable, but in this case we are specifically interested in how some external potential v affects the density response of a system.

6.3.3 Density linear response

Density linear response theory applies the general linear response concept to understand how perturbations to the external potential affect the density of a chemical system [211, 213, 212, 210]. This shift in density can give information about excited state properties without using an excited state wave function to do so. The time independent and time dependent electronic density is defined as

$$n(\mathbf{r}) = \sum_i^N \delta(\mathbf{r} - \mathbf{r}_i) \quad (6.56)$$

and

$$n(\mathbf{r}, t) = \langle \Psi(t) | n(\mathbf{r}) | \Psi(t) \rangle \quad (6.57)$$

respectively. In ground state DFT, the Hohenberg-Kohn theorem stated that a unique one-to-one map existed between an external potential and a ground state density exist. The Runge-Gross theorem extended this unique mapping between a time-dependent potential ($v(\mathbf{r}, t)$, introduced in Equation 6.37) and a time-dependent density ($n(\mathbf{r}, t)$). The time-dependent density can then be written as a functional of the time-dependent potential,

$$n(\mathbf{r}, t) = n[v](\mathbf{r}, t). \quad (6.58)$$

In this section, we are interested in how the perturbation v_1 affects the density. The density response to this potential can be expanded in terms of this v_1 perturbation as

$$n(\mathbf{r}, t) - n_0(\mathbf{r}, t) = n_1(\mathbf{r}, t) + n_2(\mathbf{r}, t) + \dots \quad (6.59)$$

where $n_1(\mathbf{r}, t)$ is the linear term of interest. This linear density response function is defined as

$$n_1(\mathbf{r}, t) = \int dt' \int d\mathbf{r}' \chi(\mathbf{r}, t, \mathbf{r}', t') v_1(\mathbf{r}', t') \quad (6.60)$$

where χ is the density-density response function of interest. The explicit form is given to be

$$\chi(\mathbf{r}, t, \mathbf{r}', t') = i\theta(t - t') \langle \Psi_0 | [n(\mathbf{r}, t - t'), n(\mathbf{r}')] | \Psi_0 \rangle \quad (6.61)$$

with Ψ_0 being the exact, ground-state wave function.

This density-density response function can then be Fourier transformed to frequency space (the Lehmann representation) [213, 212], giving

$$\chi(\mathbf{r}, \mathbf{r}', \omega) = \sum_n^{\infty} \left\{ \frac{\langle \Psi_0 | n(\mathbf{r}) | \Psi_n \rangle \langle \Psi_n | n(\mathbf{r}') | \Psi_0 \rangle}{\omega - \Omega_n + i\eta} - \frac{\langle \Psi_0 | n(\mathbf{r}') | \Psi_n \rangle \langle \Psi_n | n(\mathbf{r}) | \Psi_0 \rangle}{\omega + \Omega_n + i\eta} \right\}. \quad (6.62)$$

Using this form of the function, it is easier to see that frequencies where excitations occur. Using different forms of the wave function will shift the excitation energies via the Ω_n term (which is $E_n - E_0$).

6.3.4 Perturbation theory approach

In this work, the exact wave function will be expanded into a perturbative series,

$$|\Psi_0\rangle = |\Psi_0^{(0)}\rangle + |\Psi_0^{(1)}\rangle + \dots \quad (6.63)$$

The perturbative expansion is an infinite series, but this work is only concerned with the first order wave function, thus other terms are ignored. This truncation will be explicitly introduced shortly. Substituting the expanded wave function into the response function gives,

$$\chi(\mathbf{r}, t, \mathbf{r}', t') = i\theta(t - t') \left\langle \Psi_0^{(0)} + \Psi_0^{(1)} + \dots \left| [n(\mathbf{r}, t - t'), n(\mathbf{r}')] \right| \Psi_0^{(0)} + \Psi_0^{(1)} + \dots \right\rangle \quad (6.64)$$

$$\begin{aligned} &= i\theta(t - t') \left(\left\langle \Psi_0^{(0)} \left| [n(\mathbf{r}, t - t'), n(\mathbf{r}')] \right| \Psi_0^{(0)} \right\rangle + \right. \\ &\quad \left. \left\langle \Psi_0^{(1)} \left| [n(\mathbf{r}, t - t'), n(\mathbf{r}')] \right| \Psi_0^{(0)} \right\rangle + \right. \\ &\quad \left. \left\langle \Psi_0^{(0)} \left| [n(\mathbf{r}, t - t'), n(\mathbf{r}')] \right| \Psi_0^{(1)} \right\rangle + \dots \right) \quad (6.65) \end{aligned}$$

Note that these terms are all of the zeroth and first order terms in the expansion.

The zeroth order term can be pulled out and used to define χ_0 , which is a reference contribution to the density response function using the zeroth order (usually Hartree-Fock) wave function.

$$\chi_0(\mathbf{r}, t, \mathbf{r}', t') = i\theta(t - t') \left\langle \Psi_0^{(0)} \left| [n(\mathbf{r}, t - t'), n(\mathbf{r}')] \right| \Psi_0^{(0)} \right\rangle \quad (6.66)$$

Excluding all terms beyond first order gives,

$$\begin{aligned} \chi(\mathbf{r}, t, \mathbf{r}', t') \approx & \chi_0(\mathbf{r}, t, \mathbf{r}', t') + i\theta(t - t') \left\langle \Psi_0^{(1)} \left| [n(\mathbf{r}, t - t'), n(\mathbf{r}')] \right| \Psi_0^{(0)} \right\rangle \\ & + i\theta(t - t') \left\langle \Psi_0^{(0)} \left| [n(\mathbf{r}, t - t'), n(\mathbf{r}')] \right| \Psi_0^{(1)} \right\rangle. \end{aligned} \quad (6.67)$$

The first order wave function can be written as some operator with the zeroth order wave function,

$$\Psi_i^{(1)} = \Omega \Psi_i^{(0)}. \quad (6.68)$$

Substituting this back into the linear response function gives,

$$\begin{aligned} \chi(\mathbf{r}, t, \mathbf{r}', t') \approx & \chi_0(\mathbf{r}, t, \mathbf{r}', t') + i\theta(t - t') \left\langle \Psi_0^{(0)} \left| \Omega [n(\mathbf{r}, t - t'), n(\mathbf{r}')] \right| \Psi_0^{(0)} \right\rangle \\ & + i\theta(t - t') \left\langle \Psi_0^{(0)} \left| [n(\mathbf{r}, t - t'), n(\mathbf{r}')] \Omega \right| \Psi_0^{(0)} \right\rangle \end{aligned} \quad (6.69)$$

which can be simplified using the anticommutator relationship,

$$\chi(\mathbf{r}, t, \mathbf{r}', t') \approx \chi_0(\mathbf{r}, t, \mathbf{r}', t') + i\theta(t - t') \left\langle \Psi_0^{(0)} \left| [[n(\mathbf{r}, t - t'), n(\mathbf{r}')] , \Omega] \right| \Psi_0^{(0)} \right\rangle. \quad (6.70)$$

This expression can use any number of forms for the first order wave function. As one of the main concerns of this project is low computational cost, the CIS and MP2 wave functions will be considered first.

6.4 Preliminary results

Calculating the excitation energies of ten electron systems has already been done using the multicomponent coupled-cluster method. To accomplish this, the CIS wave function was transformed to the electron-hole representation. This will be briefly surveyed before results are discussed.

As was stated previously, the CIS wave function consists of all singly excited determinants with respect to the Hartee-Fock reference state,

$$|\Psi^{\text{CIS}}\rangle = \sum_i^N \sum_a^M c_{(i,a)} |\Phi_i^a\rangle. \quad (6.71)$$

The i and a indices are in the occupied and virtual states, respectively. Excitation energy, ω , is calculated via

$$\omega^{\text{CIS}} = E^{\text{CIS}} - E^{\text{ref}} \quad (6.72)$$

$$= \langle \Psi^{\text{CIS}} | H | \Psi^{\text{CIS}} \rangle - E^{\text{ref}} \quad (6.73)$$

$$= \sum_{ij}^N \sum_{ab}^M c_{ia}^* c_{jb} \langle \Phi_i^a | H | \Phi_j^b \rangle - E^{\text{ref}} \quad (6.74)$$

$$\begin{aligned} &= \sum_i^N \sum_a^M c_{ia}^* c_{ia} \langle \Phi_i^a | H | \Phi_i^a \rangle \\ &+ \sum_{i \neq j}^N \sum_{a \neq b}^M c_{ia}^* c_{jb} \langle \Phi_i^a | H | \Phi_j^b \rangle \\ &+ \sum_i^N \sum_{a \neq b}^M c_{ia}^* c_{ib} \langle \Phi_i^a | H | \Phi_i^b \rangle \\ &+ \sum_{i \neq j}^N \sum_a^M c_{ia}^* c_{ja} \langle \Phi_i^a | H | \Phi_j^a \rangle - E^{\text{ref}}. \end{aligned} \quad (6.75)$$

In order to transform this to the electron-hole representation, we will need the form of the Hamiltonian and wave function.

The electron-hole Hamiltonian is defined as

$$H^{\text{eh}} = h^{\text{e}} + h^{\text{h}} + v^{\text{eh}}. \quad (6.76)$$

Note that the two body terms are missing as a single excitation in the electron-hole representation will not have those. The electron-hole wave function is defined as

$$|\Psi^{\text{eh}}\rangle = \sum_i c_i^{\text{eh}} |\Phi^{\text{e}} \Phi^{\text{h}}\rangle_i \quad (6.77)$$

Remember that in the electron-hole representation, virtual states are occupied by electrons (in an excited state), while holes inhabit the occupied space (from the all electron representation). This lets us break up the above expression as,

$$\begin{aligned} \omega^{\text{CIS}} &= \sum_i^N \sum_a^M c_{ia}^* c_{ia} (\langle a|h^{\text{e}}|a\rangle + \langle i|h^{\text{h}}|i\rangle + \langle ia|v^{\text{eh}}|ia\rangle) \\ &+ \sum_{i \neq j}^N \sum_{a \neq b}^M c_{ia}^* c_{jb} \langle ja|v^{\text{eh}}|ib\rangle \\ &+ \sum_i^N \sum_{a \neq b}^M c_{ia}^* c_{ib} (\langle a|h^{\text{e}}|b\rangle + \langle ai|v^{\text{eh}}|bi\rangle) \\ &+ \sum_{i \neq j}^N \sum_a^M c_{ia}^* c_{ja} (\langle i|h^{\text{e}}|j\rangle + \langle ia|v^{\text{eh}}|ja\rangle) \end{aligned} \quad (6.78)$$

$$= \sum_{ij}^N \sum_{ab}^M c_{ia}^* c_{jb} \langle ia|h^{\text{e}} + h^{\text{h}} + v^{\text{eh}}|jb\rangle. \quad (6.79)$$

This formulation allows multicomponent methods to calculate excitation energies that are as accurate as their single component counterparts. Results for ten electron systems are summarized in [Table 6.1](#). We are pleased to see that transforming to the electron-hole space and using the CIS ansatz reproduces those excitation energies using mcCC. This is to be expected though, as it is an exact transformation of CIS to multicomponent space.

Table 6.1: **Multicomponent coupled-cluster excitations energies versus CIS, TDHF, and EOM-CCSD in eV.**

System	ω^{mcCC}	ω^{CIS}	ω^{TDHF}	$\omega^{\text{EOM-CCSD}}$
CH ₄	11.654	11.654	13.933	13.456
NH ₃	8.141	8.141	9.051	8.211
H ₂ O	8.477	8.477	9.381	8.497
HF	11.000	11.000	11.823	10.836
Ne	44.604	44.604	50.241	51.215

All systems used standard 6-31G* basis set. CIS, TDHF, and EOM-CCSD calculations were done using GAMESS.

While this is an exciting and important first step, there remains a lot of work to catch the mcCC results up to EOM-CCSD, which is one of the gold standard methods for calculating excitation energies. TDHF and EOM-CCSD excitation energies differ with CIS excitation energies by up to 20%. By augmenting the mcCC formulation, we should be able to calculate excitation energies that more closely agree with these highly accurate methods. We expect that a screening function will improve accuracy and include correlation effects that is lacking in the current formulation.

Chapter 7

Investigating mass and confinement effects in multicomponent systems

The work in this chapter further investigates effects of invoking the Born-Oppenheimer (BO) approximation. The BO approximation is very useful, but its use is not always sufficient. This purpose of this study was to compare how properties and insight from calculations that avoided the BO approximation compared to conventional wisdom from application of the BO approximation.

7.1 Introduction

Many theoretical chemistry models are built upon the well known Born-Oppenheimer (BO) approximation. The BO approximation assumes that the nuclei and electrons in a chemical system move on different timescales. Decoupling the motion of electrons and nuclei allows the wave function to be written as

$$\Psi_{\text{exact}}(\mathbf{r}, \mathbf{R}) \approx \Psi^e(\mathbf{r}; \mathbf{R})\Psi^N(\mathbf{R}). \quad (7.1)$$

The nuclei are fixed in space, hence the parametric dependence in the electronic contribution. This approximation is justified earlier in [subsection 7.2.1](#).

The BO approximation has been used to great affect. It has been used to study chemical reactions [214, 215, 216], bond dissociations [217, 218, 219, 220], and spectroscopic signatures [221, 222], among many other applications. While the BO approximation is certainly a useful and powerful tool, it is not always an appropriate approximation to make. These failures are well documented, and have been met with new methodologies that can compensate for, or reapproximate contributions from nuclear motions [223, 224, 225, 226, 227, 228, 229, 71, 68, 99, 127, 104, 78].

This study is particularly interested in investigating an artifact of solving for the BO separated wave function via the Schrödinger equation - the potential energy surface. The potential energy surface is the functional relationship between the total potential energy of a system versus nuclear geometry. The potential energy surface is a very useful quantity and has been used to properties for molecular systems such as bond distance and geometries. The bond distance of the nuclear coordinates is of particular interest to this study. Using the BO approximation, we understand that there will be an energy minima at the equilibrium bond distance. If the atoms are spread further apart, energy will increase until the atoms are noninteracting and total energy is just a sum of individual energies. If the atoms are pinched together, we expect to see an increase in potential energy. The internuclear distance decreases, the Coulombic repulsions would greatly increasing, forcing the molecule back towards a favorable geometry.

Other studies have avoided using the BO approximation to understand the influence of this approximation on system properties. Recent work by Ceperley, Hammes-Schiffer, and others has utilized quantum Monte Carlo techniques such as path integral Monte Carlo [79] and diffusion Monte Carlo [99, 230] to study small molecular systems without the BO approximation. Earlier work led by Hammes-Schiffer also

used the Nuclear-electron orbital approach to look at non-BO effects [68, 71, 96, 77]. Adamowicz and coworkers investigated similar systems using explicitly correlated methods [74, 231, 232, 233]. Other work by Abedi, Maitra, and Gross solves the time dependent Schrödinger equation using the exact factorization method [103, 104].

The goal of this study is to investigate how nuclei behave when treated without the BO approximation. We are specifically interested in looking at how the potential energy changes as a function of internuclear distance in the H₂ molecule. Since the BO approximation is not made, the internuclear distance will not be governed by setting stationary points for the hydrogen atoms, but rather, a fully non BO system of two electrons and two protons will be placed in a parabolic well. This parabolic well will span weakly confining to strongly confining potentials as a means of influencing this distance. This study will also be carried out on a two-electron, two-positron system to see how mass influences the results.

7.2 Theory

The central focus of quantum chemistry is to predict and describe chemical properties and behavior at the atomic and subatomic level. A common way to gain insights about a molecular system is to solve the time-independent Schrödinger equation. The Schrödinger equation is an eigenvalue, partial differential equation. The equation is defined below,

$$H\Psi(\mathbf{r}, \mathbf{R}) = E\Psi(\mathbf{r}, \mathbf{R}). \quad (7.2)$$

The Hamiltonian is the operator that corresponds to the energy of a chemical system. The wave function has dependence on all of the coordinates in every particle in the system. The electronic coordinates are in the set \mathbf{r} and all nuclear coordinates are in the set \mathbf{R} . The exact form of the wave function is an infinite expansion of all possible

states that the system may exist in,

$$\Psi^{\text{exact}}(\mathbf{r}, \mathbf{R}) = \sum_i \sum_j w_{ij} \Psi^e(\mathbf{r}, \mathbf{R}) \Psi^N(\mathbf{R}). \quad (7.3)$$

Solving the Schrödinger equation as an infinite expansion is unpractical, so it is commonly approximated to have a different form. A select few of these approximations will be discussed later in [section 2.1](#), [section 2.3](#), and [section 2.4](#). The Hamiltonian has the following form for an N electron and M nuclei system,

$$H^{\text{mol}} = - \sum_i^N \frac{\hbar}{2m_i} \nabla_i^2 - \sum_A^M \frac{1}{2M_A} \nabla_A^2 - \sum_i^N \sum_A^M \frac{Z_A}{r_{iA}} + \sum_{i<j}^N \sum_j^N \frac{1}{r_{ij}} + \sum_{A<B}^M \sum_B^M \frac{Z_A Z_B}{R_{AB}} \quad (7.4)$$

$$= T^e(\mathbf{r}) + T^N(\mathbf{R}) + V^{e,N}(\mathbf{r}, \mathbf{R}) + V^{e,e}(\mathbf{r}) + V^{N,N}(\mathbf{R}). \quad (7.5)$$

The first two terms are differential operators and compute the kinetic energy of the i^{th} electron and the A^{th} nuclei in the system. The third term is the nuclear-electron attraction term, with Z_A being the charge of nucleus A and r_{iA} being the interparticle distance between electron i and nucleus A . The fourth term is the electron-electron repulsion term (where r_{ij} is the electron-electron distance) while the last is the nuclear-nuclear repulsion term (with R_{AB} being the internuclear distance). This form of the Hamiltonian is called the molecular Hamiltonian since it operates on both the nuclei and electrons in a molecule.

Solving the molecular Schrödinger equation with the molecular Hamiltonian is a difficult task. Chemical systems are collections of dynamic particles that are constantly moving. The electrons repel other electrons, nuclei repel other nuclei, and the two are also attracting one another. This is known as the correlation problem in quantum mechanics. It is impossible to exactly solve the Schrödinger equation because the positions of the particles are correlated. That is to say, an electron in

space will affect where other electrons may be. The same is true for nuclei. While the correlation problem will not disappear, we first simplify the Schrödinger equation to be more manageable since all of the information in a quantum system is difficult to quantify simulatenously.

7.2.1 The Born-Oppenheimer Approximation for single component systems

The Born-Oppenheimer (BO) approximation simplifies the wave function by decoupling the motion of nuclei and electrons, which allows us to rewrite the wave function as

$$\Psi^{\text{exact}}(\mathbf{r}, \mathbf{R}) \approx \Psi^e(\mathbf{r}; \mathbf{R}) \Psi^N(\mathbf{R}). \quad (7.6)$$

The wave function is written as a product of electronic and nuclear functions. Note though, that the electronic wave function, Ψ^e , is explicitly dependent on electronic coordintes and parametrically dependent on nuclear coordinates. In order to justify this approximation, we begin by defining an electronic Hamiltonian, H^e , which ignores the kinetic energy of nuclei (T^N) and the nuclear repulsion term ($V^{N,N}$) will be considered a constant since the nuclear positions are fixed in space.

$$H^e = T^e(\mathbf{r}) + V^{e,N}(\mathbf{r}; \mathbf{R}) + V^{e,e}(\mathbf{r}) + V^{N,N}(\mathbf{R}) \quad (7.7)$$

The electronic Hamiltonian can then be used in the electronic structure Schrödinger equation to solve for electronic energy,

$$H^e \Psi^e(\mathbf{r}; \mathbf{R}) = E^e \Psi^e(\mathbf{r}; \mathbf{R}) \quad (7.8)$$

$$[T^e(\mathbf{r}) + V^{e,N}(\mathbf{r}; \mathbf{R}) + V^{e,e}(\mathbf{r}) + V^{N,N}(\mathbf{R})] \Psi^e(\mathbf{r}; \mathbf{R}) = E^e \Psi^e(\mathbf{r}; \mathbf{R}) \quad (7.9)$$

Now, substituting the BO wave function (Equation 7.6) into the Schrödinger equation (Equation 7.2) yields,

$$H^{\text{mol}} \Psi^e(\mathbf{r}; \mathbf{R}) \Psi^N(\mathbf{R}) = E^{\text{tot}} \Psi^e(\mathbf{r}; \mathbf{R}) \Psi^N(\mathbf{R}). \quad (7.10)$$

Expanding this to include the full H^{mol} is then

$$[T^e(\mathbf{r}) + T^N(\mathbf{R}) + V^{e,N}(\mathbf{r}, \mathbf{R}) + V^{e,e}(\mathbf{r}) + V^{N,N}(\mathbf{R})] \Psi^e(\mathbf{r}; \mathbf{R}) \Psi^N(\mathbf{R}) = E^{\text{tot}} \Psi^e(\mathbf{r}; \mathbf{R}) \Psi^N(\mathbf{R}). \quad (7.11)$$

If the nuclear motion is to be decoupled from the electronic motion, it is necessary to inspect how the T^N operator will effect the electronic portion of the wave function, Ψ^e , since it has dependence on nuclear terms,

$$T^N(\mathbf{R}) \Psi^e(\mathbf{r}; \mathbf{R}) \Psi^N(\mathbf{R}) = \frac{1}{2M_A} \nabla_A^2 \Psi^e(\mathbf{r}; \mathbf{R}) \Psi^N(\mathbf{R}) \quad (7.12)$$

$$= \frac{1}{2M_A} [\Psi^e(\mathbf{r}; \mathbf{R}) \nabla_A^2 \Psi^N(\mathbf{R}) + \Psi^N(\mathbf{R}) \nabla_A^2 \Psi^e(\mathbf{r}; \mathbf{R}) \quad (7.13)$$

$$+ 2(\nabla_A \Psi^e(\mathbf{r}; \mathbf{R})) \bullet (\nabla_A \Psi^N(\mathbf{R}))]. \quad (7.14)$$

Then, substituting Equation 7.8 and Equation 7.12 into Equation 7.11 we get

$$\begin{aligned} & \Psi^e(\mathbf{r}; \mathbf{R}) T^N(\mathbf{R}) \Psi^N(\mathbf{R}) + (E^e) \Psi^N(\mathbf{R}) \Psi^e(\mathbf{r}; \mathbf{R}) - \\ & \left[\sum_A \frac{1}{2M_A} (2\nabla_A \Psi^e(\mathbf{r}; \mathbf{R}) \nabla_A \Psi^N(\mathbf{R}) + \Psi^N(\mathbf{R}) \nabla_A^2 \Psi^e(\mathbf{r}; \mathbf{R})) \right] = E^{\text{tot}} \Psi^e(\mathbf{r}; \mathbf{R}) \Psi^N(\mathbf{R}). \end{aligned} \quad (7.15)$$

The terms in square brackets are said to be the derivative coupling terms as they couple the motion of the nuclear coordinates with the electronic wave function. To decouple

the motions, the term in the square brackets must be dropped to give

$$\Psi^e(\mathbf{r}; \mathbf{R})T^N(\mathbf{R})\Psi^N(\mathbf{R}) + \Psi^N(\mathbf{R})E^e\Psi^e(\mathbf{r}; \mathbf{R}) = E^{\text{tot}}\Psi^e(\mathbf{r}; \mathbf{R})\Psi^N(\mathbf{R}) \quad (7.16)$$

can then solve the electronic problem and the nuclear problem separately as the remaining terms can be factored as

$$[T^N(\mathbf{R}) + E^e(\mathbf{R})] \Psi^N(\mathbf{R}) = E^{\text{tot}}(\mathbf{R})\Psi^N(\mathbf{R}). \quad (7.17)$$

This is the nuclear Schrödinger equation. Solutions to the nuclear Schrödinger equation are not the focuses of the research in this work, so it will not be examined further; however, there are many great resources that detail it further.

Potential energy surface

Invoking the BO approximation leads to an electronic energy that is dependent on the nuclear positions. This is called the potential energy surface and it describes the energy of a chemical system as the nuclear geometry changes.

Qualitatively, this can be understood as using the H₂ molecule as an example. Assume that two individual H atoms exist infinitely far apart. The energy of this system would simply be the energy of twice a Hydrogen atom. As these two atoms were brought closer together, they would share electron density, forming a bond, which would reduce the energy of the system. If the two H atoms were continued to be pinched together, we would see E^e climb higher due to the fact that the nuclear repulsion term grows rapidly. This simple example illustrates how nuclear geometries dictate bonding behavior of molecular systems.

The H₂ example is quite simple, but it can be extended to more complex molecules, though it becomes harder to conceptualize. This is generally how molecular bonding is taught and understood with regards to the nuclear coordinates. While this is a

valuable tool for investigators to use, this work will discuss models where the BO approximation and potential energy surfaces produce erroneous results. When this happens, one must adopt a new model for investigating such systems that does not require that the nuclear and electronic motions to be decoupled. Furthermore, we will look at systems where the BO approximation cannot be used because electrons are bound to other (non-massive) subatomic particles, such as a positron or a quasi-hole.

7.2.2 The Born-Oppenheimer Approximation for multicomponent systems

A multicomponent interpretation of the BO approximation allows for particles to be classified to as many types as necessary. With this logic, the wave function can be approximated as,

$$\Psi^{\text{exact}}(\mathbf{r}^{\text{I}}, \mathbf{r}^{\text{II}}, \dots, \mathbf{r}^{\text{N}}) \approx \Psi^{\text{I,II},\dots}(\mathbf{r}^{\text{I}}, \mathbf{r}^{\text{II}}, \dots; \mathbf{R}^{\text{BOS}}) \Psi^{\text{BOS}}(\mathbf{R}^{\text{BOS}}). \quad (7.18)$$

We see that the wave function still includes BO separated bodies (\mathbf{R}^{BOS}), but also on particles that are not BO separated (\mathbf{r}^{X}). As was the case with the BO approximation, this will lead to a BOS Schrödinger equation for Ψ^{BOS} and a non-BOS Schrödinger equation for $\Psi^{\text{non-BOS}}$. This formulation allows for as many unique particle types as necessary to be defined. While this is a powerful ability, it need not be liberally applied to any system. It should be applied to systems where the motion of two types of particles is coupled.

Unfortunately, approximating the wave function to include an ambiguous number of unique particle types is as powerful as it is impractical. Such a wave function would be accompanied by a complex Hamiltonian, which would make enumerating and indexing the states and interactions enormously challenging. So, we begin by

using two types of non BO separated particles,

$$\Psi^{\text{exact}}(\mathbf{r}^{\text{I}}, \mathbf{r}^{\text{II}}, \dots, \mathbf{R}^{\text{BOS}}) \approx \Psi^{\text{I,II}}(\mathbf{r}^{\text{I}}, \mathbf{r}^{\text{II}}; \mathbf{R}^{\text{BOS}}) \Psi^{\text{BOS}}(\mathbf{R}^{\text{BOS}}). \quad (7.19)$$

with dependence on coordinates \mathbf{r}^{I} and \mathbf{r}^{II} . Note that this is nearly identical to the BO approximated single component wave function seen previously (Equation 7.6). As was the case with the single component wave function, separating the exact wave function into a product of two wave functions (one for non BO separated bodies and one for BO separated bodies) must be justified. This justification will be built upon the assumption that the motion of BO separated particles affects the non BO separated bodies to a negligible degree.

The Hamiltonian for this system will be of the form,

$$\begin{aligned} H^{\text{mc}} = & - \sum_i^{N^{\text{I}}} \frac{\hbar}{2m_i^{\text{I}}} \nabla_i^{\text{I}^2} + \sum_{i < j}^{N^{\text{I}}} \sum_j^{N^{\text{I}}} \frac{q^{\text{I}} q^{\text{I}}}{r_{ij}} + \sum_i^{N^{\text{I}}} \sum_A^{N^{\text{BOS}}} \frac{q^{\text{I}} Z_A}{r_{iA}} \\ & - \frac{\hbar}{2m_{i'}^{\text{II}}} \sum_{i'}^{N^{\text{II}}} \nabla_{i'}^{\text{II}^2} + \sum_{i' < j'}^{N^{\text{II}}} \sum_{j'}^{N^{\text{II}}} \frac{q^{\text{II}} q^{\text{II}}}{r_{i'j'}} + \sum_{i'}^{N^{\text{II}}} \sum_A^{N^{\text{BOS}}} \frac{q^{\text{II}} Z_A}{r_{i'A}} \\ & + \sum_i^{N^{\text{I}}} \sum_{i'}^{N^{\text{II}}} \frac{q^{\text{I}} q^{\text{II}}}{r_{ii'}} \\ & - \sum_A^{N^{\text{BOS}}} \frac{\hbar}{2M_A} \nabla_A^2 + \sum_{A < B}^{N^{\text{BOS}}} \sum_B^{N^{\text{BOS}}} \frac{Z_A Z_B}{R_{AB}}. \end{aligned} \quad (7.20)$$

The first and second lines are the kinetic energy, interparticle potential, and external potential for the type I and type II particles, respectively. The third line is the type I-II potential term. The final line is the kinetic energy and interparticle potential of the particles that fall under the BO separated definition. Note that the type II particle indices are primed so they are more easily distinguished from the type I counterparts.

This can be condensed to

$$\begin{aligned}
H^{\text{mc}} &= T^{\text{I}}(\mathbf{r}^{\text{I}}) + V^{\text{I,I}}(\mathbf{r}^{\text{I}}) + V_{\text{ext}}^{\text{I}}(\mathbf{r}^{\text{I}}, \mathbf{R}^{\text{BOS}}) \\
&+ T^{\text{II}}(\mathbf{r}^{\text{II}}) + V^{\text{II,II}}(\mathbf{r}^{\text{II}}) + V_{\text{ext}}^{\text{II}}(\mathbf{r}^{\text{II}}, \mathbf{R}^{\text{BOS}}) \\
&+ V^{\text{I,II}}(\mathbf{r}^{\text{I}}, \mathbf{r}^{\text{II}}) \\
&+ T^{\text{BOS}}(\mathbf{R}^{\text{BOS}}) + V^{\text{BOS,BOS}}(\mathbf{R}^{\text{BOS}})
\end{aligned} \tag{7.21}$$

$$\begin{aligned}
&= H^{\text{I,II}}(\mathbf{r}^{\text{I}}, \mathbf{r}^{\text{II}}) + V^{\text{I,II,BOS}}(\mathbf{r}^{\text{I}}, \mathbf{r}^{\text{II}}, \mathbf{R}^{\text{BOS}}) \\
&+ T^{\text{BOS}}(\mathbf{R}^{\text{BOS}}).
\end{aligned} \tag{7.22}$$

The form of $H^{\text{I,II}}$ and $V^{\text{I,II,BOS}}$ are

$$H^{\text{I,II}}(\mathbf{r}^{\text{I}}, \mathbf{r}^{\text{II}}) = T^{\text{I}}(\mathbf{r}^{\text{I}}) + V^{\text{I,I}}(\mathbf{r}^{\text{I}}) + T^{\text{II}}(\mathbf{r}^{\text{II}}) + V^{\text{II,II}}(\mathbf{r}^{\text{II}}) + V^{\text{BOS,BOS}}(\mathbf{R}^{\text{BOS}}) \tag{7.23}$$

$$V^{\text{I,II,BOS}}(\mathbf{r}^{\text{I}}, \mathbf{r}^{\text{II}}, \mathbf{R}^{\text{BOS}}) = V_{\text{ext}}^{\text{I}}(\mathbf{r}^{\text{I}}, \mathbf{R}^{\text{BOS}}) + V_{\text{ext}}^{\text{II}}(\mathbf{r}^{\text{II}}, \mathbf{R}^{\text{BOS}}). \tag{7.24}$$

This form of the Hamiltonian closely resembles the single component form from [Equation 7.4](#).

The Hamiltonian and exact wave function are then substituted into the Schrödinger equation,

$$H^{\text{mc}}(\mathbf{r}^{\text{I}}, \mathbf{r}^{\text{II}}, \mathbf{R}^{\text{BOS}})\Psi^{\text{exact}}(\mathbf{r}^{\text{I}}, \mathbf{r}^{\text{II}}, \mathbf{R}^{\text{BOS}}) = E^{\text{tot}}\Psi^{\text{exact}}(\mathbf{r}^{\text{I}}, \mathbf{r}^{\text{II}}, \mathbf{R}^{\text{BOS}}) \tag{7.25}$$

$$H^{\text{mc}}(\mathbf{r}^{\text{I}}, \mathbf{r}^{\text{II}}, \mathbf{R}^{\text{BOS}})\Psi^{\text{I,II}}(\mathbf{r}^{\text{I}}, \mathbf{r}^{\text{II}}; \mathbf{R}^{\text{BOS}})\Psi^{\text{BOS}}(\mathbf{R}^{\text{BOS}}) = E^{\text{tot}}\Psi^{\text{I,II}}(\mathbf{r}^{\text{I}}, \mathbf{r}^{\text{II}}; \mathbf{R}^{\text{BOS}})\Psi^{\text{BOS}}(\mathbf{R}^{\text{BOS}}). \tag{7.26}$$

If the Hamiltonian in the Schrödinger equation were then expanded as prescribed by [Equation 7.22](#), it would be analogous to the single component counterpart, [Equation 7.11](#). The BO extension to multicomponent systems then follows the same logical flow as the single component derivation, where the coupling terms for BO separated particle motion is decoupled from particles that are not BO separated. The steps are

not repeated here, but the following Schrödinger equations are produced,

$$H^{I,II}(\mathbf{r}^I, \mathbf{r}^{II}; \mathbf{R}^{\text{BOS}}) \Psi^{I,II}(\mathbf{r}^I, \mathbf{r}^{II}; \mathbf{R}^{\text{BOS}}) = E^{I,II}(\mathbf{R}^{\text{BOS}}) \Psi^{I,II}(\mathbf{r}^I, \mathbf{r}^{II}; \mathbf{R}^{\text{BOS}}) \quad (7.27)$$

$$[T^{\text{BOS}}(\mathbf{R}^{\text{BOS}}) + E^{I,II}(\mathbf{R}^{\text{BOS}})] \Psi^{\text{BOS}}(\mathbf{R}^{\text{BOS}}) = E^{\text{tot}}(\mathbf{R}^{\text{BOS}}) \Psi^{\text{BOS}}(\mathbf{R}^{\text{BOS}}). \quad (7.28)$$

As was the case with the single component BO approximation, decoupling the motion of BO separated particles from the others results in two equations that can be solved separately.

Multicomponent methods focus on solving the first equation above by approximating and optimizing a multicomponent wave function ($\Psi^{I,II}$). Some of these methods will be detailed in following sections and the next chapter. Solving the Schrödinger equation for BO separated particles can be done using existing techniques and is not the focus of the work presented.

Multicomponent potential energy surfaces

Applying the BO approximation to single component systems resulted in a potential energy surface. This quantity relates the nuclear geometries to a specific electronic potential energy.

The multicomponent BO approximation also produces a potential energy surface, provided that BO separated particles exist. Relating the multicomponent energy plus the BO separated potential would give similar insights about the effects the BO separated geometries have on the energy of the system.

Should no BO separated bodies exist, there would be no potential energy surface to speak of. It is important to remember this fact. Potential energy surfaces are very useful tools for investigating chemical processes, but are the result of an approximation. Ideally, quantum chemical investigations would avoid using the ap-

proximation all together since it is an abstraction from reality. This task, however, is very complex and can be an unnecessary burden. Consequences and analysis of the BO approximation as it relates to multicomponent systems is further explored later in [chapter 7](#).

7.3 Method

The two electron-two positron ($2e^-$, $2e^+$) and H_2 systems were investigated using the multicomponent configuration interaction method. This method is built on top of the multicomponent Hartree-Fock method, which were both detailed previously in [chapter 3](#), so only a quick survey will be provided here. We will then discuss the properties of interest for these systems and how those will be computed.

The mcFCI method was chosen in this study for two reason. First is that the multicomponent Hartree-Fock method is not descriptive enough for multicomponent systems. This was highlighted previously in [chapter 4](#) ([192]) and [39]. Correlation effects are extremely important when investigating multicomponent systems, so a method beyond mcHF was needed. The mcHF method was still used to construct the multicomponent molecular orbitals. For treating correlation beyond the mcHF level, there were two obvious choices of mcFCI and multicomponent coupled-cluster theory. The second reason that mcFCI was chosen was due to computational cost considerations. The properties of interest (which are discussed later) were calculated as an expectation value with respect to the multicomponent wave function. Calculating expectation values with respect to the mcCC wave function is a very complicated task. For the mcFCI wave function, it is much more straightforward.

Both the mcHF and mcFCI methods approximate a solution to the multicomponent Schrödinger equation,

$$H\Psi^{I,II}(\mathbf{r}^I, \mathbf{r}^{II}; \mathbf{R}^{\text{BOS}}) = E\Psi^{I,II}(\mathbf{r}^I, \mathbf{r}^{II}; \mathbf{R}^{\text{BOS}}). \quad (7.29)$$

The Hamiltonian used for solving the multicomponent Schrödinger equation, which was first introduced explicitly in [section 4.2](#), is defined as

$$\begin{aligned} H = & \sum_{pq} \langle p|h^I|q\rangle p^\dagger q \\ & + \sum_{pqrs} \langle pq|v^{I,I}|rs\rangle p^\dagger q^\dagger sr \\ & + \sum_{p'q'} \langle p'|h^{II}|q'\rangle p'^\dagger q' \\ & + \sum_{p'q'r's'} \langle p'q'|v^{II,II}|r's'\rangle p'^\dagger q'^\dagger s'r' \\ & + \sum_{pp'qq'} \langle pp'|v^{I,II}|qq'\rangle p^\dagger p'^\dagger qq' \end{aligned} \quad (7.30)$$

with explicit form of the one and two body operators being

$$h^\alpha(\mathbf{r}^\alpha, \mathbf{R}^{\text{BOS}}) = \frac{-\hbar}{2m_\alpha} \nabla_\alpha^2 + v_{\text{ext}}^\alpha(\mathbf{r}^\alpha, \mathbf{R}^{\text{BOS}}) \quad \alpha = \text{I, II}, \quad (7.31)$$

$$v^{\alpha,\alpha}(\mathbf{r}^\alpha) = q^\alpha q^\alpha \epsilon^{-1} r_{\alpha\alpha}^{-1}, \quad (7.32)$$

$$v^{I,II}(\mathbf{r}^I, \mathbf{r}^{II}) = q^I q^{II} \epsilon^{-1} r_{I,II}^{-1}. \quad (7.33)$$

This Hamiltonian is used for both the mcHF and mcFCI solution. Each particle was confined with a 3D parabolic potential defined as

$$v_{\text{ext}}^\alpha = \frac{1}{2} k^\alpha |\mathbf{r}^\alpha|^2 \quad \alpha = e^-, e^+, \text{H}. \quad (7.34)$$

The k values are given in [Table 7.5](#).

The mcHF method approximates the multicomponent wave function as a single Slater determinant. This determinant is a product of a type I and type II Slater determinant,

$$\Psi^{I,II}(\mathbf{r}^I, \mathbf{r}^{II}; \mathbf{R}^{\text{BOS}}) = \Phi^I(\mathbf{x}^I; \mathbf{R}^{\text{BOS}})\Phi^{II}(\mathbf{x}^{II}; \mathbf{R}^{\text{BOS}}). \quad (7.35)$$

The energy of the system is then minimized with respect to the orbitals with which the Slater determinant is constructed,

$$\langle 0^I 0^{II} | H | 0^I 0^{II} \rangle = \min_{\Phi^I, \Phi^{II}} \langle \Phi^I \Phi^{II} | H | \Phi^I \Phi^{II} \rangle. \quad (7.36)$$

This procedure is done by self consistently solving the coupled Fock equations,

$$f^I |\chi_i^I\rangle = \epsilon_i^I |\chi_i^I\rangle \quad (7.37)$$

$$f^{II} |\chi_{i'}^{II}\rangle = \epsilon_{i'}^{II} |\chi_{i'}^{II}\rangle \quad (7.38)$$

where the Fock operators are,

$$f^I = h^I + v_{\text{HF}}^I + \sum_{i'}^{N^{II}} \langle i' | v^{I,II} | i' \rangle \quad (7.39)$$

$$f^{II} = h^{II} + v_{\text{HF}}^{II} + \sum_i^{N^I} \langle i | v^{I,II} | i \rangle \quad (7.40)$$

In mcFCI theory, the wave function is approximated as a linear combination of Slater determinants in type I and type II space. The orbitals used to construct these determinants are the result of the mcHF SCF procedure. The wave function is defined

as

$$\begin{aligned}
|\Psi_{\text{mcFCI}}\rangle &= c_{(0,0),(0',0')}^{\text{I,II}} |0^{\text{I}}0^{\text{II}}\rangle \\
&+ \sum_i^{N^{\text{I}}} \sum_a^{M^{\text{I}}} c_{(i,a),(0',0')}^{\text{I,II}} a^\dagger i |0^{\text{I}}0^{\text{II}}\rangle \\
&+ \sum_{i<j}^{N^{\text{I}}} \sum_j^{N^{\text{I}}} \sum_{a<b}^{M^{\text{I}}} \sum_b^{M^{\text{I}}} c_{(ij,ab),(0',0')}^{\text{I,II}} a^\dagger b^\dagger j i |0^{\text{I}}0^{\text{II}}\rangle + \dots \\
&+ \sum_{i'}^{N^{\text{II}}} \sum_{a'}^{M^{\text{II}}} c_{(0,0),(i',a')}^{\text{I,II}} a'^\dagger i' |0^{\text{I}}0^{\text{II}}\rangle \\
&+ \sum_{i'<j'}^{N^{\text{II}}} \sum_{j'}^{N^{\text{II}}} \sum_{a'<b'}^{M^{\text{II}}} \sum_{b'}^{M^{\text{II}}} c_{(0,0),(i'j',a'b')}^{\text{I,II}} a'^\dagger b'^\dagger j' i' |0^{\text{I}}0^{\text{II}}\rangle + \dots \\
&+ \sum_i^{N^{\text{I}}} \sum_a^{M^{\text{I}}} \sum_{i'}^{N^{\text{II}}} \sum_{a'}^{M^{\text{II}}} c_{(i,a),(i',a')}^{\text{I,II}} a^\dagger i a'^\dagger i' |0^{\text{I}}0^{\text{II}}\rangle \\
&+ \sum_{i<j}^{N^{\text{I}}} \sum_j^{N^{\text{I}}} \sum_{a<b}^{M^{\text{I}}} \sum_b^{M^{\text{I}}} \sum_{i'<j'}^{N^{\text{II}}} \sum_{j'}^{N^{\text{II}}} \sum_{a'<b'}^{M^{\text{II}}} \sum_{b'}^{M^{\text{II}}} c_{(ij,ab),(i'j',a'b')}^{\text{I,II}} a^\dagger b^\dagger j i a'^\dagger b'^\dagger j' i' |0^{\text{I}}0^{\text{II}}\rangle \\
&+ \dots
\end{aligned} \tag{7.41}$$

The energy for the mcFCI method is then minimized via

$$\langle \Psi_{\text{mcFCI}} | H | \Psi_{\text{mcFCI}} \rangle = E_{\text{mcFCI}} \langle \Psi_{\text{mcFCI}} | \Psi_{\text{mcFCI}} \rangle. \tag{7.42}$$

The mcFCI method will provide exact solutions to the chosen basis for the systems of interest.

7.4 Computational details

This study is chiefly concerned with four properties for each system. For the two electron-two positron system, the relationship between average electron-electron and positron-positron repulsion energies, as well as the average electron-positron attrac-

tion energy versus the average positron-positron separation distance will be investigated. For the H_2 system, the analogous relationship will be investigated. For this study, we are curious to see how a non BO treatment of H_2 behaves compared to the two electron-two positron system which has greatly reduced mass for the positively charged particles.

These properties will be calculated by taking a given operator's expectation value with respect to the mcFCI wave function,

$$\langle \Omega \rangle = \langle \Psi_{\text{mcFCI}} | \Omega | \Psi_{\text{mcFCI}} \rangle. \quad (7.43)$$

The electron-electron, positron-positron, hydrogen-hydrogen, electron-positron, and electron-hydrogen operators have been defined above in the Hamiltonian. Note that the dielectric function (ϵ) is set to 1. The positron-positron, hydrogen-hydrogen, and electron-electron interparticle distance operator is defined as,

$$r_{1,2}^{\alpha,\alpha^2} = |\mathbf{r}_1^\alpha - \mathbf{r}_2^\alpha|^2 \quad \alpha = e^-, e^+, \text{H} \quad (7.44)$$

The masses for the electron and positron were 1 atomic unit, with charges of -1 and +1 atomic unit, respectively. The protons had a mass of 1836 atomic units. The confining potentials, k , as well as exponents for the [spd] Gaussian basis functions are given in [Table 7.5](#).

7.5 Results

The data in this study shows a very interesting deviation when compared to intuition from the BO approximation. The relationship between average positron distance and the average electron-electron, electron-positron, positron-positron potential energies, as well as the total average potential energy, is plotted in [Figure 7.1](#). The correspond-

ing plot for H_2 , showing the electron-electron, electron-hydrogen, hydrogen-hydrogen, and total potential energies versus the average hydrogen-hydrogen distance is given in [Figure 7.2](#). The inverse relationship between these quantities is plotted in [Figure 7.3](#) and [Figure 7.4](#) to understand the linear relationship. The inverse linear relationships are summarized in [Table 7.1](#) and [Table 7.2](#).

The results in [Figure 7.1](#) and [Figure 7.2](#) are very striking. As we would expect the positron-positron and hydrogen-hydrogen potential increases as the particles are drawn closer together. This agrees with intuition we already have about the bonding behavior of molecules from the BO approximation. What is unexpected is that the total potential always outpaces the positron-positron and hydrogen-hydrogen potential. Typically, the potential energy surface will have greatly increased when nuclear centers are close together which causes the system to be unbound. In this treatment of H_2 , the system is always bound.

While this finding is counter-intuitive from the BO point of view, it does not seem totally unreasonable. In each system, there are more attractive terms than repulsive. There are two repulsive terms for the $2e^-$, $2e^+$ and H_2 systems. The two electrons in each system and then the positron-positron or hydrogen-hydrogen terms. Each system then has four attractive terms. Each electron has a negative potential with each of the two positively charged particles (positrons or hydrogens).

Additionally, there are also artifacts of screening in [Figure 7.1](#) and [Figure 7.2](#). For both the two electron-two positron system and the hydrogen system, the bare Coulombic potential is plotted alongside the positron-positron and hydrogen-hydrogen potential as the orange line ($\langle r_{e^+,e^+}^2 \rangle^{-\frac{1}{2}}$ and $\langle r_{\text{H,H}}^2 \rangle^{-\frac{1}{2}}$). We see that this line is slightly lower than the repulsive potentials. The presence of electrons in the system appears to be drawing the two positively charged bodies closely together. This finding is also non-intuitive from the BO perspective since nuclear-nuclear repulsion is treated as a pure Coulombic potential.

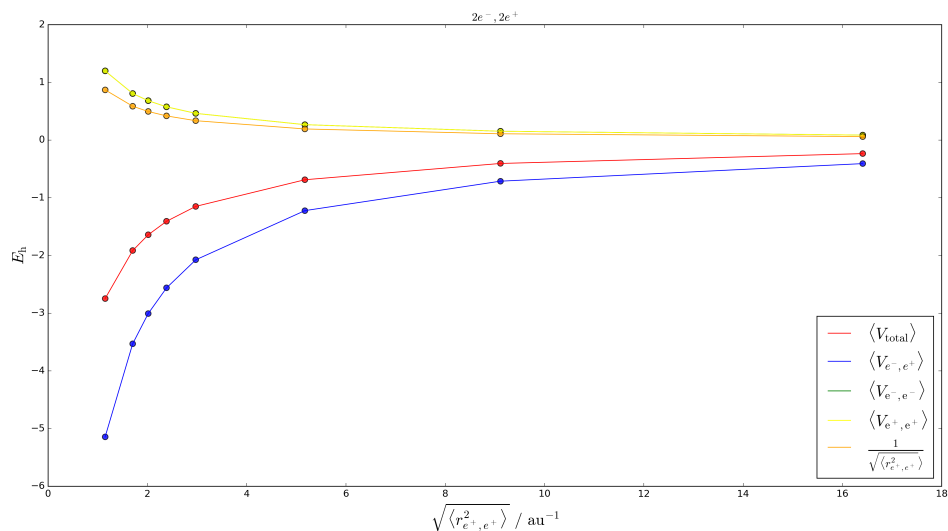


Figure 7.1: Relationship of potential electron-electron, electron-positron, and positron-positron potential energies versus the average positron-positron distance.

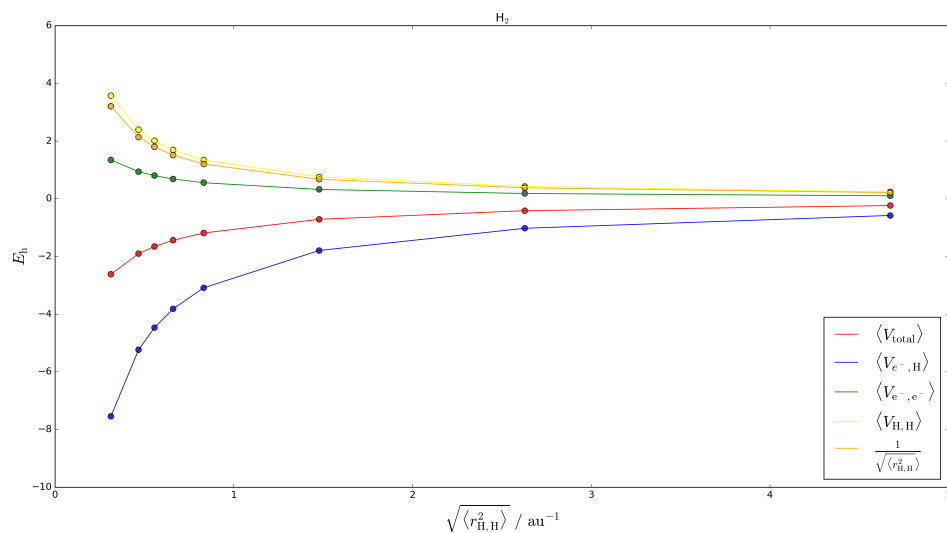


Figure 7.2: Relationship of potential electron-electron, electron-hydrogen, and hydrogen-hydrogen potential energies versus the average hydrogen-hydrogen distance.

7.6 Conclusion

This study investigated the non BO behavior of a two electron-two positron system and the hydrogen molecule. The systems were investigated by solving the multi-component full configuration interaction Schrödinger equation. Each particle was

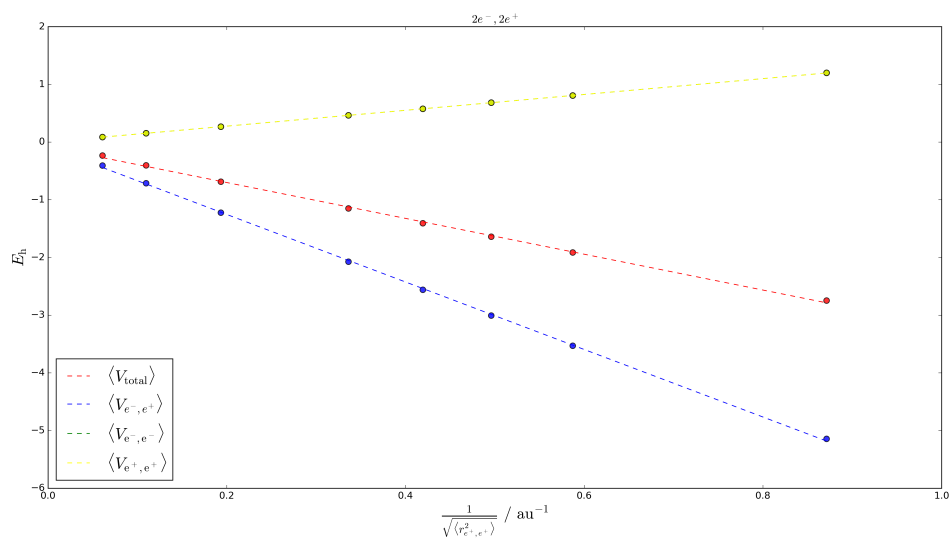


Figure 7.3: Inverse relationship of potential electron-electron, electron-positron, and positron-positron potential energies versus the average positron-positron.

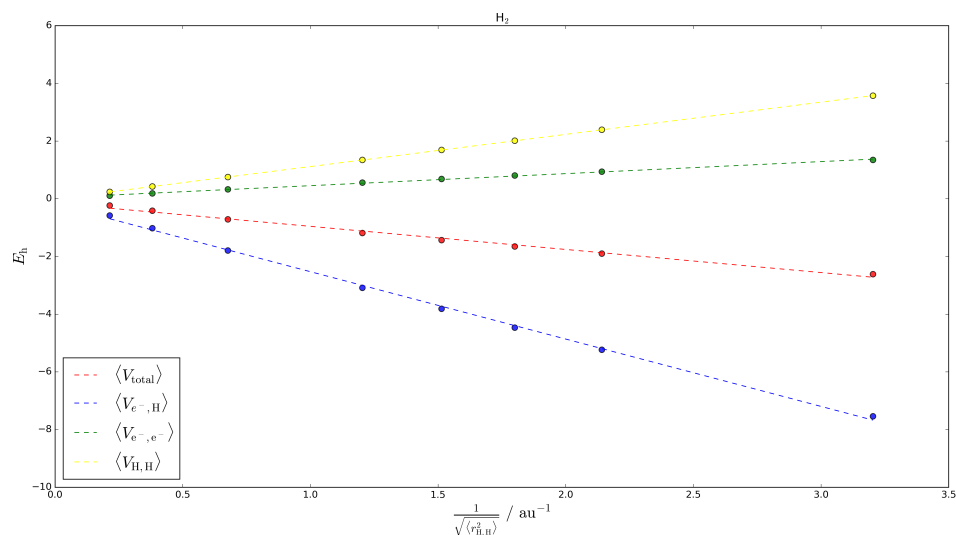


Figure 7.4: Inverse relationship of potential electron-electron, electron-hydrogen, and hydrogen-hydrogen potential energies versus the average hydrogen-hydrogen distance.

confined by a parabolic potential. The expectation value of the electron-electron, electron-positron, and positron-positron potentials were plotted versus the expectation value of positron-positron distance for a set of confining potentials. The same study was carried out for a hydrogenic system. The findings of this work constrasts

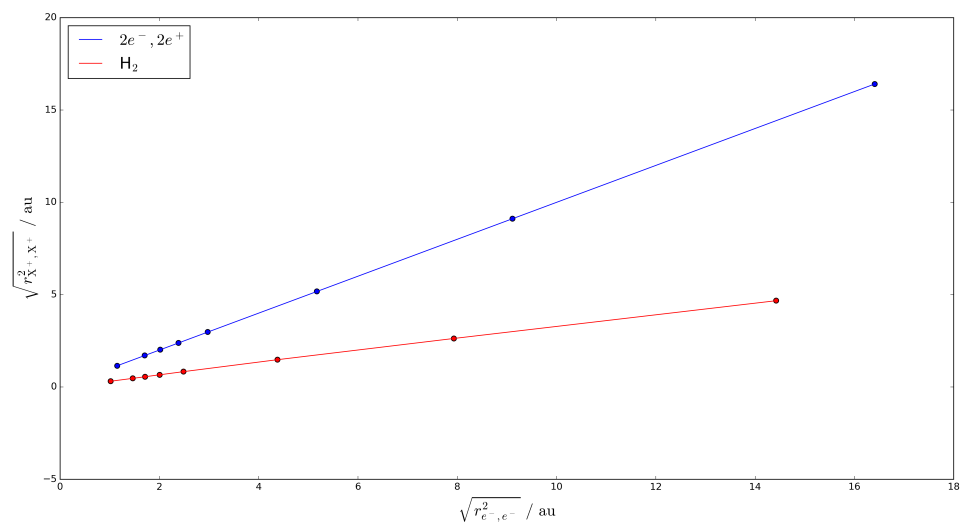


Figure 7.5: Average positron-positron and hydrogen-hydrogen distance versus average electron-electron distance.

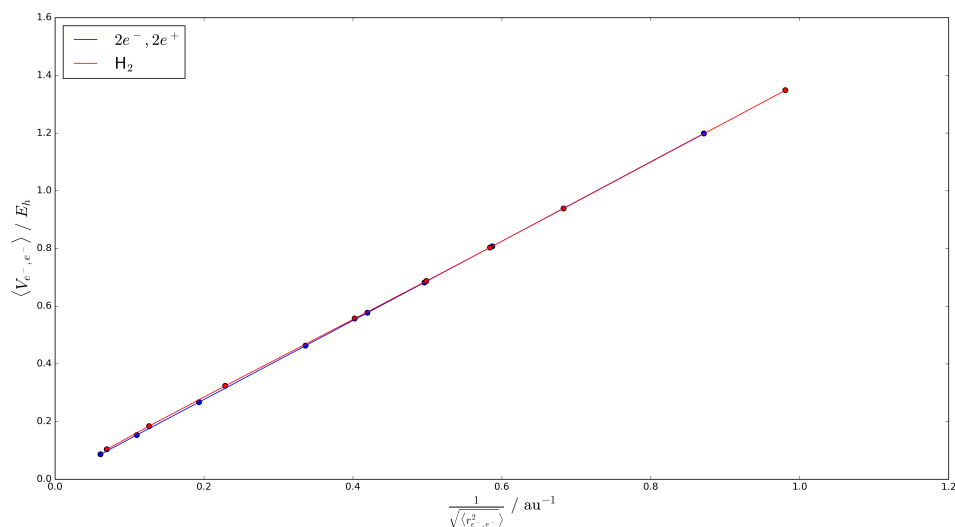


Figure 7.6: Average electron-electron potential energy versus the average electron-electron separation distance in the $2e^+, 2e^-$ and H_2 systems.

with expected behavior from invocation of the BO approximation. It was shown that, using a parabolic potential, H_2 will always be bound, regardless of how closely the two protons are confined. Additionally, it was seen that the bare Coulombic

Table 7.1: **Linear fits and RMSE of $\langle V_{e^-,e^-} \rangle$, $\langle V_{e^+,e^+} \rangle$, $\langle V_{e^-,e^+} \rangle$, and $\langle V_{\text{total}} \rangle$ (E_h) versus $\frac{1}{\sqrt{\langle r_{e^+,e^+}^2 \rangle}}$ (au^{-1}) as calculated by mcFCI for the $2e^-, 2e^+$ system.**

	Slope	Intercept	RMSE
$\langle V_{e^-,e^-} \rangle$	1.381	-7.199×10^{-4}	9.054×10^{-4}
$\langle V_{e^+,e^+} \rangle$	1.381	-7.199×10^{-4}	9.054×10^{-4}
$\langle V_{e^-,e^+} \rangle$	-5.524	2.880×10^{-3}	3.622×10^{-3}
$\langle V_{\text{total}} \rangle$	-2.762	1.440×10^{-3}	1.811×10^{-3}

Table 7.2: **Linear fits and RMSE of $\langle V_{e^-,e^-} \rangle$, $\langle V_{\text{H,H}} \rangle$, $\langle V_{e^-, \text{H}} \rangle$, and $\langle V_{\text{total}} \rangle$ (E_h) versus $\frac{1}{\sqrt{\langle r_{\text{H,H}}^2 \rangle}}$ (au^{-1}) as calculated by mcFCI for the H_2 system.**

	Slope	Intercept	RMSE
$\langle V_{e^-,e^-} \rangle$	0.398	3.795×10^{-2}	1.753×10^{-2}
$\langle V_{\text{H,H}} \rangle$	1.325	4.412×10^{-5}	1.749×10^{-5}
$\langle V_{e^-, \text{H}} \rangle$	-2.149	-0.188	8.061×10^{-2}
$\langle V_{\text{total}} \rangle$	-0.426	-0.150	6.308×10^{-2}

hydrogen-hydrogen potential was lower than the calculated value without the BO approximation.

Further investigations into parabolic confinement on this system and similar systems will help elucidate the underlying properties of these strongly confined systems. It is certainly possible that parabolic confinement is only useful for certain systems and in certain ranges.

7.A System parameters

Table 7.3: **Linear fit and RMSE of $\sqrt{\langle r_{e^-,e^-}^2 \rangle}$ (au) versus $\sqrt{\langle r_{x^+,x^+}^2 \rangle}$ (au) as calculated with mcFCL.**

	Slope	Intercept	RMSE
$2e^-, 2e^+$	1.000	0.000	0.000
H ₂	0.325	0.010	2.678×10^{-2}

Table 7.4: **Linear fit and RMSE of $\langle V_{e^-,e^-} \rangle$ (E_h) versus $\frac{1}{\sqrt{\langle r_{e^-,e^-}^2 \rangle}}$ (au⁻¹) as calculated with mcFCL.**

	Slope	Intercept	RMSE
$2e^-, 2e^+$	1.372	2.276×10^{-3}	6.358×10^{-4}
H ₂	1.361	1.041×10^{-3}	1.977×10^{-3}

Table 7.5: **External potential (k in atomic units) and Gaussian exponent parameters (α , in atomic units) for each $2e^-, 2e^+$ and H₂ calculation.**

k	$2e^-, 2e^+$		H ₂	
	α_{e^-}	α_{e^+}	α_{e^-}	α_H
0.0001	0.0050	0.0050	0.0050	0.2143
0.0010	0.0158	0.0158	0.0158	0.6775
0.0100	0.0500	0.0500	0.0500	2.1425
0.1000	0.1580	0.1580	0.1580	6.7752
0.2500	0.2500	0.2500	0.2500	10.7126
0.5000	0.3535	0.3535	0.3535	15.1499
1.0000	0.5000	0.5000	0.5000	21.4252
5.0000	1.1200	1.1200	1.1200	47.9082

Chapter 8

Conclusion

Every chemical system is a multicomponent system. Often times, it is convenient to theoretically investigate chemical systems using a single component perspective by invoking the Born-Oppenheimer approximation. The BO approximation has been, and will continue to be, one of the most important tools quantum chemistry. It's important to remember that it cannot adequately describe every system. For these cases, multicomponent methods should be used.

Accurate, efficient, and scalable treatment of multicomponent systems is of the utmost importance for multicomponent methods. While many methods already exist to theoretically study multicomponent systems, one glaring omission was a coupled-cluster approach. This thesis detailed how the foundations of single component coupled-cluster theory could be extended to treat multicomponent systems by using a multicomponent reference state and a multicomponent excitation operator. We saw that the multicomponent coupled-cluster equations were enormous in size, which highlights the need for efficient formulations and implementations of numerical solvers. The accuracy of the mcCC method was also shown using systems with exact analytical results (Hooke's atom), and by comparing results to other highly accurate

methods (multicomponent full configuration interaction and Nuclear-electron orbital configuration interaction).

The mcCC method was also used to investigate the electronic and optical properties of semiconductor quantum dots. The study spanned four dot compositions whose diameters ranged from 2nm to 20nm. Results from mcCC accurately reproduced exciton binding energies and scaling behavior which closely agrees with previous theoretical and experimental findings. Additionally, the mcCC method produced biexciton binding energies that closely agree with experiment and established a scaling trend for biexcitons that has not been previously reported.

Work has also been done to apply the mcCC method to smaller molecular systems. While preliminary results are promising, we realize that electron-hole screening is currently treated too approximately under the quasiparticle representation. Future work will build off of the early theoretical efforts reported here. Ideally, accurate treatment of electron-hole screening used with the mcCC method will produce excitation energies with accuracy competitive with established methods like equation-of-motion coupled-cluster and time dependent density functional theory.

This work also inspired curiosity about the implications of using the Born-Oppenheimer approximation. The final study investigated how a multicomponent treatment of the H_2 contrasted with the traditional BO treatment. We found that parabolic confinement of the protons and electrons produced very interesting behavior - most notably that the system will always be bound. This study was repeated for a two proton-two electron system in which we saw the same behavior. This leads to serious questions about whether parabolic confinement of multicomponent systems is appropriate for multicomponent systems, particularly those that are highly confined.

The future of applications for the mcCC method looks very bright. There is an array of potential application projects that would greatly further understanding of biexcitonic behavior in semiconductor quantum dots. Two immediate projects

that come to mind are investigating bexcitons in core-shell quantum dots, which has already been done for excitons by former group member Jen Elward [92]. Additionally, current group member Jeremy Scher has done work to investigate how quantum dot shape affects excitonic behavior. This study could be replicated for biexcitons. These are two of many possible applications for the mcCC method to quantum dot systems. Continued work on the screening for molecular systems will need further contributions. One area that the mcCC method has yet to be applied is also to investigate systems where decoupling electronic and nuclear motion is inadequate.

Bibliography

- [1] M. Born and R. Oppenheimer. Zur Quantentheorie der Molekeln. *Annalen Der Physik*, 84(20):457, 1927.
- [2] A.J. Laplante, H.D. Stidham, G.A. Guirgis, and H.W. Dukes. Vibrational spectra, ab initio calculations, and assignments of the fundamentals of the C2v conformer of n-pentane. *Journal of Molecular Structure*, 1023:170–175, 2012.
- [3] E. Kucharska, J. Michalski, W. Sasiadek, Z. Talik, I. Bryndal, and J. Hanuza. Vibrational spectra, crystal structure, DFT quantum chemical calculations and conformation of the hydrazo-bond in 6-methyl-3-nitro-2-(2-phenylhydrazinyl) pyridine. *Spectrochimica Acta - Part A: Molecular and Biomolecular Spectroscopy*, 107:317–325, 2013.
- [4] S. Li, H.-J. Zhai, L.-S. Wang, and D.A. Dixon. Structural and electronic properties of reduced transition metal oxide clusters, M4O10 and M4O10- (M = Cr, W), from photoelectron spectroscopy and quantum chemical calculations. *Journal of Physical Chemistry A*, 116(21):5256–5271, 2012.
- [5] N. Sundaraganesan, B. Anand, C. Meganathan, and B.D. Joshua. FT-IR, FT-Raman spectra and ab initio HF, DFT vibrational analysis of p-chlorobenzoic acid. *Spectrochimica Acta - Part A: Molecular and Biomolecular Spectroscopy*, 69(3):871–879, 2008.
- [6] W.B. Tzeng and K. Narayanan. Excited-state structure and vibrations of p-diaminobenzene studied by ab initio calculations. *Journal of Molecular Structure: THEOCHEM*, 434(1-3):247–253, 1998.
- [7] R.J. Bartlett. Coupled-cluster approach to molecular structure and spectra: A step toward predictive quantum chemistry. *Journal of Physical Chemistry*, 93(5):1697–1708, 1989.
- [8] T.-K. Ha and H.H. Gunthard. Quantum chemistry predicted correlations between geometric isomerism (conformation) of -OH and =NH substituents and typical group frequencies of nucleic acid bases: Cytosine. *Spectrochimica Acta - Part A Molecular and Biomolecular Spectroscopy*, 57(1):55–72, 2001.
- [9] J. Quenneville and T.J. Martinez. Ab initio study of cis-trans photoisomerization in stilbene and ethylene. *Journal of Physical Chemistry A*, 107(6):829–837, 2003.

- [10] G.A. Chasse, M.L. Mak, E. Deretey, I. Farkas, L.L. Torday, J.G. Papp, D.S.R. Sarma, A. Agarwal, S. Chakravarthi, S. Agarwal, and A.Venket Rao. An ab initio computational study on selected lycopene isomers. *Journal of Molecular Structure: THEOCHEM*, 571:27–37, 2001.
- [11] A. Del Rio, A. Boucekkine, and J. Meinnel. Reassessment of Methyl Rotation Barriers and Conformations by Correlated Quantum Chemistry Methods. *Journal of Computational Chemistry*, 24(16):2093–2100, 2003.
- [12] V.M. Petrov, G.V. Girichev, H. Oberhammer, V.N. Petrova, N.I. Giricheva, A.V. Bardina, and S.N. Ivanov. Molecular structure and conformations of para-methylbenzene sulfonamide and ortho-methylbenzene sulfonamide: Gas electron diffraction and quantum chemical calculations study. *Journal of Physical Chemistry A*, 112(13):2969–2976, 2008.
- [13] I.R. Gould, H.A.-A. Bettley, and R.A. Bryce. Correlated Ab Initio quantum chemical calculations of Di- and trisaccharide conformations. *Journal of Computational Chemistry*, 28(12):1965–1973, 2007.
- [14] S. Belaidi, Z. Almi, and D. Bouzidi. Electronic structure and physical-chemistry properties relationship for phenothiazine derivatives by quantum chemical calculations. *Journal of Computational and Theoretical Nanoscience*, 11(12):2481–2488, 2014.
- [15] C. Dahlstrand, K. Yamazaki, K. Kils, and H. Ottosson. Substituent effects on the electron affinities and ionization energies of tria-, penta-, and heptafulvenes: A computational investigation. *Journal of Organic Chemistry*, 75(23):8060–8068, 2010.
- [16] C.D. Cappa and M.J. Elrod. A computational investigation of the electron affinity of CO₃ and the thermodynamic feasibility CO₃-(H₂O)_n + ROOH reactions. *Physical Chemistry Chemical Physics*, 3(15):2986–2994, 2001.
- [17] C.A. Arrington, T.H. Dunning Jr., and D.E. Woon. Electron affinity of NO. *Journal of Physical Chemistry A*, 111(44):11185–11188, 2007.
- [18] D.A. Dixon, D. Feller, and K.A. Peterson. Accurate calculations of the electron affinity and ionization potential of the methyl radical. *Journal of Physical Chemistry A*, 101(49):9405–9409, 1997.
- [19] Y.H. Park and B.-S. Cheong. Theoretical investigation of electronic structures of the ground and excited states of pyrene and its derivatives. *Current Applied Physics*, 6(4):700–705, 2006.
- [20] A. Dreuw and M. Head-Gordon. Single-reference ab initio methods for the calculation of excited states of large molecules. *Chemical Reviews*, 105(11):4009–4037, 2005.

- [21] K. Kowalski and P. Piecuch. New coupled-cluster methods with singles, doubles, and noniterative triples for high accuracy calculations of excited electronic states. *Journal of Chemical Physics*, 120(4):1715–1738, 2004.
- [22] U. Lourderaj, M.K. Harbola, and N. Sathyamurthy. Time-dependent density functional theoretical study of low lying excited states of F 2. *Chemical Physics Letters*, 366(1-2):88–94, 2002.
- [23] Z. Yang, S. Hu, J. Cheng, J. Xu, W. Shi, B. Zhu, Y. Zhang, Z. Yao, H. Pan, and Y. Zhang. Prevalence and risk of cancer of incidental uptake in prostate identified by fluorine-18 fluorodeoxyglucose positron emission tomography/computed tomography. *Clinical Imaging*, 38(4):470–474, 2014.
- [24] X. Zhang, H. Liu, P. Balter, P.K. Allen, R. Komaki, T. Pan, H.H. Chuang, and J.Y. Chang. Positron emission tomography for assessing local failure after stereotactic body radiotherapy for non-small-cell lung cancer. *International Journal of Radiation Oncology Biology Physics*, 83(5):1558–1565, 2012.
- [25] Z. Li and P.S. Conti. Radiopharmaceutical chemistry for positron emission tomography. *Advanced Drug Delivery Reviews*, 62(11):1031–1051, 2010.
- [26] N. Avril, F. Dambha, I. Murray, J. Shamash, T. Powles, and A. Sahdev. The clinical advances of fluorine-2-D-deoxyglucose-positron emission tomography/computed tomography in urological cancers. *International Journal of Urology*, 17(6):501–511, 2010.
- [27] L. Rosso, A.D. Gee, and I.R. Gould. Ab initio computational study of positron emission tomography ligands interacting with lipid molecule for the prediction of nonspecific binding. *Journal of Computational Chemistry*, 29(14):2397–2405, 2008.
- [28] A. Uedono, H. Nakamori, K. Narita, J. Suzuki, X. Wang, S.-B. Che, Y. Ishitani, A. Yoshikawa, and S. Ishibashi. Vacancy-type defects in Mg-doped InN probed by means of positron annihilation. *Journal of Applied Physics*, 105(5), 2009.
- [29] Y.C. Wu and Y.C. Jean. Hydrogen-damaged defects near the surface in heavily deformed iron and steels investigated by slow positron annihilation spectroscopy. *Physica Status Solidi (C) Current Topics in Solid State Physics*, 4(10):3506–3509, 2007.
- [30] T. McMullen and M.J. Stott. Reemitted positron spectroscopy of near-surface defects. *Physical Review B*, 42(4):1910–1916, 1990.
- [31] A.R. Kymen, D.W. Gidley, and T.W. Capehart. Investigation of surface defects on Ni(110) with a low-energy positron beam. *Physical Review B*, 35(3):1034–1038, 1987.
- [32] A.L. Fetter and J.D. Walecka. *Quantum Theory of Many-particle Systems*. Dover Books on Physics. Dover Publications, 2003.

- [33] R. D. Mattuck. *A Guide to Feynman Diagrams in the Many-Body Problem*. Dover Publications, 1967.
- [34] J.M. Elward, F.J. Irudayanathan, S. Nangia, and A. Chakraborty. Optical signature of formation of protein corona in the firefly luciferase-CdSe quantum dot complex. *Journal of Chemical Theory and Computation*, 10(12):5224–5228, 2014.
- [35] J.M. Elward, J. Hoffman, and A. Chakraborty. Investigation of electron-hole correlation using explicitly correlated configuration interaction method. *Chemical Physics Letters*, 535:182–186, 2012.
- [36] J.M. Elward and A. Chakraborty. Effect of dot size on exciton binding energy and electron-hole recombination probability in CdSe quantum dots. *Journal of Chemical Theory and Computation*, 9(10):4351–4359, 2013.
- [37] J.M. Elward, B. Thallinger, and A. Chakraborty. Calculation of electron-hole recombination probability using explicitly correlated Hartree-Fock method. *Journal of Chemical Physics*, 136(12):124105, 2012.
- [38] M. Wimmer, S.V. Nair, and J. Shumway. Biexciton recombination rates in self-assembled quantum dots. *Physical Review B*, 73(16):165305, 2006.
- [39] J. Shumway, A. Franceschetti, and A. Zunger. Correlation versus mean-field contributions to excitons, multiexcitons, and charging energies in semiconductor quantum dots. *Physical Review B*, 63(15):1553161–15531613, 2001.
- [40] J. Shumway. Quantum Monte Carlo simulation of exciton-exciton scattering in a GaAs/AlGaAs quantum well. *Physica E (Amsterdam, Neth.)*, 32(1-2 SPEC. ISS.):273–276, 2006.
- [41] P.G. McDonald, E.J. Tyrrell, J. Shumway, J.M. Smith, and I. Galbraith. Tuning biexciton binding and antibinding in core/shell quantum dots. *Physical Review B*, 86(12):125310, 2012.
- [42] J.-W. Luo, G. Bester, and A. Zunger. Atomistic pseudopotential calculations of thickness-fluctuation GaAs quantum dots. *Physical Review B*, 79(12):125329, 2009.
- [43] A. Franceschetti and A. Zunger. Direct pseudopotential calculation of exciton Coulomb and exchange energies in semiconductor quantum dots. *Physical Review Letters*, 78(5):915–918, 1997.
- [44] A. Franceschetti, J.M. An, and A. Zunger. Impact ionization can explain carrier multiplication in PbSe quantum dots. *Nano Letters*, 6(10):2191–2195, 2006.
- [45] A. Zunger, A. Franceschetti, G. Bester, W.B. Jones, K. Kim, P.A. Graf, L.-W. Wang, A. Canning, O. Marques, C. Voemel, J. Dongarra, J. Langou, and S. Tomov. Predicting the electronic properties of 3D, million-atom semiconductor nanostructure architectures. *J. Phys: Conf. Ser.*, 46(1):040, 2006.

- [46] M. Braskén, M. Lindberg, D. Sundhölml, and J. Olsen. Full configuration interaction calculations of electron-hole correlation effects in strain-induced quantum dots. *Physical Review B*, 61:7652–7655, Mar 2000.
- [47] G.J. Choi and R.R. Knowles. Catalytic Alkene Carboaminations Enabled by Oxidative Proton-Coupled Electron Transfer. *Journal of the American Chemical Society*, 137(29):9226–9229, 2015.
- [48] S. Hammes-Schiffer. Proton-Coupled Electron Transfer: Moving Together and Charging Forward. *Journal of the American Chemical Society*, 137(28):8860–8871, 2015.
- [49] D.R. Weinberg, C.J. Gagliardi, J.F. Hull, C.F. Murphy, C.A. Kent, B.C. Westlake, A. Paul, D.H. Ess, D.G. McCafferty, and T.J. Meyer. Proton-coupled electron transfer. *Chemical Reviews*, 112(7):4016–4093, 2012.
- [50] T. Honda, T. Kojima, and S. Fukuzumi. Proton-coupled electron-transfer reduction of dioxygen catalyzed by a saddle-distorted cobalt phthalocyanine. *Journal of the American Chemical Society*, 134(9):4196–4206, 2012.
- [51] V.R.I. Kaila and G. Hummer. Energetics of direct and water-mediated proton-coupled electron transfer. *Journal of the American Chemical Society*, 133(47):19040–19043, 2011.
- [52] K. Swarnalatha, E. Rajkumar, S. Rajagopal, R. Ramaraj, I.S. Banu, and P. Ramamurthy. Proton coupled electron transfer reaction of phenols with excited state ruthenium(II) - Polypyridyl complexes. *Journal of Physical Organic Chemistry*, 24(1):14–21, 2011.
- [53] L. Evangelisti, P. Cija, E.J. Cocinero, F. Castao, A. Lesarri, W. Caminati, and R. Meyer. Proton tunneling in heterodimers of carboxylic acids: A rotational study of the benzoic acid-formic acid bimolecule. *Journal of Physical Chemistry Letters*, 3(24):3770–3775, 2012.
- [54] C. Drechsel-Grau and D. Marx. Quantum simulation of collective proton tunneling in hexagonal ice crystals. *Physical Review Letters*, 112(14), 2014.
- [55] R.a Marom, C.a Levi, T.a Weiss, S.a Rosenwaks, Y.b c Zeiri, R.d Kosloff, and I.a Bar. Quantum tunneling of hydrogen atom in dissociation of photoexcited methylamine. *Journal of Physical Chemistry A*, 114(36):9623–9627, 2010.
- [56] L.a b f Masgrau, A.a c Roujeinikova, L.O.a b Johannissen, P.a c Hothi, J.d Basran, K.E.e Ranaghan, A.J.e Mulholland, M.J.a b Sutcliffe, N.S.a c Scrutton, and D.a c Leys. Atomic description of an enzyme reaction dominated by proton tunneling. *Science*, 312(5771):237–241, 2006.
- [57] Y. Cha, C.J. Murray, and J.P. Klinman. Hydrogen tunneling in enzyme reactions. *Science*, 243(4896):1325–1330, 1989.

- [58] A. Szabo and N.S. Ostlund. *Modern Quantum Chemistry: Introduction to Advanced Electronic Structure Theory*. Dover Books on Chemistry Series. Dover Publications, 1996.
- [59] T. Helgaker, P. Jørgensen, and J. Olsen. *Molecular electronic-structure theory*. Wiley, 2000.
- [60] I. Shavitt and R.J. Bartlett. *Many-Body Methods in Chemistry and Physics: MBPT and Coupled-Cluster Theory*. Cambridge Molecular Science. Cambridge University Press, 2009.
- [61] T. Daniel Crawford and Henry F. Schaefer. *An Introduction to Coupled Cluster Theory for Computational Chemists*, pages 33–136. John Wiley & Sons, Inc., 2007.
- [62] G.H. Booth, A.J.W. Thom, and A. Alavi. Fermion monte carlo without fixed nodes: A game of life, death, and annihilation in Slater determinant space. *Journal of Chemical Physics*, 131(5), 2009.
- [63] D. Cleland, G.H. Booth, and A. Alavi. Communications: Survival of the fittest: Accelerating convergence in full configuration-interaction quantum Monte Carlo. *Journal of Chemical Physics*, 132(4), 2010.
- [64] G.H. Booth and A. Alavi. Approaching chemical accuracy using full configuration-interaction quantum Monte Carlo: A study of ionization potentials. *Journal of Chemical Physics*, 132(17), 2010.
- [65] F.R. Petruzielo, A.A. Holmes, H.J. Changlani, M.P. Nightingale, and C.J. Umrigar. Semistochastic projector monte carlo method. *Physical Review Letters*, 109(23), 2012.
- [66] S.A. Kucharski and R.J. Bartlett. Coupled-cluster methods that include connected quadruple excitations, T4: CCSDTQ-1 and Q(CCSDT). *Chemical Physics Letters*, 158(6):550–555, 1989. cited By 90.
- [67] S.A. Kucharski and R.J. Bartlett. The coupled-cluster single, double, triple, and quadruple excitation method. *The Journal of Chemical Physics*, 97(6):4282–4288, 1992.
- [68] S.P. Webb, T. Iordanov, and S. Hammes-Schiffer. Multiconfigurational nuclear-electronic orbital approach: Incorporation of nuclear quantum effects in electronic structure calculations. *Journal of Chemical Physics*, 117(9):4106–4118, 2002.
- [69] D. Sundholm and T. Vänskä. Computational methods for studies of semiconductor quantum dots and rings. *Annu. Rep. Prog. Chem. Sect. C: Phys. Chem.*, 108:96–125, 2012.

- [70] T. Vänskä, M. Lindberg, J. Olsen, and D. Sundholm. Computational methods for studies of multiexciton complexes. *Physica Status Solidi B Basic Solid State Physics*, 243(15):4035–4045, 2006.
- [71] A. Sirjoosingh, M.V. Pak, C. Swalina, and S. Hammes-Schiffer. Reduced explicitly correlated Hartree-Fock approach within the nuclear-electronic orbital framework: Theoretical formulation. *Journal of Chemical Physics*, 139(3):034102, 2013.
- [72] Bruce S Hudson and Suzanne K Chafetz. Zero-Point Corrections for Isotropic Coupling Constants for Cyclohexadienyl Radical, C₆H₇ and C₆H₆Mu: Beyond the Bond Length Change Approximation. *Molecules*, 18(5):4906–4916, 2013.
- [73] Louis E Brus. Electron–electron and electron-hole interactions in small semiconductor crystallites: The size dependence of the lowest excited electronic state. *Journal of Chemical Physics*, 80(9):4403–4409, 1984.
- [74] Mauricio Cafiero, Sergiy Bubin, and Ludwik Adamowicz. Non-Born-Oppenheimer calculations of atoms and molecules. *Physical Chemistry Chemical Physics*, 5:1491–1501, 2003.
- [75] T. Kreibich and E.K.U. Gross. Multicomponent density-functional theory for electrons and nuclei. *Physical Review Letters*, 86(14):2984–2987, 2001.
- [76] T. Ishimoto, M. Tachikawa, and U. Nagashima. Electron-electron and electron-nucleus correlation effects on exponent values of Gaussian-type functions for quantum protons and deuterons. *Journal of Chemical Physics*, 125(14):144103, October 2006.
- [77] T. Iordanov and S. Hammes-Schiffer. Vibrational analysis for the nuclear-electronic orbital method. *Journal of Chemical Physics*, 118(21):9489–9496, 2003.
- [78] A. Chakraborty, M.V. Pak, and S. Hammes-Schiffer. Development of electron-proton density functionals for multicomponent density functional theory. *Physical Review Letters*, 101(15):153001, 2008.
- [79] I. Kylänpää, T.T. Rantala, and D.M. Ceperley. Few-body reference data for multicomponent formalisms: Light-nuclei molecules. *Physical Review A*, 86(5):052506, 2012.
- [80] T. Udagawa, T. Tsuneda, and M. Tachikawa. Electron-nucleus correlation functional for multicomponent density-functional theory. *Physical Review A*, 89(5):052519, 2014.
- [81] J.E. Subotnik, E.C. Alguire, Q. Ou, B.R. Landry, and S. Fatehi. The requisite electronic structure theory to describe photoexcited nonadiabatic dynamics: Nonadiabatic derivative couplings and diabatic electronic couplings. *Accounts of Chemical Research*, 48(5):1340–1350, 2015.

- [82] D.J. Trivedi and O.V. Prezhdo. Decoherence Allows Model Reduction in Nonadiabatic Dynamics Simulations. *The Journal of Physical Chemistry A*, 119(33):8846–8853, 2015.
- [83] Alexander J White, Vyacheslav N Gorshkov, Sergei Tretiak, and Dmitry Mozyrsky. Non-adiabatic molecular dynamics by accelerated semiclassical Monte Carlo. *Journal of Chemical Physics*, 143(1):014115, 2015.
- [84] A. Marciniak, V. Despré, T. Barillot, A. Rouzée, M.C.E. Galbraith, J. Klei, C.-H. Yang, C.T.L. Smeenk, V. Loriot, S.N. Reddy, A.G.G.M. Tielens, S. Mahapatra, A.I. Kuleff, M.J.J. Vrakking, and F. Lépine. XUV excitation followed by ultrafast non-adiabatic relaxation in PAH molecules as a femto-astrochemistry experiment. *Nature Communications*, 6:7909, 2015.
- [85] Rami Gherib, Ilya G Ryabinkin, and Artur F Izmaylov. Why do mixed quantum-classical methods describe short-time dynamics through conical intersections so well? Analysis of geometric phase effects. *Journal of Chemical Theory and Computation*, 11(4):1375–1382, 2015.
- [86] Sharon Hammes-Schiffer. Proton-Coupled Electron Transfer: Moving Together and Charging Forward. *Journal of the American Chemical Society*, 137(28):8860–8871, 2015.
- [87] Y. Oba and M. Tachikawa. Theoretical investigation of a positron binding to an aspartame molecule using the ab initio multicomponent molecular orbital approach. *International Journal of Quantum Chemistry*, 114(17):1146–1149, 2014.
- [88] R. Sabry, W.M. Moslem, E.F. El-Shamy, and P.K. Shukla. Three-dimensional nonlinear Schrödinger equation in electron-positron-ion magnetoplasmas. *Physics of Plasmas*, 18(3):032302, 2011.
- [89] M. Tachikawa, H. Sainowo, K. Iguchi, and K. Suzuki. Ab initio calculation of $[\text{OH}^-; e^+]$ system with consideration of electron correlation effect. *Journal of Chemical Physics*, 101(7):5925–5928, 1994.
- [90] M. Tachikawa, Y. Kita, and R.J. Buenker. Bound states of the positron with nitrile species with a configuration interaction multi-component molecular orbital approach. *Physical Chemistry Chemical Physics*, 13(7):2701–2705, 2011.
- [91] S. Corni, M. Braskén, M. Lindberg, J. Olsen, and D. Sundholm. Stabilization energies of charged multiexciton complexes calculated at configuration interaction level. *Physica E*, 18(4):436–442, 2003.
- [92] J.M. Elward and A. Chakraborty. Effect of heterojunction on exciton binding energy and electron-hole recombination probability in CdSe/ZnS quantum dots. *Journal of Chemical Theory and Computation*, 11(2):462–471, 2015.

- [93] G.A. Narvaez, G. Bester, and A. Zunger. Pressure effects on neutral and charged excitons in self-assembled (In,Ga)As GaAs quantum dots. *Physical Review B*, 72(4):041307, 2005.
- [94] A. Franceschetti, H. Fu, L. W. Wang, and A. Zunger. Many-body pseudopotential theory of excitons in InP and CdSe quantum dots. *Physical Review B*, 60:1819–1829, 1999.
- [95] Lin-Wang Wang, Marco Califano, Alex Zunger, and Alberto Franceschetti. Pseudopotential Theory of Auger Processes in CdSe Quantum Dots. *Physical Review Letters*, 91:056404, Jul 2003.
- [96] C. Ko, M.V. Pak, C. Swalina, and S. Hammes-Schiffer. Alternative wavefunction ansatz for including explicit electron-proton correlation in the nuclear-electronic orbital approach. *Journal of Chemical Physics*, 135(5):054106, 2011.
- [97] A. Sirjoosingh, M.V. Pak, and S. Hammes-Schiffer. Multicomponent density functional theory study of the interplay between electron-electron and electron-proton correlation. *Journal of Chemical Physics*, 136(17):174114, 2012.
- [98] C. Swalina, M.V. Pak, and S. Hammes-Schiffer. Analysis of electron-positron wavefunctions in the nuclear-electronic orbital framework. *Journal of Chemical Physics*, 136(16):164105, 2012.
- [99] N.M. Tubman, I. Kylänpää, S. Hammes-Schiffer, and D.M. Ceperley. Beyond the Born-Oppenheimer approximation with quantum Monte Carlo methods. *Physical Review A*, 90(4):042507, 2014.
- [100] K.R. Brorsen, A. Sirjoosingh, M.V. Pak, and S. Hammes-Schiffer. Nuclear-electronic orbital reduced explicitly correlated Hartree-Fock approach: Restricted basis sets and open-shell systems. *Journal of Chemical Physics*, 142(21):214108, 2015.
- [101] A. Sirjoosingh, M.V. Pak, K.R. Brorsen, and S. Hammes-Schiffer. Quantum treatment of protons with the reduced explicitly correlated Hartree-Fock approach. *Journal of Chemical Physics*, 142(21):214107, 2015.
- [102] T. Ishimoto, M. Tachikawa, and U. Nagashima. Review of multicomponent molecular orbital method for direct treatment of nuclear quantum effect. *International Journal of Quantum Chemistry*, 109(12):2677–2694, 2009.
- [103] A. Abedi, N.T. Maitra, and E.K.U. Gross. Exact factorization of the time-dependent electron-nuclear wave function. *Physical Review Letters*, 105(12):123002, 2010.
- [104] A. Abedi, N.T. Maitra, and E.K.U. Gross. Correlated electron-nuclear dynamics: Exact factorization of the molecular wavefunction. *Journal of Chemical Physics*, 137(22):22A530, 2012.

- [105] F. Agostini, A. Abedi, Y. Suzuki, and E.K.U. Gross. Mixed quantum-classical dynamics on the exact time-dependent potential energy surface: A fresh look at non-adiabatic processes. *Molecular Physics*, 111(22-23):3625–3640, 2013.
- [106] A. Abedi, F. Agostini, Y. Suzuki, and E.K.U. Gross. Dynamical steps that bridge piecewise adiabatic shapes in the exact time-dependent potential energy surface. *Physical Review Letters*, 110(26):263001, 2013.
- [107] G. Albareda, H. Appel, I. Franco, A. Abedi, and A. Rubio. Correlated electron-nuclear dynamics with conditional wave functions. *Physical Review Letters*, 113(8):083003, 2014.
- [108] Y. Suzuki, A. Abedi, N.T. Maitra, K. Yamashita, and E.K.U. Gross. Electronic Schrödinger equation with nonclassical nuclei. *Physical Review A*, 89(4):040501, 2014.
- [109] A. Abedi, F. Agostini, and E.K.U. Gross. Mixed quantum-classical dynamics from the exact decomposition of electron-nuclear motion. *Europhysics Letters*, 106(3):33001, 2014.
- [110] Y.-C. Chiang, S. Klaiman, F. Otto, and L.S. Cederbaum. The exact wavefunction factorization of a vibronic coupling system. *Journal of Chemical Physics*, 140(5):054104, 2014.
- [111] L.S. Cederbaum. The exact wavefunction of interacting N degrees of freedom as a product of N single-degree-of-freedom wavefunctions. *Chemical Physics*, 457:129–132, 2015.
- [112] H. Feng, K.R. Randall, and III Schaefer, H.F. Reaction of a fluorine atom with methanol: Potential energy surface considerations. *The Journal of Physical Chemistry A*, 119(9):1636–1641, 2015.
- [113] W. Klopper, R.A. Bachorz, D.P. Tew, J. Aguilera-Iparraguirre, Y. Carissan, and C. Hättig. Accurate coupled cluster calculations of the reaction barrier heights of two $\text{CH}_3\cdot + \text{CH}_4$ reactions. *The Journal of Physical Chemistry A*, 113(43):11679–11684, 2009.
- [114] J.W. Krogh and J. Olsen. A general coupled cluster study of the N_2 molecule. *Chemical Physics Letters*, 344(5-6):578–586, 2001.
- [115] W.D. Laidig, P. Saxe, and R.J. Bartlett. The description of N_2 and F_2 potential energy surfaces using multireference coupled cluster theory. *Journal of Chemical Physics*, 86(2):887–907, 1986.
- [116] U.S. Mahapatra and S. Chattopadhyay. Potential energy surface studies via a single root multireference coupled cluster theory. *Journal of Chemical Physics*, 133(7):074102, 2010.

- [117] E. Miliordos, E. Apra, and S.S. Xantheas. Benchmark theoretical study of the π - π binding energy in the benzene dimer. *The Journal of Physical Chemistry A*, 118(35):7568–7578, 2014.
- [118] Kirk A. Peterson and Thom H. Dunning. Intrinsic Errors in Several ab Initio Methods: The Dissociation Energy of N_2 . *Journal of Physical Chemistry*, 99(12):3898–3901, 1995.
- [119] S. Samdal, H. Mollendal, and J.-C. Guillemin. Conformational properties of cis - And trans - N -cyclopropylformamide studied by microwave spectroscopy and quantum chemical calculations. *The Journal of Physical Chemistry A*, 119(14):3375–3383, 2015.
- [120] A. Dutta and C.D. Sherrill. Full configuration interaction potential energy curves for breaking bonds to hydrogen: An assessment of single-reference correlation methods. *Journal of Chemical Physics*, 118(4):1610–1619, 2003.
- [121] G. Czako, I. Szabo, and H. Telekes. On the choice of the ab initio level of theory for potential energy surface developments. *The Journal of Physical Chemistry A*, 118(3):646–654, 2014.
- [122] S. Hirata, M. Nooijen, I. Grabowski, and R.J. Bartlett. Perturbative corrections to coupled-cluster and equation-of-motion coupled-cluster energies: A determinantal analysis. *Journal of Chemical Physics*, 114(9):3919–3928, 2001.
- [123] X. Li and J. Paldus. A multireference coupled-cluster study of electronic excitations in furan and pyrrole. *The Journal of Physical Chemistry A*, 114(33):8591–8600, 2010.
- [124] Z. Liu, O. Demel, and M. Nooijen. Multireference Equation of Motion Coupled Cluster study of atomic excitation spectra of first-row transition metal atoms Cr, Mn, Fe and Co. *Journal of Molecular Spectroscopy*, 311:54–63, 2015.
- [125] J. Sous, P. Goel, and M. Nooijen. Similarity transformed equation of motion coupled cluster theory revisited: A benchmark study of valence excited states. *Molecular Physics*, 112(5-6):616–638, 2014.
- [126] J.F. Stanton and R.J. Bartlett. The equation of motion coupled-cluster method. A systematic biorthogonal approach to molecular excitation energies, transition probabilities, and excited state properties. *Journal of Chemical Physics*, 98(9):7029–7039, 1993.
- [127] Hendrik J Monkhorst. Chemical physics without the Born-Oppenheimer approximation: The molecular coupled-cluster method. *Physical Review A*, 36(4):1544, 1987.
- [128] R.J. Bartlett and M. Musiał. Coupled-cluster theory in quantum chemistry. *Reviews of Modern Physics*, 79(1):291–352, 2007.

- [129] G.D. Purvis III and R.J. Bartlett. A full coupled-cluster singles and doubles model: The inclusion of disconnected triples. *Journal of Chemical Physics*, 76(4):1910–1918, 1982.
- [130] G.E. Scuseria, C.L. Janssen, and H.F. Schaefer III. An efficient reformulation of the closed-shell coupled cluster single and double excitation (CCSD) equations. *Journal of Chemical Physics*, 89(12):7382–7387, 1988.
- [131] T. Shiozaki, E.F. Valeev, and S. Hirata. Explicitly correlated combined coupled-cluster and perturbation methods. *Journal of Chemical Physics*, 131(4):044118, 2009.
- [132] T. Van Voorhis and M. Head-Gordon. Benchmark variational coupled cluster doubles results. *Journal of Chemical Physics*, 113(20):8873–8879, 2000.
- [133] S.A. Fischer and O.V. Prezhdo. Dopant effects on single and multiple excitons in small Si clusters: High-level Ab initio calculations. *Journal of Physical Chemistry C*, 115(20):10006–10011, 2011.
- [134] E. Rabani and R. Baer. Theory of multiexciton generation in semiconductor nanocrystals. *Chemical Physics Letters*, 496(4-6):227–235, 2010.
- [135] A. Franceschetti and Y. Zhang. Multiexciton absorption and multiple exciton generation in CdSe quantum dots. *Physical Review Letters*, 100(13):136805, 2008.
- [136] T.M. Henderson, G.E. Scuseria, J. Dukelsky, A. Signoracci, and T. Duguet. Quasiparticle coupled cluster theory for pairing interactions. *Physical Review C*, 89(5):054305, 2014.
- [137] C. J. Blanton, C. Brenon, and A. Chakraborty. Development of polaron-transformed explicitly correlated full configuration interaction method for investigation of quantum-confined Stark effect in GaAs quantum dots. *Journal of Chemical Physics*, 138(5):054114, 2013.
- [138] T. Ishimoto, M. Tachikawa, and U. Nagashima. Simultaneous analytical optimization of variational parameters in Gaussian-type functions with full configuration interaction of multicomponent molecular orbital method by elimination of translational and rotational motions: Application to isotopomers of the hydrogen molecule. *Journal of Chemical Physics*, 128(16):164118, 2008.
- [139] D.I. Lyakh, V.V. Ivanov, and L. Adamowicz. Automated generation of coupled-cluster diagrams: Implementation in the multireference state-specific coupled-cluster approach with the complete-active-space reference. *Journal of Chemical Physics*, 122(2):024108, 2005.
- [140] C.L. Janssen and H.F. Schaefer III. The automated solution of second quantization equations with applications to the coupled cluster approach. *Theoretica Chimica Acta*, 79(1):1–42, 1991.

- [141] P. Piecuch, S. Hirata, K. Kowalski, P.-D. Fan, and T.L. Windus. Automated derivation and parallel computer implementation of renormalized and active-space coupled-cluster methods. *International Journal of Quantum Chemistry*, 106(1):79–97, 2006.
- [142] P. Piecuch, S.A. Kucharski, K. Kowalski, and M. Musiał. Efficient computer implementation of the renormalized coupled-cluster methods: The R-CCSD[T], R-CCSD(T), CR-CCSD[T], and CR-CCSD(T) approaches. *Computer Physics Communications*, 149(2):71–96, 2002.
- [143] X. Li and J. Paldus. Automation of the implementation of spin-adapted open-shell coupled-cluster theories relying on the unitary group formalism. *Journal of Chemical Physics*, 101(10):8812–8826, 1994.
- [144] F.E. Harris. Computer Generation of Coupled-Cluster Equations. *International Journal of Quantum Chemistry*, 75(4-5):593–597, 1999.
- [145] M. Nooijen and V. Lotrich. Brueckner based generalized coupled cluster theory: Implicit inclusion of higher excitation effects. *Journal of Chemical Physics*, 113(11):4549–4557, 2000.
- [146] M. Nooijen and V. Lotrich. Extended similarity transformed equation-of-motion coupled cluster theory (extended-STEOM-CC): applications to doubly excited states and transition metal compounds. *Journal of Chemical Physics*, 113(2):494–507, 2000.
- [147] M. Head-Gordon, P.E. Maslen, and C.A. White. A tensor formulation of many-electron theory in a nonorthogonal single-particle basis. *Journal of Chemical Physics*, 108(2):616–625, 1998.
- [148] A.A. Auer, G. Baumgartner, D.E. Bernholdt, A. Bibireata, V. Choppella, D. Cociorva, X. Gao, R. Harrison, S. Krishnamoorthy, S. Krishnan, C.-C. Lam, Q. Lu, M. Nooijen, R. Pitzer, J. Ramanujam, P. Sadayappan, and A. Sibiriyakov. Automatic code generation for many-body electronic structure methods: The tensor contraction engine. *Molecular Physics*, 104(2):211–228, 2006.
- [149] Q. Lu, X. Gao, S. Krishnamoorthy, G. Baumgartner, J. Ramanujam, and P. Sadayappan. Empirical performance model-driven data layout optimization and library call selection for tensor contraction expressions. *Journal of Parallel and Distributed Computing*, 72(3):338–352, 2012.
- [150] A. Hartono, Q. Lu, T. Henretty, S. Krishnamoorthy, H. Zhang, G. Baumgartner, D.E. Bernholdt, M. Nooijen, R. Pitzer, J. Ramanujam, and P. Sadayappan. Performance optimization of tensor contraction expressions for many-body methods in quantum chemistry. *The Journal of Physical Chemistry A*, 113(45):12715–12723, 2009.

- [151] S. Hirata. Tensor contraction engine: Abstraction and automated parallel implementation of configuration-interaction, coupled-cluster, and many-body perturbation theories. *The Journal of Physical Chemistry A*, 107(46):9887–9897, 2003.
- [152] E. Matito, J. Cioslowski, and S.F. Vyboishchikov. Properties of harmonium atoms from FCI calculations: Calibration and benchmarks for the ground state of the two-electron species. *Physical Chemistry Chemical Physics*, 12(25):6712–6716, 2010.
- [153] J. Karwowski. Influence of confinement on the properties of quantum systems. *Journal of Molecular Structure-THEOCHEM*, 727(1–3):1 – 7, 2005.
- [154] Jacek Karwowski. Inverse problems in quantum chemistry. *International Journal of Quantum Chemistry*, 109(11):2456–2463, 2009.
- [155] P.E. Adamson, X.F. Duan, L.W. Burggraf, M.V. Pak, C. Swalina, and S. Hammes-Schiffer. Modeling positrons in molecular electronic structure calculations with the nuclear-electronic orbital method. *The Journal of Physical Chemistry A*, 112(6):1346–1351, 2008.
- [156] M. Tachikawa. Simultaneous optimization of Gaussian type function exponents for electron and positron with full-CI wavefunction - Application to ground and excited states of positronic compounds with multi-component molecular orbital approach. *Chemical Physics Letters*, 350(3-4):269–276, 2001.
- [157] J Mitroy and G G Ryzhikh. Measuring the positron affinities of atoms. *J. Phys. B*, 32(15):L411, 1999.
- [158] V. Halonen, T. Chakraborty, and P. Pietiläinen. Excitons in a parabolic quantum dot in magnetic fields. *Physical Review B*, 45(11):5980–5985, 1992.
- [159] Mohammad El-Said. Ground-state energy of an exciton in a parabolic quantum dot. *Semiconductor Science and Technology*, 9(3):272–274, 1994.
- [160] S. Jaziri and R. Bennaceur. Excitons in parabolic quantum dots in electric and magnetic fields. *Semiconductor Science and Technology*, 9(10):1775–1780, 1994.
- [161] G. Lamouche and G. Fishman. Two interacting electrons in a three-dimensional parabolic quantum dot: A simple solution. *Journal of Physics: Condensed Matter*, 10(35):7857–7867, 1998.
- [162] W. Xie and J. Gu. Exciton bound to a neutral donor in parabolic quantum dots. *Physics Letters A*, 312(5-6):385–390, 2003.
- [163] W. Xie. Exciton states trapped by a parabolic quantum dot. *Phys. B (Amsterdam, Neth.)*, 358(1-4):109–113, 2005.

- [164] W. Xie. Effect of an electric field and nonlinear optical rectification of confined excitons in quantum dots. *Physica Status Solidi B Basic Solid State Physics*, 246(10):2257–2262, 2009.
- [165] M.J. Karimi and G. Rezaei. Effects of external electric and magnetic fields on the linear and nonlinear intersubband optical properties of finite semi-parabolic quantum dots. *Phys. B (Amsterdam, Neth.)*, 406(23):4423 – 4428, 2011.
- [166] F.S. Nammias, A.S. Sandouqa, H.B. Ghassib, and M.K. Al-Sugheir. Thermodynamic properties of two-dimensional few-electrons quantum dot using the static fluctuation approximation (SFA). *Physica B*, 406(24):4671 – 4677, 2011.
- [167] G. Rezaei, B. Vaseghi, and M. Sadri. External electric field effect on the optical rectification coefficient of an exciton in a spherical parabolic quantum dot. *Phys. B (Amsterdam, Neth.)*, 406(24):4596 – 4599, 2011.
- [168] Brian T Sutcliffe and R Guy Woolley. On the quantum theory of molecules. *Journal of Chemical Physics*, 137(22):22A544, 2012.
- [169] S.-W. Baek, J.-H. Shim, H.-M. Seung, G.-S. Lee, J.-P. Hong, K.-S. Lee, and J.-G. Park. Effect of core quantum-dot size on power-conversion-efficiency for silicon solar-cells implementing energy-down-shift using CdSe/ZnS core/shell quantum dots. *Nanoscale*, 6(21):12524–12531, 2014.
- [170] A. Salant, M. Shalom, Z. Tachan, S. Buhbut, A. Zaban, and U. Banin. Quantum rod-sensitized solar cell: Nanocrystal shape effect on the photovoltaic properties. *Nano Letters*, 12(4):2095–2100, 2012.
- [171] O.E. Semonin, J.M. Luther, S. Choi, H.-Y. Chen, J. Gao, A.J. Nozik, and M.C. Beard. Peak external photocurrent quantum efficiency exceeding 100% via MEG in a quantum dot solar cell. *Science*, 334(6062):1530–1533, 2011.
- [172] D.D. Wanger, R.E. Correa, E.A. Dauler, and M.G. Bawendi. The dominant role of exciton quenching in PbS quantum-dot-based photovoltaic devices. *Nano Letters*, 13(12):5907–5912, 2013.
- [173] P.O. Anikeeva, J.E. Halpert, M.G. Bawendi, and V. Bulović. Quantum dot light-emitting devices with electroluminescence tunable over the entire visible spectrum. *Nano Letters*, 9(7):2532–2536, 2009.
- [174] W. Ji, P. Jing, W. Xu, X. Yuan, Y. Wang, J. Zhao, and A.K.-Y. Jen. High color purity ZnSe/ZnS core/shell quantum dot based blue light emitting diodes with an inverted device structure. *Applied Physics Letters*, 103(5), 2013.
- [175] G.J. Supran, K.W. Song, G.W. Hwang, R.E. Correa, J. Scherer, E.A. Dauler, Y. Shirasaki, M.G. Bawendi, and V. Bulović. High-performance shortwave-infrared light-emitting devices using core-shell (PbS-CdS) colloidal quantum dots. *Advanced Materials*, 27(8):1437–1442, 2015.

- [176] D.R. Baker and P.V. Kamat. Tuning the emission of CdSe quantum dots by controlled trap enhancement. *Langmuir*, 26(13):11272–11276, 2010.
- [177] L.Y.T. Chou, H.C. Fischer, S.D. Perrault, and W.C.W. Chan. Visualizing quantum dots in biological samples using silver staining. *Analytical Chemistry*, 81(11):4560–4565, 2009.
- [178] L. Liu, S. Jin, Y. Hu, Z. Gu, and H.-C. Wu. Application of quantum dots in biological imaging. *Journal of Nanomaterials*, 2011, 2011.
- [179] J. Su, J. Zhang, L. Liu, Y. Huang, and R.P. Mason. Exploring feasibility of multicolored CdTe quantum dots for in Vitro and in Vivo fluorescent imaging. *Journal of Nanoscience and Nanotechnology*, 8(3):1174–1177, 2008.
- [180] M. Vibin, R. Vinayakan, A. John, V. Raji, C.S. Rejiya, and A. Abraham. Fluorescence imaging of stem cells, cancer cells and semi-thin sections of tissues using silica-coated CdSe quantum dots. *Journal of Fluorescence*, 21(4):1365–1370, 2011.
- [181] C. Wu, B. Bull, C. Szymanski, K. Christensen, and J. McNeill. Multicolor conjugated polymer dots for biological fluorescence imaging. *ACS Nano*, 2(11):2415–2423, 2008.
- [182] X. Chen, Y. Tang, B. Cai, and H. Fan. 'One-pot' synthesis of multifunctional GSH-CdTe quantum dots for targeted drug delivery. *Nanotechnology*, 25(23), 2014.
- [183] F. Ye, T. Barrefelt, H. Asem, M. Abedi-Valugerdi, I. El-Serafi, M. Saghafian, K. Abu-Salah, S. Alrokayan, M. Muhammed, and M. Hassan. Biodegradable polymeric vesicles containing magnetic nanoparticles, quantum dots and anti-cancer drugs for drug delivery and imaging. *Biomaterials*, 35(12):3885–3894, 2014.
- [184] N. Li, H. Li, D. Chen, H. Liu, F. Tang, Y. Zhang, J. Ren, and Y. Li. Preparation and characterization of quantum dots coated magnetic hollow spheres for magnetic fluorescent multimodal imaging and drug delivery. *Journal of Nanoscience and Nanotechnology*, 9(4):2540–2545, 2009.
- [185] T.P. Osedach, S.M. Geyer, J.C. Ho, A.C. Arango, M.G. Bawendi, and V. Bulović. Lateral heterojunction photodetector consisting of molecular organic and colloidal quantum dot thin films. *Applied Physics Letters*, 94(4), 2009.
- [186] G. Zhai, C.P. Church, A.J. Breeze, D. Zhang, G.B. Alers, and S.A. Carter. Quantum dot PbS 0.9Se 0.1/TiO₂ heterojunction solar cells. *Nanotechnology*, 23(40), 2012.

- [187] J.T. Stewart, L.A. Padilha, W.K. Bae, W.-K. Koh, J.M. Pietryga, and V.I. Klimov. Carrier multiplication in quantum dots within the framework of two competing energy relaxation mechanisms. *Journal of Physical Chemistry Letters*, 4(12):2061–2068, 2013.
- [188] C.-H.M. Chuang, P.R. Brown, V. Bulović, and M.G. Bawendi. Improved performance and stability in quantum dot solar cells through band alignment engineering. *Nature Materials*, 13(8):796–801, 2014.
- [189] C.J. Stolle, T.B. Harvey, D.R. Pernik, J.I. Hibbert, J. Du, D.J. Rhee, V.A. Akhavan, R.D. Schaller, and B.A. Korgel. Multiexciton solar cells of CuInSe₂ nanocrystals. *Journal of Physical Chemistry Letters*, 5(2):304–309, 2014.
- [190] N.J.L.K. Davis, M.L. Böhm, M. Tabachnyk, F. Wisnivesky-Rocca-Rivarola, T.C. Jellicoe, C. Ducati, B. Ehrler, and N.C. Greenham. Multiple-exciton generation in lead selenide nanorod solar cells with external quantum efficiencies exceeding 120%. *Nature Communications*, 6, 2015.
- [191] M.L. Böhm, T.C. Jellicoe, M. Tabachnyk, N.J.L.K. Davis, F. Wisnivesky-Rocca-Rivarola, C. Ducati, B. Ehrler, A.A. Bakulin, and N.C. Greenham. Lead telluride quantum dot solar cells displaying external quantum efficiencies exceeding 120%. *Nano Letters*, 15(12):7987–7993, 2015.
- [192] Benjamin H. Ellis, Somil Aggarwal, and Arindam Chakraborty. Development of the Multicomponent Coupled-Cluster Theory for Investigation of Multiexcitonic Interactions. *Journal of Chemical Theory and Computation*, 12(1):188–200, 2016.
- [193] P. Michler. *Single Quantum Dots: Fundamentals, Applications and New Concepts*. Physics and Astronomy Online Library. Springer, 2003.
- [194] S. Glutsch. *Excitons in Low-Dimensional Semiconductors: Theory Numerical Methods Applications*. Springer Series in Solid-State Sciences. Springer Berlin Heidelberg, 2013.
- [195] H. Haug and S.W. Koch. *Quantum Theory of the Optical and Electronic Properties of Semiconductors*. World Scientific, 2009.
- [196] F. Bechstedt. *Many-Body Approach to Electronic Excitations: Concepts and Applications*. Springer Series in Solid-State Sciences. Springer Berlin Heidelberg, 2014.
- [197] U. Woggon. *Optical Properties of Semiconductor Quantum Dots*. Springer Tracts in Modern Physics. Springer Berlin Heidelberg, 2014.
- [198] S.N. Inamdar, P.P. Ingole, and S.K. Haram. Determination of band structure parameters and the quasi-particle gap of CdSe quantum dots by cyclic voltammetry. *ChemPhysChem*, 9(17):2574–2579, 2008.

- [199] L.-W. Wang and A. Zunger. Pseudopotential calculations of nanoscale CdSe quantum dots. *Physical Review B - Condensed Matter and Materials Physics*, 53(15):9579–9582, 1996.
- [200] C. Querner, P. Reiss, S. Sadki, M. Zagorska, and A. Pron. Size and ligand effects on the electrochemical and spectroelectrochemical responses of CdSe nanocrystals. *Physical Chemistry Chemical Physics*, 7(17):3204–3209, 2005.
- [201] J. Jasieniak, M. Califano, and S.E. Watkins. Size-dependent valence and conduction band-edge energies of semiconductor nanocrystals. *ACS Nano*, 5(7):5888–5902, 2011.
- [202] E. Kucur, J. Riegler, G.A. Urban, and T. Nann. Determination of quantum confinement in CdSe nanocrystals by cyclic voltammetry. *Journal of Chemical Physics*, 119(4):2333–2337, 2003.
- [203] R.W. Meulenberg, J.R.I. Lee, A. Wolcott, J.Z. Zhang, L.J. Terminello, and T. Van Buuren. Determination of the exciton binding energy in CdSe quantum dots. *ACS Nano*, 3(2):325–330, 2009.
- [204] S.L. Sewall, R.R. Cooney, K.E.H. Anderson, E.A. Dias, D.M. Sagar, and P. Kambhampati. State-resolved studies of biexcitons and surface trapping dynamics in semiconductor quantum dots. *Journal of Chemical Physics*, 129(8), 2008.
- [205] S.L. Sewall, A. Franceschetti, R.R. Cooney, A. Zunger, and P. Kambhampati. Direct observation of the structure of band-edge biexcitons in colloidal semiconductor CdSe quantum dots. *Physical Review B - Condensed Matter and Materials Physics*, 80(8), 2009.
- [206] M. Achermann, J.A. Hollingsworth, and V.I. Klimov. Multiexcitons confined within a subexcitonic volume: Spectroscopic and dynamical signatures of neutral and charged biexcitons in ultrasmall semiconductor nanocrystals. *Physical Review B - Condensed Matter and Materials Physics*, 68(24):2453021–2453025, 2003.
- [207] C. Bonati, M.B. Mohamed, D. Tonti, G. Zgrablic, S. Haacke, F. Van Mourik, and M. Chergui. Spectral and dynamical characterization of multiexcitons in colloidal CdSe semiconductor quantum dots. *Physical Review B - Condensed Matter and Materials Physics*, 71(20), 2005.
- [208] L. Dworak, V.V. Matyilitsky, M. Braun, and J. Wachtveitl. Coherent longitudinal-optical ground-state phonon in CdSe quantum dots triggered by ultrafast charge migration. *Physical Review Letters*, 107(24), 2011.
- [209] M. Kuno. *Introductory Nanoscience*. Garland Science, 2011.

- [210] Andreas Dreuw and Martin Head-Gordon. Single-reference ab initio methods for the calculation of excited states of large molecules. *Chemical reviews*, 105(11):4009–4037, 2005.
- [211] C. Ullrich. *Time-Dependent Density-Functional Theory: Concepts and Applications*. Oxford Graduate Texts. OUP Oxford, 2012.
- [212] Miguel A.L. Marques, Carsten A. Ullrich, Fernando Nogueira, Angel Rubio, Kieron Burke, and Eberhard K. U. Gross, editors. *Time-Dependent Density Functional Theory*. Springer Berlin Heidelberg, 2006.
- [213] Carsten A Ullrich and Zeng-hui Yang. A brief compendium of time-dependent density functional theory. *Brazilian Journal of Physics*, 44(1):154–188, 2014.
- [214] Y. Zhou, S. Wang, and Y. Zhang. Catalytic reaction mechanism of acetylcholinesterase determined by born-oppenheimer Ab initio QM/MM molecular dynamics simulations. *Journal of Physical Chemistry B*, 114(26):8817–8825, 2010.
- [215] Z. Ke, S. Wang, D. Xie, and Y. Zhang. Born - Oppenheimer ab initio QM/MM molecular dynamics simulations of the hydrolysis reaction catalyzed by protein arginine deiminase 4. *Journal of Physical Chemistry B*, 113(52):16705–16710, 2009.
- [216] G.-J. Kroes, A. Gross, E.-J. Baerends, M. Scheffler, and D.A. McCormack. Quantum theory of dissociative chemisorption on metal surfaces. *Accounts of Chemical Research*, 35(3):193–200, 2002.
- [217] N.J. Harris and K. Lammertsma. Ab initio density functional computations of conformations and bond dissociation energies for hexahydro-1,3,5-trinitro-1,3,5-triazine. *Journal of the American Chemical Society*, 119(28):6583–6589, 1997.
- [218] I.V. Schweigert and B.I. Dunlap. Electronic structure and molecular dynamics of breaking the RO-NO₂ bond. *Journal of Chemical Physics*, 130(24), 2009.
- [219] W.-R. Zheng, J.-L. Xu, T. Huang, Z.-C. Chen, and Q. Yang. P=O bond dissociation enthalpies: High-level ab initio and DFT study. *Computational and Theoretical Chemistry*, 968(1-3):1–7, 2011.
- [220] B.S. Jursic. The evaluation of nitrogen containing bond dissociation energies using the ab initio and density functional methods. *Journal of Molecular Structure: THEOCHEM*, 366(1-2):103–108, 1996.
- [221] M.E.A. Benmalti, A. Krallafa, and M.-P. Gaigeot. Born Oppenheimer Molecular Dynamics calculation of the o-H IR spectra for acetic acid cyclic dimers. *Journal of Physics: Conference Series*, 574(1), 2014.

- [222] W. Lin and F. Paesani. Infrared spectra of $\text{HCl}(\text{H}_2\text{O})_n$ clusters from semiempirical Born-Oppenheimer molecular dynamics simulations. *Journal of Physical Chemistry A*, 119(19):4450–4456, 2015.
- [223] M. Baer. *Beyond Born-Oppenheimer: Electronic Nonadiabatic Coupling Terms and Conical Intersections*. 2006.
- [224] S. Bubin, M. Pavanello, W.-C. Tung, K.L. Sharkey, and L. Adamowicz. Born-oppenheimer and non-born-oppenheimer, atomic and molecular calculations with explicitly correlated gaussians. *Chemical Reviews*, 113(1):36–79, 2013.
- [225] J.M. Bowman. Chemistry: Beyond born-oppenheimer. *Science*, 319(5859):40–41, 2008.
- [226] T. Yonehara, K. Hanasaki, and K. Takatsuka. Fundamental approaches to nonadiabaticity: Toward a chemical theory beyond the born-oppenheimer paradigm. *Chemical Reviews*, 112(1):499–542, 2012.
- [227] M. Cafiero, S. Bubin, and L. Adamowicz. Non-Born-Oppenheimer calculations of atoms and molecules. *Physical Chemistry Chemical Physics*, 5(8):1491–1501, 2003.
- [228] Ahren W. Jasper, Shikha Nangia, Chaoyuan Zhu, and Donald G. Truhlar. Non-Born-Oppenheimer Molecular Dynamics. *Accounts of Chemical Research*, 39(2):101–108, 2006.
- [229] Joseph F. Capitani, Roman F. Nalewajski, and Robert G. Parr. Non-Born-Oppenheimer density functional theory of molecular systems. *Journal of Chemical Physics*, 76(1):568–573, 1982.
- [230] How large are nonadiabatic effects in atomic and diatomic systems? *Journal of Chemical Physics*, 143(12), 2015.
- [231] S. Bubin, M. Stanke, and L. Adamowicz. Accurate non-Born-Oppenheimer calculations of the complete pure vibrational spectrum of ditritium using all-particle explicitly correlated Gaussian functions. *Journal of Chemical Physics*, 140(15), 2014.
- [232] L. Adamowicz, E.I. Tellgren, and T. Helgaker. Non-Born-Oppenheimer calculations of the HD molecule in a strong magnetic field. *Chemical Physics Letters*, 639:295–299, 2015.
- [233] N. Kirnosov, K.L. Sharkey, and L. Adamowicz. Non-Born-Oppenheimer variational method for calculation of rotationally excited binuclear systems. *Journal of Physics B: Atomic, Molecular and Optical Physics*, 48(19), 2015.

Benjamin H. Ellis

ellis.bh89@gmail.com (414) 305-0784
 103 Croyden Ln
 Apt B
 Syracuse, NY 13224

Personal Statement

My objective is to pursue my professional and personal interest in solving large, complex problems with real world impact. I am particularly passionate about computationally challenging problems where creative and critical thinking provides data driven solutions and expands the boundaries of current technology.

Experience

- | | |
|---|---|
| Syracuse University | SYRACUSE, NY |
| Graduate Teaching Assistant | <i>Fall 2011 – Fall 2013, Fall 2015 – present</i> |
| <ul style="list-style-type: none"> • Taught general and organic chemistry • Led laboratory and discussion sections • Reviewed and reinforced key concepts | |
| Graduate Research Assistant | <i>Spring 2013 – Summer 2015</i> |
| <ul style="list-style-type: none"> • Wrote and maintained numerically intensive software • Deployed software on HPC platforms • Collected, explored, and analyzed data • Authored reports and manuscripts for publication | |
-

Education

- | | |
|---|---------------------|
| Syracuse University | SYRACUSE, NY |
| Doctorate of Philosophy, Physical Chemistry | <i>October 2016</i> |
| Thesis: Development of multicomponent coupled-cluster theory and applications to molecular and semiconductor systems | |
| Syracuse University | SYRACUSE, NY |
| Master of Philosophy, Physical Chemistry | <i>August 2013</i> |
| Thesis: Development of multicomponent semistochastic quantum Monte Carlo for investigating nuclear-electron correlation | |
| University of Wisconsin-Madison | MADISON, WI |
| Bachelor of Science, Chemistry | <i>May 2011</i> |
-

Qualifications

Skills:

- | | |
|--|--|
| <ul style="list-style-type: none"> • Software development • Object oriented design principles • Algorithm development • High performance and parallel computing • Numerical methods | <ul style="list-style-type: none"> • Data analysis • Problem solving, troubleshooting, and debugging • Technical reporting and documentation • Teaching, training, and support |
|--|--|

Technologies:

- | | |
|--|--|
| <ul style="list-style-type: none"> • Python • FORTRAN • C and C++ • MPI, OpenMP, and multithreading • Numerical and data analysis libraries (LAPACK, BLAS, MKL, SciPy, NumPy, Pandas) | <ul style="list-style-type: none"> • Microsoft Office (Word, Excel, PowerPoint) and latex (\LaTeX) • Version control and collaboration software (Git) • Cluster (TACC Stampede) and cloud HPC platforms using SLURM, PBS, and Condor schedulers • Comfortable with *nix systems |
|--|--|

Publications and Exhibitions

Exhibitions

National American Physical Society March Meeting 2013

Baltimore, MD

Development of multicomponent semistochastic quantum Monte Carlo, Session W24, Abstract ID: BAPS.2013.MAR.W24.4

National American Chemical Society Fall Meeting 2015

Boston, MA

Development of the multicomponent coupled-cluster theory for investigating non-adiabatic electron-nuclear interactions in confined chemical systems, Paper Number: COMP 192

Publications

- Development of multicomponent coupled-cluster theory for investigation of multiexciton interactions, *Journal of Chemical Theory and Computation*
- Investigation of many-body correlation in biexcitonic systems using electron-hole multicomponent coupled-cluster theory (submitted 2016)
- Non-perturbative determination of electron-hole screening from explicitly correlated geminal functions without using unoccupied states (in prep 2016)

Research Experience

Development of multicomponent coupled-cluster theory

- Formulated coupled-cluster theory capable of quantifying correlation between multiple particle types
- Deigned algorithms, implemented solutions, and optimized code that considered both memory footprint and CPU cost
- Developed symbolic and numerical software to both derive and automatically implement large sets of equations
- Deployed code on HPC cluster computing environment (TACC Stampede)

Investigation of exciton and biexciton binding energy in semiconductor quantum dots

- Used multicomponent coupled-cluster method to investigate and predict properties of semiconductor quantum dots
- Modified theoretical formulation and implementation of the method to favorably scale computational cost
- Analyzed and explored data to find unique and novel trends

Formulation of electron-hole Hamiltonian for investigating excited electronic states in molecular systems

- Developed theory to treat excitations in chemical systems using multicomponent methods
- Wrote software that transforms single component mathematical models to multicomponent models